



HAL
open science

Direct functionalization by C-H activation of s-tetrazine for the development of new materials in medicine

Ahmad Daher

► **To cite this version:**

Ahmad Daher. Direct functionalization by C-H activation of s-tetrazine for the development of new materials in medicine. Organic chemistry. Université Bourgogne Franche-Comté, 2023. English. NNT : 2023UBFCK030 . tel-04427189

HAL Id: tel-04427189

<https://theses.hal.science/tel-04427189>

Submitted on 30 Jan 2024

HAL is a multi-disciplinary open access archive for the deposit and dissemination of scientific research documents, whether they are published or not. The documents may come from teaching and research institutions in France or abroad, or from public or private research centers.

L'archive ouverte pluridisciplinaire **HAL**, est destinée au dépôt et à la diffusion de documents scientifiques de niveau recherche, publiés ou non, émanant des établissements d'enseignement et de recherche français ou étrangers, des laboratoires publics ou privés.



**THESE DE DOCTORAT DE L'ETABLISSEMENT UNIVERSITE BOURGOGNE FRANCHE-COMTE
PREPAREE A L'INSTITUT DE CHIMIE MOLECULAIRE DE L'UNIVERSITE DE BOURGOGNE**

Ecole doctorale n°553

Dénomination école doctorale

Doctorat de chimie

Par

M. DAHER Ahmad

Direct functionalization by C-H activation of s-tetrazine

for the development of new materials in medicine

Thèse présentée et soutenue à Dijon , le 15/05/2023

Composition du Jury :

Mr. AUDEBERT, Pierre	Professeur, École Normale Supérieure Paris-Saclay	Rapporteur
Mme. OBLE, Julie	Maître de conférences, Sorbonne Université	Rapporteuse
Mr. BOUIT, Pierre-Antoine	Chargé de recherches CNRS, Université de Rennes 1	Examineur
Mr. SOULE, Jean-François	L'École nationale supérieure de chimie de Paris	Examineur
Mme. MALACEA, Raluca	Chargée de recherches CNRS, Université de Bourgogne	Membre invité
Mr. HIERSO, Jean-Cyrille	Professeur, Université de Bourgogne	Directeur de thèse
Mr. ROGER, Julien	Maître de conférences, Université de Bourgogne	Codirecteur de thèse

Contents

Abbreviations	7
General introduction	9
Chapter 1: Alkali halides as reagents for <i>N</i>-directed <i>ortho</i>-C–H halogenation	11
I. Introduction to organic halides formation	11
II. Nitrogen directed C–H bond electrophilic halogenation	13
1) Palladium-catalyzed C–H bond electrophilic halogenation	13
A. Phenylpyridine, phenylpyrazole and oxime as directing groups	13
B. Phenylpyrimidine as directing group	14
C. Azobenzene as directing groups	15
D. Benzoquinoline as directing group	18
E. Nitriles as directing groups	19
F. Amides as directing groups.....	20
G. Thiazole as directing groups	21
H. Benzimidazole, quinazoline and imidazo[1,2 <i>b</i>]pyridine directing groups.....	22
I. Diarylmethylamines derivatives directing groups	23
2) Rhodium-catalyzed C–H bond electrophilic halogenation	25
3) Copper-catalyzed C–H bond electrophilic halogenation	26
4) Nickel-catalyzed C–H bond electrophilic halogenation	28
5) Cobalt-catalyzed C–H bond electrophilic halogenation	29
6) Ruthenium-catalyzed C–H bond electrophilic halogenation	30
7) Mechanism proposed for the electrophilic Pd-catalyzed C–H bond halogenation	31
III. Nitrogen-directed C–H bond halogenation using nucleophilic halogen sources MX (M = Ca, Na, K, H and X = I, Br, Cl).	33
1) Palladium C–H bond nucleophilic halogenation	33
A. Phenylpyridine, pyrimidine and benzoquinoline directing groups.....	33
B. Benzothiadazole as directing groups	34
2) Copper catalyzed C–H bond nucleophilic halogenation	35
3) Rhodium-catalyzed C–H bond nucleophilic halogenation	39

4)	Mechanisms proposed for C–H bond halogenation using nucleophilic halogen sources.....	41
IV.	Results and discussion: <i>Nitrogen</i> -directed C–H halogenation of <i>s</i> -aryltetrazines	44
1)	Screening of the conditions for the iodination of 3,6-bis(2-fluorophenyl)-1,2,4,5-tetrazine	44
A.	Study of the oxidant.....	47
B.	Study of the catalyst	48
C.	Study of the solvent	49
D.	Study of the halogen source	50
2)	General iodination of <i>s</i> -aryltetrazines and other <i>N</i> -containing substrates	52
3)	Screening of conditions for the bromination of 3,6-bis(2-fluorophenyl)-1,2,4,5-tetrazine ..	55
4)	Bromination of <i>s</i> -aryltetrazines and other <i>N</i> -containing substrates	56
5)	Screening of conditions for the chlorination of 3,6-bis(2-fluorophenyl)-1,2,4,5-tetrazine ..	58
6)	Chlorination of <i>s</i> -tetrazines and other <i>N</i> -containing substrates	59
7)	Unequal trihalogenated phenylpyrazole derivatives	60
8)	Proposed mechanism for the <i>N</i> -direct palladium-catalyzed iodination with nucleophilic source	61
9)	Conclusion and perspectives	62
	Supporting Information	64
I.	General procedures	65
1)	General procedure for the halogenation of heteroaryl derivatives	65
2)	General procedure for the acetoxylation	74
	Chapter 2: <i>bis</i> -Tetrazo[1,2- <i>b</i>]indazoles: access to highly nitrogen-containing polyaromatics	77
I.	Introduction	77
II.	Insertion of azides on heteroaryl aromatic	78
1)	Insertion of azides via organic pathways.....	79
A.	Azidation by nucleophilic aromatic substitution on arenes	79
B.	Azidation via lithium organometallic reagents	84
C.	Diazotization general approaches.....	85
2)	Insertion of azide <i>via</i> catalytic azidation	88

A.	Interconversion of pre-inserted groups into azide	88
3)	The insertion of azide by ligand-directed C–H bond activation.....	92
A.	Copper-catalyzed ligand-directed C–H bond azidation	92
4)	Mechanism of <i>N</i>-directed catalytic C–H bond azidation.....	95
D.	General mechanism for Rh(III)-catalyzed C–H bond azidation	96
III.	Selected applications of <i>N</i>-containing heteroaryl azides as platforms	98
1)	Introduction to click chemistry: the synthesis of triazoles	98
A.	Cu-catalyzed cycloaddition of aliphatic alkynes and azide on heteroarenes	99
2)	Strain-promoted [3+2] cycloaddition of azides and cyclooctynes	100
3)	General mechanisms of the [3+2] cycloaddition reactions	101
A.	Sodium ascorbate-mediated Cu-catalyzed [3+2] cycloaddition of terminal alkynes	101
B.	Metal free [3+2] cycloaddition reaction of cyclooctynes and aryl azides.....	102
IV.	Indazole derivatives as N–N bond containing molecules.....	103
1)	General synthesis.....	103
A.	The synthesis of indazoles from aryl azide and the nitrene intermediate	104
V.	Results and discussion	109
1)	Azidation of <i>s</i>-aryltetrazines: synthesis and applications	109
A.	Azide <i>s</i> -aryltetrazine in click chemistry.....	109
B.	Cycloaddition chemistry: The Huisgen and iEDDA cycloaddition reactions	110
2)	Azide <i>s</i>-aryltetrazine in <i>N</i>-cyclisation: formation of tetrazo[1,2-<i>b</i>]indazole	114
A.	Formation of 3-aryltetrazo[1,2- <i>b</i>]indazole	114
B.	Formation of the <i>bis</i> -tetrazo[1,2- <i>b</i>]indazole	115
VI.	Mechanism formation of the tetrazo[1,2-<i>b</i>]indazole	118
1)	Formation of 3-(aryl)-tetrazo[1,2-<i>b</i>]indazole	118
2)	Formation of the <i>bis</i>-tetrazo[1,2-<i>b</i>]indazole.....	120
VII.	Post-functionalization of 3-(aryl)-tetrazo[1,2-<i>b</i>]indazole	120
1)	Palladium metallacycle formation	120
2)	<i>Ortho</i>-functionalization of tetrazo-indazole	122
VIII.	Photophysical analysis of the mono and bistetrazo[1,2-<i>b</i>]indazole	124
1)	UV-visible analysis	124

A.	UV-visible analysis of 3-(aryl)-tetrazo[1,2- <i>b</i>]indazoles	124
B.	UV-visible analysis of bis-tetrazo[1,2- <i>b</i>]indazoles	125
2)	Cyclic voltammetry measurements	125
IX.	Conclusion and perspectives	127
	Supporting Information	128
	Typical experimental procedures	129
1)	General procedure of functionalization of 3,6-diaryl-1,2,4,5-tetrazine	129
2)	General procedure of the synthesis of 3-(aryl)-[1,2,4,5]-tetrazo[1,2-<i>b</i>]indazole	132
	3-(2-fluorophenyl)-[1,2,4,5]-tetrazo-[1,2-<i>b</i>]indazole	132
3)	General procedure of the functionalization of 3-(aryl)-tetrazo[1,2-<i>b</i>]indazole	133
X.	Thermal properties	137
XI.	Optical properties	137
1)	UV-visible analyses	137
2)	Emission spectra	139
XII.	Cyclic voltammetry	140
	General conclusion and perspectives	144
	References	148

Abbreviations

ACN	Acetonitrile
Ac ₂ O	Acetic anhydride
S _N Ar	Aromatic nucleophilic substitution
bz-Leu-OH	N-Benzoyl-L-leucine
Bn	Benzyl
BtSO ₂ N ₃	Benzotriazol-1-yl-sulfonyl azide
CF ₃ CO ₂ H	Trifluoroacetic acid
CV	Cyclic voltammetry
DCE	Dichloroethane
DMF	Dimethylformamide
DCM	Dichloromethane
DMSO	Dimethyl sulfoxide
Equiv	Equivalent
E ⁺	Electrophile
HMPA	Hexamethylphosphoramide
<i>K_{app}</i>	Kinetic rate
Mw (μw)	Microwave
NBS	<i>N</i> -bromosuccinimide
NCS	<i>N</i> -chlorosuccinimide
NFSI	<i>N</i> -fluorobenzenesulfonimide
Nu ⁻	Nucleophile
CH ₃ NO ₂	Nitromethane
OLEDs	Organic light emitting diode

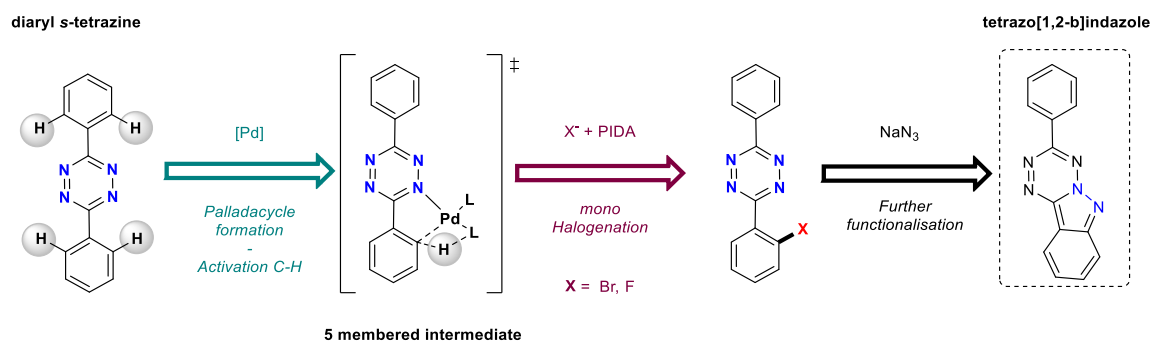
PivOH	Pivalic acid
Pd	Palladium
PIDA	Phenyl iodane diacetate
POCl ₃	Phosphoryl chloride
AgSbF ₆	Silver hexafluoroantimonate
[TM]	Transition metal
TsOH	Tosylic acid
<i>t</i> -amylOH	<i>Tert</i> -amyl alcohol
TFA	Trifluoroacetic acid
TBAI	Tetra- <i>n</i> -butylammonium iodide
C ₂ H ₂ Cl ₄	Terachloroethane
THF	Tetrahydrofuran
PhCF ₃	Trifluorotoluene
TsN ₃	Tosyl azide
TCP	1,2,3-Trichloropropane
TMEDA	Tetramethylethylenediamine
TEMPO	(2,2,6,6-Tetramethylpiperidin-1-yl)-oxy
Rh	Rhodium
UV-Vis	Ultraviolet–visible spectroscopy

General introduction

Heterocycles comprise an essential category of organic compounds. Numerous heterocyclic compounds, both natural and manufactured have pharmacological activity and are in clinical use.^[1] Distinctly, *s*-tetrazines have to be active heterocycles in several fields. The 1,2,4,5-tetrazines or *s*-tetrazine is a six-membered hetero-aromatic benzene-type molecule that has the maximum permitted ratio of nitrogen to carbon in a single ring (indeed, pentazine and hexazine are not stable. Tetrazines were slightly neglected after their discovery by Pinner in the 19th century.^[2] However, with the nearly simultaneous appearance of two major discoveries regarding their properties, the situation completely shifted. The first was the (re)discovery of tetrazines optical characteristics.^[3] The second, and more significant, was the remarkable reactivity in inverse Electron Demand Diels-Alder (IEDDA) reactions (also known as tetrazine click chemistry), specifically with strained alkenes. The tetrazines are particularly reactive because of their low aromaticity energy ($E = 14\text{--}15$ kcal/mol, as opposed to benzene, which is 33 kcal/mol). This cycloaddition coupling is uncommon, incredibly quick, clean, and tolerant. Their broad use in biochemistry and pharmaceutical applications —referred to in this context as "biorthogonal click chemistry"— was the reason for this increase far more than their synthetic usefulness.^[4] One of the main topics of study conducted by Pr. J.-C. Hierso's group at the Institute of Molecular Chemistry at the University of Bourgogne is the synthesis and design of polyfunctionalized *s*-tetrazines *via* transition metal catalyzed C–H bond activation methods. We demonstrated the efficiency of *ortho*-directed palladium C–H activation in the efficient building of topical sensitive heterocyclic tetrazine-core and its further use in selective halogenation/acetoxylation.^[5] These functionalized tetrazines were then involved in various important reactions such as Suzuki cross-coupling reactions and biorthogonal cycloaddition reactions.^[6] Previously, the reported synthetic methods for tetrazine synthesis suffered from the use of toxic materials (such as PCl_5), long reaction times and most importantly low yields when halides are presents.^[7] We then became interested in extending the introduced functional groups to beyond halides. The presence of different hetero-atoms on a *s*-tetrazine derivative can be highly beneficial and of great use.

Our present project aims at developing new catalytic conditions with transition metal (Pd, Ir, Ru, Rh, Cu or Ni) to efficiently achieve challenging direct *ortho*-C–H activation on *s*-aryltetrazines in presence of suitable halogen providing reagents to reach new materials and medical applications. In this context, we first addressed the challenging *ortho*-C–H halogenation of *s*-diaryltetrazine (and others relevant heteroaryls) in presence of nucleophilic halogen source. We then target to involve the halogenated *s*-tetrazines, specifically the brominated and fluorinated forms in possible post-functionalization processes involving the introduction of an additional nitrogen atom and the

formation of a new novel family of molecules, the tetrazo[1,2-*b*]indazoles *via* a unique N–N bond formation. The properties of these molecules will be studied and compared to their parental origin, *s*-tetrazines (Scheme 1.).



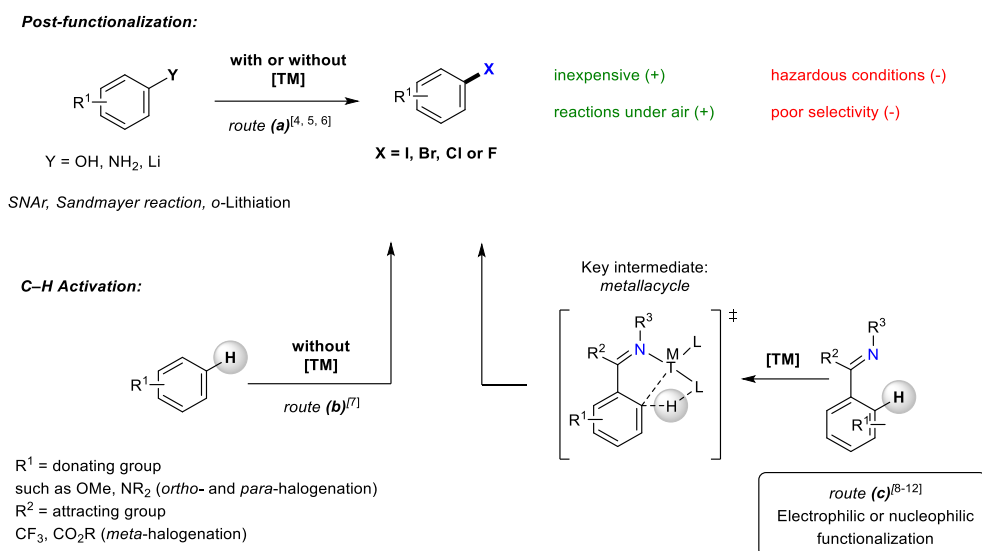
Scheme 1. Concept: Halogenation of aryl *s*-tetrazines and their transformation into a new family of tetrazo[1,2-*b*]indazoles

Chapter 1: Alkali halides as reagents for *N*-directed *ortho*-C–H halogenation

I. Introduction to organic halides formation

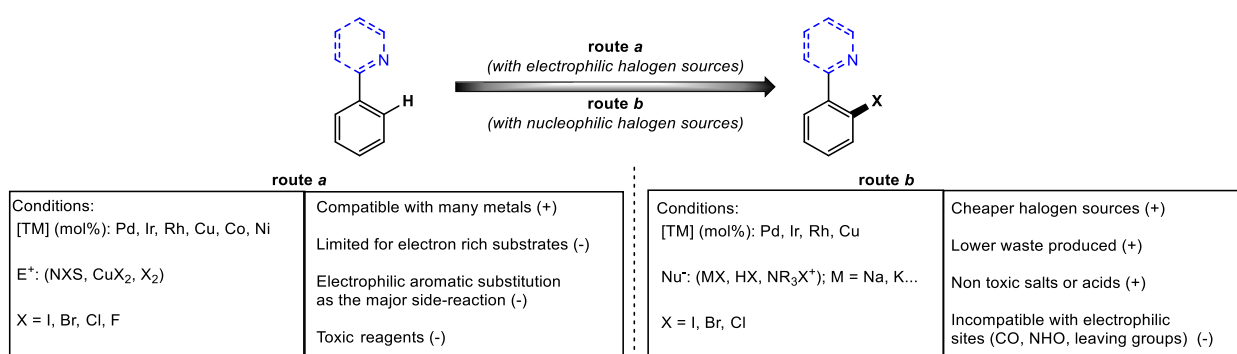
Halides' numerous synthetic applications are crucial to the current advancement of organic chemistry. The formation of halide chemicals in nature involves enzyme metabolic pathways, photochemistry,^[8,9] and uncontrolled geothermal events.^[10] Early on, alcohols were the primary starting material for addition and substitution processes that produced halogenated aromatic and aliphatic molecules, and these reactions later constituted the foundation of synthetic organic chemistry.^[11] On the other hand, the Sandmeyer reaction then enabled amines to be converted into halides.^[12] Another technique used to introduce various halides was *ortho*-lithiation.^[13] Although these reactions are beneficial, they have several drawbacks, such as risky reaction processes, hazardous halogenation chemicals, harsh reaction temperatures and most importantly, generally low site selectivity.

The concept of C–H bond activation emerged as a greener and more efficient method with respect to the more common organic pathways. C–H Bond halogenation can be described in the absence or presence of transition metals. For example, the group of Watkins illustrated efficient metal free C–H bond halogenation of quinolones.^[14] For other substrates, transition metal-promoted reactions seemed more efficient to achieve carbon–halogen bond chemistry development.^[15,16,17,18,19] Selective and efficient metal catalysis served at breaking carbon–hydrogen bonds towards straightforward carbon atom functionalization, and was also used to form C–X bonds (X = F, Cl, Br and I, Scheme 1). Metal-catalyzed C–H bond halogenation for C–X bond formation thus, experienced fast development and improved efficiency. Relevant reviews concerning general palladium-catalyzed C–H activation/functionalization and halogenation are available with relevant complementary perspectives.^[20,21,22,23,24,25]



Scheme 1. General synthetic routes for the C–X (X = halides) bonds formation

Therefore, the development of methods for the direct C–H halogen insertion on aromatics is preferable. A directing atom (nitrogen, oxygen, *etc.*) coordinates to transition metals and promotes selectively the C–H bond in the *ortho*-position on the aryl. Late transition metals that are efficient in such reactions are mainly palladium, copper, ruthenium, iridium and rhodium. The halogen sources used for such purposes might be divided into two categories: a) electrophilic halogenation sources such as *N*-halosuccinimide reagents (NXS), metal dihalides and halogen gases, and b) nucleophilic halogen sources using mainly metal halide salts (Scheme 2). We discuss below the halogenation reactions that are reported in the literature according their “formal” electrophilic and nucleophilic nature, depending on the transition metal, and arranged according suitable directing groups and substrates.



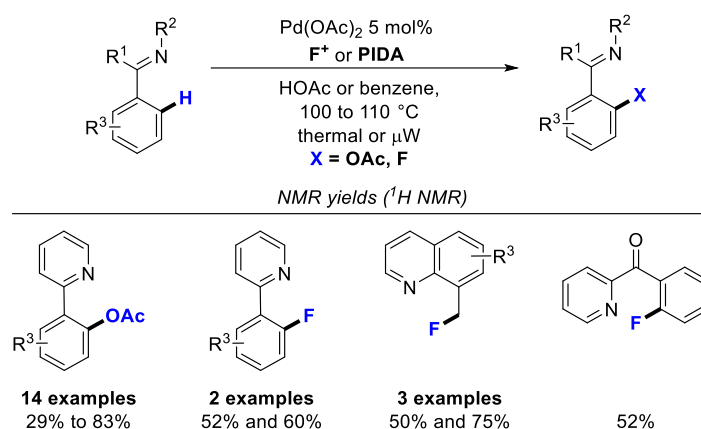
Scheme 2. Electrophilic and nucleophilic pathways on the N-directed C–H bond activation/halogenation

II. Nitrogen directed C–H bond electrophilic halogenation

1) Palladium-catalyzed C–H bond electrophilic halogenation

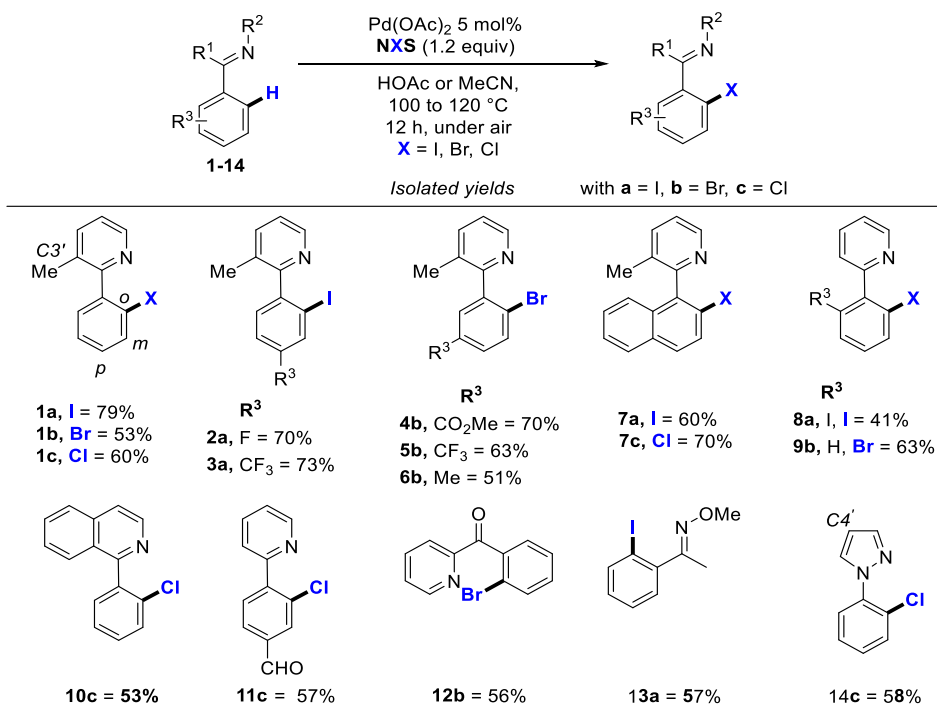
A. Phenylpyridine, phenylpyrazole and oxime as directing groups

The group of Sanford demonstrated the efficiency of different *N*-containing molecules in C–X bond formation *via* C–H bond activation (X = OAc, F). For example, they reported the Pd(II)-catalyzed chelate-directed oxidative functionalization of C–H bonds using hypervalent iodine(III) reagents, such as phenyl iodane diacetate (PIDA) as terminal oxidants to insert the acetoxy (OAc) group (Scheme 3). Moreover, utilizing the presence of electrophilic fluorine source, *N*-fluoro-2,4,6-trimethylpyridinium and the presence of a nitrogen directing group, they were able to introduce fluorine atom through a C–H bond activation on C_{sp2} and C_{sp3} in the presence of a palladium catalyst.^[26]



Scheme 3. *N*-directed Pd-catalyzed acetoxylation and fluorination

Accordingly, the same group was able to extend the principle of C–H functionalization to halogen insertion based on the same chelation principle and on similar substrates. In 2006, Sanford *et al.* reported the electrophilic Pd(II)-catalyzed halogenation on heteroarenes by a directing group strategy (Scheme 4).^[27] Monohalogenation takes place at the *ortho*-position (*o*) of the directing group. 1 equiv of 3-methyl-2-phenylpyridine **1** reacts with 1.2 equiv of *N*-halosuccinimides (NXS; X = I, Br, Cl) in the presence of 5 mol% Pd(OAc)₂ in HOAc or acetonitrile at 100 to 120 °C under air. The corresponding monoiodinated, brominated and chlorinated products **1a**, **1b** and **1c** were obtained in 87%, 53% and 60% respectively.



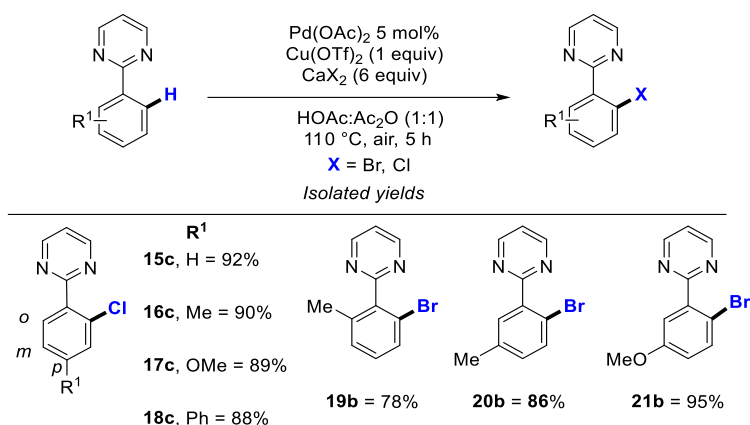
Scheme 4. N-directed Pd C–X bond formation on different heteroarenes

Both donating (Me) and withdrawing groups (CHO, CF₃, F and CO₂Me) were tolerated, and the mono halogenated products (**2a**, **3a**, **4b** to **6b**) were obtained in good yields of 51% to 73% with a clear preference for electron-withdrawing groups. The scope of the reaction, yields, and regioselectivity were controlled by electronic and steric factors for the halogenation reactions of phenylpyridine **1** to **12** that were obtained in 41% to 79% yields. For example, steric factors contributed highly in the determining the number of halogens inserted on **1** to **7** bearing a C3'-methyl group on the pyridine ring that contributed in blocking a second *o*-halogenation of the phenyl. Indeed, the position of the halogen inserted is opposite to the methyl (**6**)—or other *meta*-substituents—when they are present (**1** to **7** to **10** respectively). Amide **12** and oxime **13** afforded one type of insertion each that was either the bromination (56%) or iodination (57%) for **12b** and **13a**, respectively. Phenylpyrazole **14** yielded the chlorinated product in 58%. Notably, in the absence of palladium catalyst the C4'-halogenated product was generated (**14**, Scheme 4).

B. Phenylpyrimidine as directing group

Similarly to phenylpyridines, phenylpyrimidines are efficient directing groups for C–H bond halogenation. The group of Xu initiated their optimization on phenylpyrimidine **15** (Scheme 5). For selective mono halogenation, the reaction of one equiv of **15** with 5 mol% of Pd(OAc)₂, 6 equiv of CaCl₂

as the nucleophilic halogen source, 1 equiv of cupric triflate $\text{Cu}(\text{OTf})_2$ as an oxidant in mixture of HOAc and acetic anhydride (1:1) was performed at 110°C for 5 h to give **15c** in 92% yield.



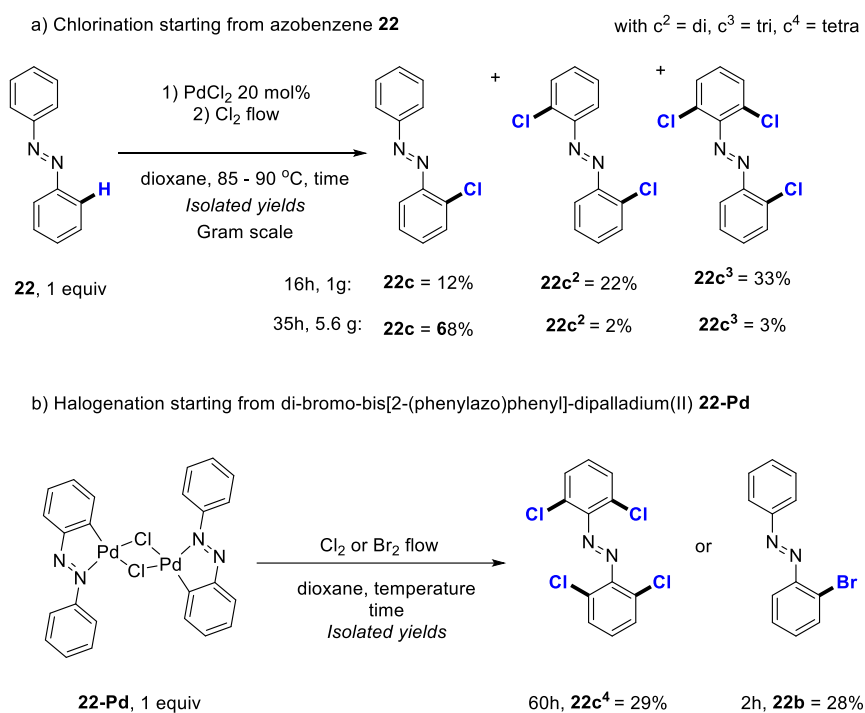
Scheme 5. N-directed Pd-catalyzed C–X bond formation on phenylpyrimidine derivatives

Using $\text{Pd}(\text{OAc})_2$ as catalyst achieved superior yields (92%) than using PdCl_2 (67%). Other electrophilic halogen sources such as *N*-chlorosuccinimide were tested in 1.2 equiv, which led to balanced mixture of **15c** and its *o*-dichlorinated derivative. Copper chloride (CuCl_2) was tested as a source of chlorine, using two equivalents, and produced a mixture of mono and di-halogenated derivatives. In HOAc as the only solvent, two equiv of CaCl_2 gave **15c** in 74% yield together with the dichlorinated derivative (20%). Other solvents, like acetonitrile or DCE, also yielded mixtures of the products with low conversions. Cupric trifluoroacetate ($\text{Cu}(\text{OTf})_2$) was required for the reaction to proceed well. Conversely, benzoquinone, $\text{K}_2\text{S}_2\text{O}_8$ and O_3 were also tested as oxidants with lower conversion. *Para*-donating (Me, OMe or Ph) groups were tolerated for chlorination in yields of 88% to 90% for compounds **16** to **18**. Bromination was presented with compounds **19** to **21**, with donating (Me and OMe) on the *ortho*- and *meta*-positions and afforded **19b** to **21b** in yields 78% to 95%. Halogenation reactions were not presented on compounds with electron-withdrawing groups.

C. Azobenzene as directing groups

Typical azobenzene has four identical C–H bonds in the *ortho*-position of the directing group which can undergo four concurrent C–H bond activations, making those substrates challenging to perform selective mono-C–H bond functionalization. Fahey reported the *ortho*-halogenation on azobenzenes in the presence of palladium catalysts *via* halogen quenching using halogen gas flow (Cl_2 , Scheme 6).^[28]

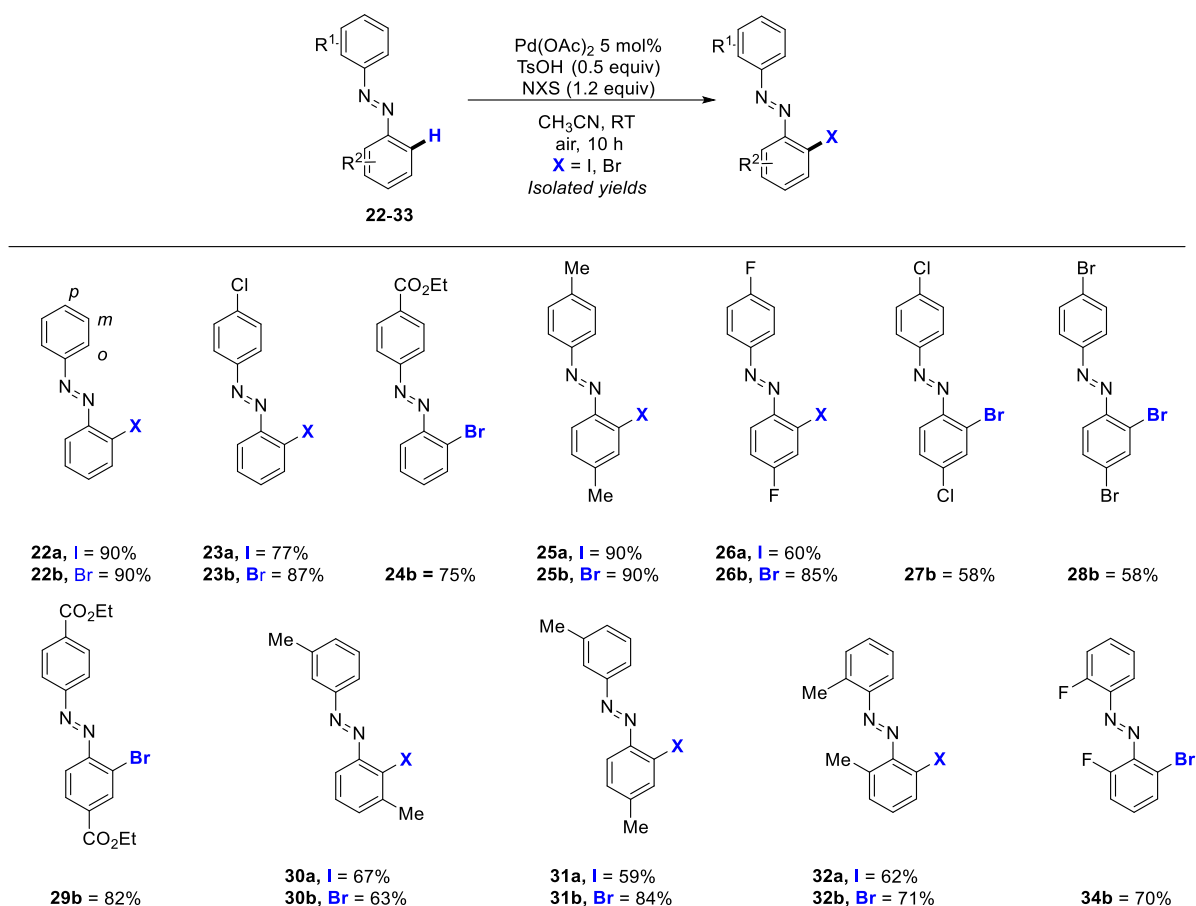
Starting from azobenzene **22** (in 1 gram scale), all three mono, di and trichlorinated azobenzenes were produced in 12%, 22% and 33% yields for **22c**, **22c²** and **22c³**, respectively in the presence of 20 mol% PdCl₂, under Cl₂ flow and increased temperature of 85 to 90 °C. The scale of the reaction proved to be of huge importance for controlling the number of chlorine atoms inserted. Increasing the scale of the reaction to 5.6 g directed the reactivity towards the monochlorinated azobenzene **22c** which was obtained in 68%. The tetrachlorinated azobenzene or the brominated azobenzene could not be obtained starting from azobenzene. These products were targeted from starting from dibromo-bis[2-(phenylazo)phenyl]-dipalladium(II) **22-Pd**, which is the intermediate complex produced and isolated *in situ* from azobenzene and PdCl₂. This allowed the production of the tetrachlorinated azobenzene **22c⁴** as the major product in 29% yield. In addition, bromination was realized by reacting this complex with Br₂, albeit only the monobrominated form was obtained in 28% yield for **22b**.



Scheme 6. *N*-directed Pd-catalyzed C–X bond formation on azobenzene

o-Halogenation achieved *via* halogen quenching mainly suffered from using toxic halogen gases and achieving moderate yields. In addition, this method was only performed on a single unsubstituted azobenzene. Therefore, Tian *et al.* reported a more efficient Pd(II)-catalyzed C–H bond iodination and bromination on azobenzene substrates, using more conveniently the *N*-halosuccinimides (X = I, Br) as the electrophilic halogen sources. Monohalogenation was performed with 1 equiv of the azobenzene

22, 5 mol% Pd(OAc)₂, 1.2 equiv of *N*-halosuccinimide and 0.5 equiv of tosylic acid (TsOH) additive in acetonitrile at RT and afforded **22a** in 90% yield in 10 h (Scheme 7).^[29]



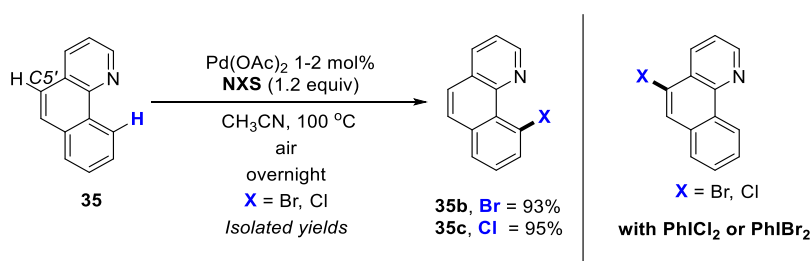
Scheme 7. *N*-directed Pd-catalyzed C-X bond formation on azobenzene derivatives

The bromination of **22** to yield **22b** is achieved in 90% yields. Brønsted acid additives were apparently needed in the reaction for activating both the Pd(II)-catalyst and NBS.^[30] The tosylic acid produced the palladium tosylate complex Pd(OTs)₂, which proved to be the active catalyst. By using prepared Pd(OTs)₂, the bromination reaction of **22** is promoted in 72% and 89% yield, in the absence and presence of TsOH, respectively. In the case of unsymmetric azobenzenes bearing substituents only on one phenyl in **23** and **24**, the halogenation occurred selectively on the more electron-rich phenyl and not on the phenyl bearing the electron-withdrawing group. C-H bond halogenation gave 77% and 87% for **23a** and **23b**, respectively, but only afforded bromination of **24** in 75% yields. Azobenzene substrates bearing electron-donating methyl groups or electron-withdrawing groups (F, Cl, Br, CO₂Et and Br) afforded *o*-monohalogenation in 58% to 90% yield for substrates **25-30**. With halogen bearing

substituents in **27** and **28** (*p*-Cl and *p*-Br), the regioselectivity of the bromination reaction towards the monohalogenated form was limited to 58% in both cases. When the substituents are positioned on the *meta* or *ortho* in **31** to **34**, the yields obtained ranged between 59% to 84% and were generally lower in comparison to those bearing *para*-substituents in **25** to **30**. Recently, some heterogeneous Pd(II)-catalyzed chlorination have been described, albeit in moderate yields of 32%.^[31]

D. Benzoquinoline as directing group

Sanford *et al.* also reported the C–H bond activation of benzoquinolines from Pd(II)-catalyzed C–H bond activation (Scheme 8).^[19] The optimal condition reaction for monohalogenation proceeded with 1 equiv of the benzoquinoline **35**, 1 to 2 mol% of Pd(OAc)₂, and 1.2 equiv of *N*-halosuccinimide at 100 °C in acetonitrile. The reaction was successful with NBS or NCS, and produced **35b** in 93% and **35c** in 95%.

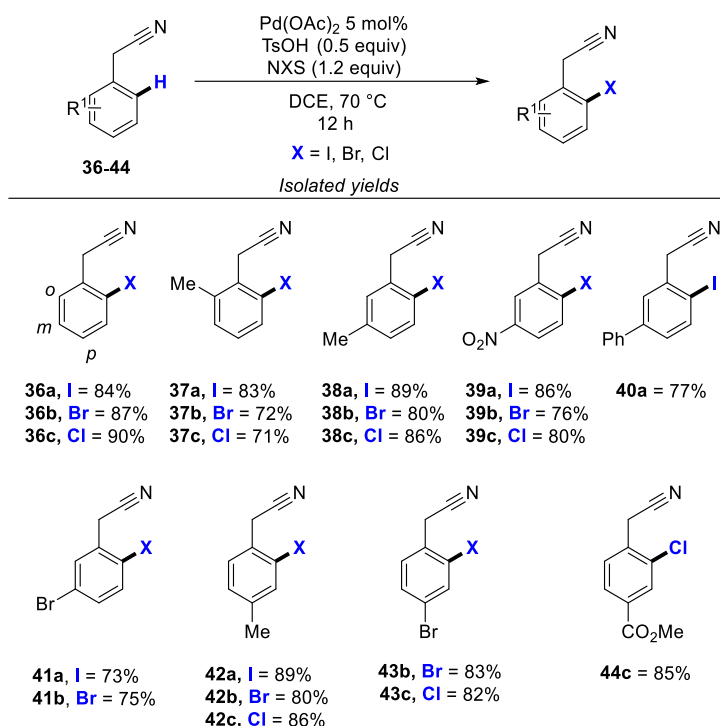


Scheme 8. *N*-directed Pd-catalyzed C–X bond formation on benzoquinoline

Other chlorinating or brominating sources PhICl₂ and PhIBr₂ lead to exclusive C5'–H halogenation (Scheme 8, right). With NIS or any other iodide sources, only traces of unidentified isomers of iodinated product were obtained, while the starting material remained largely unconsumed. Because of the rigid and planar nature of this substrate and the congested location of the *o*-C–H bond, steric constraints may prevent the introduction of the iodine atom. Homogenous Pd(II) *N*-directed halogenation on benzoquinolines still needs development. Such reaction is not described with other metals, and it is difficult to control concurrent undirected C5' activation. Iodine insertion onto such derivatives is still unsuccessful through homogenous catalysis and is narrowed to heterogeneous catalysis with Pd-metal–organic framework (MOF) or Pd@MOF nanoparticles, until now in average yields (27%).^[32]

E. Nitriles as directing groups

In the absence of transition metals, the electrophilic aromatic substitution of benzonitriles does not provide *o*-halogenated benzonitriles because of the mesomeric directing effect of this electron-withdrawing group.^[33] In this case, *o*-halogenation occurs *via* the coordination of the π bond of the cyano group. Sun group used benzonitrile **36** and achieved its iodination with 1 equiv of a benzonitrile derivative, 5 mol% of Pd(OAc)₂, 1.2 equiv of *N*-halosuccinimide, 0.5 equiv PTSA at 70 °C in DCE to give **36a** in 84% (Scheme 9).^[34]



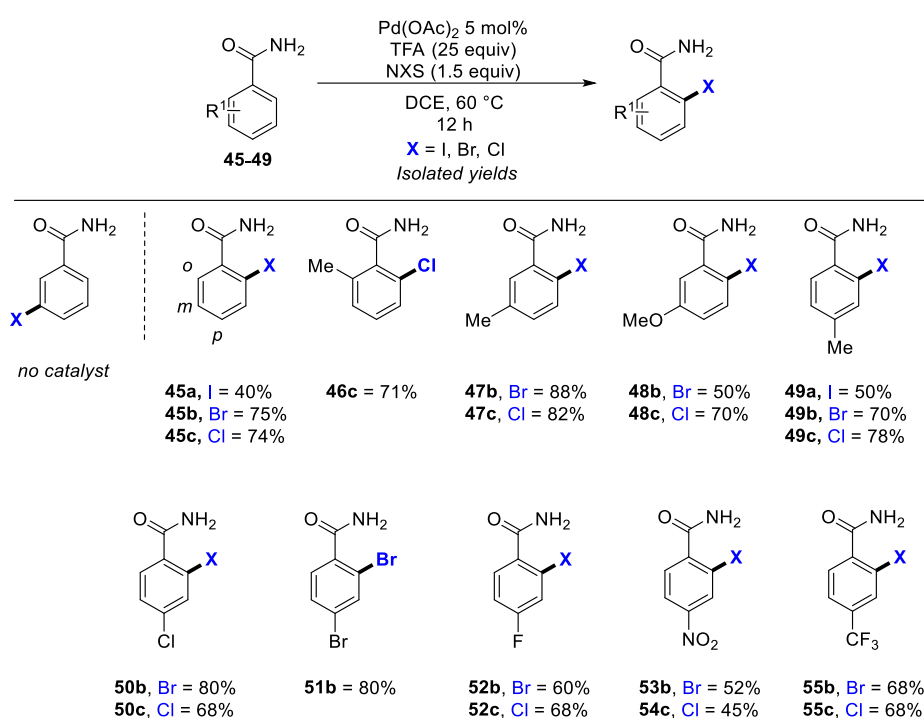
Scheme 9. N-directed Pd-catalyzed C–X bond formation on benzonitrile derivatives

PTSA was used as an additive, activating the succinimide halogen sources similarly to TsOH in the halogenation of azobenzenes substrates (Scheme 7). The use of other acid additives, PivOH and TFA provided **36a** with yields of 58% and 63%, respectively. Various solvents have been tried out such as toluene, 1,4-dioxane, DMF, HOAc and acetonitrile. Only DMF as a solvent produced 55% of monohalogenated product **36a**, while other solvents yielded the targeted product **36a** in less than 40% yields. On **36**, all three halogens were successfully inserted, thus giving yields of 87% and 90% for Br and Cl, respectively. Donating (OMe, Me and Ph) and withdrawing (NO₂, Cl, Br and CO₂Me)

substituents were well tolerated on *ortho*-, *meta*- and *para*- **37-44** and afforded their halogenated forms in 71% to 89% yields.

F. Amides as directing groups

C–H Bond functionalization with amides as directing groups and Pd(II)-catalysts was reported by Kumar *et al.*, who described the halogenation of benzamides (Scheme 10).^[35] 1 equiv of the benzamide react with 1.5 equiv of the *N*-bromosuccinimide in a catalyzed reaction in the presence of 5 mol% of Pd(OAc)₂, 25 equiv of TFA at 60 °C in DCE, the brominated benzamide **45b** was obtained in 75%.



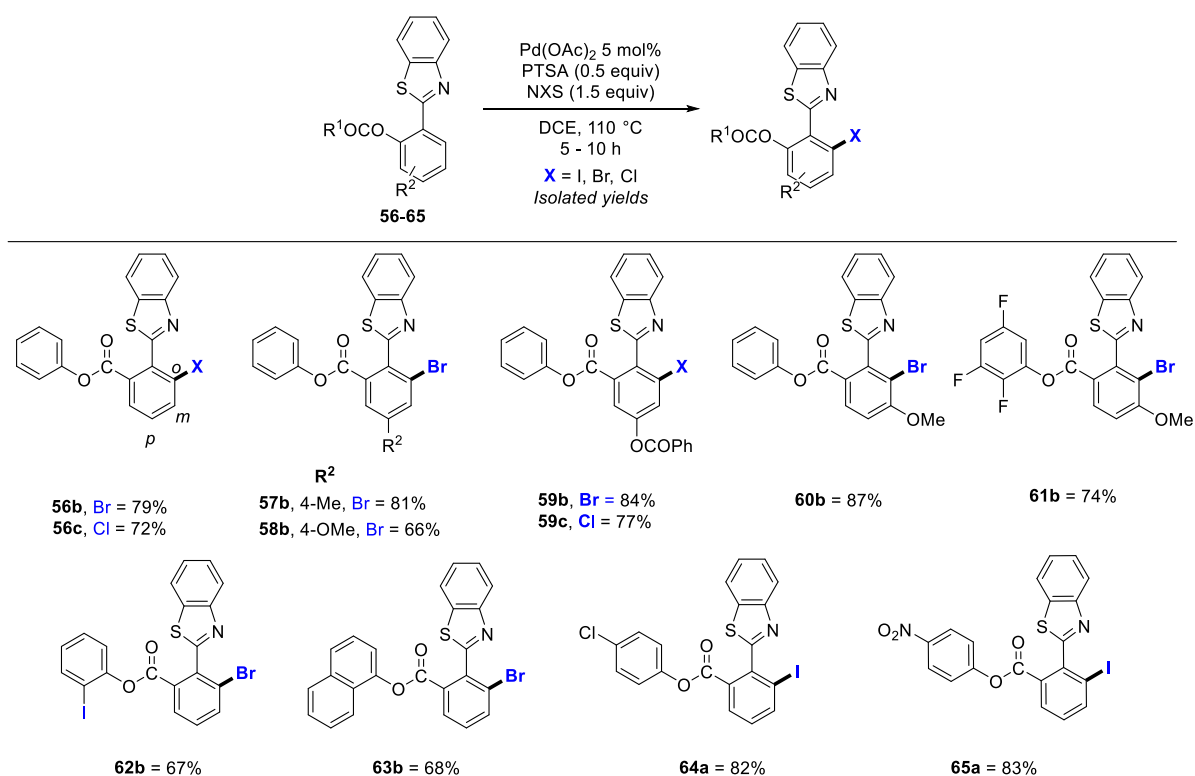
Scheme 10. *N*-directed Pd-catalyzed C–X bond formation on aryl amide derivatives

A reaction without catalyst favoured the formation of a *meta*-substituted product *via* aromatic electrophilic substitution (SEAr) (Shown in Scheme 10, left). TFA or pivalic acid as Brønsted acid were necessary for the reaction to proceed. Reaction times longer than 12 h and reaction temperatures higher than 60 °C increased dihalogen insertion. Iodination reaction was found to be the least successful on simple benzamides with only 40% yield for **45a** formation; bromination and chlorination were achieved in 75% and 74% yield for **45b** and **45c**. For compounds **46** to **55**, halogenation was only represented by bromine and chlorine insertion but for iodine, only for **49** which produced **49a** in 50% yields. Generally, for **46** to **55**, bromine and chlorine C–H insertion gave rather similar yields for both

halogens, ranging from 45% to 80%. The reaction tolerated donating (Me and OMe) and withdrawing (Cl, Br, F, NO₂ and CF₃) groups on the substrate, but was favoured for electron-donating groups over electron-withdrawing groups. Notably, for the benzamides functionalized at the *meta*-position, like **47** and **48**, the halogen was inserted at *para*-position similarly to phenylpyridines and azobenzenes, presumably because of steric factors.

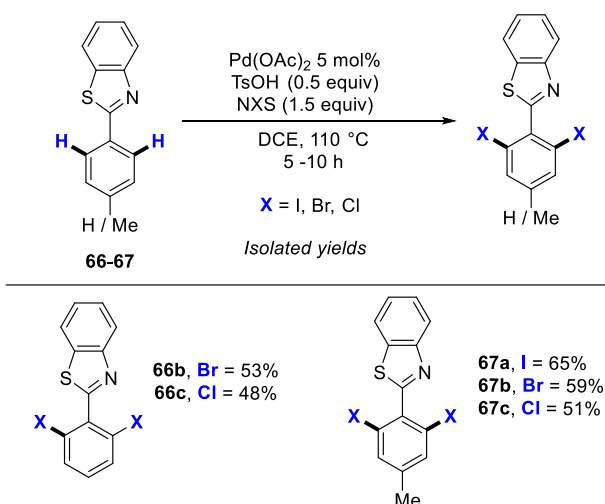
G. Thiazole as directing groups

Previously, the groups of Marder and Zhang initiated the transition metal catalyzed C–H bond activation of such substrates through C–H arylation reactions on benzthiazoles.^[36] Then, the groups of Babu and Patel reported the C–heteroatom bond formation *via* C–H bond acetoxylation reactions of C_{sp2} and C_{sp3}.^[37] The group of Patel extended their work to include C–H bond halogenation reactions through Pd(II)-based systems using 2-(benzo[*d*]thiazol-2-yl)phenyl benzoate **56** and its derivatives (Scheme 11).



Scheme 11. N-directed Pd-catalyzed C–X bond formation on benzothiazole derivatives

The use of 2-(benzo[*d*]thiazol-2-yl)phenyl benzoate **56** in 1 equiv, 1.5 equiv of the *N*-halosuccinimides NXS (X = Br, Cl), 5 mol% of Pd(OAc)₂ and 0.5 equiv of the acid additive PTSA between 60 °C to 110 °C in DCE afforded bromination and chlorination of **56** for yielding **56b** and **56c** in 79% and 72%, respectively (Scheme 12). Electron-donating (Me and OMe) and withdrawing groups (OCOPh) were present on the *para*- or *meta*- of the phenyl rings on compounds **57** to **60** and afforded good yields (66% to 87%) but most presented reactions were with bromination only with the exception of for chlorination of **59** in 77%. The compounds **61** to **65** bearing phenyl groups with electron-withdrawing moieties (2,3,5-triF, I, Cl and NO₂) were well-tolerated on the *o*-carboxyl group afforded monohalogenation in 67% to 83% yield. Naphtalene as an electron-donating group in **63** produced **63b** in 68% yield. In the absence of an *o*-protecting group, the dihalogenation proceeds to the major products like in using **66** and **67**. This is explained by the periplanar orientation structure of the mono *o*-halogenated 2-arylbenzothiazole which contains sulphur...halide interaction that facilitates *o*-palladation, then a second *o*-halogenation.^[38] Using of 1.5 equiv of the corresponding *N*-halosuccinimide on **66**, dibromination and dichlorination were achieved, giving **66b** and **66c** in 53% and 48% yield, respectively. In the presence of an electron-donating group *p*-Me group, 59% and 51% of the dibrominated **67b** and diiodination **67c** were formed, respectively. On the same molecule **67**, iodination gave 65% yield for **67a**.

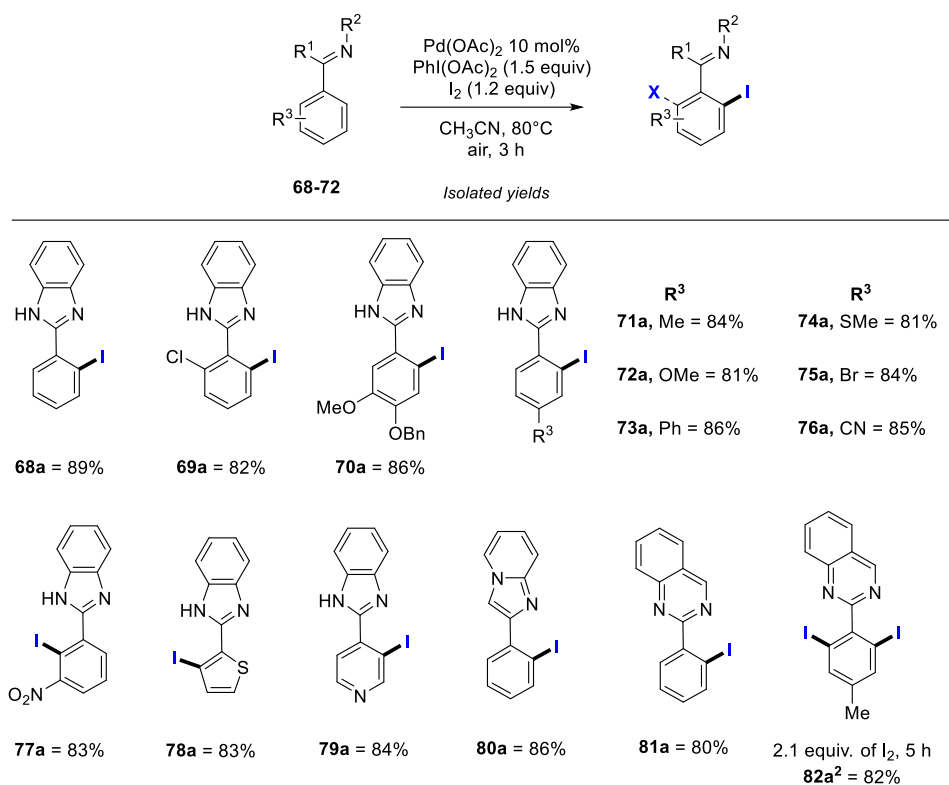


Scheme 12. *N*-directed Pd-catalyzed C–X bond formation on benzothiazole derivatives

H. Benzimidazole, quinazoline and imidazo[1,2*b*]pyridine directing groups

Another report illustrating the use of I₂ as the iodide source was reported by Das *et al.* on benzimidazole, quinazoline and imidazo[1,2*b*]pyridine derivatives (Scheme 13).^[39] One equivalent of

the benzimidazole substrate **68** reacts with 1.2 equiv of I₂, in the presence of 10 mol% of Pd(OAc)₂, and 1.5 equiv of PIDA as the oxidant at 80 °C in acetonitrile for 3 h produced **68a** in 89 % yield.

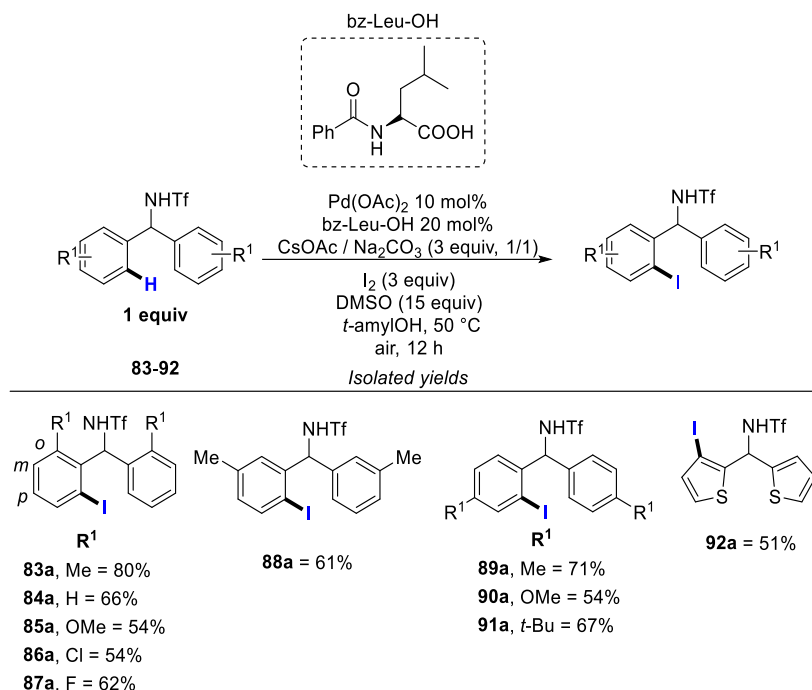


Scheme 13. N-directed Pd-catalyzed C–X bond formation on benzimidazoles and pyrimidines

Using either nucleophilic sources in KI or TBAI produced **68a** in lower yields (11% and 44%) compared to I₂ (89%). The scope of the reaction was performed on benzimidazoles bearing electron-donating (Me, OMe, Ph and SMe) or *electron*-withdrawing substituents (Cl, Br, CN and NO₂) in either the *ortho*-, *meta*- or *para*- positions of the phenyl ring. These groups were tolerated and the iodinated products of **69** to **77** were formed in 81% to 86% yields. With **77**, the iodine was inserted adjacent to a *meta*-NO₂ group. Iodination of benzimidazole substrates incorporating heteroarenes instead of the phenyl group gave **78a** and **79a** in 83% and 84% yield, respectively. 2-Imidazo[1,2*b*]pyridine **80** and phenylquinazoline **81** produced **80a** and **81a** in 86% and 80% yields, respectively. By increasing the I₂ loading to 2 equiv and with a longer reaction times to 5 h, instead of 3 h for the monohalogenation step, produced the diiodinated **82a²** in 82% yield.

I. Diarylmethylamines derivatives directing groups

Similarly to benzimidazole, metal-catalyzed electrophilic halogenation was conducted by Yu *et al.*, using I₂ gas as the iodine source on diarylmethylamine **83** and some derivatives (Scheme 14).^[40]



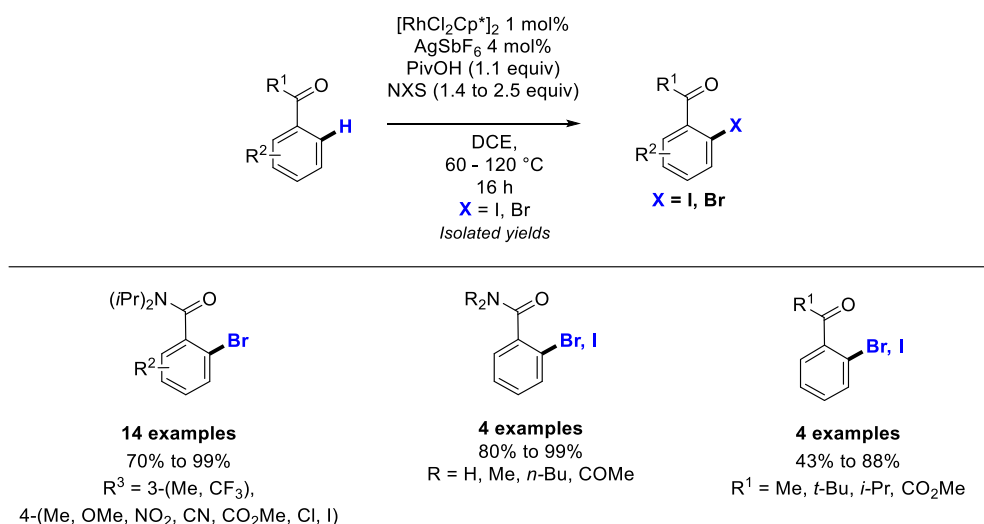
Scheme 14. N-directed Pd-catalyzed C–X bond formation on diarylmethylamine derivatives

Selective monoiodination on diarylmethylamine **83** yielded **83a** in 80% by loading the substrate with 10% Pd(OAc)₂, 3 equiv of I₂, 20% of an amine ligand (bz-Leu-OH), 3 equiv of an equimolar base mixture of CsOAc and Na₂CO₃. The reaction also required the addition of 15 equiv of DMF in *t*-amyl alcohol as the solvent. The reaction was performed under 50 °C and for 12 h. No reaction was achieved without palladium catalyst. On the other hand, substituting bz-Leu-OH with different amino-acid ligands such as Boc-Leu-OH, Boc-Phe-OH, Piv-Leu-OH either inhibited the reaction or produced **83a** in traces or modest amounts (< 30% yield). Removing the bases mixture also stopped the reaction. Different metal acetate (LiOAc, KOAc or NaOAc), carbonate (NaHCO₃, KHCO₃, K₂CO₃ or Cs₂CO₃) and phosphate (Na₂HPO₄, K₃PO₄ or K₂HPO₄) compounds were tested as bases with very little or trace amounts of the product **83a** formed. Surprisingly, loading Na₂CO₃ or CsOAc solely, affected the reaction. Only when these two bases teamed-up as a mixture the reaction proceeded. With the substrate **84** bearing no substituents the iodination occurred in 66% yields. Electron-donating groups (OMe) and electron-withdrawing (Cl and F) were tolerated on the *o*-position, and iodination of the substrates bearing these groups were obtained in 54% to 62% for **85a** to **87a**. When electron-donating (Me, OMe and *t*-Bu)

groups were present on the *meta*- and *para*-positions, the corresponding iodinated products were obtained in 54% to 71% for **89** to **91**. Initiating the reaction with **92**, bearing thienyl groups instead of the phenyl groups also affords the *o*-iodination in 51% yields. The iodination reaction to produce **88a** was performed at gram scale in 67%, consistent with lower scale reaction (61%).

2) Rhodium-catalyzed C–H bond electrophilic halogenation

Glorius *et al.* initiated the study of rhodium catalyzed C–H bond monohalogenation, mainly by using oxygen atoms of benzamides as directing atom (Scheme 15).^[41] Pyridine was used as a nitrogen directing group but only within dihalogenation reactions. The monohalogenation using benzamides derivatives yielded 70% to 99% for bromination from NBS. Few other *o*-directing substrates such as ketones or esters were also tested for the introduction of halogens in 43% to 88% yields.

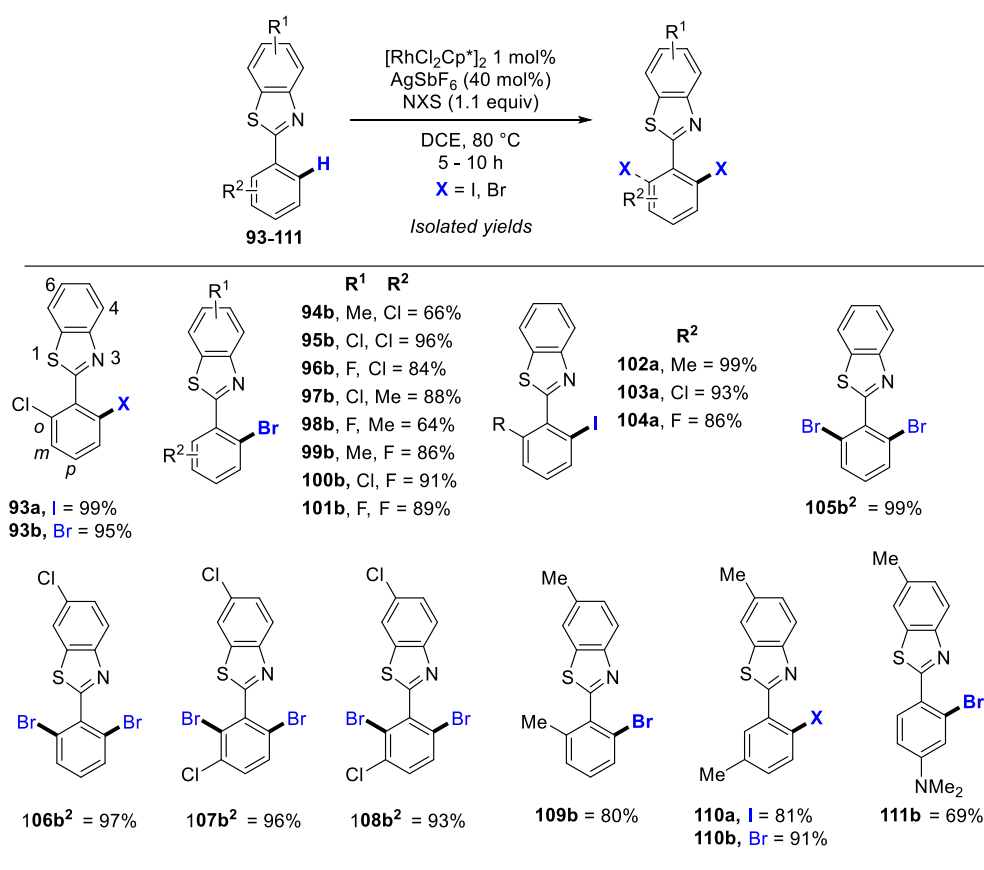


Scheme 15. *O*-directed Rh-catalyzed C–X bond formation on phenylamide derivatives

Cao *et al.* extended the Rh-catalyzed C–H bond halogenation on benzothiazoles under similar conditions. 2-(6-methyl-phenyl)-benzo[*d*]thiazole **93** reacts with 1.1 equiv of *N*-halosuccinimide in the presence of 1 mol% $[\text{RhCp}^*\text{Cl}_2]_2$, 40 mol% of AgSbF_6 , and, under 80 °C in DCE, **93a** was quantitatively produced in 99% yields (Scheme 16).^[42]

The use of *o*-substituted substrates avoids uncontrolled double C–H halogenation that is observed when two identical and reactive C–H bonds are present. The bromination of **93** afforded 95% of the bromine derivative **93b**. In the absence of rhodium catalyst, no reaction was observed. On the other hand, removing the silver salt additive much lowered the yield of the target product (<20%).

Compounds **94-104** were formed in 64% to 99% yields with high tolerance with the donating (CH₃) and withdrawing (Cl or F) groups on either the *o*-position of the phenyl ring and/or the benzothiazole ring. Dihalogenation was also achieved in high yields, ranging from 93% to 99%, with compounds **105-108** by employing 2.1 equiv of NBS. The presence of a *m*-chlorine atom in compounds **107** and **108** does not prevent dihalogenation. Conversely, in compounds **109** to **111** the tertiary amine (or Me group) at the *meta* or *para*-position of the phenyl ring directed the reaction towards the monosubstituted derivatives in 69% to 91% yields. The position of the inserted halogen is on the opposite side of the *m*-substituent of the phenyl ring. Bromination are easier than iodination that showed limitations and were restricted to fewer compounds like **102** to **104** and **105**.



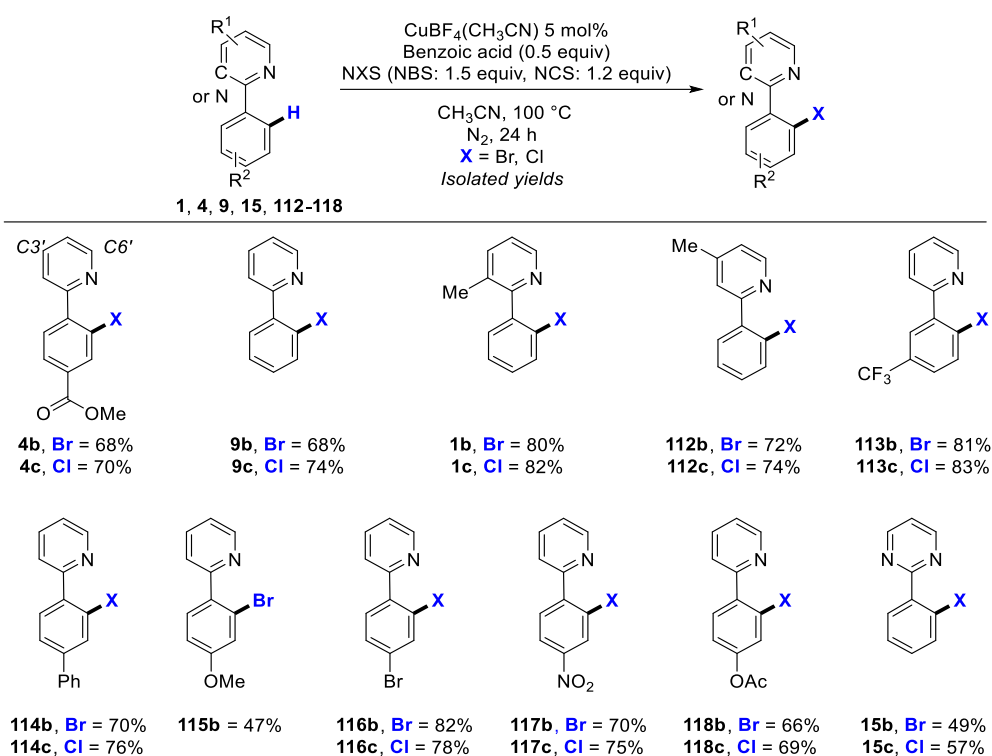
Dihalogenation of **105** to **108** were done with 2.1 equiv of NBS

Scheme 16. N-directed Rh-catalyzed C-X bond formation on benzothiazole derivatives

3) Copper-catalyzed C-H bond electrophilic halogenation

High cost and less abundant palladium and rhodium can be sometimes replaced by cheaper copper catalysts for C-H bond activation in successful arylation and acetoxylation reactions.^[43]

Copper-based C–H bond halogenation reactions are still scarce and the major reactions were presented by Yingjie *et al.* reporting first copper catalyzed C–H bond halogenation of phenylpyridines (Scheme 17).^[44] Methyl 4-(pyridine-2-yl)benzoate **4** was *o*-halogenated using 5 mol% of CuBF₄(CH₃CN) and 0.5 equiv of benzoic acid 1.5 equiv of NBS or 1.2 of NCS, in CH₃CN under 100 °C. Monobrominated **4b** was selectively obtained in 68% yields and monochlorinated **4c** in 70% yield.



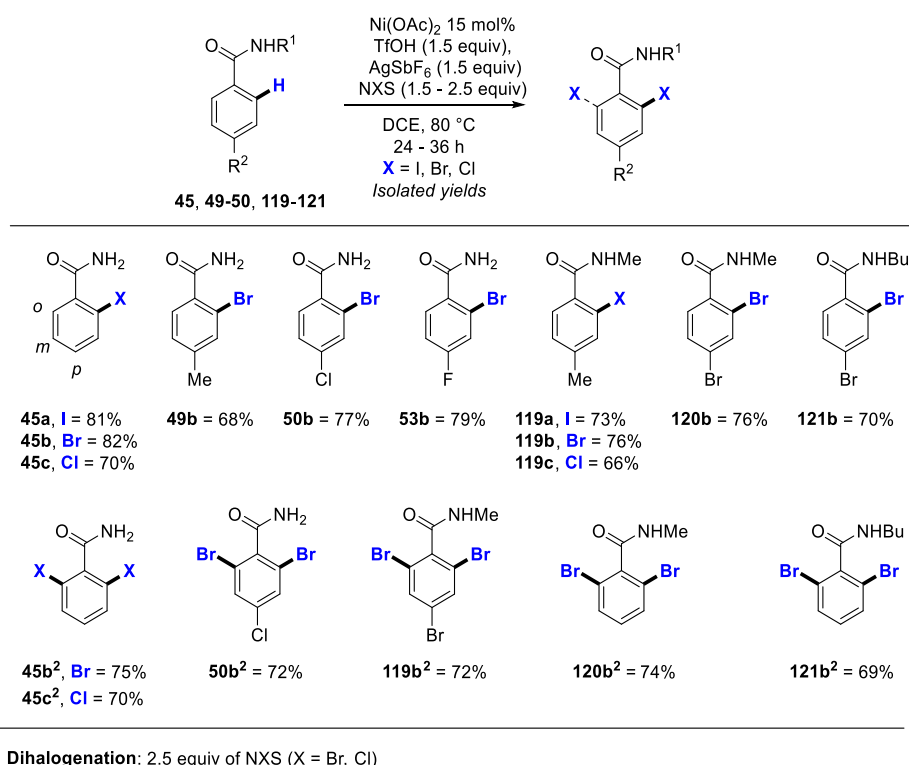
Scheme 17. N-directed Cu-catalyzed C–X bond formation on phenylpyridines and pyrimidines

Cu(II) and Cu(I) catalysts such as Cu(OTf)₂, Cu(OAc)₂, Cu(OAc), and CuPF₆(CH₃CN) were found less effective than CuBF₄(CH₃CN) in the absence of benzoic acid. With CuBF₄(CH₃CN) as the catalyst, and assuming that acyl hypobromite generated *in situ* from carboxylic acid and NBS was more active than NBS, HOAc or benzoic acid were tested as additive, with better success for benzoic acid. A lower loading of NCS in comparison to NBS (1.2 equiv instead of 1.5 equiv), was used to better control the selectivity of mono- and dihalogenation. Iodination with NIS was too fast and uncontrollable and led to major regioselectivity issues. From this protocol, phenylpyridine **9** gave bromination and chlorination in good yields of 68% for **9b** and 74% of **9c** (Scheme 17). With **1** and **112**, where methyl groups are present at C3' and C4' position of the pyridine ring, monohalogenation was obtained between 72% and 82% yields, respectively. Electron-donating groups (OMe and Ph) and electron-

withdrawing groups (Br, NO₂, OAc, CO₂Me and CF₃) were tolerated at the *m*- and *p*-positions, giving yields of 47% to 83% with substrates **113** to **118**. Substituents positioned in *m*-position helped for selectivity towards monohalogenation (compared to *p*-substituents) due to the proximate steric hindrance for compound **113**. With the phenylpyrimidine **15**, halogenation was reported in moderate yields of 49% and 57% for bromination and chlorination, respectively for **15b,c**. A major effect of the counter anions at the cationic copper catalysts was observed. Using non-coordinating anions, such as PF₆⁻ and BF₄⁻ as counter ions improved the reactivity toward halogenation because the anion may accelerate the reductive elimination from Cu(III) centers to form Cu(I) species.^[45] The possible formation of a bimetallic complex hypothetically affected the regioselectivity, and thus dihalogenation would decrease the yield of monohalogenated products.

4) Nickel-catalyzed C–H bond electrophilic halogenation

In 2013 Cai described the C–H bond electrophilic halogenation of benzoamide derivatives (Scheme 18).^[46] Monohalogenation of the amide **45** was achieved in the presence of 15 mol% Ni(OAc)₂, 1.5 equiv of the *N*-halosuccinimide NXS (X = I, Br, Cl), AgSbF₆ and TfOH as additives under 80 °C in DCE. Brominated **45b** was formed in 82% yield.

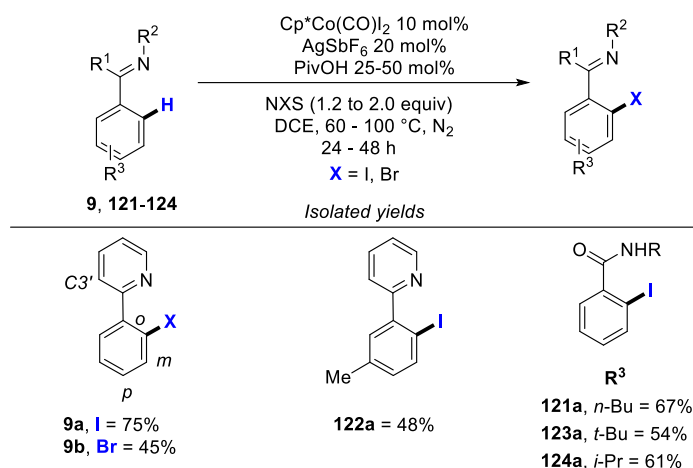


Scheme 18. N-directed Ni-catalyzed C–X bond formation on phenylpyridine derivatives

Without Ni(OAc)₂ catalyst the *m*-substituted product was exclusively formed through SEAr. In the presence of Ni(OAc)₂ in less than 15 mol%, the desired *o*-halogenated products are formed together with in majority the SEAr product. The addition of AgSbF₆ silver salt and TfOH improved the *N*-directed C–H halogenation. The iodine and chlorine derivatives **45a** and **45c** were obtained in 81% and 70% yields, respectively. Halogenation was illustrated with **45**, **49**, **50**, **119** to **121** in yields ranging between 68% and 79%, tolerating different groups: electron-donating (Me) and electron-withdrawing (F, Br, Cl), albeit mostly for bromination. The presence of alkyl donating groups on the directing nitrogen increase the coordination efficiency of this directing group, and facilitates the production of all three halogen derivatives **119a-c** (66% to 76%). Dihalogenation of **45**, **50**, **119**, **120** and **121** was also achieved by increasing the reaction time to 36 h and the amount of the halogen sources to 2.5 equiv. The amide **45** tolerated bromination from bromide and chloride in 75% and 70% yield, respectively. Diiodination seemed difficult owing to the larger size of the iodine that prevents two halides to be inserted in the presence of a proximate amino group. Compounds **50**, **119**, **120** and **121** tolerated bromination with resulting products obtained in 69% to 74% yield.

5) Cobalt-catalyzed C–H bond electrophilic halogenation

The groups of Kanai and Matsunaga reported C–H bond activation through Co(III)-catalysts for the formation of C–C and C–heteroatom bonds (oxygen and nitrogen). However, halide insertion using such systems was not performed.^[47] Focused on phenylpyridines and amides as directing groups, the group of Glorius reported the first Co-catalyzed C–H bond halogenation reactions (Scheme 19).^[48]



Scheme 19. N-directed Co-catalyzed C–X bond formation on phenylpyridines and amides

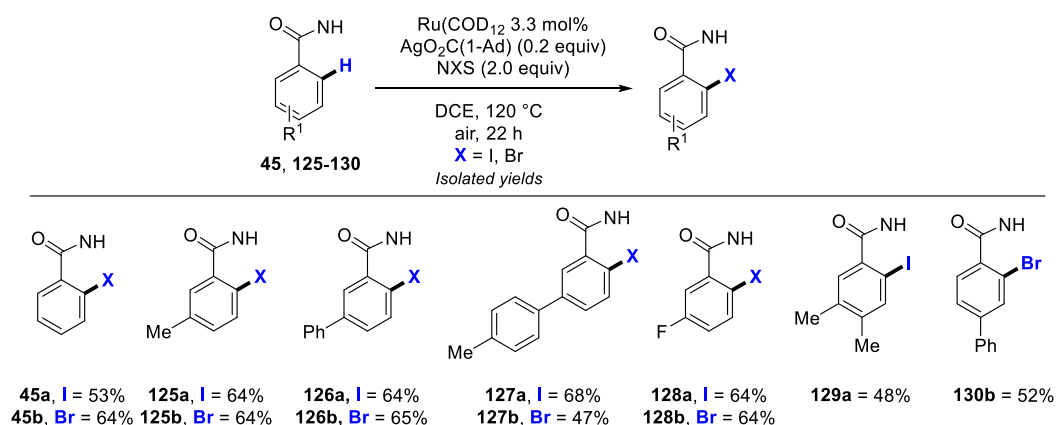
The complex $\text{CoCp}^*(\text{CO})\text{I}_2$ catalyzed the reaction between one equiv of **9** and 1.2 equiv of *N*-halosuccinimides in the presence of two additives: 20 mol% AgSbF_6 and 25-50 mol% PivOH under 60-100 °C in DCE under N_2 for 24 to 48 h, monohalogenation was selectively achieved. For example, iodination on **9** affords **9a** in 75% yield. Bromination to reach **9b** was achieved in 45% yield. The scope with this system is limited for other substrates and halogen insertions. Moreover, PivOH was required for the reaction. Methylated compound **122** only produced the brominated product in 48% yield. On the other hand, benzamides **121**, **123** and **124** afforded their corresponding iodinated products in yields ranging from 54% to 67%. The roles of the acid additive and silver salts might be the activation of NXS reagent through its protonation, increasing its electrophilicity. C–H halogenation with Co(III)-catalyst is still at its early stages. For such cobalt-based systems and directing groups, the yields limitation, the lack of general conditions, the limitations to certain halogens, and the selectivity in mono- and dihalogenation altogether leave a large room for improvement.

6) Ruthenium-catalyzed C–H bond electrophilic halogenation

Different ruthenium complexes have been identified as powerful catalysts for the oxidative transformation of C–H bonds into C–C,^[49] C–O,^[50] or C–N^[51] bonds. Ackermann *et al.* described the first transformation of C–H bonds to C–X bonds. For this purpose, benzamide and its derivatives were studied as substrates (Scheme 20).^[52] For selective mono halogenation, 1 equiv of benzamide **45** reacts with two equiv of NBS, 3.3% of the $\text{Ru}_3(\text{COD})_{12}$, 20% of $\text{AgCO}_2(1\text{-Ad})$ as an additive under 120 °C, for 22h and produced the *ortho*-brominated benzamide **45b** in 64%. Without the catalyst or the additive, no products were detected. The addition of certain silver (AgCl , Ag_2CO_3 , AgSbF_6), potassium (KPF_6) and

CsOAc additives proved to be inefficient as **45b** was produced in low yields (<30%). Other additives, used in 2 equiv, such as AgCO₂CF₃, AgOAc, PivOH, 1-AdCO₂H were more efficient and produced **45b** in 41% to 58% yields yet slightly lower than with the use of AgCO₂(1-Ad) (64%).

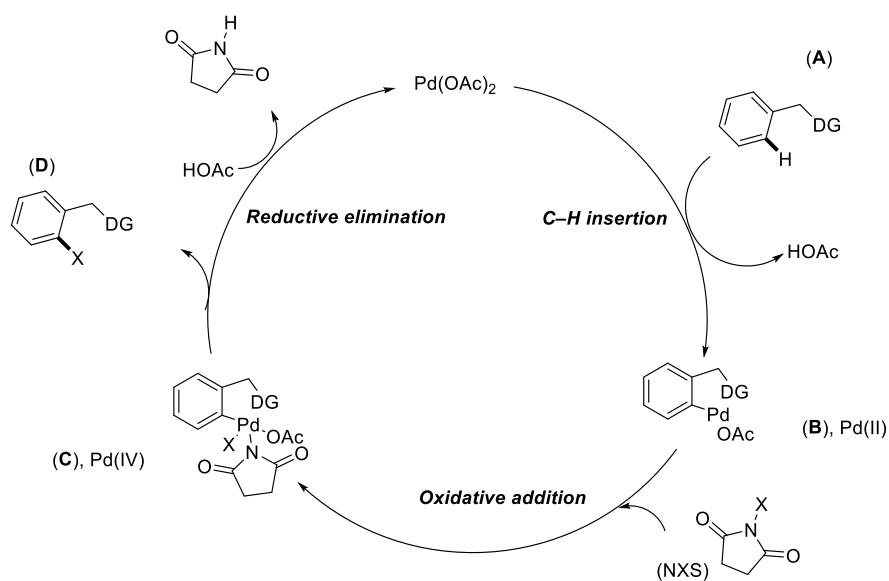
The scope of the reaction was done on various benzamides derivatives **125** to **130**. Iodination on unsubstituted benzamide **45** was afforded in 53% yields. The halogenation of substrates **125** to **127** and **127** with bulky *m*-substituents, such as Me or Ph, afforded the iodination and bromination products on less hindered C–H bond in 64% to 68%, except for the bromination of **127**, which was obtained in 47%. In contrast, in the presence of smaller *m*-fluorine groups, the reaction occurs on the adjacent position to the fluorine group, in 64% for both halogens. With *p*-substituted compounds **129** and **130**, iodination and bromination were achieved in 48% and 52%, respectively. The lower yields with *p*-substituted molecule were due to the increase of dihalogenation products in the presence of two equivalents of the halogen source.



Scheme 20. N-directed Ru-catalyzed C–X bond formation on phenylamide derivatives

7) Mechanism proposed for the electrophilic Pd-catalyzed C–H bond halogenation

From the use of electrophilic halogen sources an example of the global mechanism generally proposed (in a first approach) is presented in Scheme 21, with Pd(OAc)₂, NXS as the halogen source and a suitable directing group.^[53]



Scheme 21. Proposed mechanism for the electrophilic Pd-catalyzed C-X bond formation

The catalytic cycle starts with the C-H insertion of Pd(OAc)₂ with oxidation state +2 [Pd(II)] into the substrate of interest **A** to give **B** with the abstraction of one acetate from the catalyst and the activated hydrogen in the form of HOAc. Oxidative addition of NXS occurs on **B** to give the Pd(IV) species in **C**. Reductive elimination terminates the cycle by producing **D** as the product of interest. The succinimide on the Pd abstracts the hydrogen from the previously produced HOAc and is released to the medium. Finally, the free OAc⁻ in the medium restores the Pd(OAc)₂ catalyst which was first employed.

Overall, huge advancement in terms of substrates and metal compatibility has been realized with *N*-directed C-H bond halogenation using electrophilic halogen sources. This field has been mostly dominated by palladium catalysis, particularly Pd(II)-based catalysts and fewer examples presented with other transition metals such rhodium, copper, cobalt, nickel and ruthenium. The most studied substrates were phenylpyridine and its derivatives. Other substrates such benzamides, benzothiazoles, phenylpyrimidine and pyrazoles were also compatible with several metals. This method mainly presented efficient insertion of different halogens such as I, Br and Cl. Iodination and bromination reactions were found to be more efficient and the access to C-I or C-Br bonds from C-H bonds was found to be a lot smoother than C-Cl with many substrates. Despite this significant advancement, C-H bond halogenation reactions utilizing electrophilic halogen sources still suffered from the use of toxic reagents such as *N*-halosuccinimides and halogen gases and the need to block *o*-positions to avoid concurrent dihalogenation. Metal halide halogen sources such as sodium,

potassium, and other readily available metal halides, and other nucleophilic halogen sources, were studied as potential sources of halogen for better reactivity.

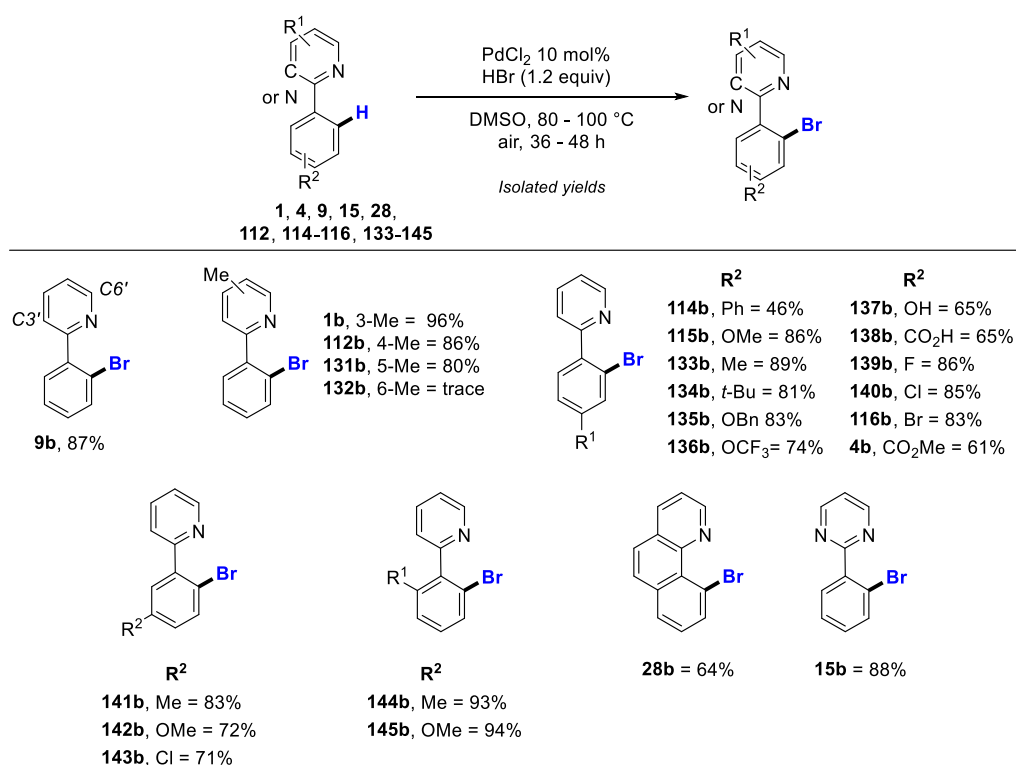
III. Nitrogen-directed C–H bond halogenation using nucleophilic halogen sources MX (M = Ca, Na, K, H and X = I, Br, Cl).

1) Palladium C–H bond nucleophilic halogenation

A. Phenylpyridine, pyrimidine and benzoquinoline directing groups

Palladium-catalyzed C–H bond activation reactions directed by phenylpyridine groups in the presence of “nucleophilic” halogen sources are quite rare in comparison to the electrophilic approaches above-described, and are generally focused on bromination. Jiao *et al.* recently published the monobromination of *N*-directing group arylpyridines (Scheme 22).[†]

^{54]} Starting from 1 equiv of phenylpyridine **9**, with 10 mol% PdCl₂ loading, 1.2 equiv of HBr reacted in DMSO at 80-100 °C for 36 h to 48 h, afforded **9b** in 87% yield. In this reaction, DMSO acts both as an oxidant and solvent.



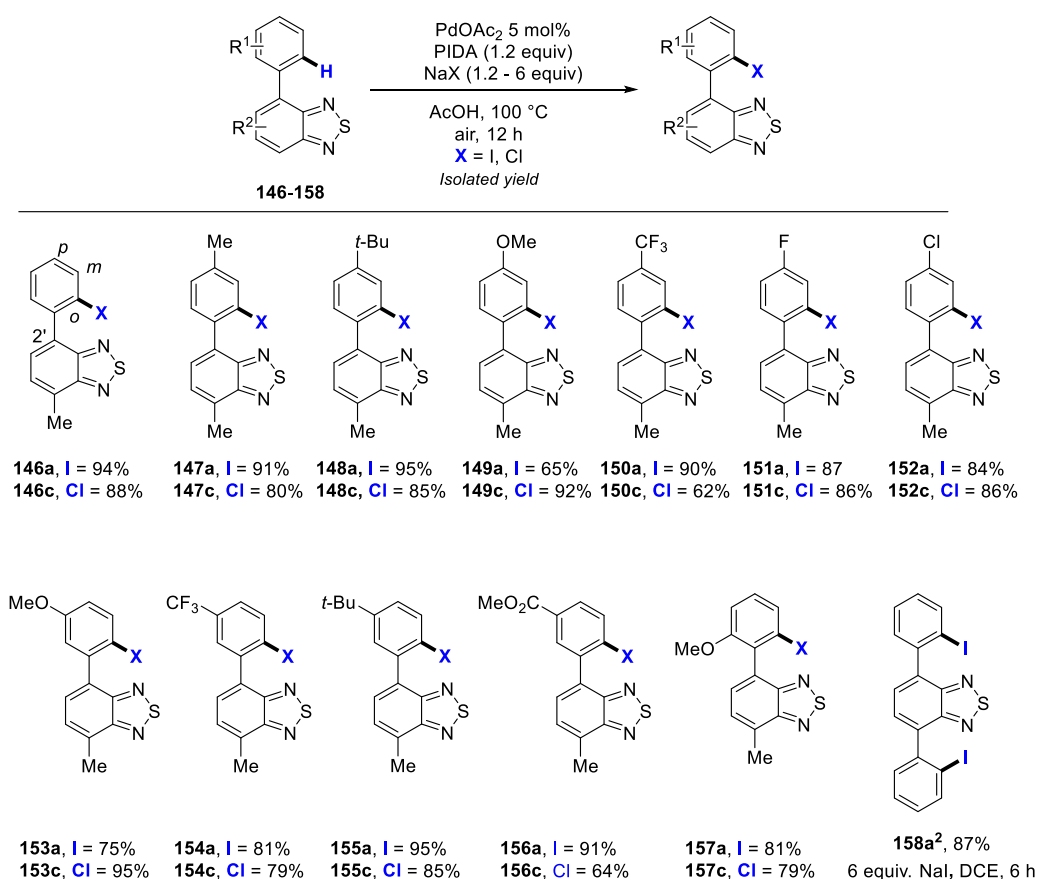
Scheme 22. *N*-directed Pd-catalyzed C–X bond formation on different phenyl heteroarenes

The reaction was tested using 1.2 equiv of DMSO as an oxidant and PdBr₂ in DMF as solvent, and the product **9b** was obtained in only 16% yield. Increasing the amount of DMSO enhanced the production of **9b** to 82%. DMSO is the main oxidant even in the presence of O₂ from air. The reaction was extended to compounds **1**, **4**, **9**, **15**, **28**, **112**, **114-116**, **130**, **131** and **145** (Scheme 22). Methyl groups were tolerated on all the positions of the pyridine ring except the position C6'. The halogenation of these products **1**, **112**, **131** and **132** were achieved in yields ranging between 80% to 96%. When the methyl group is closer to the directing-nitrogen, the reaction yield decreased. Functional groups on the *para*-position are well-tolerated, including electron-donating (OMe, Me, *t*-Bu, Ph, OH and OBn) and electron-withdrawing (F, Cl, Br, CF₃ and COOH) groups in **133** to **140**, furnishing 61% to 89% yields, with apparently little effect of the substituent. Compound **114b** only was produced with a lower 46% yield. Phenylpyridine substrates **141** to **145** with donating (Me, OMe) and withdrawing (Cl) functional groups on the *ortho*- or *meta*-positions are well tolerated and produced halogenated derivatives in yields ranging between 71% and 94%. The yields for bromination with *o*-substituents in **144b** and **145b** were considerably higher than their *meta* counterparts (**141b** to **143b**). The scope of the reaction extended to benzoquinoline **28** and phenylpyrimidine **15** in 64% and 88% yield, respectively.

B. Benzothiadazole as directing groups

The C–H bond functionalization on *o*-position of benzothiadiazole **146** and its derivatives, potentially achieved through less-favoured six-membered palladacycles, was found fairly challenging (Scheme 23). Benzothiadiazoles incorporate several accessible acidic C–H bonds and two nitrogen atoms as potential coordinating groups, in addition to the sulphur atom (Scheme 23).^[55] Benzothiadiazole **146** has a blocking methyl group at the *p*-position of the phenyl group attached to the fused cycles, which leaves two positions for *N*-directed C–H bond activation. From 1 equiv of 4-methyl-7-phenyl-benzothiadiazole **146**, 5 mol% of Pd(OAc)₂, 1.2 equiv of NaI, 1.2 equiv of PIDA, in HOAc under 100 °C, **146a** was formed in 94% yield. DCE, toluene, acetonitrile and acetic anhydride were also tested as solvents, but produced lower amounts of monohalogenated products. Employing KI or the electrophilic NIS produced **146a** in yields of 80% and 82% for **146a** with KI and NIS, respectively; yet lower than using NaI (94%). Chlorinated **146c** was obtained in 88% yield. The monoiodinated and monochlorinated derivatives of **147** to **152** were formed with good tolerance for electron-donating (Me, *t*-Bu and OMe) and electron-withdrawing (F, CF₃ and Cl) groups on the *p*-position of the peripheral phenyl ring. The formation of **147** to **152** and **153** to **156** illustrated the substrates bearing electron-donating and electron-withdrawing groups on the *meta*- or *ortho*-positions of the peripheral phenyl ring, respectively. The yields obtained ranged from 75% to 95%,

except for chlorination or iodination of **149a** (65%), **150c** (65%) and **156c** (64%). The change of the *p*-methyl group by a phenyl group, opens the access to four C–H bond accessible for C–H activation/functionalization. Thus, **158a**² is preferentially formed from the use of six equiv of NaI in DCE, in 87% yield. Dichlorination was not achieved, and bromination reactions with NaBr or any nucleophilic halogen source, failed while electrophilic NBS efficiently achieved monobromination.

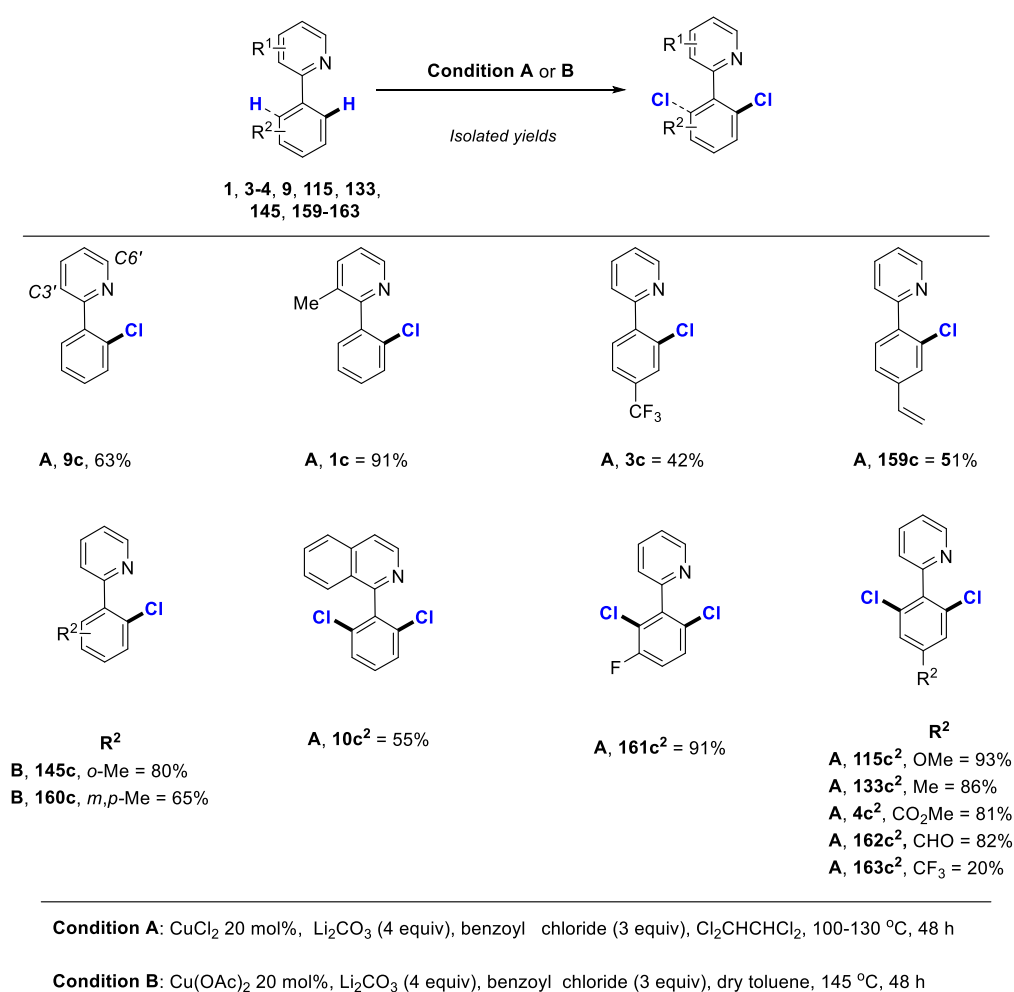


Scheme 23. N-directed Pd-catalyzed C–X bond formation on benzothiadazole derivatives.

2) Copper catalyzed C–H bond nucleophilic halogenation

In 2006, Yu *et al.* realized the *ortho*-halogenation of phenylpyridine **9** and its derivatives. This group employed 1,1,2,2-tetra-haloethane as both the solvent and the halogen source, in the presence of the Cu(II)-catalysts, CuCl₂ or Cu(OAc)₂ (Scheme 24).^[56] However, one main difficulty was overcoming the problem of obtaining both mono- and dihalogenated products. For this purpose, the group of Cheng proposed acyl halides as a replacement for halogenated solvents, but were not able to overcome the selectivity issues. Moreover, only chlorine was successfully inserted in a copper catalyzed C–H bond halogenation reaction using phenylpyridines as substrates and acyl chlorides as the chlorine source

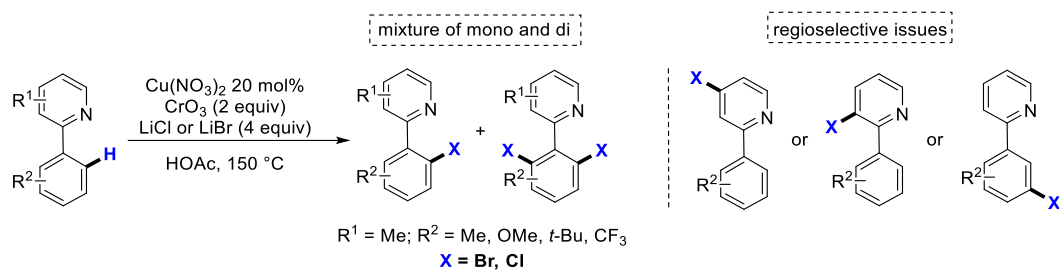
(Scheme 24).^[57] This group adopted two different conditions for selective mono chlorination. For 1 equiv of *p*-substituted phenylpyridines **1**, **3**, **9**, **159**, 20 mol% of CuCl₂, benzoyl chloride (3 equiv) and Li₂CO₃ (4 equiv) were added in C₂H₂Cl₄ at 130 °C for 48 h. The chlorinated derivatives **1c**, **3c**, **9c**, **159c** were obtained in 42% to 91% yields. On the other hand, for *o*-substituted derivatives **145** and **160**, monohalogenation occurred in the presence of 20 mol% of Cu(OAc)₂, and dry toluene were required instead of CuCl₂ and tetrachloroethane. Compounds **145c** and **160c** were obtained in 55% and 91% yields, respectively. For all other substituted phenylpyridines **4**, **10**, **115**, **133**, **161** to **163** dichlorination was achieved in 20% to 93% yields (Scheme 24), using CuCl₂ as the catalyst in the conditions [a].



Scheme 24. N-directed Cu-catalyzed halogenation of phenylpyridine derivative

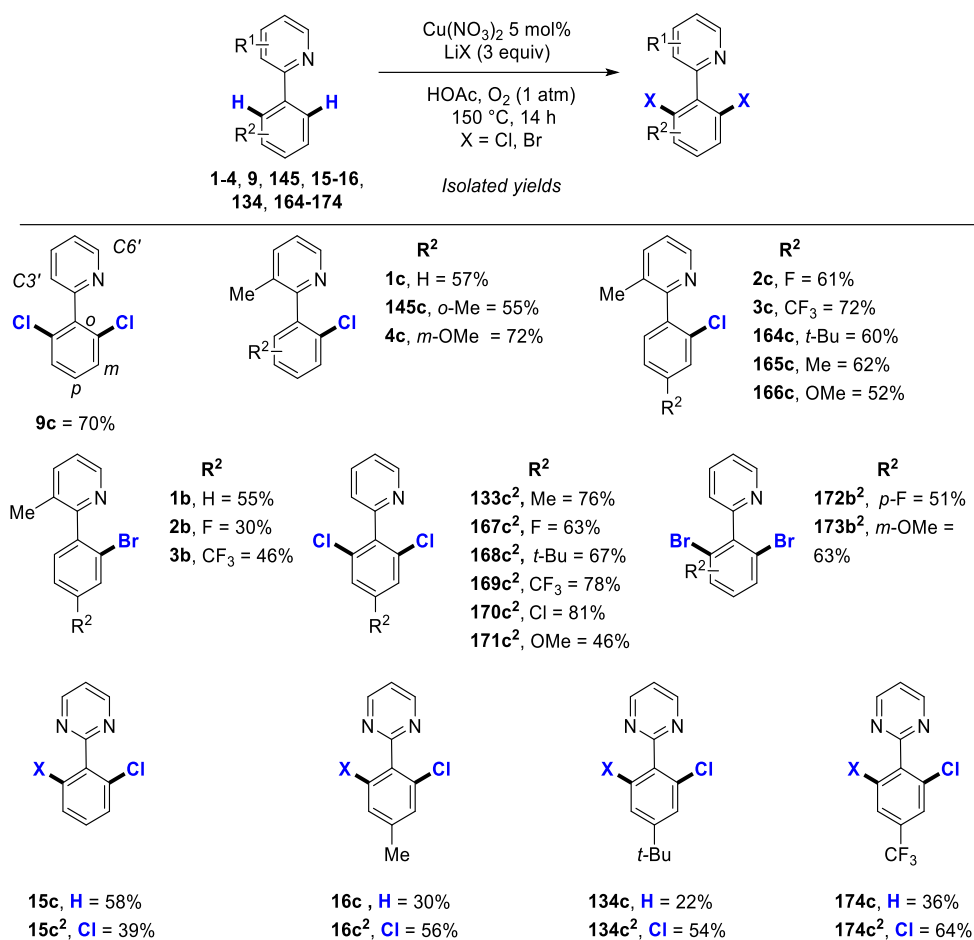
The problems of regioselectivity, low control of the reaction, and narrow substrate scope also appeared in the first work by Shen et al.,^[58] where they used lithium halide salts as halogen sources, Cu(NO₃)₂ as the catalyst, HOAc as additive and CrO₃ as the oxidant. Stoichiometric amounts of the

halide salts were required for good conversion of the reaction. These amounts lead to the production of a mixture of mono- and di- halogenated products. Moreover, halogenation on undesired positions on the pyridine ring or either the *meta*- or *para*- positions of the phenyl group also occurred (Scheme 25).



Scheme 25. N-directed Cu-catalyzed C-H bond halogenation of aryl pyridine derivatives

The same group overcame the regioselective issues by replacing CrO_3 by dioxygen as the oxidant. Starting from *o*-C-H bonds on phenylpyridine, lithium halide salts as halogen sources, $\text{Cu}(\text{NO}_3)_2$ as the catalyst, HOAc as additive and O_2 , C-Cl and C-Br bonds were successfully formed (Scheme 26).^[59]



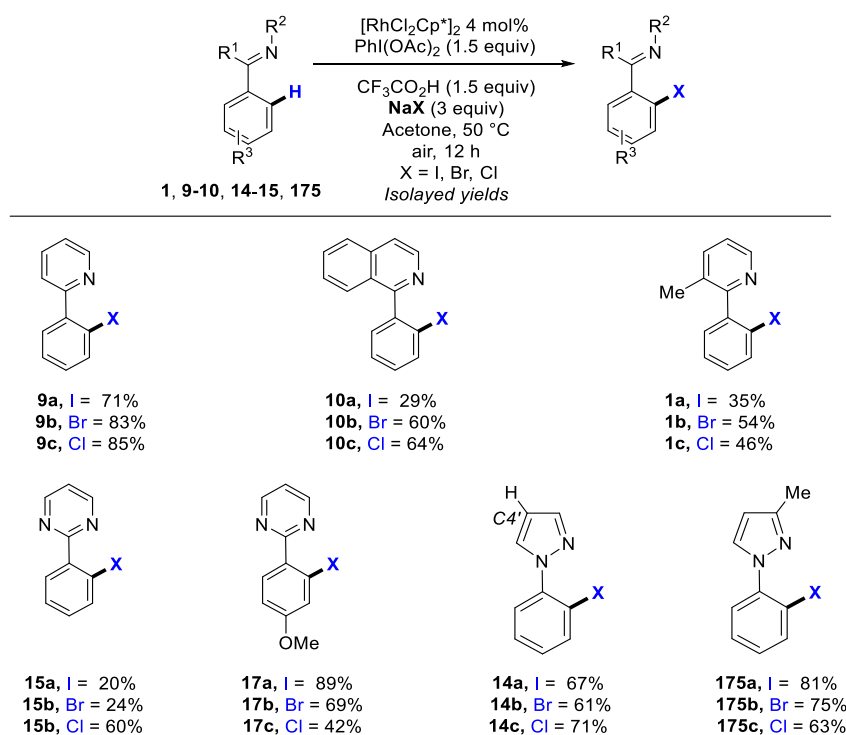
Scheme 26. N-directed Cu-catalyzed C–X bond formation on phenylpyridine and pyrimidine derivatives

Yet, on phenylpyridine **9**, monochlorination was hard to selectively achieve. Dichlorination was targeted instead and 20% of Cu(NO₃)₂ were employed with 3 equiv of LiCl in acetic acid, and in the presence of O₂ (1 atm) under 150 °C for 14 h to give the dichlorinated **9c²** in 70% yield. Several copper catalysts were tested. The loading of Cu(OH)₂, CuSCN, CuCl₂, Cu(acac)₂, CuCN and CuSO₄ in 20 mol% produced **9c²** in yields ranging from 27% to 66%. However, a longer reaction was required, 32 h to 96 h instead of 14 h for Cu(NO₃)₂. Steric effects were needed to achieve selective monohalogenation. This was achieved by employing blocking or bulky groups on the C3' of the pyridine ring or the *ortho*- and *meta*-positions of the phenyl ring. Monochlorinated derivatives **1c**, **4c** and **145c** were afforded in 55% to 72% yields. Phenylpyridine derivatives lacking C3' or *ortho*-substituents on the pyridine or phenyl ring afforded both their mono halogenation, and dihalogenation products. Dichlorination was obtained from substrates **2**, **3**, **164** to **166** in 52% to 72% yields. Fewer examples were presented on monobromination. Substrates **1**, **2** and **3**, containing blocking methyl group on the C3' position of the pyridine ring produced their corresponding mono brominated products in 55%, 30% and 46% for **1b**, **2b** and **3b** respectively. Abstraction of the methyl group from the pyridine group leads to dichlorinated

and dibrominated products. Substrates **133**, **167** to **171** afforded their dichlorinated products **133c²**, **167c²** to **171c²** in 63% and 81% yields. Dibromination was done on **172** and **173** in 51% and 63% for **172b²** and **173b²** respectively. The halogenation was extended to phenylpyrimidines **15**, **16**, **134** and **174**. Phenylpyrimidines showed less practical reactions, in comparison to phenylpyridines, since each substrate systematically afforded a mixture of mono- and dihalogenation products in yields ranging from 22% to 58% (Scheme 26, bottom).

3) Rhodium-catalyzed C–H bond nucleophilic halogenation

The rhodium-catalyzed bromination and iodination of arenes with electrophilic halogen sources NBS and NIS,^[60] were found limited by: *a*) using reactive *electron*-rich substrates and expensive electrophilic halogenating reagents (*i. e.* iodobenzene dichloride (PhICl₂), *N*-halosuccinimides) *b*) being suited for only one or two types of C–H bond transformations, and *c*) resulted often in the formation of a mixture of mono- and dihalogenated products. For less expensive nucleophilic reagents, Wang *et al.* developed a Rh(III)-based system for *N*-directed catalytic C–H halogenation with phenylpyridine **9** (Scheme 27).^[61] One equiv of **9**, 4 mol% of [RhCl₂Cp*]₂, 3 equiv of the sodium halide NaX, 1.5 equiv of PIDA and CF₃CO₂H as the oxidant, reacted for 12 h at 50 °C in acetone to produce **9a** in 71% yield.



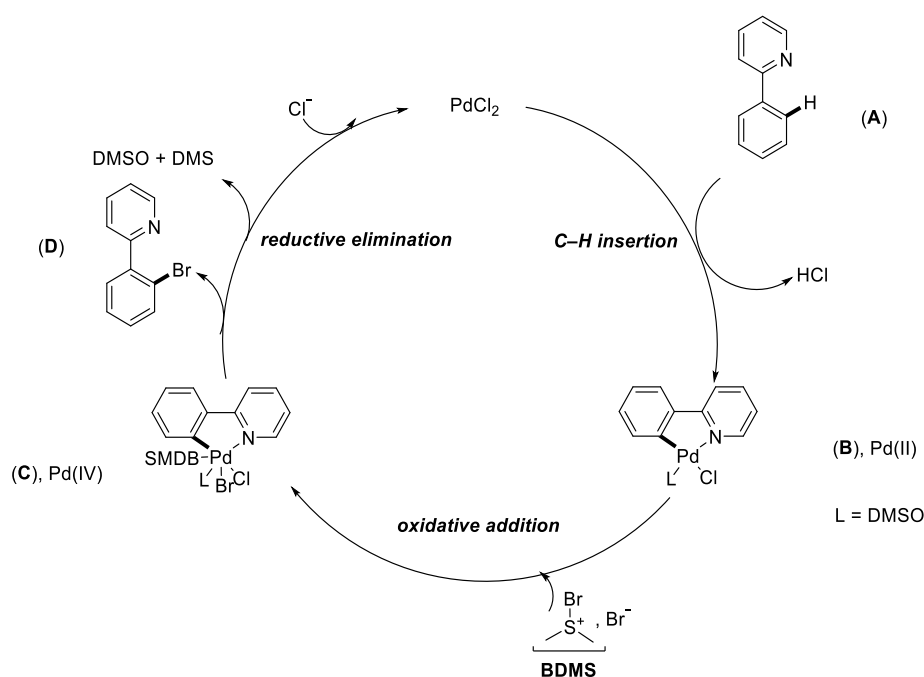
Scheme 27. *N*-directed Rh-catalyzed C–X bond formation on phenylpyridine, pyrimidine and pyrazole derivatives

By using di-*tert*-butyl peroxide and *tert*-butyl hydroperoxide as oxidants lower amounts of **9a** <40% were obtained. Bromination and chlorination provided **9b** and **9c** in 83% and 85%, respectively. 2-Naphthylpyridine **10** was also compatible with C–H halogenation to yield **10a-c** in 29% to 64% yields with the iodination occurring in 29%. The reaction with 3-methyl-2-phenylpyridine **1**, yielded the compounds **1a** in 35% yield, **1b** in 54%, **1c** in 46% from *o*-C–H iodination, bromination and chlorination, respectively. From unsubstituted phenylpyrimidine **15**, iodinated **15a** was obtained in 20% yield and brominated **15b** in 24% yield, and 60% for chlorinated **15c**. When using phenylpyridimines with a OMe *p*-donating group **17**, the reaction yields were enhanced for iodination and bromination, respectively 89% for **17a**, 69% for **17b**, and 42% for **17c**. The use of sodium halides in less than 3 equiv lead to low conversions even after 12 h, while utilizing 3 equiv of the halogen source increase the dihalogenation process. Phenylpyrazoles **14** and **175** provided halogenated products in 61% to 81% yields. Low amounts of electrophilic C4'–H bond activation also occurred on the directing group of phenylpyrazole **14**.

4) Mechanisms proposed for C–H bond halogenation using nucleophilic halogen sources

From the use of nucleophilic halogen sources, examples of the global mechanisms proposed in a first approach are presented in Schemes 28 and 29. The mechanistic studies showed that there are similarities in the major steps. C–H insertion is followed by oxidative addition and reductive elimination terminates the cycle. However, further additives are used due to the need to produce the active halogen source that can perform oxidative addition during the cycle. The groups of Jiao and Glorius presented different pathways to give active reactive halogen sources produced *in situ* and with different metals.

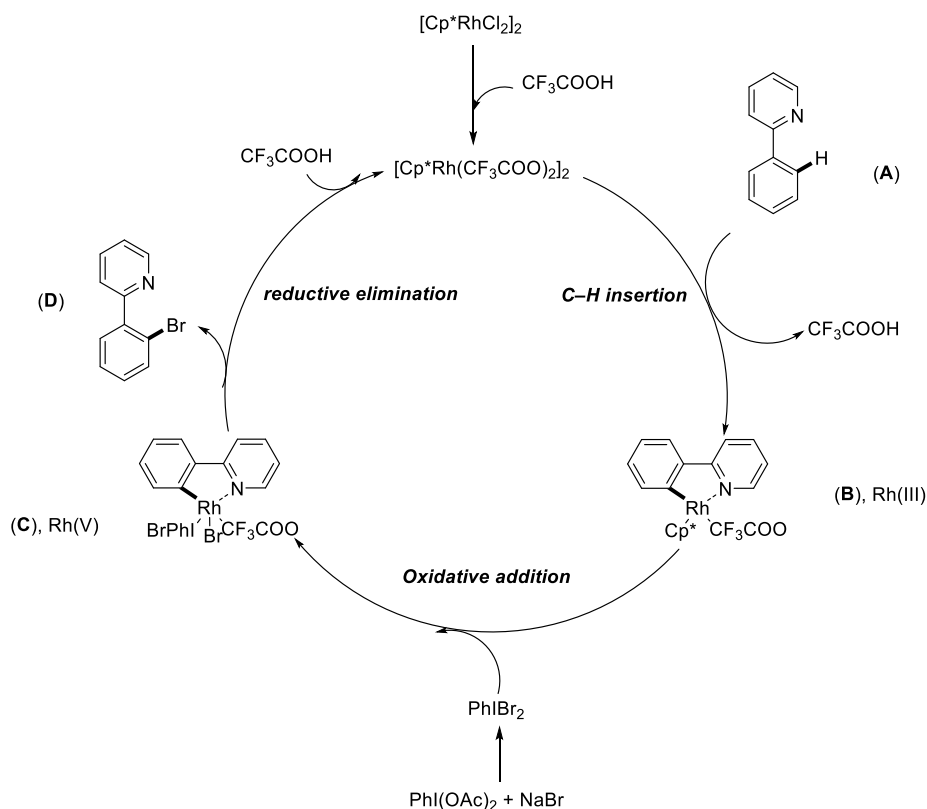
The mechanism presented by the group of Jiao for palladium-catalysis is illustrated with phenylpyridine **A** (Scheme 28).^[45] It starts with C–H bond insertion of the PdCl₂ into **A** to give the metallacycle complex **B**. Oxidative addition of the halogen source formed *in situ*, (BDMS⁺, Br⁻) gives the Pd(IV) species **C**. It is believed that in the acidic environment, DMSO oxidizes the Br⁻ to BDMS, Br which then becomes the halogen source.^[62] Reductive elimination produces the desired product **D** and the anionic Cl⁻ reenters the cycle and restores the initial catalyst PdCl₂.



Scheme 28. Proposed mechanism for the Pd-catalyzed halogenation using nucleophilic halogen sources

For rhodium-catalysis, similarly to palladium catalyzed reactions, the additives play a crucial role in directing the catalytic cycle, which is also presented with phenylpyridine **A** as substrate (Scheme

29).^[51] First, the added CF_3COOH replaces the two chlorines present in the $[\text{RhCl}_2\text{Cp}^*]_2$ to produce the active catalyst $[\text{Cp}^*\text{Rh}(\text{CF}_3\text{COOH})_2]_2$ and HCl . C–H Insertion occurs to give **B** and releases CF_3COOH . The other additive $\text{PhI}(\text{OAc})_2$ interacts with NaBr to produce PhIBr_2 . Oxidative addition of PhIBr_2 into **B** give **C**. Finally, reductive elimination gives the desired product **D**. Initially, in the catalyst used the rhodium has a +3 formal oxidation state which stay identical after C–H insertion and abstraction. Oxidative addition gave Rh(V) in **C** while Rh(III) is restored after reductive elimination.



Scheme 29. Proposed mechanism for the Rh-catalyzed halogenation using a NaBr nucleophilic halogen sources

Overall, transition metal-catalyzed C–H bond halogenation on *N*-containing molecules using the directing abilities of donor-atoms on the heteroaryl has been investigated with Pd, Rh, Cu, Ni, and Co-based catalytic systems. The reported methods might be roughly divided into two categories, depending on the nature of the halogen source used: reactions based on electrophilic halogen sources, like mostly *N*-halosuccinimides, are opposed to nucleophilic halogen sources such acid halides and metal halides based on sodium, calcium, etc. Each type of halogen source requires different conditions for better efficiency. For the electrophilic halogenation reaction acidic additives such *p*-TSA, TsOH or TFA were used. Possibly, the acid initially reacts with the halosuccinimides to

produce more reactive sources of X^+ that generally increases the rate and improve the yield of the halogenation. Regarding the catalytic loading, metal is generally used between 5% to 10%. Mono- and di-halogenation were examined, and for limiting undesired halogenation the pre-functionalization of the substrates either at *ortho*-position or in the adjacent *meta* or distal *para*-position was mostly reported.

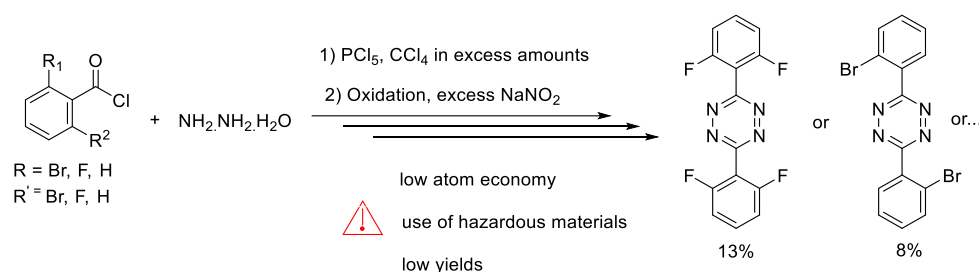
Cobalt and nickel catalysts are being considered as possible replacements for more expensive metals such as palladium and rhodium, an interest that is due to their abundance and cheap prices, but their systems still suffer from narrow scope and lower yield. While nickel(II) catalyzed bromination is developed, chlorination was illustrated with very few examples, and the iodine C–H insertion was unsuccessful. Cobalt(III)-catalyzed halogenation required the use of both an acidic additive and silver salt in high amounts, probably as halide attractor. Yet, the yields remained moderate for bromine and chlorine C–H insertion.

The cheaper nucleophilic halogen sources were taken into consideration for new catalytic and main transition metals halides were tested with palladium, rhodium and copper metals. The presence of an oxidant and oxygenated solvents in this system is needed since the oxidant allows transitioning from Pd(II) to Pd(IV). As an oxidant, PIDA may play another role in transforming the metal halide halogen source into a hypervalent halogen source $PhI(OAc)(X)$ ($X = I, Br, Cl$), which is more reactive than the metal halide, and in many instances such transformation was needed to the reaction, especially with palladium. Oxygenated solvents assist the oxidant or even act as oxidants themselves (DMSO). Acetic acids, DMSO and acetic anhydrides (Ac_2O) all allowed the catalytic systems to work efficiently. Regarding the selectivity of the insertion, the same trends were used to favour the production of monohalogenated products. A notable advantage of using nucleophilic halogen sources is the variety of salt couples (Li, Na, K, Cs with I, Br, Cl and F, etc.) that remains to be studied for such reactions, as a function also of the desired direct groups and substrates.

IV. Results and discussion: *Nitrogen*-directed C–H halogenation of *s*-aryltetrazines

1) Screening of the conditions for the iodination of 3,6-bis(2-fluorophenyl)-1,2,4,5-tetrazine

Tailored aryl tetrazine framework is classically derived from the Pinner-like synthesis using hydrazine derivatives with either cyanoaryl or chlorobenzoyl co-reagents (Scheme 30). Such procedure involves the use of toxic reagents and suffers from low yields of the desired product. Moreover, because of sterics and its multistep pathway under harsh conditions, this synthesis failed to give efficient access to functionalized *s*-tetrazines, and notably *ortho*-substituted ones.

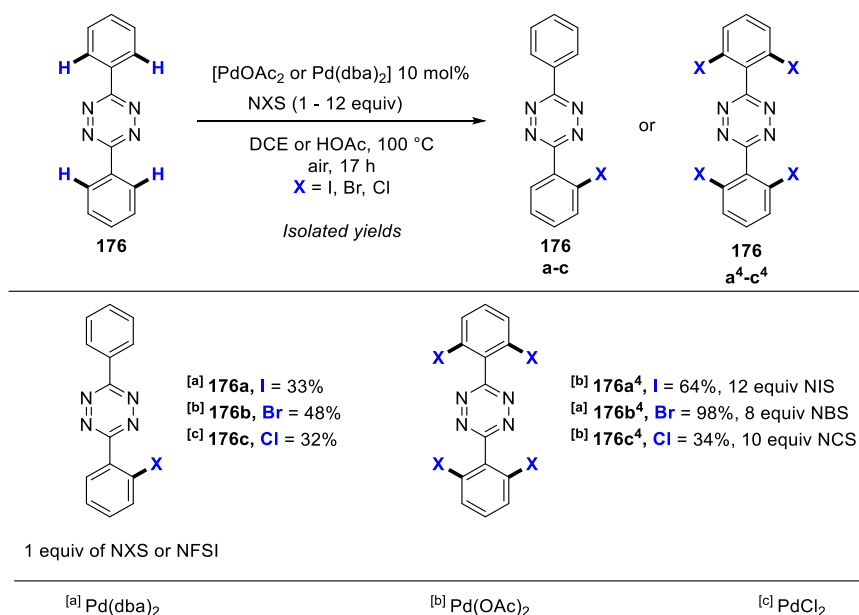


Scheme 30. The Pinner synthesis of *o*-halogenated *s*-aryltetrazines

Interested by the diverse properties and applications of functionalized tetrazines,^[63] the Hierso group targeted the palladium catalyzed C–H halogenation as a possible efficient pathway for the synthesis of tailored platform *s*-tetrazines. In 2016, Hierso *et al.* explored the presence of directing nitrogen atoms on *s*-aryltetrazines for metal-catalyzed ligand directed C–H bond halogenation.^[5, 64] Starting from 3,6-diphenyl-1,2,4,5-tetrazine **176**, they introduced in *ortho*-position all the possible halogen elements (I, Br, Cl and F) by using 1 equiv of either *N*-halosuccinimides (NXS, X = I, Br and Cl) or NFSI for the insertion of fluorine. By employing 10 mol% of Pd(0)- or Pd(II)-catalysts from $\text{Pd}(\text{dba})_2$, $\text{Pd}(\text{OAc})_2$ or PdCl_2 precatalysts, depending on the type of halogen, C–H activation/halogenation in DCE or HOAc was performed at 100 °C for 17 h. Monohalogenation was achieved in isolated yields ranging between 32% and 48%.

Compound **176b** was formed in 48% isolated yields for monobromination (Scheme 31). Iodination and chlorination produced **176a** and **176c** in 33% and 32% isolated yields, respectively. After screening the adequate conditions, monohalogenation products were isolated in general in fairly good yields, even in the presence of four identical C–H bonds readily available for C–H activation. Taking advantage of these multiple C–H bonds, tetrahalogenation was successfully carried out on **176** by increasing the

halogen source loading to 8-12 equiv to produce **176a⁴**, **176b⁴**, **176c⁴** in 64%, 98% and 34% respectively. These compounds are unprecedented derivatives of the chloro-*s*-aryltetrazine agrochemical known as Clofentezine.

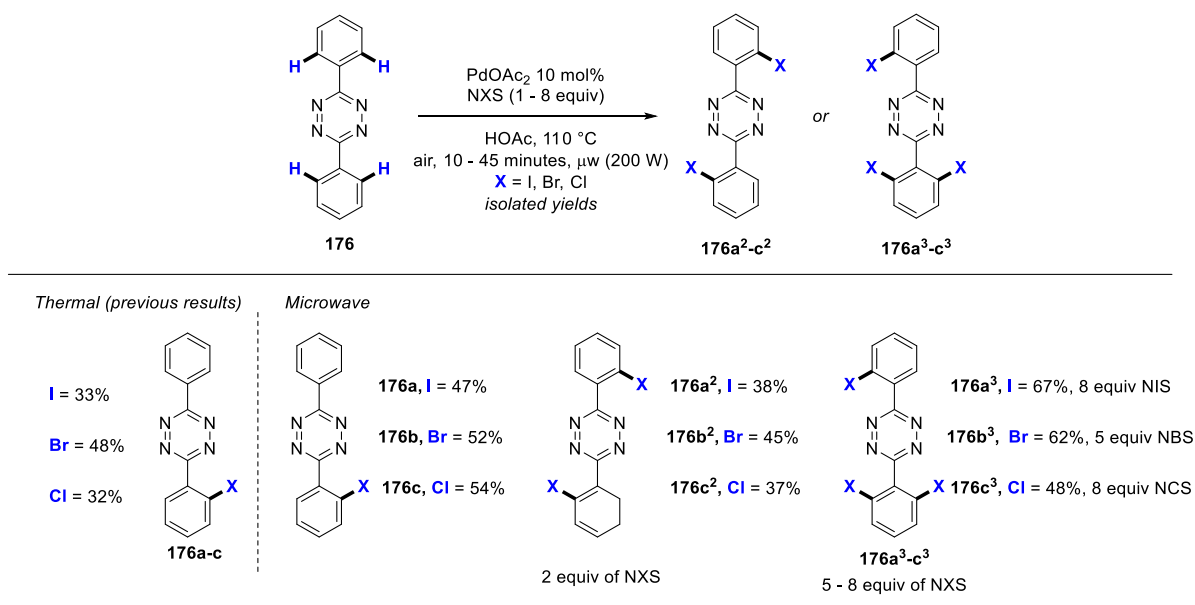


Scheme 31. *N*-directed Pd-catalyzed C–H bond halogenation on *s*-tetrazine **176** thermally

The Hierso group also achieved selective di- and trihalogenation reactions starting from 3,6-diphenyl-1,2,4,5-tetrazine **176** (Scheme 32).^[5a] Under thermal reactions, it is difficult to control the reaction to di- or trihalogenation due to the long-time reactions. Thus, new conditions for the convenient production of di- and trihalogenated derivatives of **176** were required. In HOAc under 200 W microwave irradiation for 10 minutes at 110 °C, starting from **176**, in the presence of 10 mol% Pd(OAc)₂ and 1 equiv of the *N*-halosuccinimide, products **176a-c** were obtained in yields ranging from 47% to 54%. The reactions conducted under microwave radiations allowed for fast C–H activation and halogenation. The amounts of NXS were increased to 2-4 equiv and 5-8 equiv to reach di- and trihalogenation, respectively. **176a^{2-c2}** and **176a^{3-c3}** were obtained in 37% to 45% and 48% to 67%, respectively. The amounts of halogen sources varied depending on each halogen (Scheme 32).^[5b]

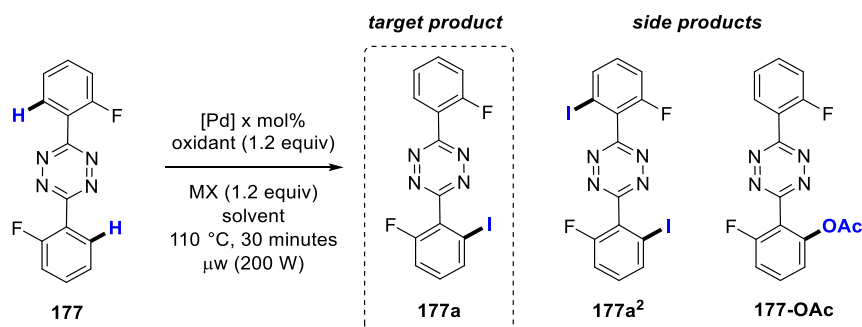
Fairly efficient pathways for the insertion of different halides by a Pd-catalyzed C–H bond activations were thus reported. Finding new conditions to increase conversions and selectivity for C–H bond halogenation, this by substituting the use of NXS halogen sources by cheaper and less toxic metal halides as nucleophilic halogen sources was the first goal of the present work. We first optimized

monohalogenation on *s*-aryltetrazine derivative **176**, and then extended the appropriate catalytic system to various *N*-containing substrates.



Scheme 32. *N*-directed Pd-catalyzed C–H bond halogenation on *s*-aryltetrazine **176** under microwave irradiation

For the optimization process, we opted to perform a series of iodination reactions where we investigated the best combination of all reagents (oxidant, catalyst, solvent and halogen source) to produce the desired monoiodinated product as the major product (Scheme 33). In all the optimization procedure, the monoiodinated product, **177a** is the desired product. Diiodination and acetoxylation reactions also occurred as competing reactions, to give the products **177a²** and **177-OAc** respectively. Pd-catalyzed acetoxylation is well-known on substrates containing nitrogen as directing groups reacted in the presence of OAc sources.^[65] In the absence of a more reactive halogen source, acetoxylation reactions occurs as the major reaction in the presence of OAc sources such as PIDA.

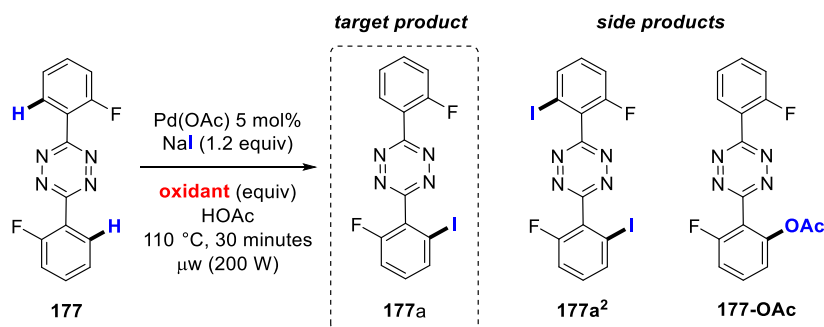


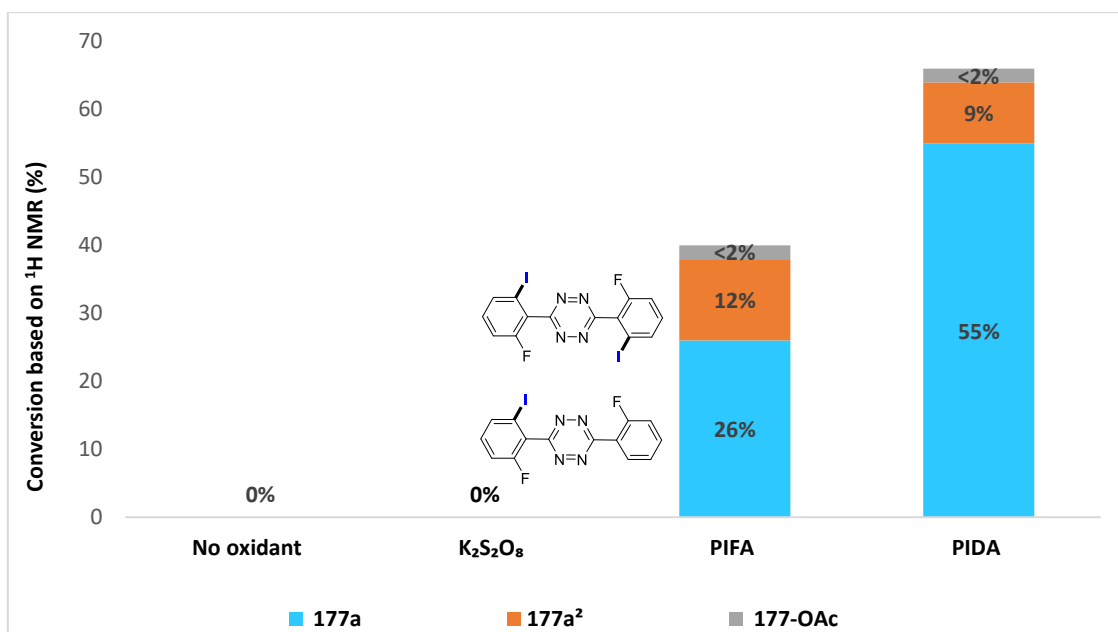
Scheme 33. The general conditions for the optimization process

A. Study of the oxidant

To choose a suitable oxidant, we performed a series of iodination reactions with unchanged conditions for 5 mol% Pd(OAc)₂, 1.2 equiv NaI, and HOAc as solvent (Graph 1). The most suitable oxidant was chosen according to the highest yield of **177a** determined by ¹H and ¹⁹F NMR of the crude reaction.

The reaction did not proceed without oxidant (Column 1), so several oxidants of different nature and reactivity were examined. Organic oxidants (PIDA, PIFA) and inorganic oxidant potassium persulfate (K₂S₂O₈) were tested. Product **177a** was obtained in 55% with PIDA as the oxidant (Column 4). With K₂S₂O₈ (Column 2) as the oxidant, the reaction did not proceed. The use of PIFA as an oxidant led to the production of the desired product in 26% (Column 3). Unsurprisingly, the production of a hypervalent halogen form PhI(OAc)(X) is decisive. This hypervalent form, which is produced *in situ* with both PIDA and PIFA is facilitated using PIDA (see our proposal for mechanism, below). Conversely, K₂S₂O₈ does not interact with the halogen metal salts and can only participate in oxidizing the Pd(II) to Pd(IV). However, even the highest yield (55%) with PIDA was limited due to some concurrent reactions, including fast dihalogenation and acetoxylation. The process of dihalogenation provided **177a**² in 12% and 9% with PIFA and PIDA, respectively, while the acetoxylation product **177-OAc** appeared in trace amounts in both cases. More convenient conditions for higher conversion, along with better selectivity, for the production of **177a** were investigated.

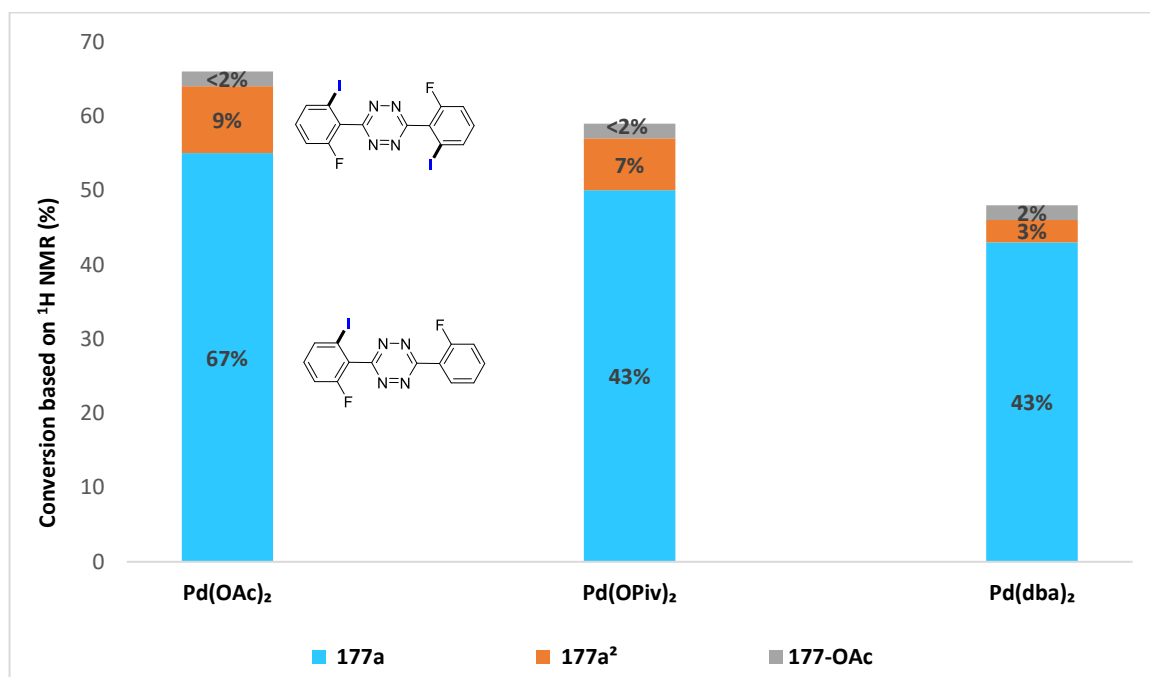
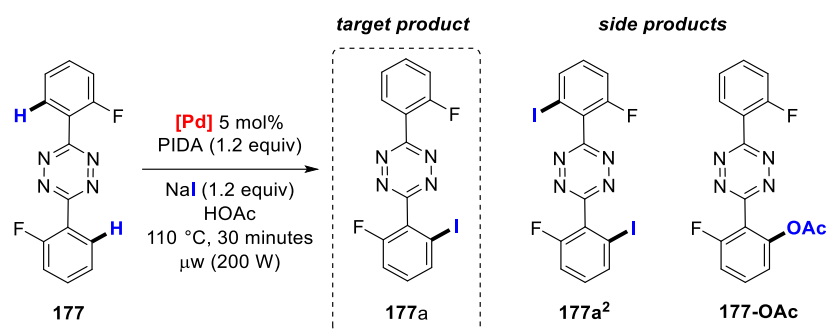




Graph 1. Iodination of 3,6-bis(2-fluorophenyl)-1,2,4,5-tetrazine **177** with different oxidants

B. Study of the catalyst

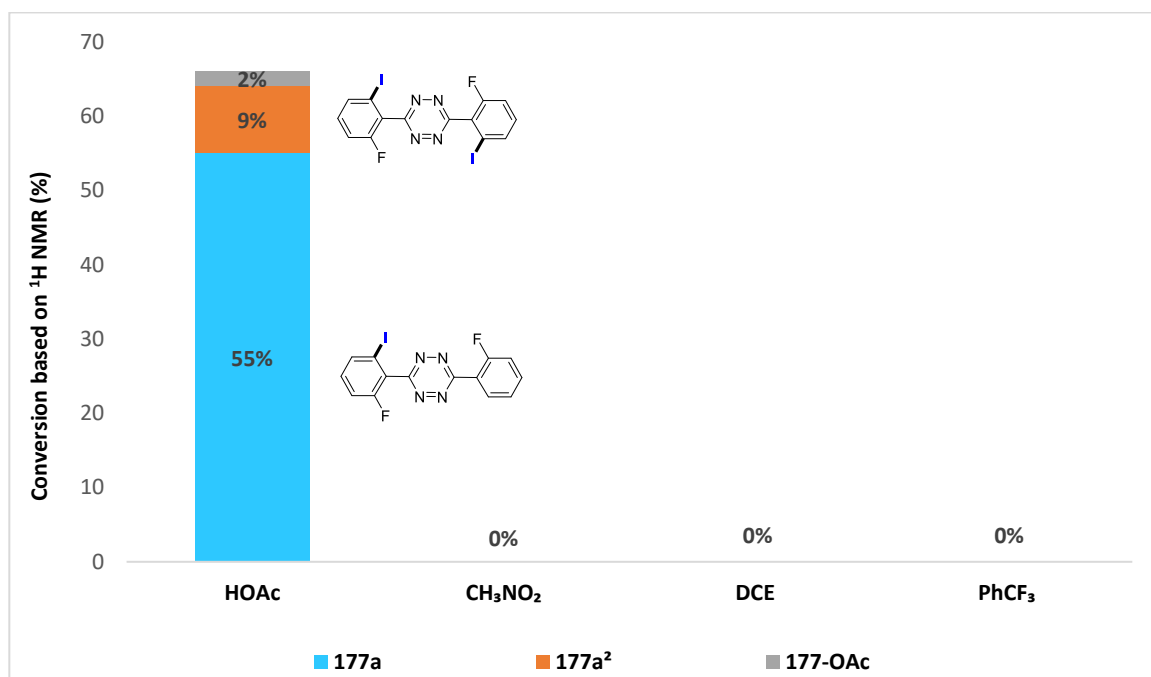
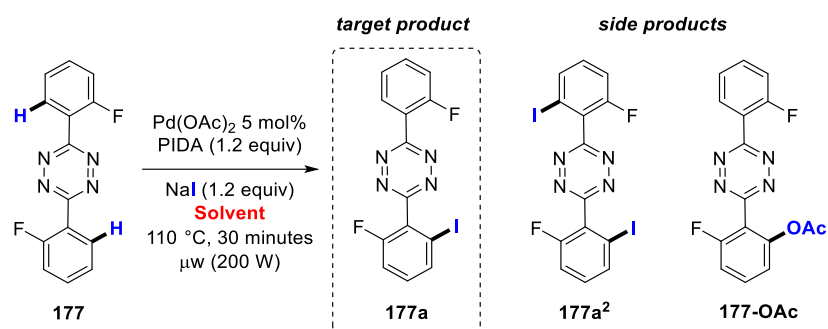
A series of reactions to identify the best catalyst for this reaction was done. We fixed the halogen source as NaI, the oxidant as PIDA and HOAc as the solvent of the reaction (Graph 2). Without Pd-catalyst the starting material remained unchanged, which infers that no products are formed from purely organic reactions with this substrate.^[25] By using 5 mol% of Pd(OAc)₂, **177a** was produced in 67% yield (Column 1). Loading other Pd(II)-catalysts such as Pd(OPiv)₂ (Column 2) produced **177a** in 43%, and the dihalogenated product **177a²** in 7% yield (Column 2). On the other hand, from Pd(dba)₂ [Pd(0)] formed **177a** and **177a²** in 43% and 3% yield (Column 3), respectively. Acetoxylation products **177-OAc** appeared in trace amount in all three reactions. This suggest a higher efficiency of Pd(II)-catalysts: Pd(OAc)₂ overwhelms Pd(0)-catalysts for conversion and selectivity towards the desired product **177a** (Column 4).



Graph 2. Iodination of 3,6-bis(2-fluorophenyl)-1,2,4,5-tetrazine **177** with different palladium catalysts

C. Study of the solvent

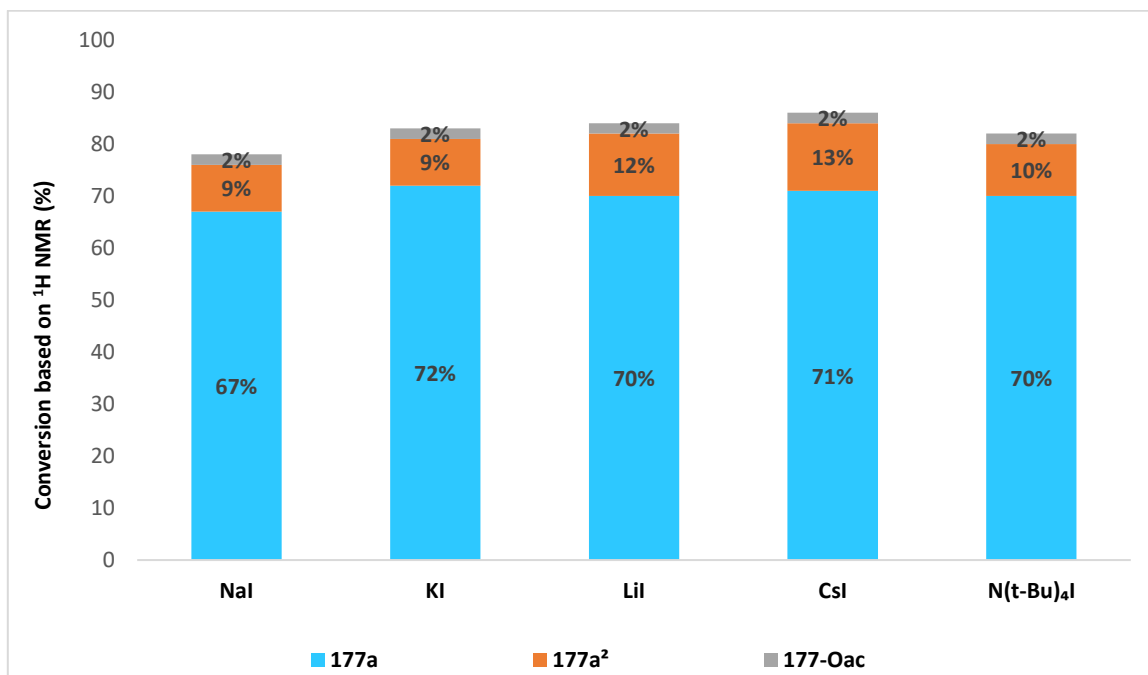
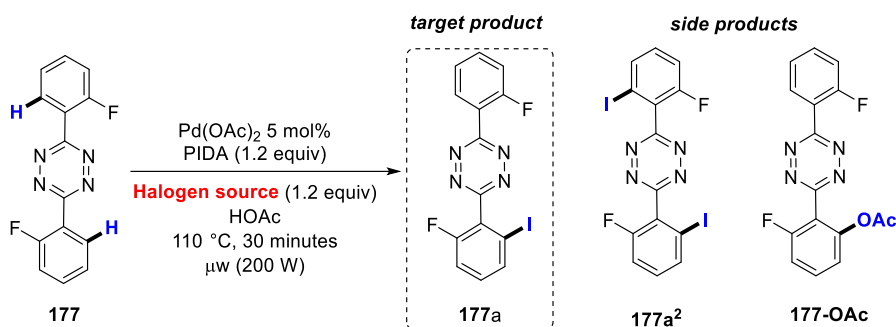
We tested different solvents and fixed the other conditions on 5 mol% of Pd(OAc)₂ and 1.2 equiv of PIDA, and used 1.2 equiv of the halogen salt as halogen sources (Graph 3). CH₃NO₂, DCE and PhCF₃ trifluorotoluene were compatible solvents for electrophilic C–H bond halogenation under microwave conditions.^[40] However, in the present system, such solvents provided no efficiency and only HOAc (Column 1) solvent promoted the nucleophilic halogenation as such (Graph 3).



Graph 3. Iodination of 3,6-bis(2-fluorophenyl)-1,2,4,5-tetrazine **177** with different solvents

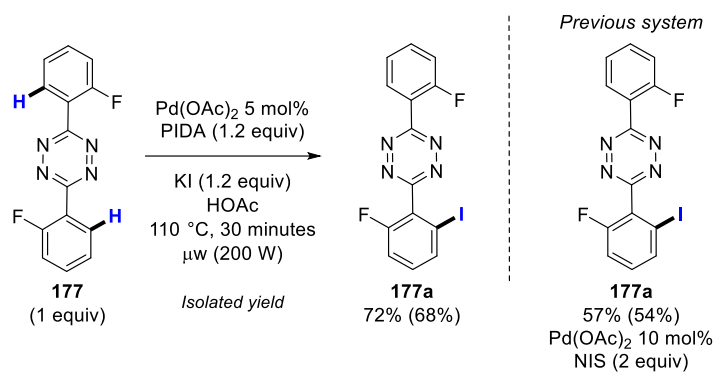
D. Study of the halogen source

Different iodide salts (M^+, I^-) were selected where $M = Na, K, Li, Cs, N(t-Bu)_4$. All of the mentioned nucleophilic halogen sources produced the desired monohalogenated product **177a** in yields higher than 65% (Graph 4). Despite the fact that all metal iodides gave very close values of conversion within the standard error, we opted for potassium iodide as it is a cheaper and more abundant salt with respect to the other iodide salts. $N(t-Bu)_4I$ was also compatible in such reaction and gave **177a** in similar 70% crude yield (Column 5).



Graph 4. Iodination of 3,6-bis(2-fluorophenyl)-1,2,4,5-tetrazine **177** with different nucleophilic halogen sources

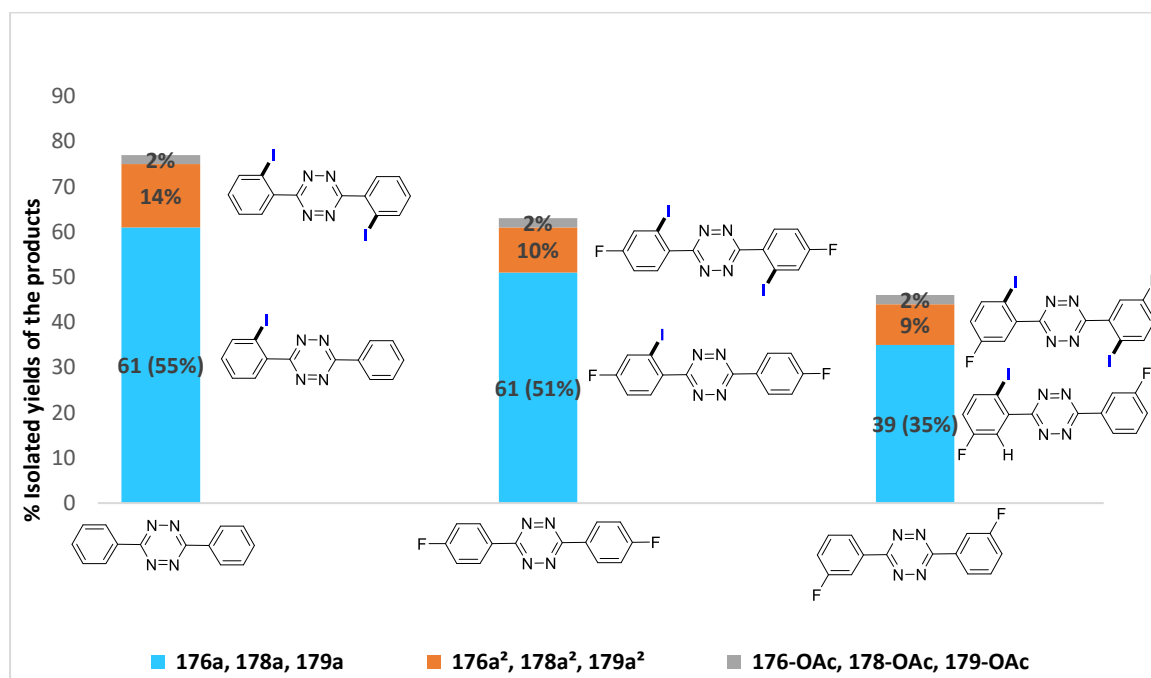
After having tested different oxidants, catalysts, solvents and halogen sources, the best yield for selective monoiodination was obtained with 1.2 equiv of PIDA as the oxidant, 5% of Pd(OAc)₂, HOAc as the solvent and 1.2 equiv of KI as the nucleophilic halogen source (Scheme 34). The monoiodinated product **177a** was obtained with 72% conversion, and was isolated in 68% yields. From the same substrate **177**, with the reported conditions from NIS electrophile use,^[61] conversion to **177a** was 57% yield and isolated yields was 54%. With the nucleophilic halide system, we reached an improvement of 14 units of percent in isolated yields. In addition, we cut the catalytic loading by half to 5 mol% Pd(OAc)₂ and use 1.2 equiv of KI salt instead of 2 equiv of the more toxic NIS. Notably, 1.2 eq of PIDA as expensive oxidant was also needed.



Scheme 34. Iodination of **177** with nucleophilic source (left) or electrophilic source (right)

2) General iodination of *s*-aryltetrazines and other *N*-containing substrates

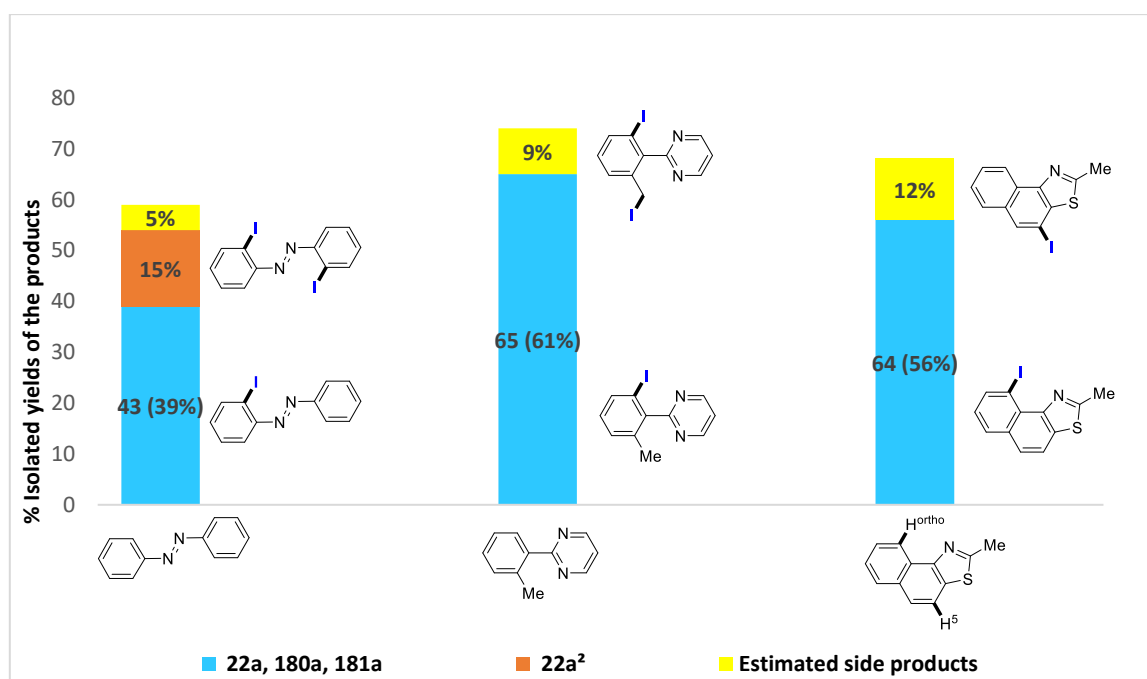
The selective monohalogenation of 1 equiv of the tetrazine substrate **177** was achieved using 1.2 equiv of PIDA as the oxidant, 1.2 equiv of KI as the nucleophilic halogen source in HOAc at 110 °C for 30 minutes (Graph 5). These conditions were employed for different *s*-aryltetrazines and heteroarenes. The results for iodination of 3,6-bisphenyl-6-phenyl-1,2,4,5-tetrazine **176**, 3,6-bis(4-fluorophenyl)-1,2,4,5-tetrazine **178** and 3-(5-fluoro-2-iodophenyl)-6-(3-fluorophenyl)-1,2,4,5-tetrazine **179** are reported in Graph 5.



Graph 5. *o*-Iodination of *s*-aryltetrazines **176**, **178** and **179**

The reaction with **176** and **178** lead to isolated monoiodinated **176a** and **178a** in 55% and 51% yields, respectively. The isolated yield for **179a** (35%) decreased considerably because of the presence of an *electron*-withdrawing fluorine atom at the *m*-position. Usually, *m*-substituents block their adjacent *o*-position site, leading to the selective monohalogenation in the other distant *o*-position.

We further achieved the scope extension on several substrates of interest (Graph 6). The conversion for these reactions were generally above 65% except in the case of the azobenzene **22** that has a challenging *N*-directing activation similar to *s*-aryltetrazine **176**, with multiple accessible *o*-C–H bonds. In this case, *c.a.* 15% of halogenation occurred in addition to trace amounts (<5%) of tri- and tetrahalogenation. For heterocycles other than *s*-aryltetrazines, 5 mol% Pd(OAc)₂ was found to be less efficient, and 10 mol% Pd(OAc)₂ was required for more efficient activation reactions.

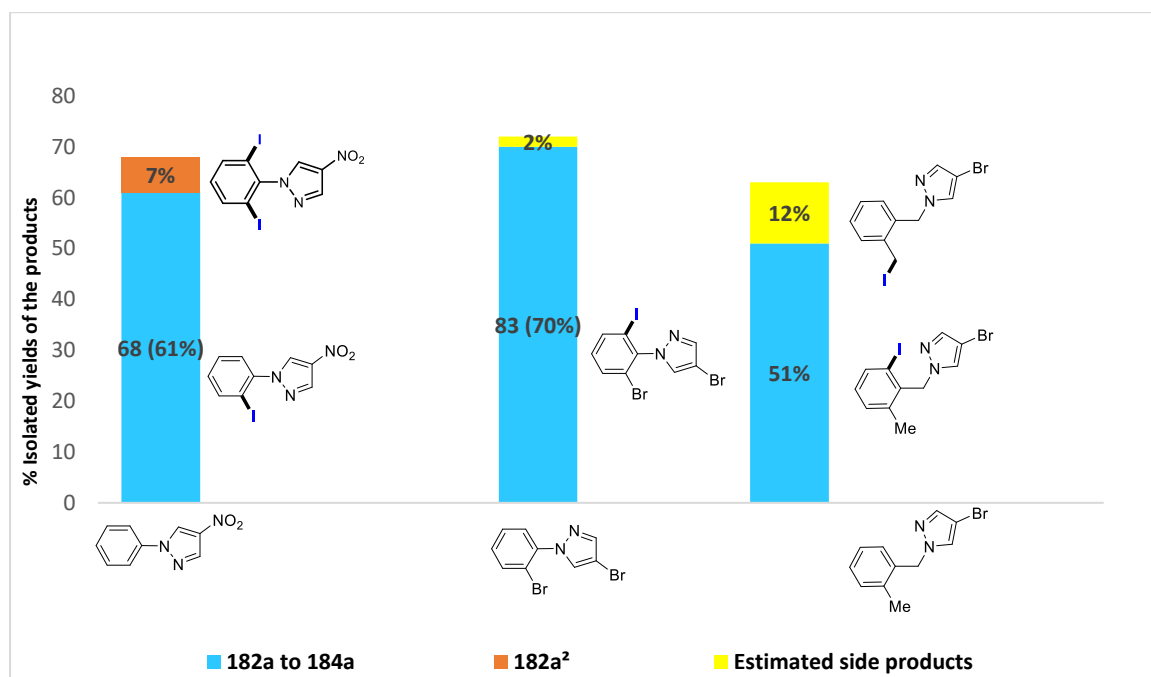


Graph 6. *o*-Iodination of azobenzene **22** and phenylpyridine and thiazole **180**, **181**

In the case of *o*-methylated pyrimidine **180** also, only a single *o*-position is accessible to C–H bond activation that explains the good conversion of 65% for **180a**. An interesting side product was obtained through the C–H bond iodination of the methyl group in **180**. Acetoxylation on activated C_{sp3}–H is well-known and was reported with directing nitrogen containing substrates such as quinolones.^[66] Compound **181**, like its benzoquinoline analogue, was compatible with iodination but suffered from a similar side-reaction that is the organic direct C–H iodination of C5'–H bond (12%), thus **181a** was

obtained in 56% isolated yield, from an incomplete conversion of 64%. The iodination of 2-methylnaphtho[1,2-*d*]thiazole **181** provided **181a** in 56% isolated yields, respectively

In addition to the iodination of phenylpyridines and pyrimidines, the nucleophilic approach nicely operated with challenging phenylpyrazole substrates: phenylpyrazoles 4-nitro-1-phenyl-1*H*-pyrazole **182**, 4-bromo-1-(2-bromophenyl)-1*H*-pyrazole **183**, 4-bromo-1-(2-methylbenzyl)-1*H*-pyrazole **184** were successfully converted (Graph 7).

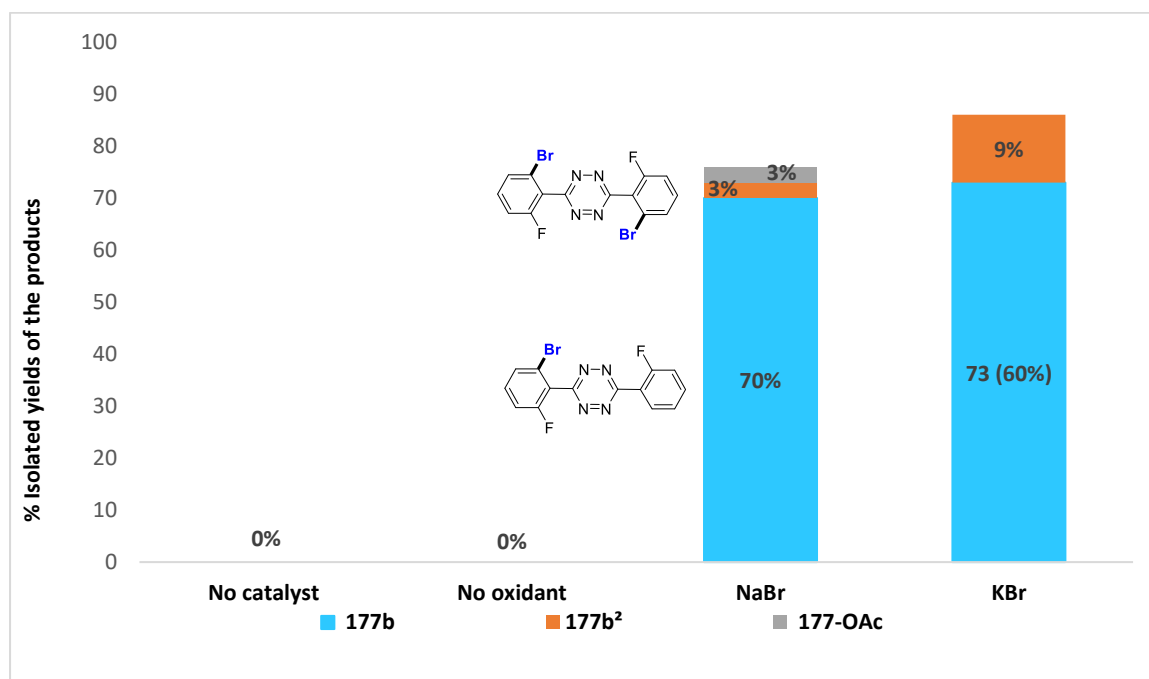
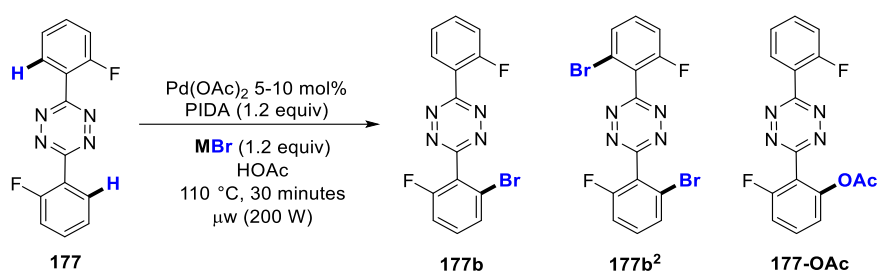


Graph 7. *o*-Iodination of phenylpyrazole derivatives **182** to **184**

From **182**, the monohalogenated product **182a** was isolated in 61% yield, despite the presence of two accessible C–H bonds. The kinetics for the occurrence of a second halogenation is hampered by a palladacycle very congested intramolecularly or by ancillary ligands.^[64] From **183**, only a single C–H bond is accessible for activation, **183a** was obtained exclusively in 70% isolated yields. From **184**, the *o*-monoiodinated molecule **184a** was isolated as major product in 51% yield. However, **184** was not fully converted and additional side products from the halogenation of the aliphatic *o*-methyl group was observed, either alone or accompanied with *o*-halogenation. In principle, benzylpyrazole **184** is a challenging *N*-directing substrates since C–H activation occurs through a less stable six-membered palladacycle (compared to more frequent five-membered metallacycles). Only few reports described that cycles for C–H bond activation mechanisms.^[67] Despite some minor side-reactions observed, the *N*-directed *o*-iodination of different *s*-aryltetrazines, and other challenging *N*-containing molecules, generally proceed nicely but must be extended to bromination and chlorination.

3) Screening of conditions for the bromination of 3,6-bis(2-fluorophenyl)-1,2,4,5-tetrazine

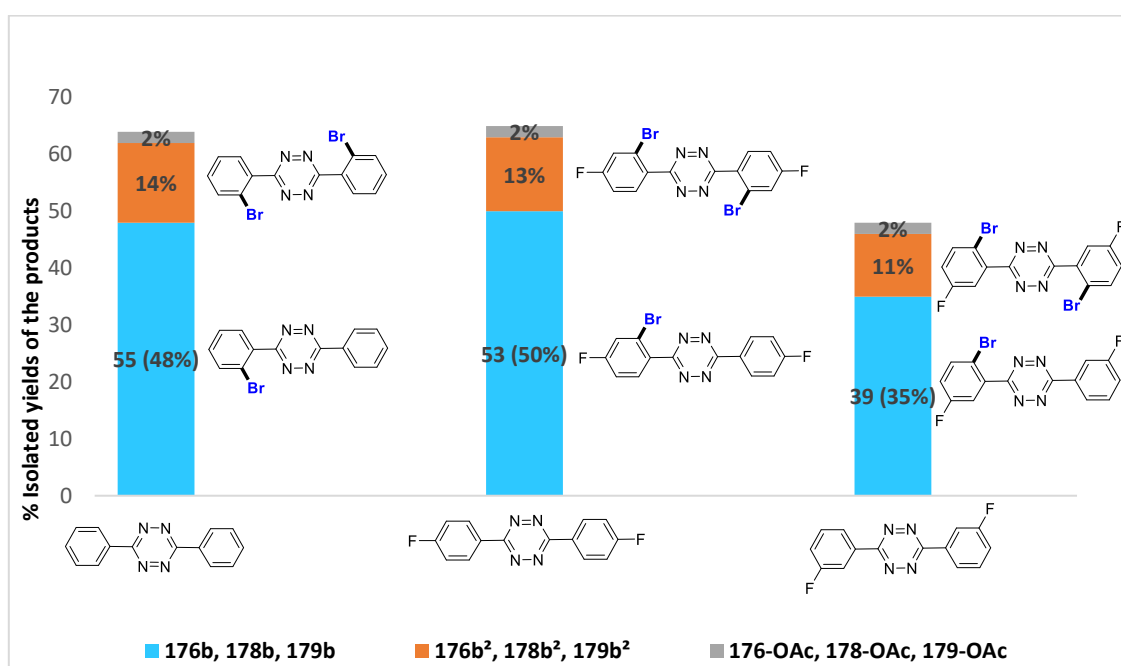
For control experiments, we performed the reaction in the absence of either the catalyst or the oxidant where both reactions failed to give any result (Graph 8). Both NaBr and KBr yielded the monobrominated product **177b** as the major product in 70% and 73% yields. Similarly to iodination, dihalogenated **177b²** products appeared as side products in addition to traces of the acetoxyated product **177-OAc**. Monobromination to reach **177b** using potassium bromide and potassium iodide afforded similar results with *c. a.* 70% conversion, and thus KBr appeared as a suitable nucleophilic source of bromide.



Graph 8. Impact of the brominated sources for the bromination of *s*-aryltetrazine **177**

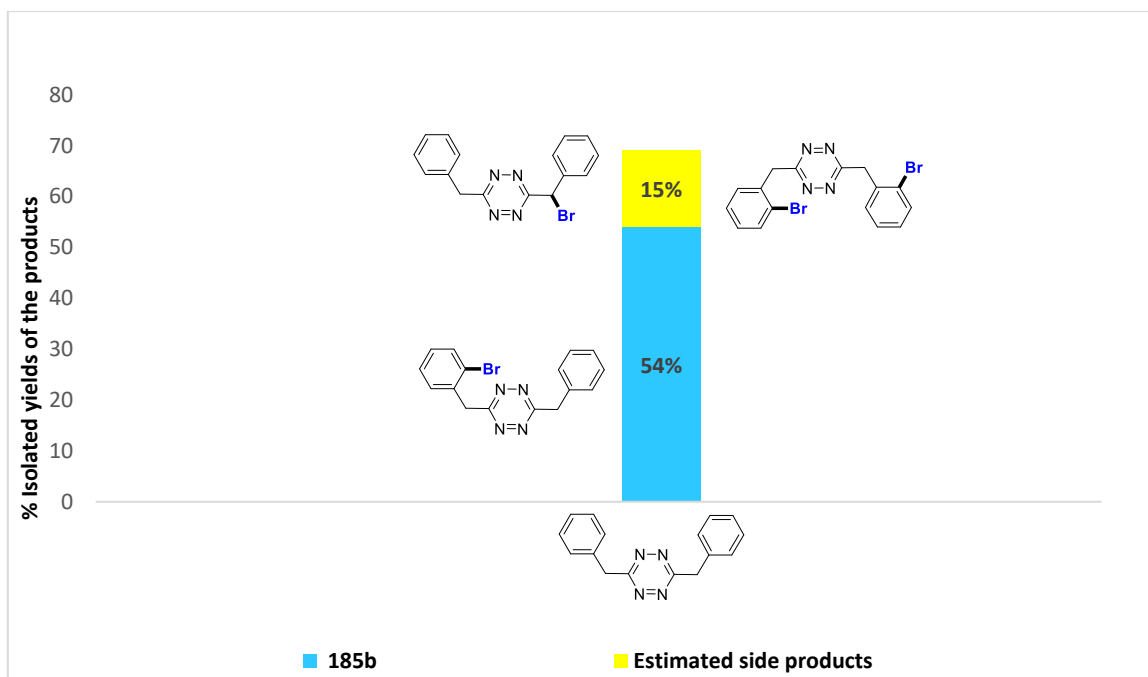
4) Bromination of *s*-aryltetrazines and other *N*-containing substrates

Using the optimized conditions for bromination, the monobromination on the *s*-tetrazines **176**, **178** and **179** afforded their monohalogenated products **176b**, **178b** and **179b** in 48%, 50% and 35% isolated yields, respectively (Graph 9). The presence of four accessible *o*-C–H bonds lead to concurrent mono and polyhalogenation. Compared to iodination, the selectivity of the bromination was found more difficult to control: **176b** was isolated in (48%) in a lower yield than to **176a** (Graph 5, 55%). Replacing KBr with NaBr affords the bromination reaction of **178** and **179** in 46% and 32% crude yields respectively, lower than with KBr.



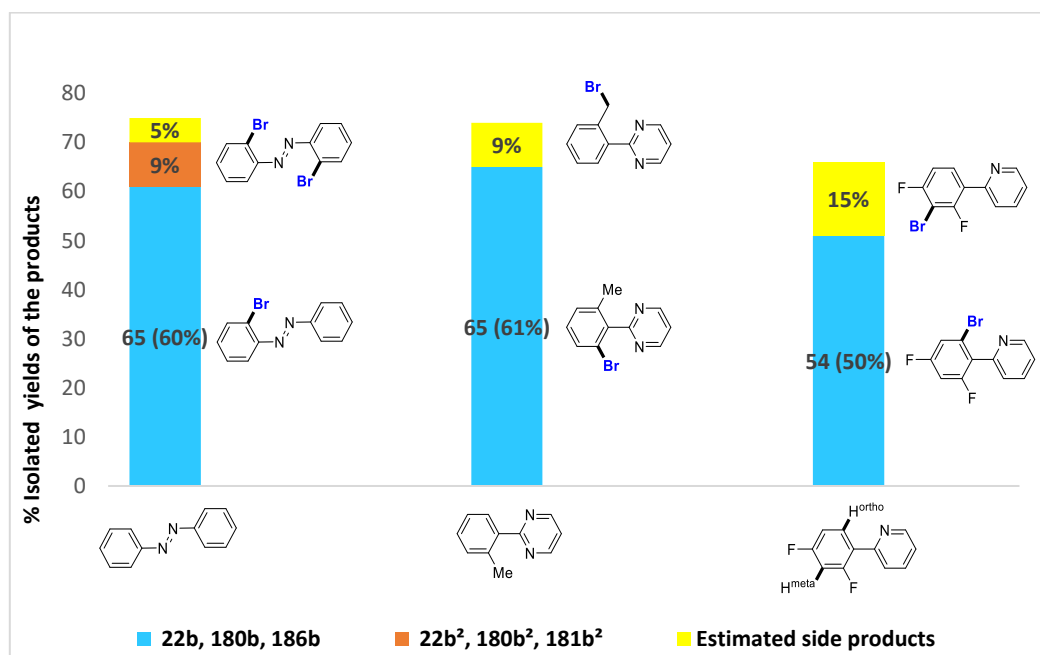
Graph 9. *o*-Bromination of **176**, **178**, and **179** from KBr

We performed the nucleophilic bromination on challenging *s*-tetrazines 3,6-dibenzyl-1,2,4,5-tetrazine **185** (Graph 10). The *N*-directed C–H bond bromination on the C_{Sp2} of the phenyl, leading to **185b** with 54% isolated yields. Side products were comprised of electrophilic C–H bromination on the benzyl C_{Sp3} (yellow). Another side product realized from the bromination on both phenyl C_{Sp2} and benzyl C_{Sp3} simultaneously.



Graph 10. *o*-Bromination of **185**.

Azobenzene **22**, 2-(*o*-tolyl)pyrimidine **180**, 2-(2,4-difluorophenyl)pyridine **186** were brominated using KBr (Graph 11).

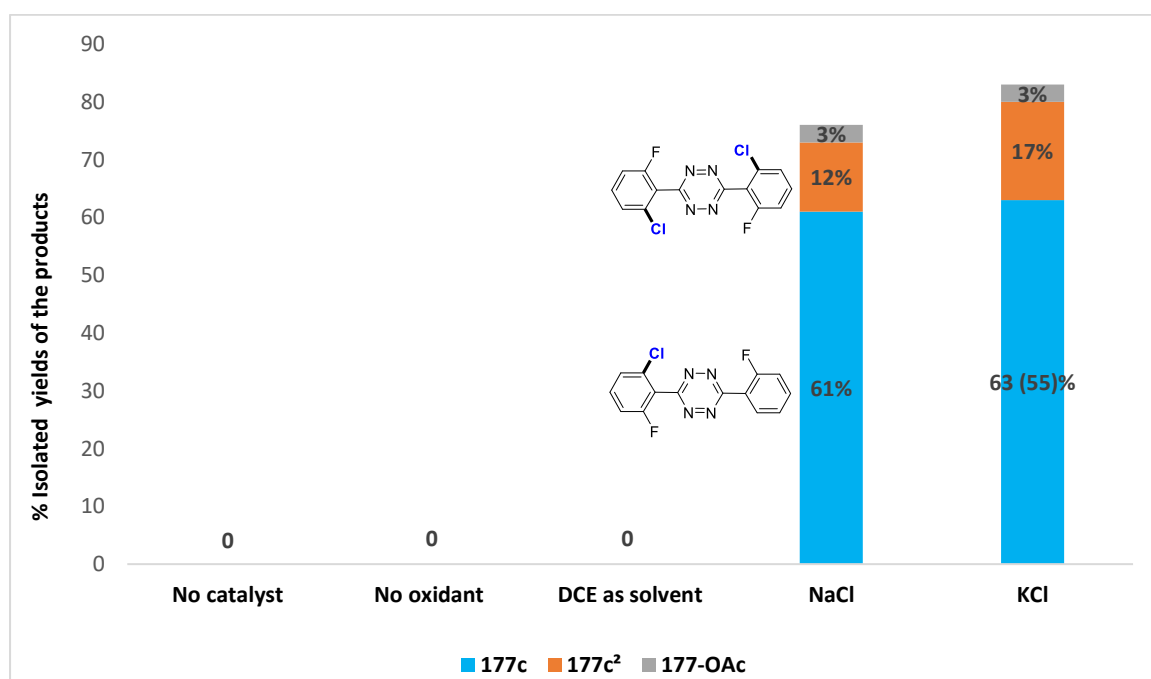
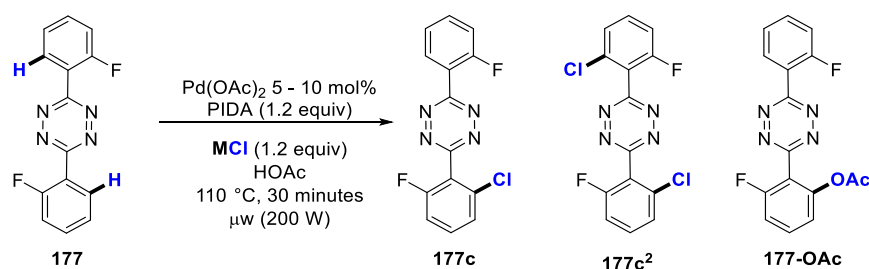


Graph 11. *o*-Bromination of **22**, **180**, and **186**

With these substrates, 10 mol% Pd(OAc)₂ was required instead of the usual 5 mol%. Compound **22b** was isolated in 60% yield, showing a significant improvement compared to the synthesis of iodinated derivative **22a** (39%). From the bromination of methylated pyrimidine **180**, the compound **180b** was isolated in 61% yield together with side-products from *N*-directed bromination of the methyl group. With arylpyridine **186**, the bromination the brominated product **186b** was isolated in 50% yield.

5) Screening of conditions for the chlorination of 3,6-bis(2-fluorophenyl)-1,2,4,5-tetrazine

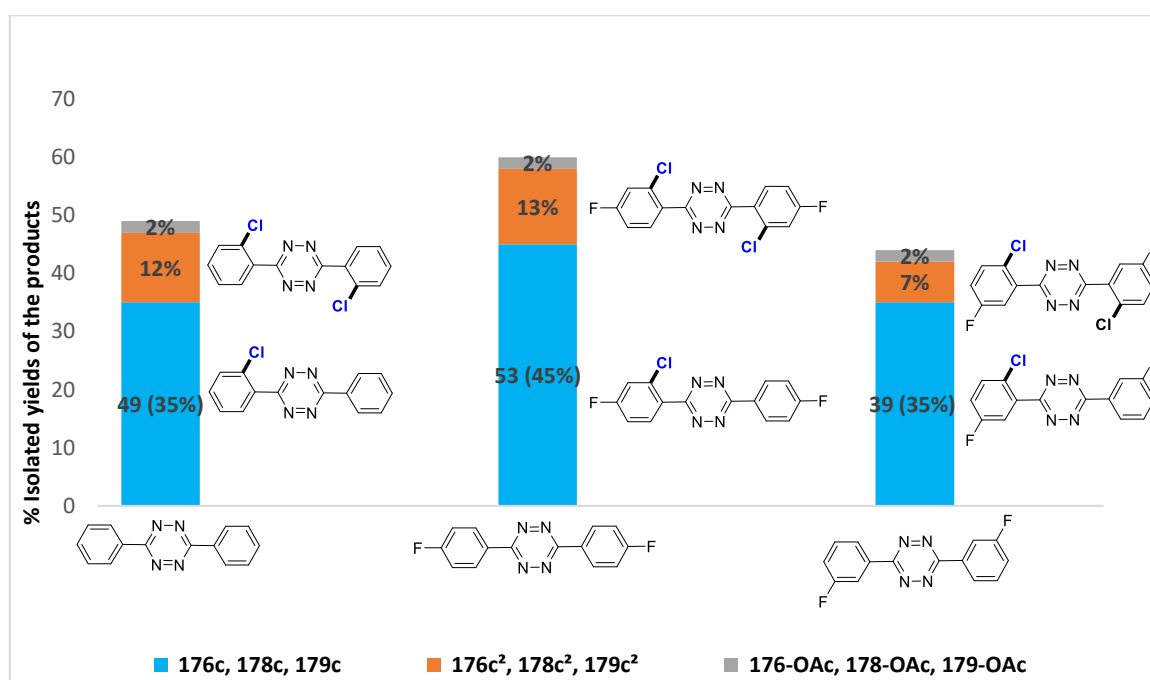
We compared the results obtained when using NaCl and KCl as the chlorine sources, to produce **177c** in crude 61% and 63%, respectively (Graph 12). We were able to isolate the monochlorinated product **177c** in 55% yield using KCl as the halogen source.



Graph 12. Impact of the chlorinated sources for the bromination of *s*-aryltetrazine **177**

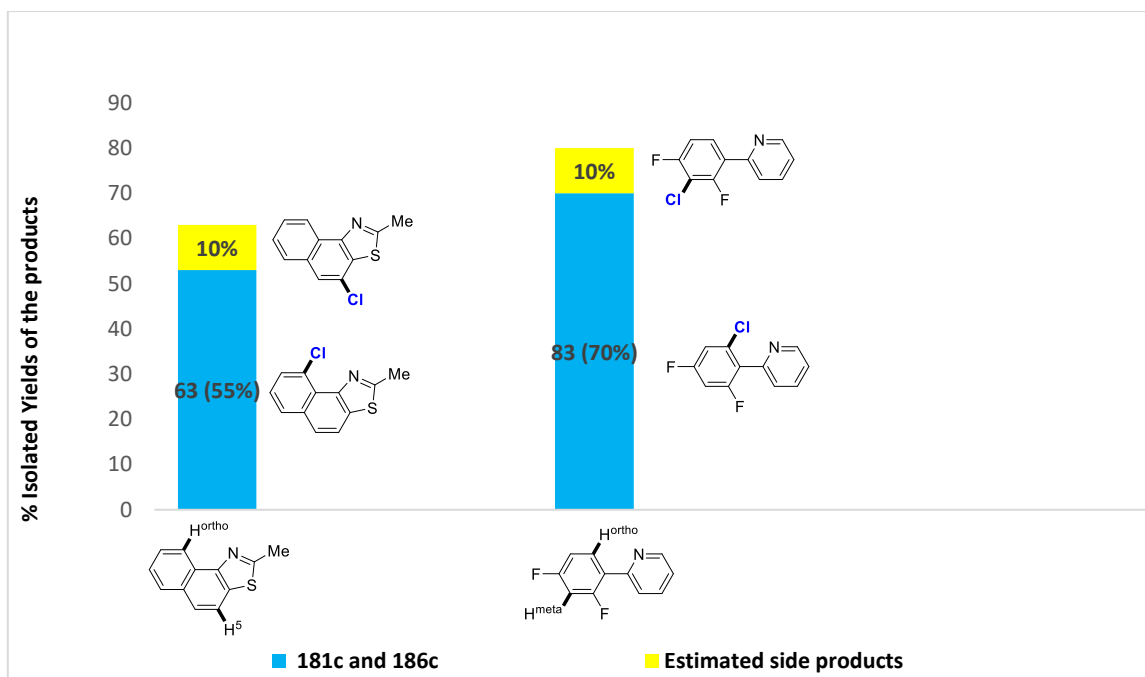
6) Chlorination of *s*-tetrazines and other *N*-containing substrates

We achieved under standard conditions the *N*-directed *o*-C–H-chlorination of *s*-tetrazines 3,6-bisphenyl-6-phenyl-1,2,4,5-tetrazine **176**, 3,6-bis(4-fluorophenyl)-1,2,4,5-tetrazine **178** and 3-(5-fluoro-2-iodophenyl)-6-(3-fluorophenyl)-1,2,4,5-tetrazine **179** (Graph 13). The monochlorinated products **176c**, **178c**, and **179c** were obtained in 35%, 45% and 35% isolated yields, respectively. Unfortunately, both the conversion and the isolated yields are minored in comparison with other halogenated analogous products. We also performed the reactions of **178** and **179** with NaCl as halogen source. However, we obtained 46% and 28% of crude yield for **178c** and **179c**, which is lower than obtained with KCl, at 53% and 39% crude yield.



Graph 13. *o*-chlorination of substrates **176**, **178**, and **179**.

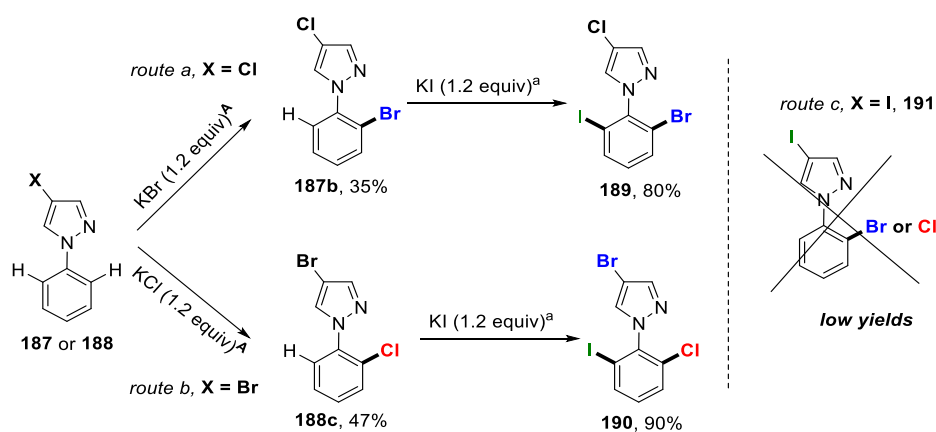
Conversely, good isolated yields for chlorination were obtained with 2-methylnaphtho[1,2-*d*]thiazole **181** (55%, Graph 14) and 2-(2,4-difluorophenyl)pyridine **186** (70%). Using **181** as the substrate, the main product was the *o*-monochlorinated product isolated in 55% yields. The total conversion of this late reaction for **186** was estimated at 83% with 70% isolated yields for the *o*-chlorinated product **186c**, and the main side product was the *m*-electrophilic chlorination at the C5'–H bond with 10% of *meta*-insertion of chlorine.



Graph 14. *o*-chlorination of **181** and **186** with KCl

7) Unequal trihalogenated phenylpyrazole derivatives **189** and **190**

We synthesized phenylpyrazole derivatives with unequal halogen functionalizations, especially for further diversification in post-functionalization (Scheme 35).



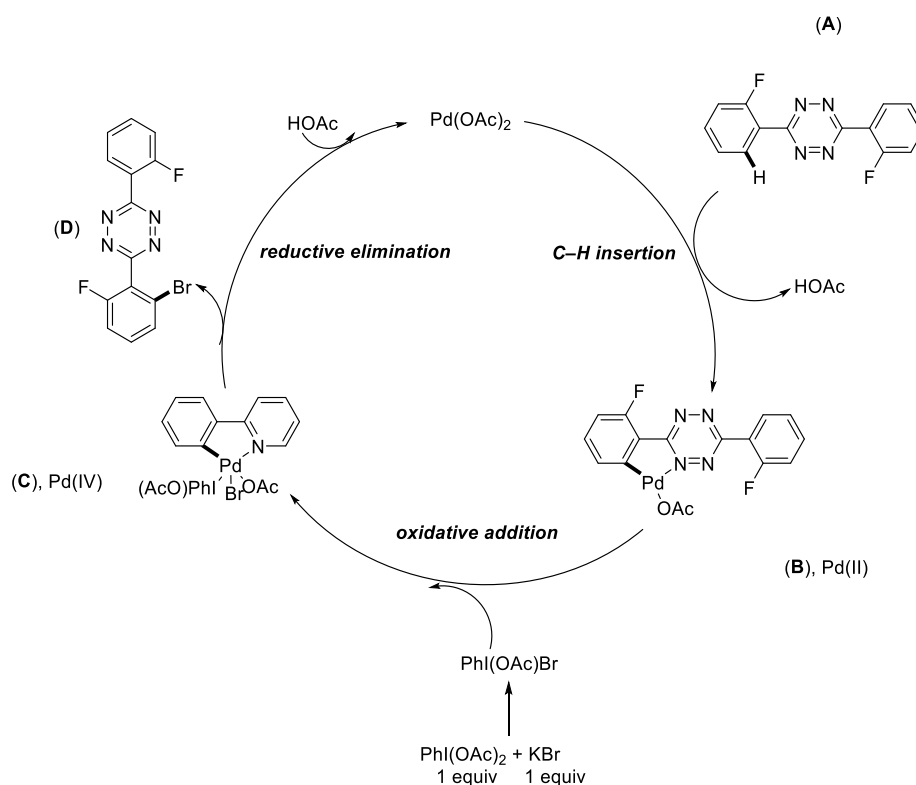
Conditions A: Pd(OAc)₂ 5 mol%, PIDA (1.2 equiv), HOAc, 110 °C, 30 minutes, μ W (200 W)
All yields are isolated

Scheme 35. Synthesis of unequally trihalogenated phenylpyrazole derivatives **189** and **190**

We initially started from the halogenated phenylpyrazoles at the *C4'*-position of the pyrazole ring, which is the most reactive site for initial organic halogenation with NXS. The compounds **187** and **188** bear chlorine and bromine at the *C4*-position of the pyrazole ring, respectively. By using the conditions previously established for selective monohalogenation with KX (X = I, Br, Cl); we applied *o*-bromination to **187**, bearing a chlorine on the pyrazole ring by C–H chlorination to obtain **187b** in 35% isolated yield (Scheme 35, *route a*). We performed then iodination on the other free *o*-position in high yields of 80% to obtain **189**. From **188** (Scheme 35, *route b*), bearing a bromine on the pyrazole ring, undergoes *o*-chlorination through the conditions reported previously.^[56b] Then, suitable iodination produced **190** in 90% yield, this compound bearing three different halogen atoms isomeric to **189** from its halogens in different positions. *Route c*, which started from **191** bearing iodine on the pyrazole ring suffered from low selectivity towards monobromination and chlorination, and produced a mixture of mono- and dihalogenated products instead.

8) Proposed mechanism for the *N*-direct palladium-catalyzed iodination with nucleophilic source

We choose to present the cycle with bromination and used **177** (called in this case **A**) as the substrate of interest (Scheme 36).



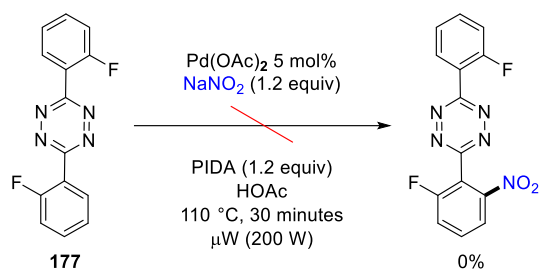
Scheme 36. The plausible mechanism of our work

The catalytic cycle begins from Pd(OAc)₂ and C–H bond insertion occurs with the substrate of interest **177** = **A** to give the tetrazine-palladium complex **B** with Pd(II) species upon the extraction of the acetate. Meanwhile, PhI(OAc)Br is produced as active halogen transfer agent *in situ* from the reaction of 1 equiv of the “nucleophilic” halogen source KBr and PhI(OAc)₂ (PIDA) on **B**. The oxidative addition of the active halogen transfer agent PhI(OAc)Br occurs to give rise to the Pd(IV) complex **C**. Reductive elimination on **C** gives the desired product. HOAc which was previously produced reenters the cycle to finally restore the Pd(OAc)₂. The halogen source PhI(OAc)Br would be hypothetically produced in similar fashion to the rhodium catalyzed cycle from Glorius et al. work. However, these authors used excess NaBr (3 equiv) in comparison to PhI(OAc)₂ (1 equiv) and this led to the production of PhIBr₂ instead of PhI(OAc)Br, which would be produced in our case (Scheme 36).

9) Conclusion and perspectives

We illustrated in this first chapter a *N*-directed C–H bond halogenation method based on cheap and non-toxic available nucleophilic halogen sources MX (M = Li, Na, K, Cs, NH₄ and X = I, Br, Cl). The reaction proceeds under microwave irradiation (200 Watt), at 110 °C and in short reaction times (30 minutes) in HOAc. These conditions were employed with success on various *N*-heteroaryls for iodination, bromination and chlorination and improved some results compared to reported C–H bond electrophilic halogenation with NXS, either in terms of complexity of the substrates, total conversion and/or isolated yields, catalytic loading, or reaction times.

The next step will be to investigate the possible insertions of other heteroatoms such as nitrogen, oxygen, sulphur, phosphorus and others in *ortho*-position with other nucleophilic sources. Interestingly, many available sources of such heteroatoms are commercially available in the nucleophilic forms. For example, we applied similar conditions to what we used before in terms of solvent, catalyst, reaction time and heating method with NaNO₂ (Scheme 37). However, the reactions did not proceed as expected.



*Scheme 37. N-directed Pd-insertion of nitro on 3,6-bis(2-fluorophenyl)-1,2,4,5-tetrazine **177***

Supporting Information

General Conditions

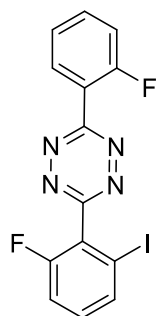
All reagents were purchased from commercial suppliers and used without purifications. All experiments were carried out under air using a microwave reaction vessel. Microwave heating was carried out using a CEM Discover microwave reactor. The microwave reactions were run in closed reaction vessels with magnetic stirring and with the temperature controlled via IR detection. Flash chromatography was performed on silica gel (40-63 μm). The identity and purity of the products were established at the "Chemical Analysis Platform and Molecular Synthesis University of Burgundy" (PACSMUB Platform – SATT SAYENS) using high-resolution mass spectrometry, elemental analysis and multinuclear NMR. ^1H (500, 400 or 300 MHz), ^{13}C (125 or 101 MHz), ^{19}F (470 or 282 MHz) spectra were recorded on Bruker AVANCE III instruments in CDCl_3 or CD_2Cl_2 solution. Chemical shifts are reported in ppm relative to CDCl_3 (^1H : 7.26 and ^{13}C : 77.16) or CD_2Cl_2 (^1H : 5.32 and ^{13}C : 54.00) and coupling constants J are given in Hz. High resolution mass spectra (HRMS) were obtained on a Thermo LTQ-Orbitrap XL with ESI source. Elemental analysis experiments were performed on a Thermo *Electron* Flash EA 1112 Series.

I. General procedures

1) General procedure for the halogenation of heteroaryl derivatives

As a typical experiment, in a microwave reaction vessel equipped with a magnetic stirring bar was charged with heteroaryls (1 equiv, 0.25 mmol), $\text{Pd}(\text{OAc})_2$ (5 mol%), PIDA (1.2 equiv, 0.3 mmol) and NaX or KX (1.2 equiv, 0.3 mmol) in HOAc [0.125 M] under air. The mixture was heated at 110 $^\circ\text{C}$ during the corresponding time under microwaves irradiations (200 W). After cooling down to room temperature, the solvent was removed under vacuum and the residue was analysed by ^1H and ^{19}F NMR spectroscopy to determine the conversion and selectivity of the halogenation reaction. The crude mixture was purified by silica gel column chromatography using an appropriate ratio of eluent (Dichloromethane or Ethyl Acetate/Heptane or Pentane) to afford the targeted product.

3-(2-Fluoro-6-iodophenyl)-6-(2-fluorophenyl)-1,2,4,5-tetrazine (**177a**) CAS: 2099072-60-1

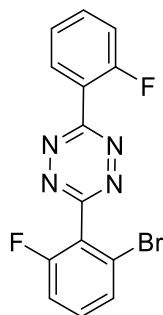


$R_f = 0.51$ ($\text{CH}_2\text{Cl}_2/\text{Heptane}$: 7/3). Isolated yield: 68% (67 mg, as a purple solid).

^1H NMR (300 MHz, CDCl_3): δ (ppm) = 8.46–8.40 (m, 1H), 7.88–7.84 (m, 1H), 7.71–7.63 (m, 1H), 7.46–7.30 (m, 4H).

$^{19}\text{F}\{^1\text{H}\}$ NMR (282 MHz, CDCl_3): δ (ppm) = –108.8 (1F), –111.0 (1F).

3-(2-Bromo-6-fluorophenyl)-6-(2-fluorophenyl)-1,2,4,5-tetrazine (177b) CAS: 2099072-59-8

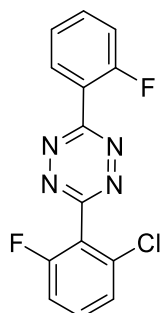


R_f = 0.52 (CH₂Cl₂/Heptane: 7/3). Isolated yield: 60% (52 mg, as a purple solid).

¹H NMR (500 MHz, CDCl₃): δ (ppm) = 8.42 (td, *J* = 7.6 and 1.8 Hz, 1H), 7.69–7.65 (m, 1H), 7.62 (dt, *J* = 8.2 and 1.0 Hz, 1H), 7.48 (td, *J* = 8.3 and 5.8 Hz, 1H), 7.43 (td, *J* = 7.6 and 1.1 Hz, 1H), 7.36 (ddd, *J* = 10.9, 8.4 and 1.1 Hz, 1H), 7.30 (td, *J* = 8.9 and 1.0 Hz, 1H).

¹⁹F{¹H} NMR (470 MHz, CDCl₃): δ (ppm) = -110.0 (1F), -111.0 (1F).

3-(2-Chloro-6-fluorophenyl)-6-(2-fluorophenyl)-1,2,4,5-tetrazine (177c) CAS: 2099072-61-2

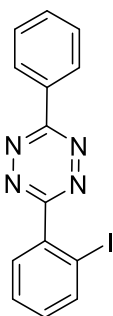


R_f = 0.55 (CH₂Cl₂/Heptane: 7/3). Isolated yield: 55% (42 mg, as a purple solid).

¹H NMR (300 MHz, CDCl₃): δ (ppm) = 8.42 (td, *J* = 7.6 and 1.8 Hz, 1H), 7.70–7.63 (m, 1H), 7.55 (td, *J* = 8.3 and 5.8 Hz, 1H), 7.46–7.43 (m, 2H), 7.41–7.33 (m, 1H), 7.29–7.23 (m, 1H).

¹⁹F{¹H} NMR (282 MHz, CDCl₃): δ (ppm) = -111.1 (1F), -111.1 (1F).

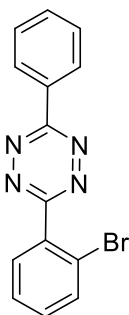
3-(2-Iodophenyl)-6-phenyl-1,2,4,5-tetrazine (176a) CAS: 1893365-17-7



R_f = 0.44 (CH₂Cl₂/Heptane: 1/1). Isolated yield: 61% (55 mg, as a purple solid).

¹H NMR (500 MHz, CDCl₃): δ (ppm) = 8.73–8.71 (m, 2H), 8.12 (dd, *J* = 8.0 and 1.0 Hz, 1H), 7.99 (dd, *J* = 7.7 and 1.6 Hz, 1H), 7.70–7.58 (m, 4H), 7.31–7.26 (m, 1H).

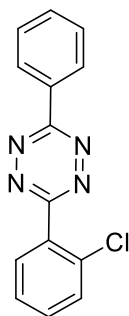
3-(2-Bromophenyl)-6-phenyl-1,2,4,5-tetrazine (176b) CAS: 1893365-13-3



R_f = 0.34 (CH₂Cl₂/Heptane: 1/1). Isolated yield: 48% (37 mg, as a purple solid).

¹H NMR (500 MHz, CDCl₃): δ (ppm) = 8.72–8.70 (m, 2H), 8.02 (dd, *J* = 7.7 and 1.7 Hz, 1H), 7.83 (dd, *J* = 8.0 and 1.1 Hz, 1H), 7.69–7.62 (m, 3H), 7.57 (td, *J* = 7.6 and 1.2 Hz, 1H), 7.49 (td, *J* = 7.8 and 1.7 Hz, 1H).

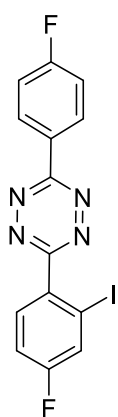
3-(2-Chlorophenyl)-6-phenyl-1,2,4,5-tetrazine (176) CAS: 74115-26-7



Rf = 0.45 (CH₂Cl₂/Heptane: 1/1). Isolated yield: 35% (23 mg, as a purple solid).

¹H NMR (500 MHz, CD₂Cl₂): δ (ppm) = 8.69–8.67 (m, 2H), 8.05 (dd, *J* = 7.4 and 2.0 Hz, 1H), 7.71–7.64 (m, 4H), 7.61–7.54 (m, 2H).

3-(4-Fluoro-6-Iodophenyl)-6-(4-fluorophenyl)-1,2,4,5-tetrazine (178a)



¹H NMR (300 MHz, CDCl₃): δ (ppm) = 8.46–8.40 (m, 1H), 7.88–7.84 (m, 1H), 7.71–

Rf = 0.36 (CH₂Cl₂/Heptane: 1/1). Isolated yield: 51% (50 mg, as a purple solid).

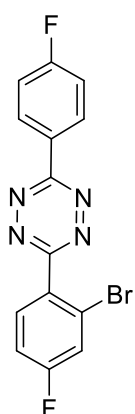
¹H NMR (500 MHz, CDCl₃): δ (ppm) = 8.74–8.71 (m, 2H), 8.03 (dd, *J* = 8.7 and 5.7 Hz, 1H), 7.85 (dd, *J* = 8.0 and 2.6 Hz, 1H), 7.35–7.30 (m, 3H).

¹⁹F{¹H} NMR (470 MHz, CDCl₃): δ (ppm) = –105.3 (1F), –107.3 (1F).

¹³C NMR (125 MHz, CD₂Cl₂): δ (ppm) = 167.6 (d, *J* = 254.1 Hz), 167.1, 164.9 (d, *J* = 256.7 Hz), 163.0, 134.0 (d, *J* = 3.5 Hz), 133.4 (d, *J* = 9.1 Hz), 131.3 (d, *J* = 9.2 Hz), 128.9 (d, *J* = 24.3 Hz), 128.4 (d, *J* = 3.2 Hz), 117.2 (d, *J* = 22.3 Hz), 116.7 (d, *J* = 21.5 Hz), 95.8 (d, *J* = 8.4 Hz).

HRMS + p ESI (*m/z*) [*M*+*H*]⁺ calcd for C₁₄H₈F₂IN₄: 396.97562; Found: 396.97519.

3-(4-Fluoro-6-bromophenyl)-6-(4-fluorophenyl)-1,2,4,5-tetrazine (178b)



Rf = 0.36 (CH₂Cl₂/Heptane: 2/3). Isolated yield: 50% (43 mg, as a purple solid).

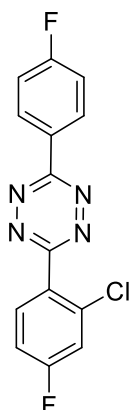
¹H NMR (400 MHz, CDCl₃): δ (ppm) = 8.74–8.71 (m, 2H), 8.06 (dd, *J* = 8.7 and 5.9 Hz, 1H), 7.58 (dd, *J* = 8.2 and 2.5 Hz, 1H), 7.35–7.27 (m, 3H).

¹⁹F{¹H} NMR (470 MHz, CDCl₃): δ (ppm) = –105.3 (1F), –106.3 (1F).

¹³C NMR (125 MHz, CDCl₃): δ (ppm) = 167.2 (d, *J* = 255.2 Hz), 165.8, 165.1 (d, *J* = 256.9 Hz), 162.5, 133.7 (d, *J* = 9.2 Hz), 130.9 (d, *J* = 9.0 Hz), 130.0 (d, *J* = 3.5 Hz), 127.7 (d, *J* = 3.0 Hz), 123.3 (d, *J* = 9.9 Hz), 122.2 (d, *J* = 24.8 Hz), 116.9 (d, *J* = 22.1 Hz), 115.7 (d, *J* = 21.5 Hz).

HRMS + p ESI (*m/z*) [*M*+*H*]⁺ calcd for C₁₄H₈BrF₂N₄: 348.98949; Found: 348.98915.

3-(4-Fluoro-6-chlorophenyl)-6-(4-fluorophenyl)-1,2,4,5-tetrazine (178c)



Rf = 0.33 (CH₂Cl₂/Heptane: 2/3). Isolated yield: 45% (34 mg, as a purple solid).

¹H NMR (400 MHz, CDCl₃): δ (ppm) = 8.74–8.70 (m, 2H), 8.10 (dd, *J* = 8.7 and 5.9 Hz, 1H), 7.39 (dd, *J* = 8.4 and 2.5 Hz, 1H), 7.34–7.30 (m, 2H), 7.28–7.23 (m, 1H).

¹⁹F{¹H} NMR (470 MHz, CDCl₃): δ (ppm) = –105.3 (1F), –106.0 (1F).

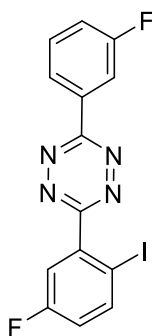
¹³C NMR (125 MHz, CDCl₃): δ (ppm) = 167.2 (d, *J* = 255.0 Hz), 165.3 (d, *J* = 256.2 Hz), 165.1, 162.5, 135.3 (d, *J* = 10.7 Hz), 133.8 (d, *J* = 9.6 Hz), 130.9 (d, *J* = 9.2 Hz), 128.1 (d, *J* = 3.7 Hz), 127.7 (d, *J* = 3.2 Hz), 119.0 (d, *J* = 25.0 Hz), 116.9 (d, *J* = 22.2 Hz), 115.2 (d, *J* = 21.6 Hz).

HRMS + p ESI (*m/z*) [*M*+*H*]⁺ calcd for C₁₄H₈ClF₂N₄: 305.04001; Found: 305.03974.

3-(3-Fluoro-6-iodophenyl)-6-(3-fluorophenyl)-1,2,4,5-tetrazine (179a)

Rf = 0.2 (CH₂Cl₂/Pentane: 3/7). Isolated yield: 35% (35 mg, as a purple solid).

¹H NMR (400 MHz, CDCl₃): δ (ppm) = 8.52 (ddd, *J* = 7.8, 1.6 and 1.0 Hz, 1H), 8.41 (ddd, *J* = 9.7, 2.6 and 1.5 Hz, 1H), 8.08 (dd, *J* = 8.8 and 5.3 Hz, 1H), 7.78 (dd, *J* = 8.9 and 3.0 Hz, 1H), 7.62 (td, *J* = 8.1 and 5.7 Hz, 1H), 7.38 (tdd, *J* = 8.3, 2.7 and 1.0 Hz, 1H), 7.07 (ddd, *J* = 8.7, 7.8 and 3.0 Hz, 1H).



¹⁹F{¹H} NMR (470 MHz, CDCl₃): δ (ppm) = -110.7 (1F), -112.4 (1F).

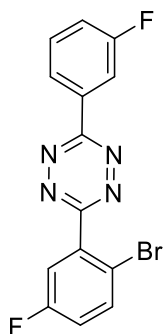
¹³C NMR (101 MHz, CDCl₃): δ (ppm) = 166.8 (d, *J* = 2.4 Hz), 164.7 (d, *J* = 247.7 Hz), 164.3 (d, *J* = 250.1 Hz), 162.7 (d, *J* = 3.2 Hz), 142.8 (d, *J* = 7.6 Hz), 138.5 (d, *J* = 7.7 Hz), 133.7 (d, *J* = 8.2 Hz), 131.2 (d, *J* = 8.0 Hz), 124.4 (d, *J* = 3.1 Hz), 120.5 (d, *J* = 21.3 Hz), 120.2 (d, *J* = 21.6 Hz), 119.2 (d, *J* = 24.3 Hz), 115.6 (d, *J* = 24.0 Hz), 88.7 (d, *J* = 3.7 Hz).

HRMS + p ESI (m/z) [M+H]⁺ calcd for C₁₄H₈F₂IN₄: 396.97562; Found: 396.97516.

3-(3-Fluoro-6-bromophenyl)-6-(3-fluorophenyl)-1,2,4,5-tetrazine (179b)

Rf = 0.35 (CH₂Cl₂/Pentane: 3/7). Isolated yield: 35% (30 mg, as a purple solid).

¹H NMR (500 MHz, CDCl₃): δ (ppm) = 8.52 (d, *J* = 7.8 Hz, 1H), 8.41 (d, *J* = 9.5 Hz, 1H), 7.81–7.78 (m, 2H), 7.62 (td, *J* = 8.0 and 5.6 Hz, 1H), 7.38 (td, *J* = 8.3 and 2.7 Hz, 1H), 7.22 (td, *J* = 8.2 and 3.1 Hz, 1H).



¹⁹F{¹H} NMR (470 MHz, CDCl₃): δ (ppm) = -110.7 (1F), -113.1 (1F).

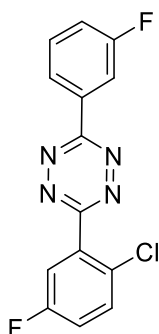
¹³C NMR (125 MHz, CD₂Cl₂): δ (ppm) = 166.5 (d, *J* = 2.3 Hz), 164.9 (d, *J* = 246.8 Hz), 163.5 (d, *J* = 248.6 Hz), 163.2 (d, *J* = 3.2 Hz), 136.6 (d, *J* = 7.8 Hz), 135.6 (d, *J* = 8.2 Hz), 134.2 (d, *J* = 8.3 Hz), 131.8 (d, *J* = 7.9 Hz), 124.7 (d, *J* = 3.0 Hz), 120.7 (d, *J* = 21.5 Hz), 120.5 (d, *J* = 22.2 Hz), 119.8 (d, *J* = 25.1 Hz), 117.2 (d, *J* = 3.4 Hz), 115.7 (d, *J* = 24.0 Hz).

HRMS + p ESI (m/z) [M+H]⁺ calcd for C₁₄H₈BrF₂N₄: 348.98949; Found: 348.98911.

3-(3-Fluoro-6-chlorophenyl)-6-(3-fluorophenyl)-1,2,4,5-tetrazine (179c)

Rf = 0.4 (CH₂Cl₂/Pentane: 3/7). Isolated yield: 28% (21 mg, as a purple solid).

¹H NMR (400 MHz, CDCl₃): δ (ppm) = 8.51 (d, *J* = 7.9 Hz, 1H), 8.40 (dt, *J* = 9.6 and 2.0 Hz, 1H), 7.83 (dd, *J* = 8.5 and 3.1 Hz, 1H), 7.65–7.59 (m, 2H), 7.38 (td, *J* = 8.0 and 2.5 Hz, 1H), 7.31–7.26 (m, 1H).



¹⁹F{¹H} NMR (470 MHz, CDCl₃): δ (ppm) = -110.7 (1F), -113.6 (1F).

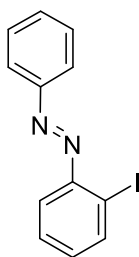
¹³C NMR (125 MHz, CD₂Cl₂): δ (ppm) = 165.8 (d, *J* = 2.2 Hz), 164.9 (d, *J* = 254.4 Hz), 163.2 (d, *J* = 3.2 Hz), 162.9 (d, *J* = 255.6 Hz), 134.2 (d, *J* = 8.3 Hz), 133.6 (d, *J* = 8.2 Hz), 133.4 (d, *J* = 8.2 Hz), 131.8 (d, *J* = 8.1 Hz), 129.3 (d, *J* = 3.5 Hz), 124.7 (d, *J* = 3.0 Hz), 120.7 (d, *J* = 21.4 Hz), 120.4 (d, *J* = 22.8 Hz), 119.5 (d, *J* = 25.3 Hz), 115.7 (d, *J* = 24.1 Hz).

HRMS + p ESI (*m/z*) [M+H]⁺ calcd for C₁₄H₈ClF₂N₄: 305.04001; Found: 305.03989.

1-(2-Iodophenyl)-2-phenyl-diazene (22a)^[29] CAS: 51343-11-4

Rf = 0.4 (CH₂Cl₂/Heptane: 2/3). Isolated yield: 39% (46 mg, as an orange solid).

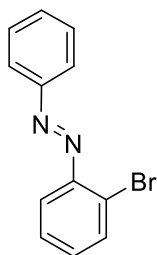
¹H NMR (400 MHz, CDCl₃): δ (ppm) = 8.04 (dd, *J* = 7.9 and 1.3 Hz, 1H), 8.02–7.99 (m, 2H), 7.64 (dd, *J* = 8.0 and 1.6 Hz, 1H), 7.57–7.50 (m, 3H), 7.45–7.41 (m, 1H), 7.19–7.15 (m, 1H).



1-(2-Bromophenyl)-2-phenyl-diazene (22bc) CAS: 4103-29-1

Rf = 0.4 (CH₂Cl₂/Heptane: 2/3). Isolated yield: 60% (39 mg, as an orange solid).

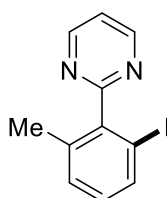
¹H NMR (400 MHz, CDCl₃): δ (ppm) = 7.99 (dd, *J* = 8.1 and 1.7 Hz, 2H), 7.76 (dd, *J* = 7.9 and 1.4 Hz, 1H), 7.68 (dd, *J* = 8.0 and 1.7 Hz, 1H), 7.56–7.50 (m, 3H), 7.40 (td, *J* = 7.6 and 1.4 Hz, 1H), 7.32 (td, *J* = 7.5 and 1.7 Hz, 1H).



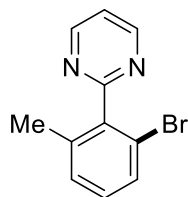
2-(2-Iodo-6-methylphenyl)-pyrimidine (180a)^[68] CAS: 1245636-15-0

Rf = 0.3 (CH₂Cl₂/Heptane: 3/7). Isolated yield: 65% (48 mg, as a colourless oil).

¹H NMR (400 MHz, CDCl₃): δ (ppm) = 8.90 (d, *J* = 4.9 Hz, 2H), 7.76 (dd, *J* = 7.9 and 0.4 Hz, 1H), 7.32 (t, *J* = 4.9 Hz, 1H), 7.25 (d, *J* = 7.8 Hz, 1H), 7.01 (t, *J* = 7.8 Hz, 1H), 2.12 (s, 3H).



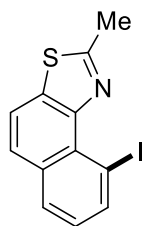
2-(2-Bromo-6-methylphenyl)-pyrimidine (180b) ^[69] CAS: 1200123-98-3



R_f = 0.3 (CH₂Cl₂/Heptane: 1/1). Isolated yield: 61% (38 mg, as a colourless oil).

¹H NMR (400 MHz, CDCl₃): δ (ppm) = 8.90 (d, *J* = 4.9 Hz, 2H), 7.49 (d, *J* = 7.7 and 0.6 Hz, 1H), 7.32 (t, *J* = 4.9 Hz, 1H), 7.24–7.21 (m, 1H), 7.17 (t, *J* = 7.7 Hz, 1H), 2.11 (s, 3H).

9-Iodo-2-methyl-naphthol[1,2-*d*]thiazole (181a)



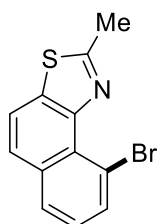
R_f = 0.33 (Ethyl acetate/Heptane: 1.5/8.5). Isolated yield: 56% (45 mg, as a white solid).

¹H NMR (500 MHz, CDCl₃): δ (ppm) = 8.40 (d, *J* = 7.4 Hz, 1H), 7.92 (dd, *J* = 8.3 and 5.6 Hz, 2H), 7.75 (d, *J* = 8.7 Hz, 1H), 7.16 (t, *J* = 7.7 Hz, 1H), 2.97 (s, 3H).

¹³C NMR (101 MHz, CDCl₃): δ (ppm) = 163.0, 147.0, 141.9, 134.9, 133.3, 129.4, 128.6, 126.5, 126.1, 119.7, 88.7, 20.5.

HRMS + p ESI (*m/z*) [*M*+*H*]⁺ calcd for C₁₂H₉INS: 325.94949; Found: 325.94913.

9-Chloro-2-methyl-naphthol[1,2-*d*]thiazole (181c)



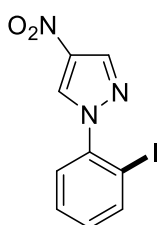
R_f = 0.37 (Ethyl acetate/Heptane: 1.5/8.5). Isolated yield: 53% (31 mg, as a yellow solid).

¹H NMR (400 MHz, CDCl₃): δ (ppm) = 7.93 (d, *J* = 8.7 Hz, 1H), 7.86 (dd, *J* = 8.1 and 1.0 Hz, 1H), 7.79 (d, *J* = 8.7 Hz, 1H), 7.74 (dd, *J* = 7.5 and 1.2 Hz, 1H), 7.45 (t, *J* = 7.8 Hz, 1H), 2.99 (s, 3H).

¹³C NMR (101 MHz, CDCl₃): δ (ppm) = 164.3, 147.6, 135.5, 134.4, 130.3, 129.7, 127.8, 126.1, 125.8, 125.7, 120.0, 20.7.

HRMS + p ESI (*m/z*) [*M*+*H*]⁺ calcd for C₁₂H₉CINS: 234.01387; Found: 234.01377.

1-(2-Iodophenyl)-4-nitro-1*H*-pyrazole (182a)



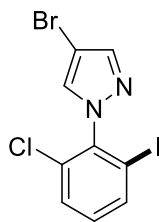
R_f = 0.25 (CH₂Cl₂/Heptane: 3/7). Isolated yield: 62% (49 mg, as a white solid).

¹H NMR (400 MHz, CD₂Cl₂): δ (ppm) = 8.45 (d, *J* = 0.5 Hz, 1H), 8.27 (s, 1H), 8.03 (dd, *J* = 8.0 and 1.3 Hz, 1H), 7.54 (td, *J* = 7.6 and 1.4 Hz, 1H), 7.46 (dd, *J* = 7.9 and 1.7 Hz, 1H), 7.28 (t, *J* = 8.0 and 1.7 Hz, 1H).

¹³C NMR (101 MHz, CD₂Cl₂): δ (ppm) = 142.4, 140.9, 140.5, 136.9, 132.1, 131.0, 130.0, 128.4, 94.3.

HRMS + p ESI (*m/z*) [*M*+*H*]⁺ calcd for C₉H₇IN₃O₂: 315.95775; Found: 315.95757.

1-(2-chloro-6-iodophenyl)-4-bromo-1H-pyrazole (190)



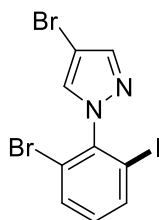
Rf = 0.25 (Ethyl acetate/Heptane: 1/9). Isolated yield: 80% (76 mg, as a white solid).

^1H NMR (400 MHz, CDCl_3): δ (ppm) = 7.86 (dd, J = 8.0 and 1.3 Hz, 1H), 7.75 (s, 1H), 7.55 (s, 1H), 7.51 (dd, J = 8.1 and 1.3 Hz, 1H), 7.13 (t, J = 8.0 Hz, 1H).

^{13}C NMR (101 MHz, CDCl_3): δ (ppm) = 141.8, 140.5, 138.3, 133.6, 132.1, 131.2, 130.4, 98.5, 95.0.

HRMS + p ESI (m/z) $[\text{M}+\text{H}]^+$ calcd for $\text{C}_9\text{H}_6\text{BrClIN}_2$: 382.84421; Found: 382.84384.

1-(2-bromo-6-iodophenyl)-4-bromo-1H-pyrazole (183a)



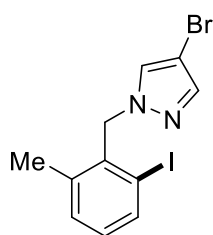
Rf = 0.4 (CH_2Cl_2 /Heptane: 1/9). Isolated yield: 70% (75 mg, as a white solid).

^1H NMR (400 MHz, CDCl_3): δ (ppm) = 7.90 (dd, J = 8.0 and 1.3 Hz, 1H), 7.75 (s, 1H), 7.68 (dd, J = 8.1 and 1.3 Hz, 1H), 7.55 (d, J = 0.5 Hz, 1H), 7.05 (t, J = 8.0 Hz, 1H).

^{13}C NMR (101 MHz, CDCl_3): δ (ppm) = 141.8, 141.7, 139.0, 133.6, 132.4, 131.0, 122.9, 98.4, 95.0.

HRMS + p ESI (m/z) $[\text{M}+\text{H}]^+$ calcd for $\text{C}_9\text{H}_6\text{Br}_2\text{IN}_2$: 426.79369. Found 426.79311.

4-Bromo-1-[(2-iodo-6-methylphenyl)methyl]-1H-pyrazole (184a)



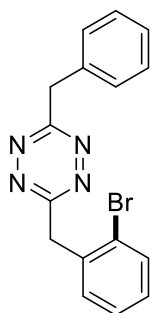
Rf = 0.37 (Ethyl acetate/Heptane: 1.5/8.5). Isolated yield: 51% (48 mg, as a white solid).

^1H NMR (400 MHz, CDCl_3): δ (ppm) = 7.78 (d, J = 7.6 Hz, 1H), 7.47 (s, 1H), 7.25 (s, 1H), 7.20 (d, J = 7.7 Hz, 1H), 6.97 (t, J = 7.7 Hz, 1H), 5.5 (s, 2H), 2.37 (s, 3H).

^{13}C NMR (101 MHz, CDCl_3): δ (ppm) = 140.4, 139.8, 138.2, 135.6, 131.4, 130.8, 129.0, 103.0, 93.2, 59.0, 20.9.

HRMS + p ESI (m/z) $[\text{M}+\text{H}]^+$ calcd for $\text{C}_{11}\text{H}_{11}\text{BrIN}_2$: 376.91448. Found: 376.91405.

3-(2-Bromophenylmethyl)-6-(phenylmethyl)-1,2,4,5-tetrazine (185b)



Rf = 0.35 (Ethyl acetate/Heptane: 1/9). Isolated yield: 54% (46 mg, as a purple solid).

^1H NMR (400 MHz, CDCl_3): δ (ppm) = 7.58 (dd, J = 8.0 and 1.2 Hz, 1H), 7.42–7.38 (m, 3H), 7.34–7.29 (m, 3H), 7.28–7.25 (m, 1H), 7.16 (td, J = 7.7 and 1.7 Hz, 1H), 4.79 (s, 2H), 4.62 (s, 2H).

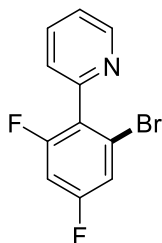
^{13}C NMR (101 MHz, CDCl_3): δ (ppm) = 169.2, 168.7, 135.9, 135.6, 133.2, 132.0, 129.4, 129.3, 129.0, 127.9, 127.5, 125.1, 41.4, 41.3.

HRMS + p ESI (m/z) $[\text{M}+\text{H}]^+$ calcd for $\text{C}_{16}\text{H}_{14}\text{BrN}_4$: 341.03964; Found: 341.03923.

2-(2,4-Difluorophenyl)-6-bromo-pyridine (186b)

R_f = 0.35 (Ethyl acetate/Heptane: 3/7). Isolated yield: 51% (34 mg, as a colourless oil).

¹H NMR (500 MHz, CDCl₃): δ (ppm) = 8.75 (dd, *J* = 4.8 and 0.6 Hz, 1H), 7.80 (td, *J* = 7.7 and 1.8 Hz, 1H), 7.38–7.33 (m, 2H), 7.26 (dt, *J* = 8.0 and 2.2 Hz, 1H), 6.92 (td, *J* = 8.9 and 2.5 Hz, 1H).



¹⁹F{¹H} NMR (470 MHz, CDCl₃): δ (ppm) = -107.7 (d, *J* = 7.3 Hz, 1F), -108.6 (d, *J* = 7.3 Hz, 1F).

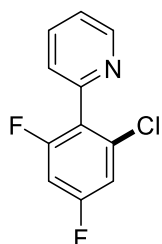
¹³C NMR (125 MHz, CDCl₃): δ (ppm) = 163.4 (dd, *J* = 252.9 and 13.4 Hz), 161.7 (dd, *J* = 252.5 and 13.1 Hz), 152.9, 149.8, 136.5, 126.8 (dd, *J* = 18.7 and 4.4 Hz), 125.8, 124.1 (dd, *J* = 11.7 and 5.4 Hz), 123.3, 116.6 (dd, *J* = 24.3 and 3.9 Hz), 104.1 (dd, *J* = 26.8 and 25.1 Hz).

HRMS + p ESI (*m/z*) [M+H]⁺ calcd for C₁₁H₇BrF₂N: 269.97244; Found: 269.97211.

2-(2,4-Difluorophenyl)-6-chloro-pyridine (186c)

R_f = 0.3 (Ethyl acetate/Heptane: 3/7). Isolated yield: 70% (39 mg, as a colourless oil).

¹H NMR (400 MHz, CDCl₃): δ (ppm) = 8.75 (d, *J* = 4.4 Hz, 1H), 7.80 (td, *J* = 7.7 and 1.8 Hz, 1H), 7.39 (dd, *J* = 7.8 and 1.0 Hz, 1H), 7.34 (ddd, *J* = 7.6, 4.9 and 1.2 Hz, 1H), 7.08 (dt, *J* = 8.3, 2.4, 1H), 6.87 (td, *J* = 8.9 and 2.5 Hz, 1H).



¹⁹F{¹H} NMR (470 MHz, CD₂Cl₂): δ (ppm) = -109.4 (d, *J* = 7.0 Hz, 1F), -109.5 (d, *J* = 7.0 Hz, 1F).

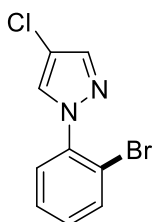
¹³C NMR (101 MHz, CDCl₃) δ (ppm) = 163.5 (dd, *J* = 252.1 and 14.4 Hz), 162.2 (dd, *J* = 249.2 and 11.17 Hz), 151.5, 149.8, 136.5, 135.3 (dd, *J* = 12.7 and 6.6 Hz), 125.9, 125.0 (dd, *J* = 19.0 and 4.2 Hz), 123.3, 113.6 (dd, *J* = 24.7 and 4.0 Hz), 103.6 (dd, *J* = 26.8 and 25.2 Hz).

HRMS + p ESI (*m/z*) [M+H]⁺ calcd for C₁₁H₇F₂NCl: 226.02296. Found: 226.02279.

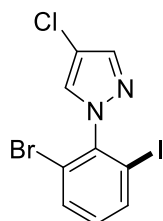
1-(2-Bromophenyl)-4-chloro-1H-pyrazole (187b) CAS: 1780323-95-6

R_f = 0.35 (Ethyl acetate/Heptane: 1.5/8.5). Isolated yield: 46% (29 mg, as a white solid).

¹H NMR (400 MHz, CDCl₃): δ (ppm) = 7.82 (s, 1H), 7.71 (dd, *J* = 8.0 and 1.4 Hz, 1H), 7.67 (s, 1H), 7.49 (dd, *J* = 7.9 and 1.8 Hz, 1H), 7.43 (td, *J* = 7.6 and 1.4 Hz, 1H), 7.30 (td, *J* = 7.8 and 1.8 Hz, 1H).



1-(2-Bromo-5-iodophenyl)-4-chloro-1H-pyrazole (189)



R_f = 0.37 (Ethyl acetate/Heptane: 1.5/8.5). Isolated yield: 90% (86 mg, as a white solid).

¹H NMR (400 MHz, CDCl₃): δ (ppm) = 7.86 (dd, *J* = 8.0 and 1.3 Hz, 1H), 7.75 (s, 1H), 7.55 (s, 1H), 7.51 (dd, *J* = 8.1 and 1.3 Hz, 1H), 7.13 (t, *J* = 8.1 Hz, 1H).

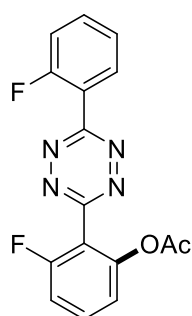
¹³C NMR (101 MHz, CDCl₃): δ (ppm) = 141.8, 140.5, 138.3, 133.6, 132.1, 131.2, 130.4, 98.5, 95.0.

HRMS + p ESI (*m/z*) [M+H]⁺ calcd for C₉H₆BrClI₂: 382.84421; Found: 382.84380.

2) General procedure for the acetoxylation

As a typical experiment, in a microwave reaction vessel equipped with a magnetic stirring bar was charged with 3,6-bis(2-fluorophenyl)-1,2,4,5-tetrazine **177** (1 equiv, 0.25 mmol), 5 mol% Pd(OAc)₂, and PIDA (1,2 equiv, 0.3 mmol) in HOAc [0.125 M] under air. The mixture was heated at 110 °C during 30 min under microwaves irradiations (200 Watts). After cooling down at room temperature, the solvent was removed in vacuum and the residue was analysed by ¹H and ¹⁹F NMR to determine the conversion and the selectivity of the acetoxylation reaction. The crude mixture was purified by silica gel column chromatography using an appropriate ratio of eluent (DCM/Heptane) to afford the desired product.

3-(2-Fluoro-6-acetylphenyl)-6-(2-fluorophenyl)-1,2,4,5-tetrazine (177-OAc)



R_f = 0.3 (CH₂Cl₂/Heptane: 3/1). Isolated yield: 40% (33 mg, as a purple solid).

¹H NMR (500 MHz, CD₂Cl₂): δ (ppm) = 8.36 (td, *J* = 7.7 and 1.7 Hz, 1H), 7.72–7.63 (m, 2H), 7.46 (td, *J* = 7.8 and 0.9 Hz, 1H), 7.37 (dd, *J* = 11.0 and 8.4 Hz, 1H), 7.28 (t, *J* = 8.7 Hz, 1H), 7.20 (d, *J* = 8.3 Hz, 1H), 2.18 (s, 3H).

¹⁹F{¹H} NMR (470 MHz, CD₂Cl₂): δ (ppm) = -112.7 (1F), -113.8 (1F).

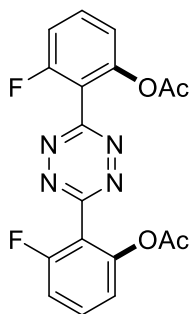
¹³C NMR (125 MHz, CD₂Cl₂): δ (ppm) = 169.5, 164.0 (d, *J* = 5.7 Hz), 162.2 (d, *J* = 259.3 Hz), 162.8 (d, *J* = 255.7 Hz), 162.2 (d, *J* = 3.9 Hz), 150.7 (d, *J* = 4.3 Hz), 135.1 (d, *J* = 8.8 Hz), 133.7 (d, *J* = 10.2 Hz), 132.2 (d, *J* = 0.7 Hz), 125.6 (d, *J* = 3.9 Hz), 121.0 (d, *J* = 9.9 Hz), 120.5 (d, *J* = 23.6 Hz), 118.0 (d, *J* = 21.6 Hz), 116.4 (d, *J* = 14.9 Hz), 114.8 (d, *J* = 21.5 Hz), 21.0.

HRMS + p ESI (*m/z*) [M+Na]⁺ calcd for C₁₆H₁₀F₂N₄O₂Na: 351.06640; Found: 351.06613.

3-(2-Fluoro-6-acetylphenyl)-6-(2-fluorophenyl)-1,2,4,5-tetrazine (177-OAc)

R_f = 0.20 (CH₂Cl₂/Heptane: 3/1). Isolated yield: 40% (39 mg, as a purple solid).

¹H NMR (500 MHz, CD₂Cl₂): δ (ppm) = 7.70–7.65 (m, 2H), 7.29 (t, *J* = 9.0 Hz, 2H), 7.21 (d, *J* = 8.3 Hz, 2H), 2.17 (s, 6H).



¹⁹F{¹H} NMR (470 MHz, CD₂Cl₂): δ (ppm) = -113.8 (2F).

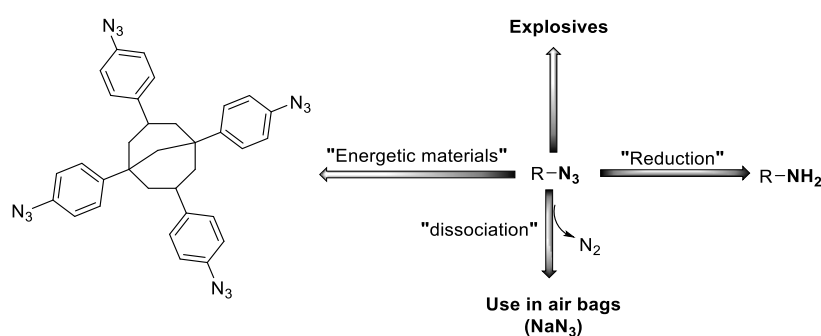
¹³C NMR (125 MHz, CD₂Cl₂): δ (ppm) = 169.4, 162.8 (d, *J* = 255.9 Hz), 162.4 (d, *J* = 3.1 Hz), 150.7 (d, *J* = 4.3 Hz), 133.9 (d, *J* = 10.3 Hz), 120.5 (d, *J* = 3.5 Hz), 116.2 (d, *J* = 14.8 Hz), 114.8 (d, *J* = 21.4 Hz), 21.0.

HRMS + p ESI (*m/z*) [M+Na]⁺ calcd for C₁₈H₁₂F₂N₄O₄Na: 409.07188; Found: 409.07130.

Chapter 2: *bis*-Tetrazo[1,2-*b*]indazoles: access to highly nitrogen-containing polyaromatics

I. Introduction

The first organic azide, phenyl azide was discovered by Peter Griess in 1864 (Scheme 1).^[70] Since then, there has been a lot of interest in these versatile, energy-dense molecules.^[71] Generally, the addition of an azido group often results in an increase of energy for the resulting organic compound ranging between 290 to 355 kJ/mol.^[72] Organic azides possess the suitable traits that classify some of them as efficient energetic materials. The reactivity of inorganic azides relies in the highly energetic N_3 polarized π -bond, which involves strong exothermic dissociation reactions and release of molecular dinitrogen^[73]. In fact, the latter compounds can be suitable N_2 releasing products in air bags and explosives. Additionally, the reduction of azides allows them to be used as precursors to amine derivatives (Scheme 1)^[74].

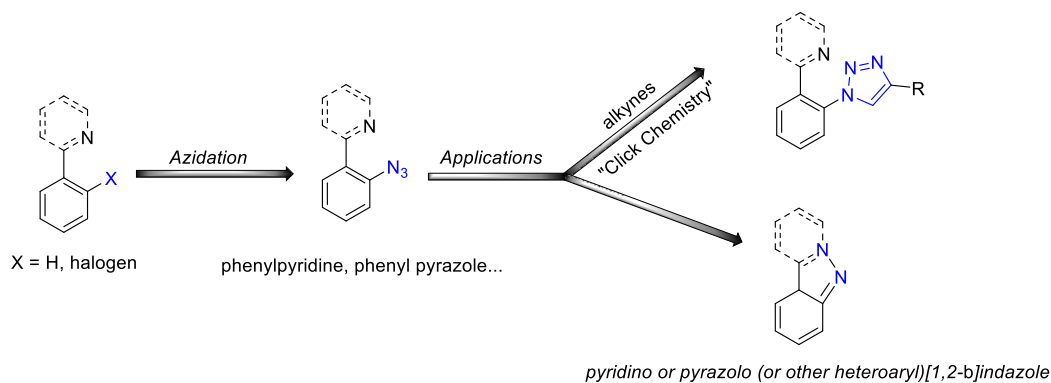


Scheme 1. Some applications of organic and inorganic azides

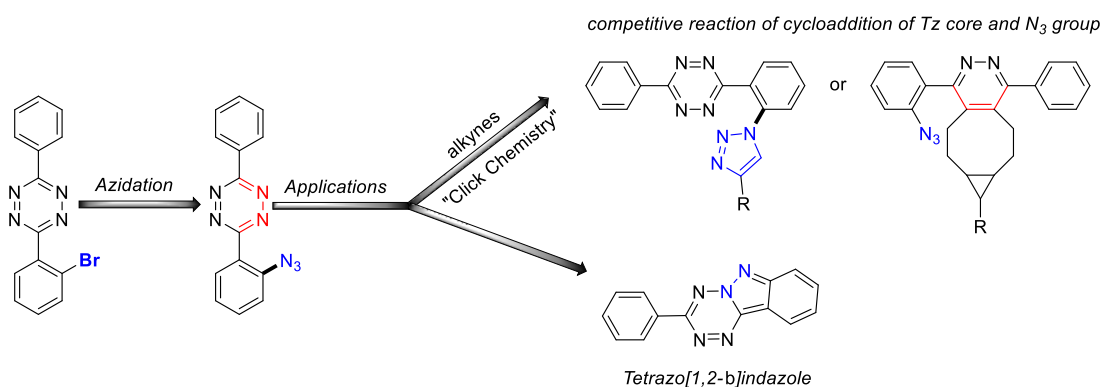
In addition to their physical properties, organic azides are widely employed reagents in multistep synthesis. Notably, they are involved in the synthesis of heterocycles like triazoles and tetrazoles, involved in easy reaction from the “click chemistry” concept (Scheme 2, (a)). These heteroaryl compounds mainly served as building blocks in pharmaceuticals. The nitrogen-containing heteroaryl azides are used as precursors for pyridinio- or pyrazolo[1.2-*b*]indazole and heteroaryl derivatives, which are employed in medicine (Scheme 2, (b)).^[75] Based on these applications, we envisioned that azide groups on the novel family of *s*-tetrazines,^[3] can be of great significance. This chapter reports

the synthesis of azido *s*-tetrazines and their synthetic applications in “click chemistry” and the synthesis of novel tetrazo[1,2-*b*]indazole.

a) Previous work: major applications of heteroaryl organic azides



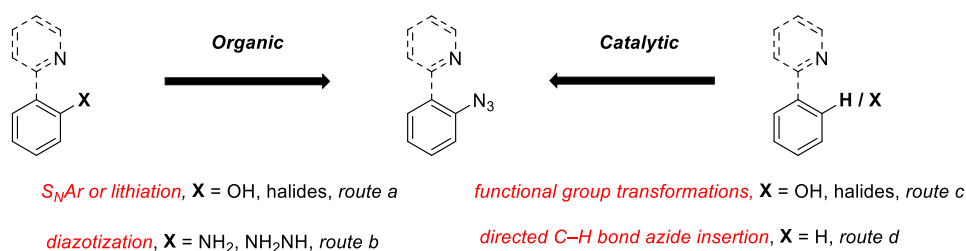
b) Our work: major applications of azido *s*-tetrazines



Scheme 2. Azidation reaction and applications (top) and general approach of our work (bottom)

II. Insertion of azides on heteroaryl aromatic

The synthesis of aryl and heteroaryl azides is extensively documented and proceeds mostly *via* organic (Scheme 3, left) and catalytic (Scheme 3, right) strategies.^[76] Organic methodologies are substitution reactions using organic or organometallic reagents or alternatively diazotization of aromatic amines (Scheme 3, routes *a* and *b*, respectively). Catalytic pathways for azide formation use transition metal-catalyzed functional group exchange, or chelation assisted C– N_3 bond formation *via* transition metal catalyzed C–H bond activation on heteroarenes (Scheme 3, routes *c* and *d*, respectively).



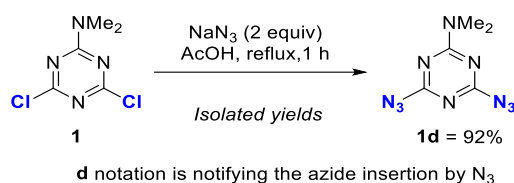
Scheme 3. Organic (left) and catalytic (right) approaches for the synthesis of aryl azides

1) Insertion of azides via organic pathways

A. Azidation by nucleophilic aromatic substitution on arenes

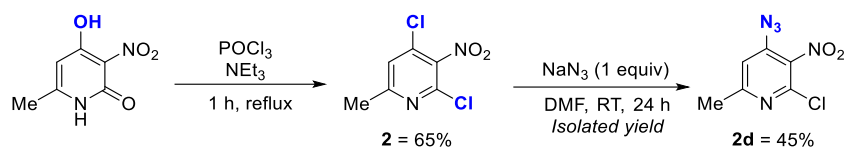
a. Halogen atoms substitution

Displacement of halogen atoms by azide is achieved by direct reaction under suitable conditions. In 1982, Stevens *et al.* isolated the 4,6-diazo-*N,N*-dimethyl-1,3,5-triazin-2-amine **1d** in 92% (Scheme 4).^[77] They prepared **1d** starting from 4,6-chloro-*N,N*-dimethyl-1,3,5-triazin-2-amine **1** by reacting it with 2 equiv of NaN₃, and two azide groups replaced the chlorine atoms on the triazine (HOAc reflux, 1 h)



Scheme 4. Azide insertion by NaN₃ reaction on triazine derivative **1** by chlorine substitution

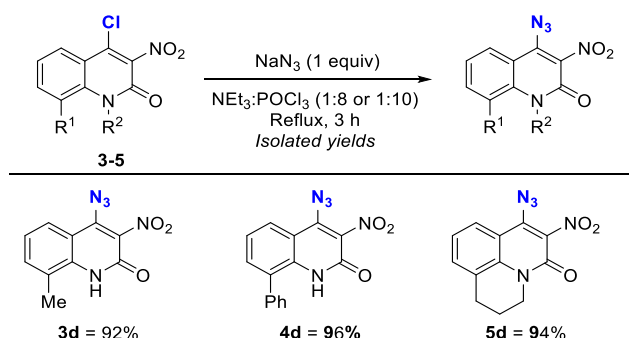
The groups of Wilson and Hojas,^[78] induced the N₃⁻ attack on the 2,4-dichloro-6-methyl-3-nitropyridine **2** to produce the 4-azido-2-chloro-6-methyl-3-nitropyridine **2d**, thus substituting the chlorine atom in 45% yields (Scheme 5). Monoazidation was realized in 45% with 1 equiv of NaN₃ at RT in DMF. Replacing DMF by other organic solvents, such as MeOH or CH₂Cl₂, or by increasing the temperature, afforded the diazido **2d²** derivative with two azides moieties as the major product.^[9a,9b]



Scheme 5. Azide insertion by NaN_3 reaction on pyridine derivative **2** by chlorine substitution

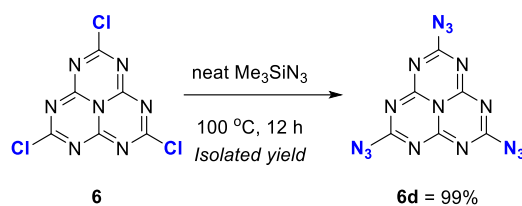
Stadlbauer *et al.* developed the chemistry of azidoquinolone (Scheme 6),^[79] with the synthesis of the 4-azido-8-methyl-3-nitroquinolin-2(1H)-one **3d**, 4-azido-3-nitro-8-phenylquinolin-2(1H)-one **4d**, and 7-azido-6-nitro-2,3-dihydro-1H,5H-pyrido[3,2,1-ij]8quinoline-5-one **5d**, from their corresponding chloro-derivatives **3-5** in 92%, 96% and 94%, respectively.

The reaction also occurred in the presence of other electrophilic groups on the molecule such as carbonyl and nitro, which mainly did not react with N_3^- . The carbon holding the nitro group remained untouched, as the carbonyl group. A co-solvent system of NEt_3 and POCl_3 (1:8 or 1:10) were needed for the reaction to occur under reflux from a 3 h reaction.



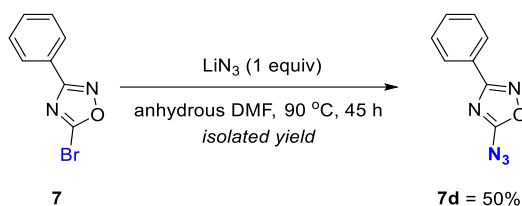
Scheme 6. The azide insertion by NaN_3 reaction on phenyl amide derivative **3-5** by chlorine substitution

Another relevant example is the synthesis of 2,5,8-triazido-heptazine **6d** (Scheme 7).^[80] This heteroaryl azide, which is entirely conjugated and only contains carbon and nitrogen atoms, exhibits visible light-activation photoluminescence and decomposes quickly at 185 °C to produce carbon nitrides enriched in nitrogen. **6d** is obtained by the nucleophilic aromatic substitution of chlorine by azides. 2,5,8-trichloro-heptazine **6** reacts with neat trimethylsilane azide, reacted as both the solvent and azide source, provided the target product **6d** in 99% yields. Heating to 100 °C and 12 h were needed to obtain this high yield.



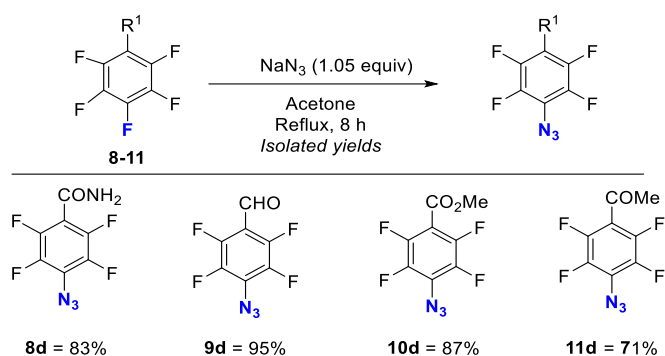
Scheme 7. The azide insertion by Me_3SiN_3 on heptazine **6** by chlorine substitution

Bromine can also be replaced by azide anions. The group of Smith performed the reaction on five-membered heterocyclic ring: 5-bromo-3-phenyl-1,2,4-oxadiazole **7** (Scheme 8).^[81] The substitution of the halide by the azide anion reactions occurs on **7** using a strong N_3^- donor, LiN_3 (1 equiv). To obtain 50% of 3-azido-5-phenyl-1,2,4-oxadiazole **7d**, the reaction was achieved in anhydrous DMF, at 90 °C and for 45 h. Using LiN_3 as the azide source was effective only when the solvent was anhydrous DMF. Replacing LiN_3 by a weaker donor of the azide anion, such as NaN_3 or $n\text{-Bu}_4\text{NN}_3$, did not achieve the reaction, even in DMF.



Scheme 8. The azide insertion by reaction of LiN_3 on phenyl oxadiazole derivative **7** by bromine substitution

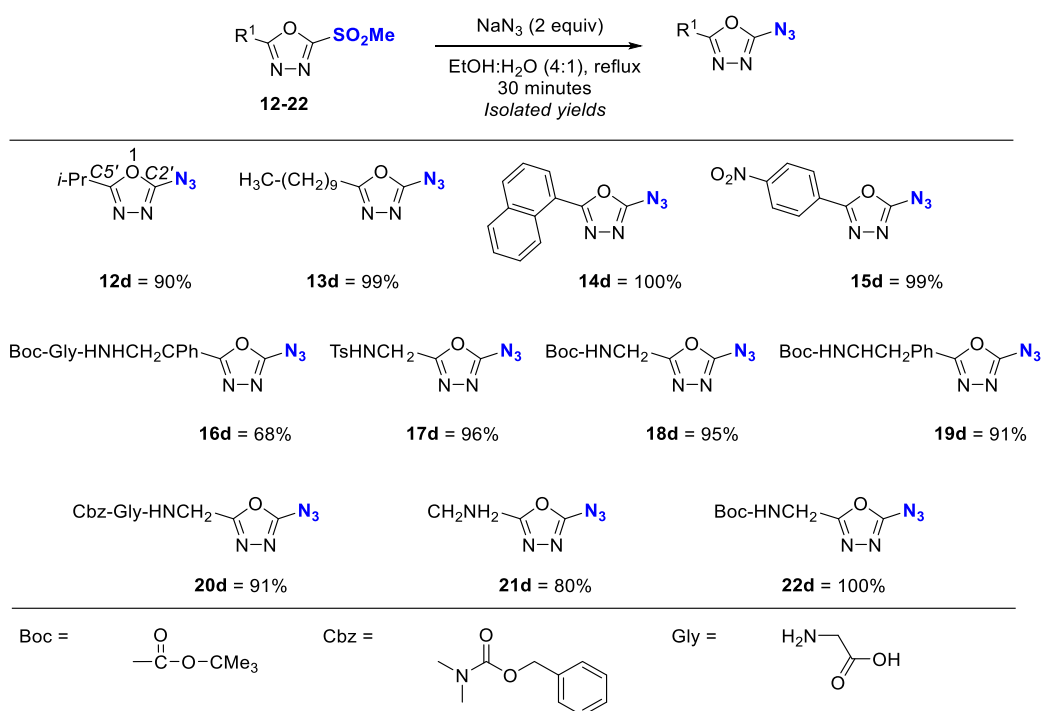
Fluoro-functionalized derivatives have been employed for nucleophilic aromatic substitution. The group of Cai proposed the introduction of azide group on fluorinated compounds and used pentafluorophenyl derivatives as the starting materials (Scheme 9).^[82] The corresponding azide derivatives 2,3,4,5,6-pentafluorobenzamide **8d**, 2,3,4,5,6-pentafluorobenzaldehyde **9d**, methyl 2,3,4,5,6-pentafluorobenzoate **10d** and 1-(perfluorophenyl)ethan-1-one **11d** were obtained by adding 1.05 equiv of the NaN_3 in acetone under reflux for 8 h. Compounds **8d**, **9d**, **10d** and **11d** were isolated in 83%, 95%, 87% and 71%, respectively. The carbonyl group remained untouched because of the high nucleophilic character of fluorine for these substitution, in addition to the presence of strictly 1.05 equiv of NaN_3 , which limited multiple azidation.



Scheme 9. The azide insertion on fluorinated aryls **8-11** by fluorine substitution

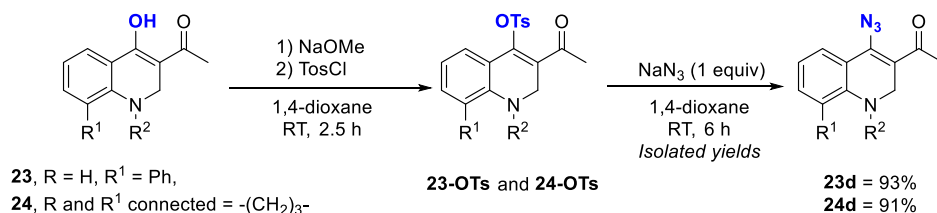
b. Other nucleophilic leaving groups

Several known electron-poor leaving groups such as sulfones, nitro groups and others are reactive towards azidation. Nucleophilic aromatic substitution of functionalized aromatics by azide has been illustrated by Woodward *et al.* with methyl sulfone groups on oxadiazole derivatives **12** to **22**. They were substituted by azide (Scheme 10),^[78b] by using 2 equiv of NaN_3 in ethanol under reflux for 30 minutes. *iso*-Propyl and *n*-undecyl were used as aliphatic substituents at the $C5'$ position of the oxadiazole derivatives **12** and **13**. Their corresponding azide derivatives were obtained in 90% and 99% yields for **12d** and **13d** respectively. Naphthyl and *para*-nitrophenyl groups were employed as the aromatic substituents on **14** and **15**, where azidation was achieved in 100% and 99% to give **14d** and **15d**, respectively. The rest of the molecules **16** to **22** in the series contain protected amine groups as substituents on the $C5'$ position of the oxadiazole. Different protecting groups were used such as Boc and Cbz (structures in Scheme 10). The yields of azidation on these molecules were between 80% and 100% for **17d** to **22d**. Only **16d**, with Boc-Gly as the protecting groups afforded the azide derivative in 68% yields.



Scheme 10. The azide insertion on oxadiazole derivative **12-22** by methyl sulfonate substitution

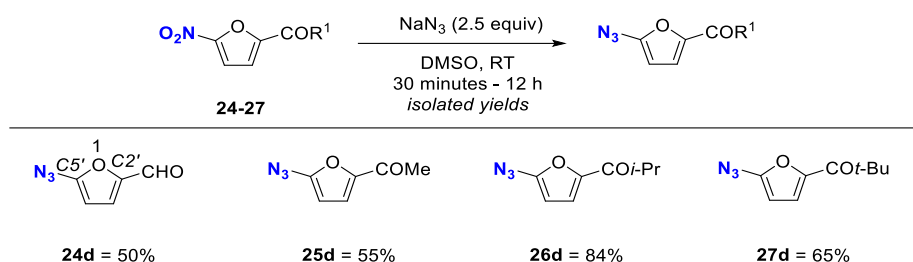
On the other hand, the group of Stadlbauer employed tosylate group-based derivatives as starting materials for azidation (Scheme 11).^[83b] They reported a two-step synthesis of azidoquinoline derivatives from hydroxyquinoline derivatives. The hydroxyl groups on aromatic compounds **23** and **24** were transformed into the corresponding tosylate to give **23-OTs** and **24-OTs**. The addition of 1 equiv of NaN_3 on these compounds affords the azidoquinoline derivatives **23d** and **24d** were obtained in 93% and 91% isolated yields, respectively.



Scheme 11. The azide insertion on quinoline derivatives **23-24** by tosylate substitution

Norris *et al.* used nitroso functionalized furan derivatives as precursors for the introduction of azides by reactions (Scheme 12).^[84] For this approach, 2.5 equiv of NaN_3 were added to the starting materials with different substituents on the carbonyl on the C2' position of the furan derivative. The substitution

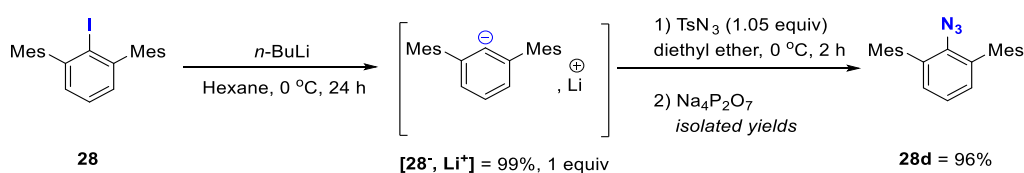
reactions were performed at RT in DMSO, while the time of the reactions depended on the starting material used. Normally, acyl furans with ketone groups on the C2' were generally more well-tolerated than aldehydes. For example, the 5-nitro-2-furaldehyde **24** afforded its azide derivative in 50% yields. On the other hand, the azide derivatives from ketone substituents (Me, *i*-Pr and *t*-Bu) were obtained in 55%, 84% and 65% yields for **25d** to **27d**, respectively.



Scheme 12. The azide insertion on furan derivatives **24-27** by nitro substitution

B. Azidation via lithium organometallic reagents

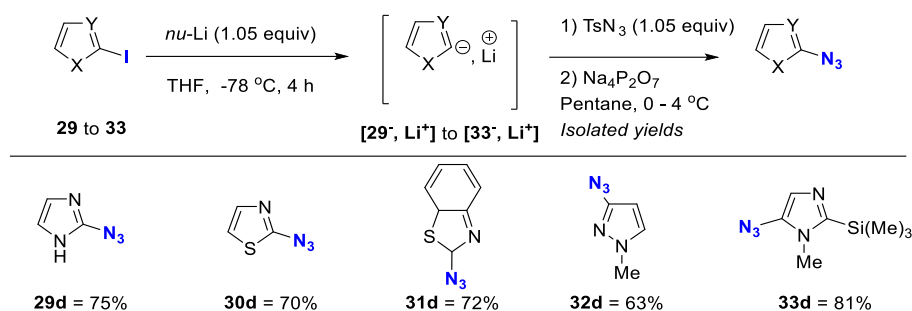
Organo halides transformation into lithium salts that are highly reactive nucleophilic species has been described. Tilley and *al.* adopted lithiation instead of the formation of a Grignard intermediate.^[85] The lithiated salt [**28⁻**, Li⁺] was obtained starting from 2'-iodo-2,6-dimesitylphenyliodide **28** at 0 °C. Compound **28** was lithiated by *n*-BuLi in dry hexane to give the corresponding intermediate salt [**28⁻**, Li⁺] in 99% yields. On [**28⁻**, Li⁺], TsN₃ was added in excess with Na₄P₂O₇ to give the desired aryl azide **28d** in 96% yield (Scheme 13).



Scheme 13. The azide insertion on phenyl derivative **28** by lithiation

The group of Cerini widened the scope of this approach on different five membered heterocycles (Scheme 14).^[86] They performed lithiation from on the starting materials by the addition of *n*-BuLi to obtain the lithiated salts [**29⁻**, Li⁺] to [**33⁻**, Li⁺]. The dissociation of these salts by the addition **29** to **33**

of TsN_3 followed by $\text{Na}_4\text{P}_2\text{O}_7$ lead to the corresponding azides. 2-Azido-1-methyl-1H-imidazole **29d**, 2-azido-1,3-thiazole **30d**, 2-azidobenzo-1,3-thiazole **31d**, 5-azido-1-methyl-1H-pyrazole **32d**, 5-azido-1-methyl-2-(trimethylsilyl)-1H-imidazole **33d** were obtained in 75%, 70%, 72%, 63% and 81%, respectively.

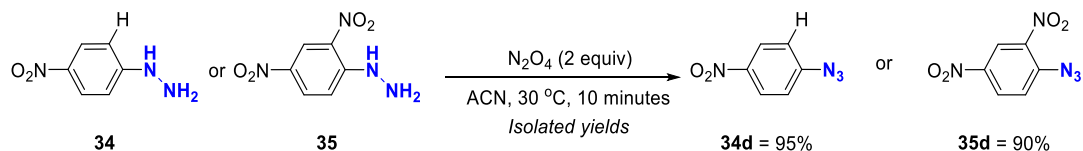


Scheme 14. The azide insertion on thiazole and imidazole derivatives **29** to **33** by lithiation

C. Diazotization general approaches

a. Diazotization of aryl hydrazine

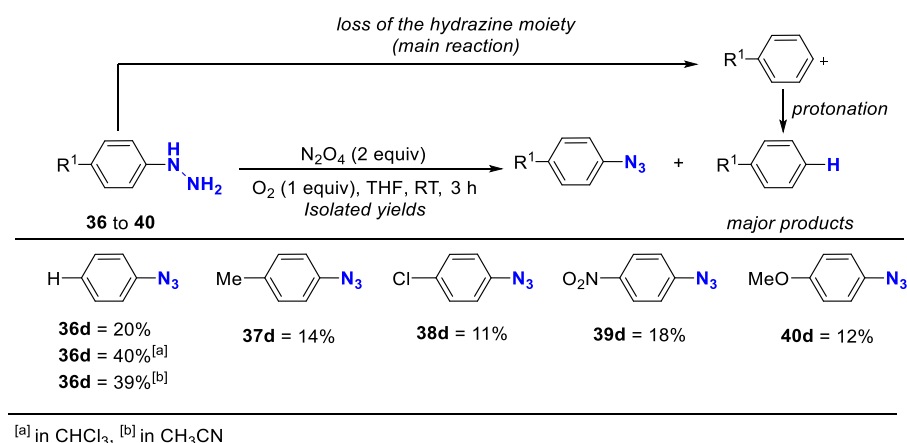
In 1986, Shim *et al.* reported that nitroso aryl hydrazines can react rapidly with nitrogen tetroxide (N_2O_4) to produce nitroso aryl azides in high yields (Scheme 15).^[87] The reaction proceeds in acetonitrile under moderate temperature $30\text{ }^\circ\text{C}$, and in short reaction times of 10 minutes. (4-nitrophenyl)hydrazine **34** and (2,4-dinitrophenyl)hydrazine **35** were loaded in 1 equiv and reacted with N_2O_4 (2 equiv) to give the aryl azides **34d** and **35d** in 95% and 90% isolated yields, respectively.



Scheme 15. The azide insertion on phenyl derivatives **34-35** by diazotization of hydrazine

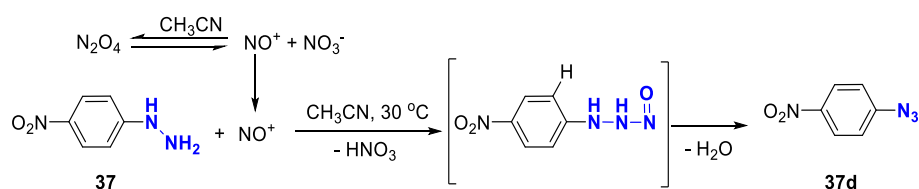
The group of Ohsawa proposed other aryl hydrazines (**36** to **40**) as the starting materials for the synthesis of the corresponding aryl azides (Scheme 16).^[88] N_2O_4 (2 equiv) was added to the substrate in the presence of O_2 (1 equiv), to furnish aryl azides **36d** to **40d** in limited 11% to 40% isolated yields. Phenylhydrazine **36**, produced its corresponding phenyl azide in 20% isolated yields in THF. The

amount of **36d** increased to 40% in CHCl_3 and 39% in CH_3CN . Electron-withdrawing groups (NO_2 and Cl) and groups (Me and OMe) on arylhydrazines **37** to **40** showed similar reactivity to **36**, producing their corresponding azido derivatives in 14%, 11%, 18% and 12% for **37d**, **38d**, **39d** and **40d** respectively in THF. In fact, the major reaction occurring was the loss of the hydrazine moiety followed by the protonation of the corresponding cationic aryl and this explains the lower yields obtained for the azides products (Scheme 16, top).



Scheme 16. The azide insertion on phenyl derivatives **36-40** by diazotization of hydrazine

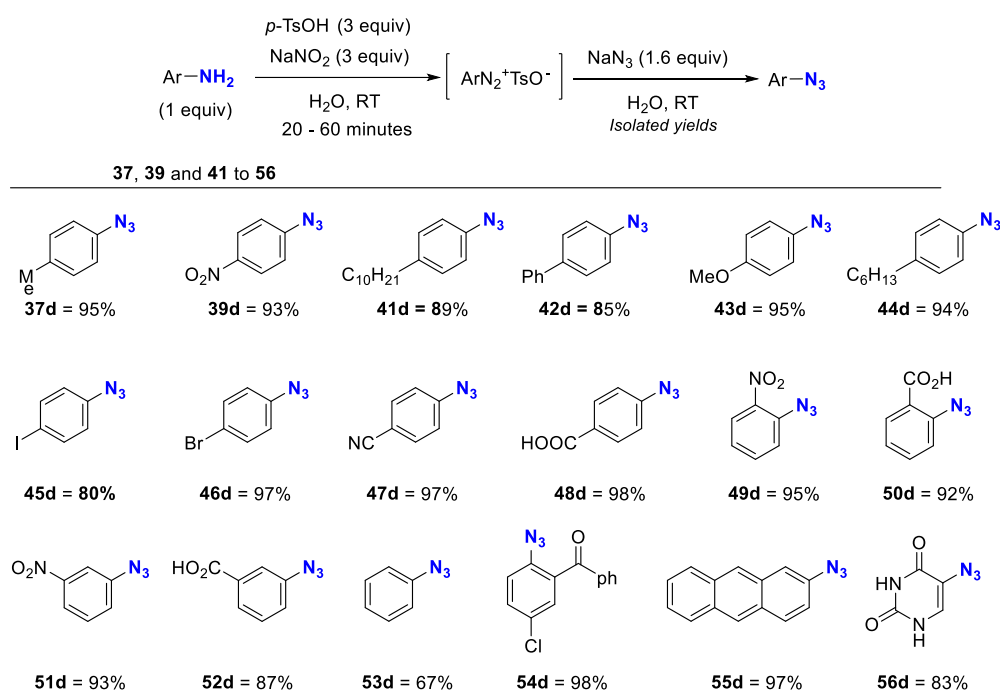
The methods to obtain aryl azides from aryl hydrazines illustrated by both Shim and Oshawa plausibly followed similar mechanisms. A model using N_2O_4 and nitroso aryl hydrazine **37** as the reagent was proposed (Scheme 17). First, N_2O_4 produces the electrophilic reactive species NO^+ in solution. The nucleophilic amine reacts with NO^+ and produces the β -nitroso hydrazine intermediate of **37** and HNO_3 . This intermediate releases H_2O and the corresponding aryl azide **37d**.



Scheme 17. Mechanism proposed for the insertion of azide by diazotization of aryl hydrazines

b. Diazotization of aryl amines

Azides containing molecules can be employed as masked amines due to their easy reduction. Inversely, the opposite reaction is also possible to produce azides from amines. Notably, this is based on the reaction of intermediates diazonium salts with the right azide sources.^[89] The generation of diazonium salts suffered mainly from their thermal stability and potential explosive properties.^[90] Moreover, classical diazonium salts are not fully soluble in water and required the use of an organic co-solvents.^[91] Recently, Parello synthesized a family of aryldiazonium tosylates ($\text{ArN}_2^+\text{OTs}^-$) that apparently possessed high reactivity, tolerance to harsh conditions, and solubility in both aqueous and organic mediums (Scheme 18).^[92]



Scheme 18. The azide insertion on phenyl derivatives **37-56** by diazotization of hydrazine

This family was used to synthesize aryl azides by reaction with 1.6 equiv of sodium azide, and isolated yields ranging between 67% and 97% were obtained for **37d**, **39d** and **41d** to **54d**, with OTs^- as the leaving group. This $\text{S}_{\text{N}}2$ reaction occurs in water at RT. The method proposed achieved a general applicability including aromatic azides with electron-withdrawing or substituents, as well as groups with a marked lipophilic character. In addition, polycyclic and heterocyclic azides with different degrees of steric hindrance are formed in yields ranging from 97% to 83% for **55d** and **56d**, respectively.

Despite these progresses, the organic stoichiometric pathways to aryl azide synthesis still suffer from the use of toxic reagents (N_2O_4 or POCl_3), rather narrow scope, especially for the direct reaction from aryl halides, and mostly involve multistep procedures. The harsh conditions that are required might be non-compatible with several substrates. For example, the lithiation of arenes and the further introduction of azide is not compatible with several electrophilic functional groups such as carboxylic functions.

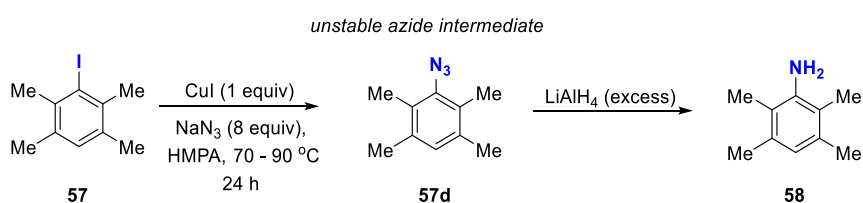
The transition metal catalyzed reactions used for the introduction of azide functions are often more straightforward. These reactions can be achieved according the main functional group transformation of pre-functionalized arenes, or more interestingly could involve direct C–H bond activation reaction.

2) Insertion of azide *via* catalytic azidation

A. Interconversion of pre-inserted groups into azide

a. From functional group interconversion of halides to azide

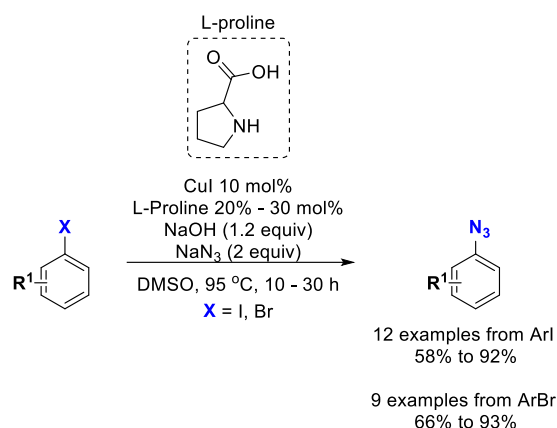
Shinoda *et al.* reported the use of metal precursors, specifically copper, for the efficient introduction of azide from halides (Scheme 19).^[93] As an example, the 2,3,5,6–tetramethyl iodide **57** reacted in the presence of a stoichiometric amount of CuI (1 equiv) and a large excess of NaN_3 (8 equiv) to form **57d** in HMPA at 70 to 90 °C for 24 h. The resulting product was produced *in situ* and directly reduced to 2,3,5,6–tetramethyl aniline **58**.



Scheme 19. The azide insertion on **57** copper-mediated by CuI

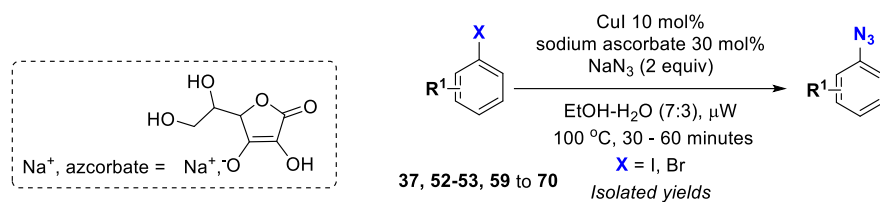
In 2004, Ma *et al.* reported a copper-catalyzed azidation starting from aryl halides in the presence of L-proline as a ligand additive (Scheme 20).^[94] The introduction of the nitrogen-based amino acid ligand L-proline, in 20 mol% loading, allowed using the copper precursor in 10 mol% catalytic amounts. Aryl bromides and iodides were used as the starting materials to produce the corresponding aryl azides in

ranges between 58% to 92% yield starting from aryl iodides, and 66% to 93% yield starting from aryl bromides.

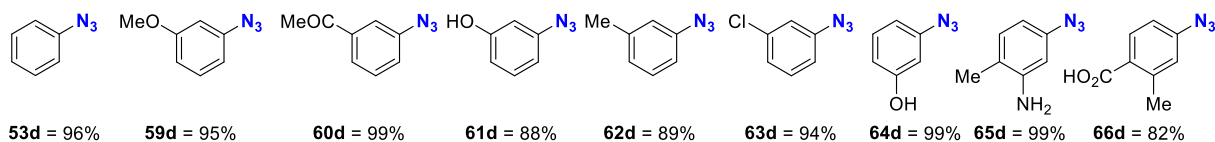


Scheme 20. Copper-catalyzed azide insertion on haloarenes in the presence of additional L-proline ligand

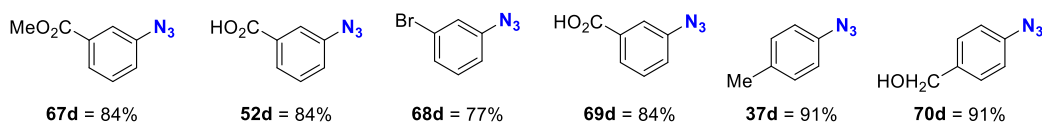
Despite this substantial advancement, the reaction was still plagued by lengthy reaction times and the use of arguably toxic and intractable solvents like DMSO. The group of Liang reported a catalyzed azidation from aryl halides under mild conditions using microwave irradiation (Scheme 21).^[95] They performed the reaction in a co-solvent system EtOH/H₂O (7:3) with 30% of sodium ascorbate as additional ligand (Scheme 21). The phenyl azide **53d** was obtained in 99% by the reaction of 1 equiv of **53**, 10 mol% of CuI, 5 mol% of sodium ascorbate, and 2 equiv of NaN₃ in EtOH/H₂O (7:3) at 100 °C under microwave irradiation for 30 min. The authors tested different azidation reaction conditions, starting from either aryl bromides or aryl iodides. From aryl bromides (Scheme 21, row 1), unsubstituted aryl bromide **53** afforded aryl azide **53d** in 99% yield. The electron-donating groups (Me, OMe or OH) and electron-withdrawing functions (COMe, CO₂H and Cl) were equally tolerated, on either the *meta*- or *para*-positions. The corresponding azide derivatives were produced in 84 to 99% isolated yield for **59d** to **64d**. Aryl bromide derivatives bearing two substituents on *meta* and *para* positions had no clear effect and the azide derivatives **65d** and **66d** were obtained in 99% and 82%, respectively. Similarly, aryl iodide derivatives showed high reactivity as well, and their corresponding aryl azides were obtained in 77% to 91% yields. For instance, the *para*-substituted derivatives **37d** and **70d** were obtained in 91% yields (Scheme 21, row 2).



row 1: from ArBr



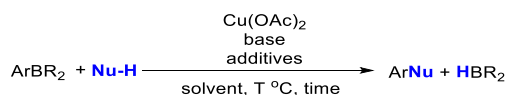
row 2: from ArI



Scheme 21. Copper-catalyzed azide insertion on **37**, **52-53**, **59-70** in the presence of additional ascorbate ligand

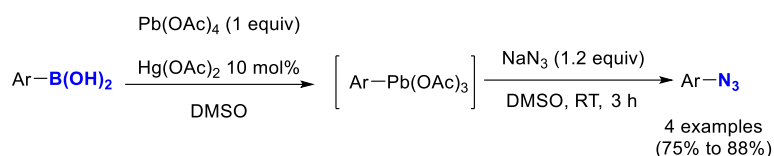
b. From functional group interconversion boranes to azide

Cu(II)-catalyzed synthesis of aryl azides from arylboronic acids, is inspired from the Chan-Lam coupling of arylboronic acids with N–H containing heteroarenes, anilines, phenols, and amides (all Nu–H).^[96] This reaction occurs in the presence of stoichiometric amount of Cu(II) acetate in aprotic solvents, and a base such as pyridine or triethylamine (Scheme 22).



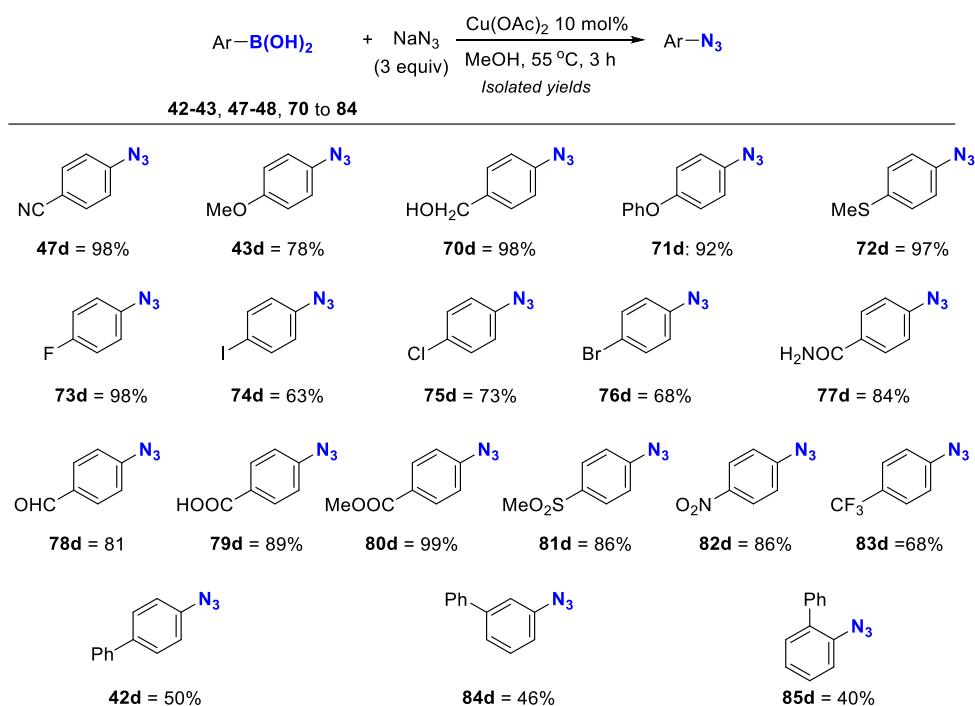
Scheme 22. General Chan–Lam coupling

In the nineties, Pinhey and coworkers converted arylboronic acids into aryl azides by using stoichiometric Pb(IV) acetate and Hg(II) acetate, through an intermediate aryl-lead species which reacted with sodium azide in DMSO to afford the desired aryl azides (Scheme 23).^[97]



Scheme 23. From organoboranes to organic azides using lead or mercury organometallics

The previous methods mainly suffered from using toxic metal precursors (Pb, Hg) and narrow scope of substrates. Then, Aldrich's group disclosed the Cu(II)-catalyzed transformation of organoboranes to organoazides, illustrating a large substrate range, detailing the role of ligands, the electronics effect of the substrate, and the functional groups compatibility (Scheme 24).^[98]



Scheme 24. The azide insertion on phenyl derivatives 42-43, 47-48, 70 to 85 by boronic acid substitution

1 equiv of the (4-cyanophenyl)boronic acid **47** reacted with 10 mol% Cu(OAc)₂, 3 equiv of NaN₃ in methanol at 55 °C for 3 h, furnished **47d** in 98% isolated yield. This reaction afforded also **43d**, **47d-48d** and **70d** to **83d** in yields ranging from 63% to 99%, where electron-donating (OPh, CH₂OH, SMe and OMe) and electron-withdrawing groups (halides, SO₂Me, NO₂, CF₃, CONH₂, and carboxyl) were similarly tolerated. Only with a biphenyl group, the azidation decreased to furnished *ca* 50% yield. Reagents **42d**, **84d** and **85d** gave the corresponding azide derivatives in 50%, 46% and 40%,

respectively. As the phenyl group is closer to the reactive C–N₃ bond, the yield decreased, from *para*-substituted **85d** (50%) to *ortho*-substituted **42d** (40%).

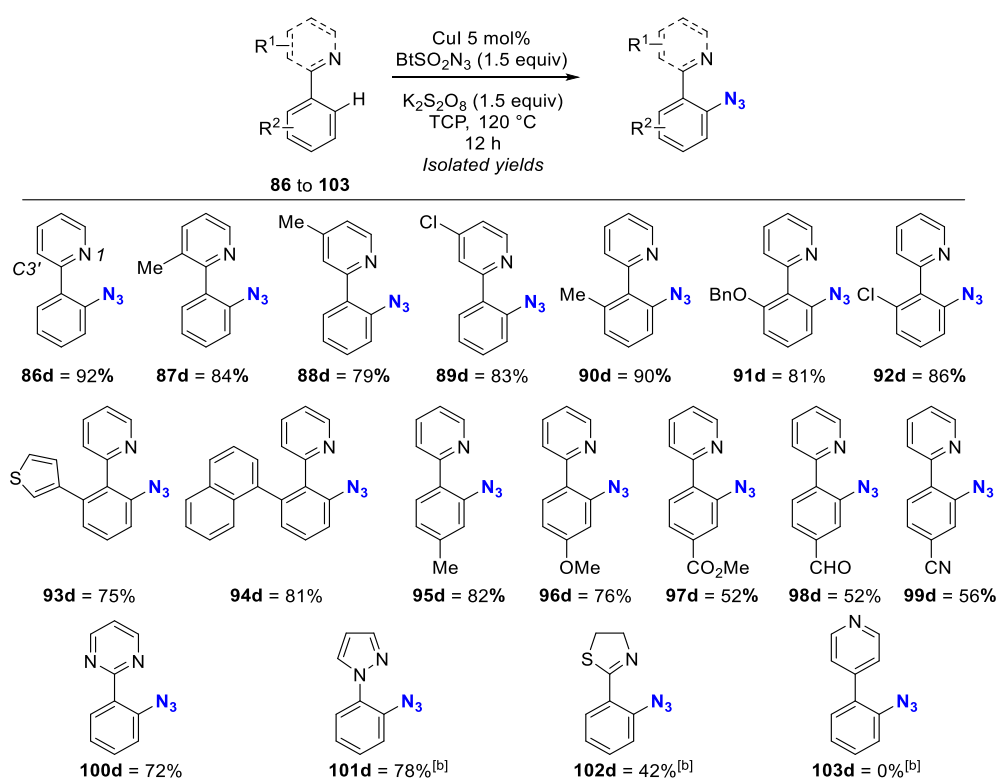
3) The insertion of azide by ligand-directed C–H bond activation

Direct metal-catalyzed C–H azidation is arguably considered as a more atom-economic route. The ligand-directed *ortho*-azidation with a *N*-directing group are the most common reactions. Different metals have been used for such purpose and the main reactions are presented below.

A. Copper-catalyzed ligand-directed C–H bond azidation

a. With pyridines as the directing group

In 2015, Narula *et al.* reported a directed Cu(I)-catalyzed C–H bond azidation on phenylpyridine and its derivatives (Scheme 25).^[99] Monoazidation was achieved from phenylpyridine **86** using 5 mol% of CuI, 1.5 equiv of K₂S₂O₈ as the oxidant and BtSO₂N₃ as azide source. The solvent used was TCP and the reaction was done under 120 °C for 12 h, **86d** was obtained in 92% yield.



^[b] 24 h instead of 12 h

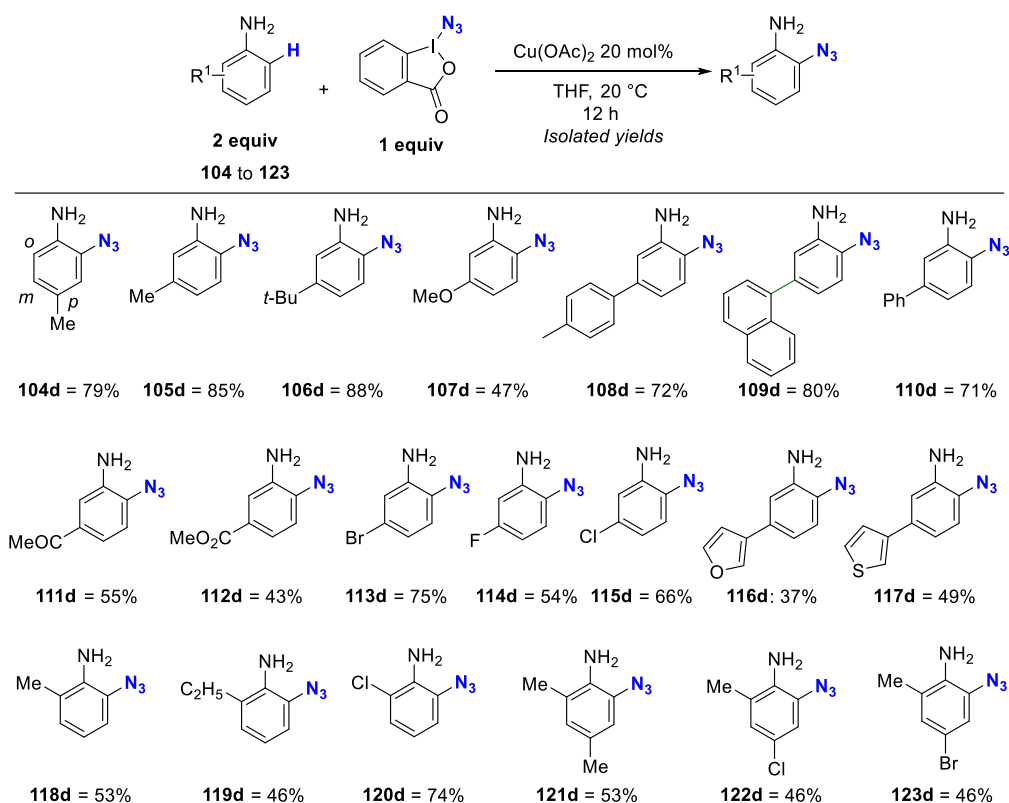
Scheme 25. Copper-catalyzed C–H bond azidation on phenylpyridine, pyrimidine andazole derivatives

The presence of an oxidant was found mandatory. The scope of the reaction was studied from heteroarenes **87** to **103**, and their corresponding azide adducts were obtained in 52% to 90% yield. When the methyl substituent is on the pyridine ring in **87** and **88**, the yields of the azidation were 84% and 79% for **87d** and **88d**, respectively. The substituents on the C3' position of the pyridine ring helped in controlling the selectivity of the reaction. The azidation on *o*-substituted phenylpyridine occurred smoothly (81% to 90% yield) with both electron-donating and electron-withdrawing groups present in compounds **89** to **92**. In addition, similar high yields were obtained in the presence of cyclic substituents in thienyl and naphthalene compounds to give **93d** and **94d** in 75% and 81%, respectively. With *p*-substituted phenylpyridines, the azidation reaction in the presence of electron-donating groups was easier (82% and 76% for **95d** and **96d**, respectively) than in the presence of electron-withdrawing groups (52% to 56% for **97d** to **99d**). This copper-catalyzed azidation was extended to other heteroaryls such as phenylpyrimidine **100**, pyrazole **101** and thiazole **102**, to produce **100d**, **101d** and **102d** in 72%, 78% and 42%, respectively. Azidation on 4-phenylpyridine **103** did not proceed, which is arguably considered as an indirect proof of the directing effect from the *o*-position of the nitrogen atom.

b. With primary amine as the directing group

Because of the explosive hazard related to azide sources such as NaN_3 or TMSN_3 at high temperature,^[100] some iodane (*hypervalent iodine*) azide sources, generated *in situ* from the reaction of NaN_3 and TMSN_3 with PIDA, were used as alternative reagent.^[101] The use of these azidoiodanes for introducing the azido function into organic compounds was, however, still constrained by their instability and high reactivity. Nevertheless, some five-membered azidoiodane heterocycles exhibited high thermal and storage stability,^[102] and could be notably used for azidation on $\text{Csp}^3\text{-H}$.^[103] The group of Hao reported the first aryl azidation using five-membered iodane azides (Scheme 26).^[104] Cu(II)-catalysts were more efficient than Cu(I) counterparts. The optimized conditions employed 4-methyl aniline **104** (2 equiv), 20 mol% of $\text{Cu}(\text{OAc})_2$ as a Lewis acid catalyst, and 1 equiv of azidoiodane in THF at RT. These conditions provided **104d** in 75% isolated yield. *meta*-Substituted anilines were tested and both electron-donating (with Ph, Me, *t*-Bu, OMe, xylyl or naphthyl groups) and electron-withdrawing (carboxyl or halide) were tolerated, and compounds **105d** to **115d** were formed in 47% to 88% yield. On the other hand, heteroaryl *p*-substituents on the aryl anilines were also employed as substrate, but afforded the corresponding azide derivatives in lower yields of 37% and 49% for **116d** and **117d**. Azidation reaction with *ortho*- (46% to 74% in **118d** to **120d**) and *para*-substituted substrates occurred with less efficiency in comparison to *m*-substituted reactants albeit presented in a lower scope. With reagents **121** to **123**, which bear both *para*- and *ortho*-substituents, lower yields

were obtained (46% to 53% for **121d** to **123d**) in comparison to the *o*-mono-functionalized products **118d** to **120d**.

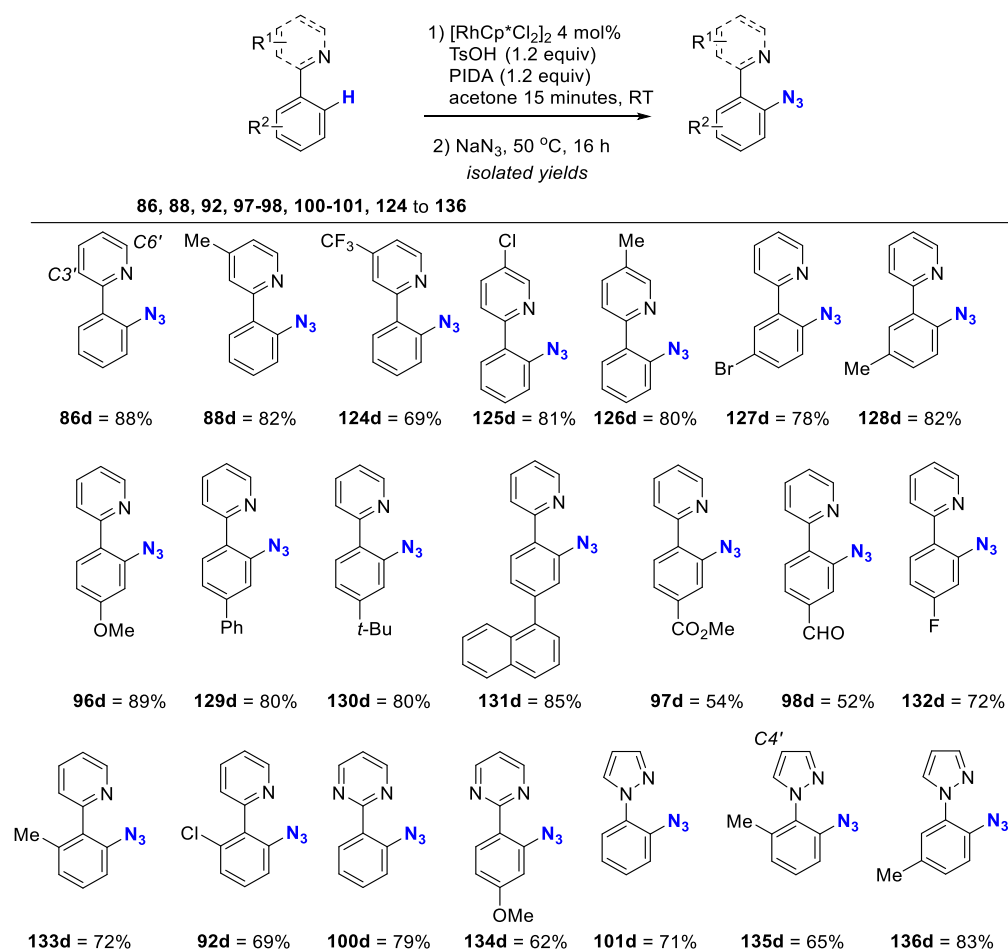


Scheme 26. Cu-catalyzed C–H bond azidation on phenylaniline derivatives using iodanes

B. Rhodium-catalyzed ligand-directed C–H bond azidation

As seen in Chapter I, rhodium catalysts are also commonly used in ligand-directed C–H bond activation of arenes for the direct introduction of aryl, acyl and heterocyclic groups.^[105] Rh(III)-catalyzed C–H azidation of *N*-directing substrate phenylpyridines, pyrazoles and pyrimidines using NaN_3 have been studied (Scheme 27). Initially, the complexation reaction was achieved through mixing phenylpyridine **86** (1 equiv), 1.2 equiv of PIDA as the oxidant, tosylic acid, and 4 mol% of $[\text{RhCl}_2\text{Cp}^*]_2$ as the catalyst, in acetone for 15 minutes. To the monometallic complex obtained was added 2 equiv of **86** to produce **86d** in 88% yield. The monocomplexation reaction was needed to insure the monoazidation. For the scope of the reactions, introducing an electron-donating (Me) or a more electron-withdrawing groups (CF_3 , Cl) on the $C4'$ and $C5'$ position of the pyridine ring helped in yielding **88d**, **124d**, **125d** and **126d** in 69% to 82% amount. Moreover, phenylpyridines holding electron-donating (naphthyl, Me, OMe and *t*-Bu) or electron-withdrawing (Cl, Br, F, CF_3 , CO_2Me and CHO) substituents in *ortho*, *meta* or *para* on the phenyl ring were similarly compatible with this reaction. Azide derivatives **92d**, **97d**, **98d**, **100d**, **101d**, **124d** to **133d** were obtained in 69% to 85% yields. With

ortho- and *para*-substituted molecules, the yields decreased when electron-withdrawing groups were present, especially with **92**, **97** and **98** where their corresponding azidation yielded in 69%, 52% and 54%, respectively. Other heterocycles such as phenylpyrimidine and pyrazole derivatives were also used in azidation to give yields of 62% to 83% of products **100d**, **101d** and **134d** to **136d**.



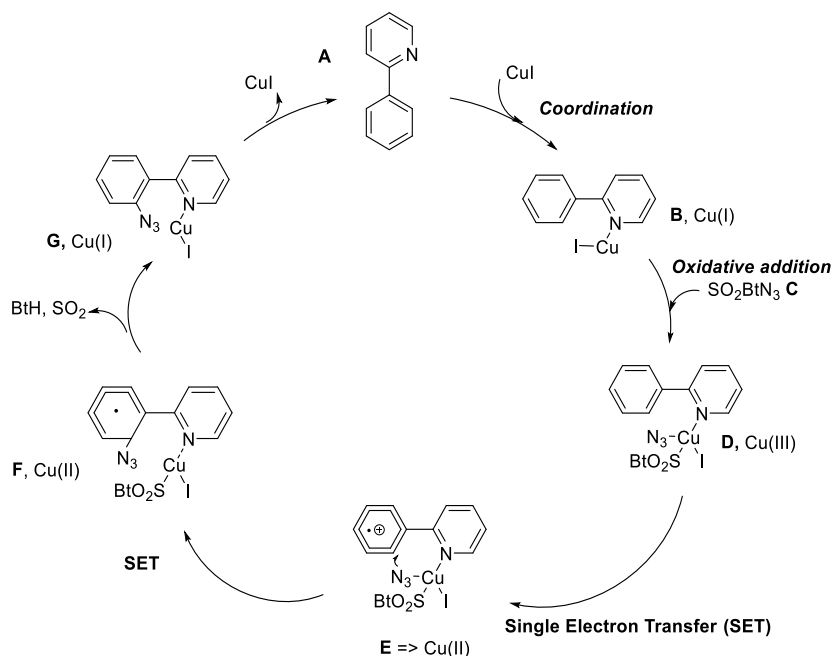
Scheme 27. Rhodium-catalyzed C–H bond azidation on phenylpyridine, pyrimidine and pyrazole derivatives

4) Mechanism of *N*-directed catalytic C–H bond azidation

The plausible mechanism for the directed C–H bond azidation of *N*-containing heterocycles depends obviously on the metal used. The different oxidation states that are possible for each metal reflect essential differences in the steps of the reaction mechanisms. We present the proposed plausible mechanisms by the authors for C–H bond azidation using copper or rhodium, and using different halogen sources and reaction conditions.

Copper(I)/copper(III) catalyzed C–H bond azidation by single *electron*-transfer (SET)

From CuI precatalyst and phenylpyridine **A**, a first step involves the coordination of the pyridine, through the nitrogen atom, to give the Cu(I)-based complex **B** (Scheme 28).



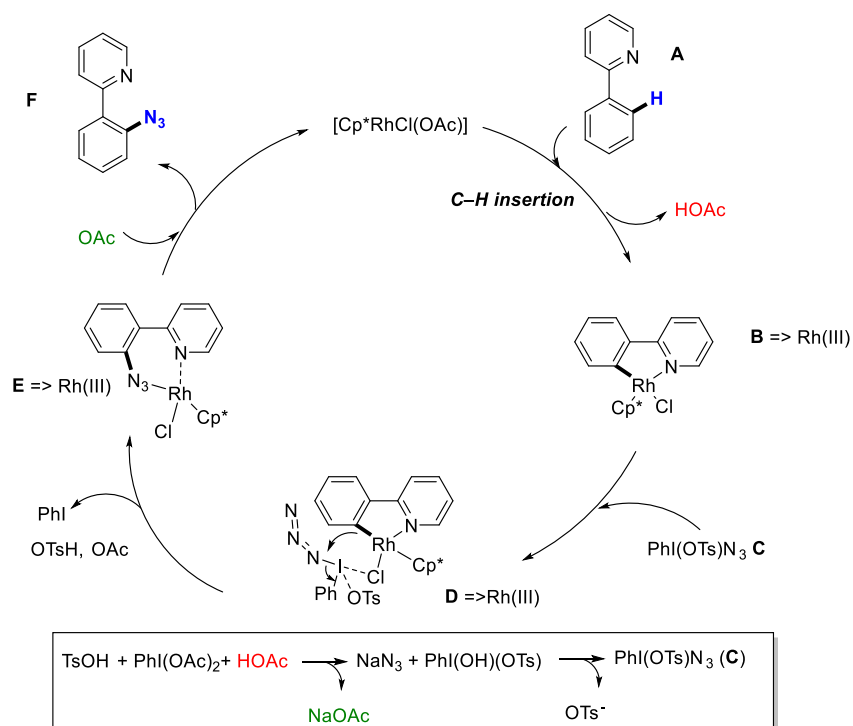
Scheme 28. Mechanism proposed for the Cu-catalyzed C–H bond azidation

The oxidative addition at copper complex **B** of the azide source BtSO_2N_3 **C**, occurs to produce the Cu(III) complex **D**. In the presence of the oxidant $\text{K}_2\text{S}_2\text{O}_8$, intramolecular single *electron*-transfer (SET) occurs on **D**, from the phenyl connected to the pyridine to the copper causing its reduction to Cu(II), while leaving an electron-deficient radical cation aryl, as **E**. Intramolecular azide transfer occurs simultaneously to reach the radical **F**. From **F**, a further single electron-transfer occurs from the same phenyl carbon on the phenyl resulting in the formation of the Cu(I) complex **G**, while releasing SO_2 and BtH. CuI is restored by rupture of coordination from the desired product **H**. The reaction failed upon the addition of the aminoxyl radical scavenger TEMPO suggesting that indeed a radical mechanism is occurring. The mechanism of the Cu-catalyzed C–H bond azidation with amines as the directing groups also involves a radical pathway also detected by the applying Tempo.^[106]

D. General mechanism for Rh(III)-catalyzed C–H bond azidation

Li *et al.* proposed a mechanism for their rhodium-catalyzed C–H bond azidation (Scheme 29), in which the initial Rh(III) in the $\text{RhCl}(\text{OAc})\text{Cp}^*$ complex maintained this oxidation state throughout the catalytic cycle. The cycle is initiated by $\text{RhCl}(\text{OAc})\text{Cp}^*$ with C–H metalation and OAc anionic ligand

exchange that occurs after coordination of phenylpyridine **A** to generate the Rh(III)-based complex **B**. The active azide transfer iodane reagent **C** dually interacts with the chlorine on the rhodium center and the Rh–C bond, giving an intermediate **D** also as a Rh(III)-species. From **D**, a concerted rearrangement occurs to give the six-membered Rh(III)-metallacycle, **E**, releasing PhI and introducing the azide on the C. Subsequent release of the resulting azide product **F**, and acetate ligand exchange regenerates RhCl(OAc)Cp*.



Scheme 29. Proposed mechanism for the Rh catalyzed C–H bond azidation

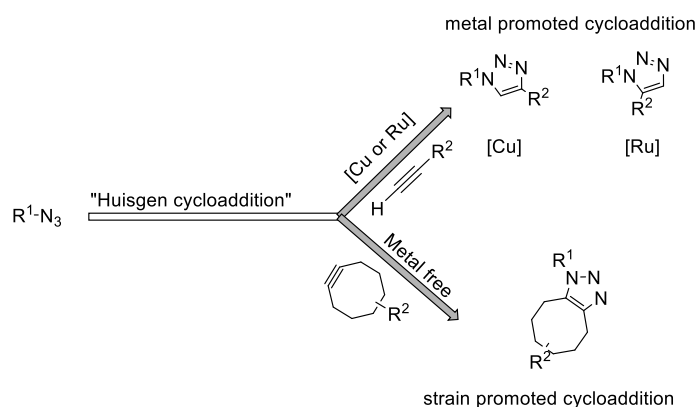
Overall, the organic synthesis of azides usually involved direct modification at halide or nitrogen-containing functional groups, such as amines and hydrazines. However, the harsh conditions were incompatible with many substrates. Conversely, milder catalytic methods using transition metals were developed. The copper-catalyzed functional group interconversions initially proposed required the pre-functionalization of substrates by halide or borane, for instance, which meant that multistep reaction was still required. Transition metal catalyzed C–H bond azidation was then proposed as mild, single-step and atom-economic approach. Heteroarenes with *N*-directing groups such as phenylpyridines and pyrimidines can be used to direct the C–H bond azidation through the metal-coordinating nitrogen. The most commonly used transition metals in these C–H bond azidation are copper and rhodium. Therefore, various synthetic routes to organic azides were presented and the

best possible way depends on the substrate employed. As mentioned before, organic azides besides NaN_3 like hypervalent iodine reagents are highly reactive and useful reagents especially for the heteroaryl azides. A selection of the notable reactivity and application of heteroaryl azides is presented in the next part.

III. Selected applications of *N*-containing heteroaryl azides as platforms

1) Introduction to click chemistry: the synthesis of triazoles

In the sixties, R. Huisgen developed the synthesis of 1,3-disubstituted triazoles from the cyclizing condensation of an aryl azide with an alkyne.^[107] He presented a metal-free [3+2] cycloaddition reaction between the azide group on aryl or alkyl azides, and bulky cyclooctynes. This cycloaddition reaction was then described as “click chemistry” due to its high rate and spontaneous action. Since then, the formation of triazoles *via* cycloaddition “click” of azides is mostly performed in two ways: a) the reaction between an aliphatic, or aromatic alkyne with aryl azides, which requires the presence of a transition metal catalysts like typically copper or ruthenium, and b) the reaction between a cyclic alkyne, like cyclooctynes, and the azide group in metal-free reactions. Several examples of azides in aryl and alkyl reacting as dienophiles are known (Scheme 30).^[108]

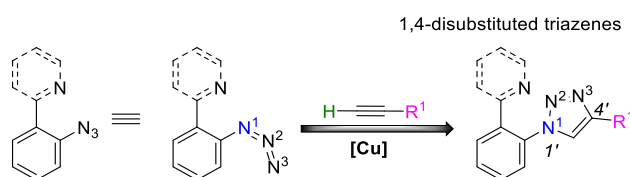


Scheme 30. The Huisgen cycloaddition reaction of azides with different alkynes

Herein, we focus on the description of Cu-catalyzed cycloaddition reaction of terminal alkynes and different heteroaryl organic azides.

A. Cu-catalyzed cycloaddition of aliphatic alkynes and azide on heteroarenes

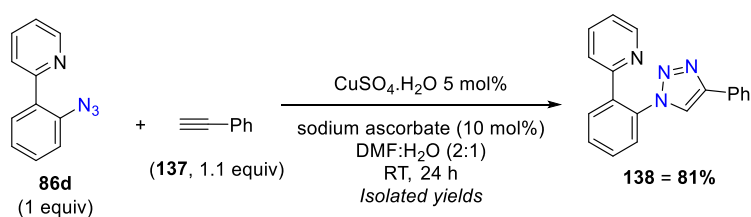
In the presence of copper catalysts, the 1,4-disubstituted triazoles are produced from the reaction between organic azides and terminal alkynes (Scheme 30, route a). In 1,4-disubstituted triazoles, the nitrogen (N^1), which is directly connected to the phenyl ring, is bonded to the unsubstituted terminal carbon of the alkyne. Using 2-(2-azidophenyl)pyridine **86d** is presented showing the target product that is obtained in [3+2] cycloaddition products in the presence of copper. Selected examples using copper-catalyzed cycloaddition are introduced afterwards (Scheme 31).



Scheme 31. An example of Huisgen cycloaddition of azide on heteroaryl

a. Huisgen cycloaddition of azide on phenylpyridine

Narula *et al.* presented the click chemistry reaction of 2-(2-azidophenyl)pyridine **86d** (Scheme 32).^[99] One equiv of **86d** reacts with 1.1 equiv of phenyl acetylene **137**, in the presence of 5 mol% of $\text{CuSO}_4 \cdot \text{H}_2\text{O}$ and 10 mol% of sodium ascorbate. Huisgen cycloaddition was achieved in DMF:H₂O (2:1) at RT in 24 h. The resulting 1,4-disubstituted triazole product **138** was obtained in 81% yield.

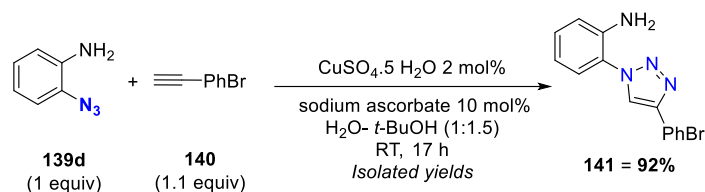


Scheme 32. An example of Huisgen cycloaddition of azides on phenylpyridine

b. Huisgen cycloaddition of azide on phenylanilines

Hao employed CuSO_4 as the catalyst for the [3+2] alkyne–azide cycloaddition (Scheme 33).^[102] Hao *et al.* were interested in phenylanilines, particularly 2-azidoaniline **139d** as a substrates for cycloaddition reactions. 1.1 equiv of 1-bromo-4-ethynylbenzene **140** reacted with **139d**, in the presence of 2 mol% of CuSO_4 and 10 mol% sodium ascorbate. The reaction was achieved in co-solvent

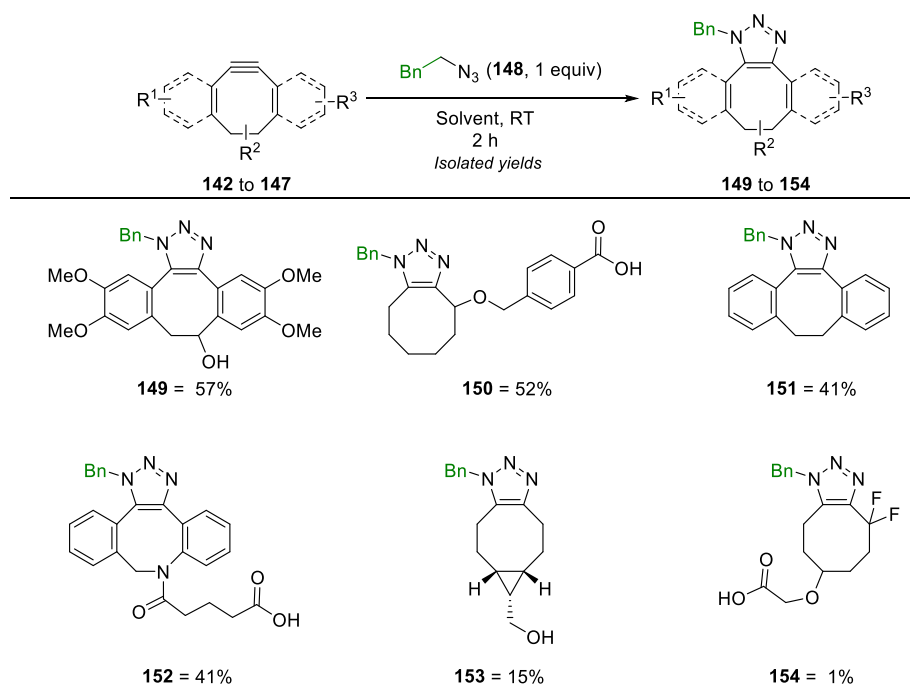
system of H₂O/*t*-BuOH (1:1.5) at RT and 17 h reaction time where 2-(4-(4-bromophenyl)-1H-1,2,3-triazol-1-yl)aniline **141** was afforded in 92% yield as the 1,4-disubstituted triazene product.



Scheme 33. An example of Huisgen cycloaddition of azides on phenylaniline

2) Strain-promoted [3+2] cycloaddition of azides and cyclooctynes

In employing cycloalkynes instead of unstrained alkynes, the balance stability/reactivity must be well-controlled. The strain of cycloalkynes is estimated through the ring size.^[109] Cyclooctyne provides a good compromise –stable enough to be isolated and stored– and highly reactive towards azides, even at RT.^[43] The cyclooctyne reactivity is adjusted by increasing the lateral ring strain sterically. Delf *et al.* illustrated this reactivity with benzyl azide through the “click chemistry” reaction (Scheme 34).^[110]



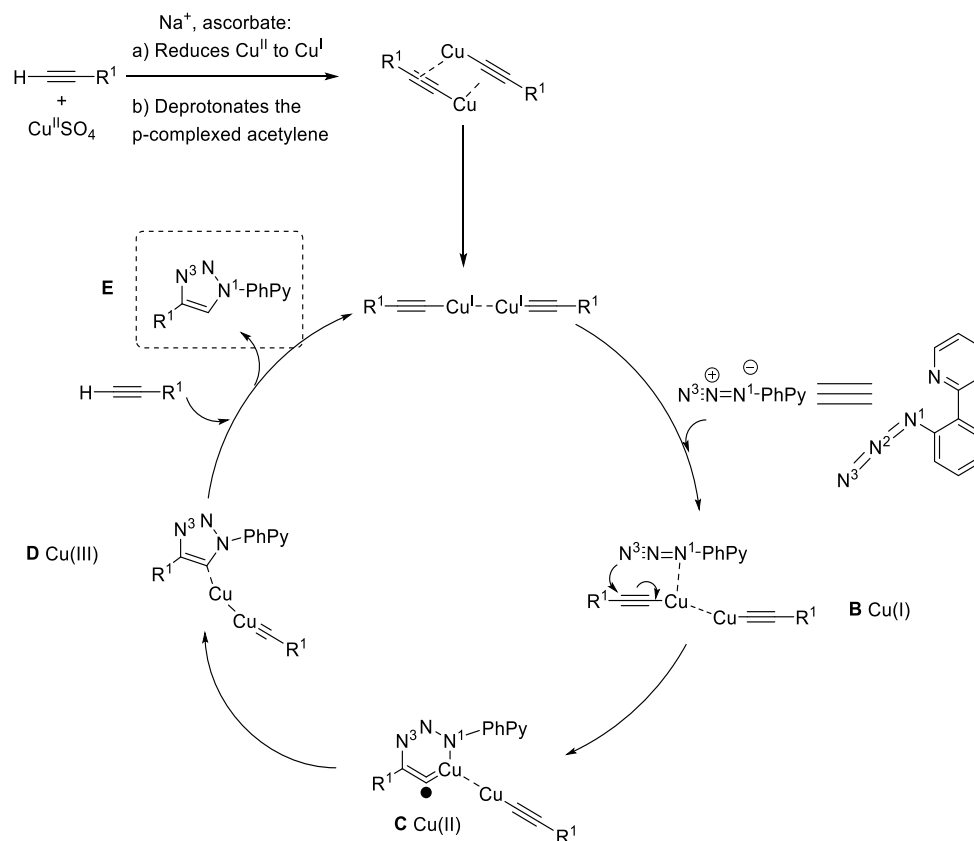
Scheme 35. An example of strained cycloaddition on aryls

The strained cyclooctynes being mostly more reactive than normal alkynes, their cycloaddition with organic azides does not necessarily require the presence of a catalyst. Thus, the cyclooctynes **142** to **145** are more reactive than cyclooctynes **146** and **147** (Scheme 27). Their reaction with benzyl azide produced the corresponding triazoles in 57%, 52%, 41% and 41% yield for **149** to **152**, respectively. The reactivity of the cyclooctynes was also related to their solubility, and thus controlled by the lipophilic character adjusted from the R¹ groups on the cyclooctynes. Accordingly, cyclooctynes **144** and **145** were less reactive than **142** and **143** despite being less strained.

3) General mechanisms of the [3+2] cycloaddition reactions

A. Sodium ascorbate-mediated Cu-catalyzed [3+2] cycloaddition of terminal alkynes^[111]

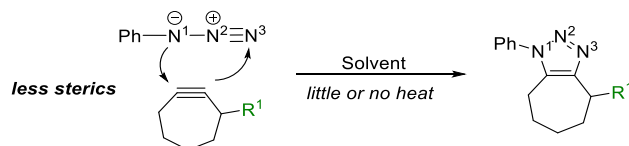
In a cycle involving both Cu₂SO₄ and sodium ascorbate, the Cu-catalyzed [3+2] cycloaddition reaction occurs with a terminal alkyne (Scheme 36). The sodium ascorbate plays two crucial roles in this reaction: a) reduction of the initial Cu(II)SO₄ to Cu(I) and b) deprotonation of the terminal hydrogen of the alkyne to give the alkyne anion that coordinates to the copper metal. These two processes end in giving dinuclear Cu(I) in (copper)acetylide **A**. After the formation of **A**, the coordination of the azide occurs from the partially negatively charged nitrogen (N¹), which is connected to the phenyl to give the Cu(I) complex **B**. Cyclization occurs from **B** by bonding N³ and the external unsubstituted carbon to give the metallacycle complex **C**, from which a rearrangement produces **D**. The approach on a new alkyne releases the cyclization product **E** and the initial Cu(I)-catalyst.



Scheme 36. Proposed mechanism for Cu-catalyzed Huisgen cycloaddition to triazoles

B. Metal free [3+2] cycloaddition reaction of cyclooctynes and aryl azides

Cyclooctynes and aryl azides can be involved in a [3+2] cycloaddition reaction in the absence of a metal catalyst. A model reaction mechanism is presented with simple cyclooctyne and phenyl azide (Scheme 37). In fact, the mechanism of the [3+2] addition reaction is a classical reaction starting from the attack of nucleophilic azide nitrogen (N^1) on the less sterically affected carbon, to yield the 1,4-disubstituted triazene. This reaction gives the same products as Cu-catalyzed cycloaddition, but the high reactivity of the cyclooctyne allows this reaction without metal.

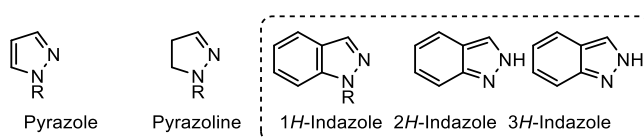


Scheme 37. The mechanism of the strain promoted cycloaddition

IV. Indazole derivatives as N–N bond containing molecules

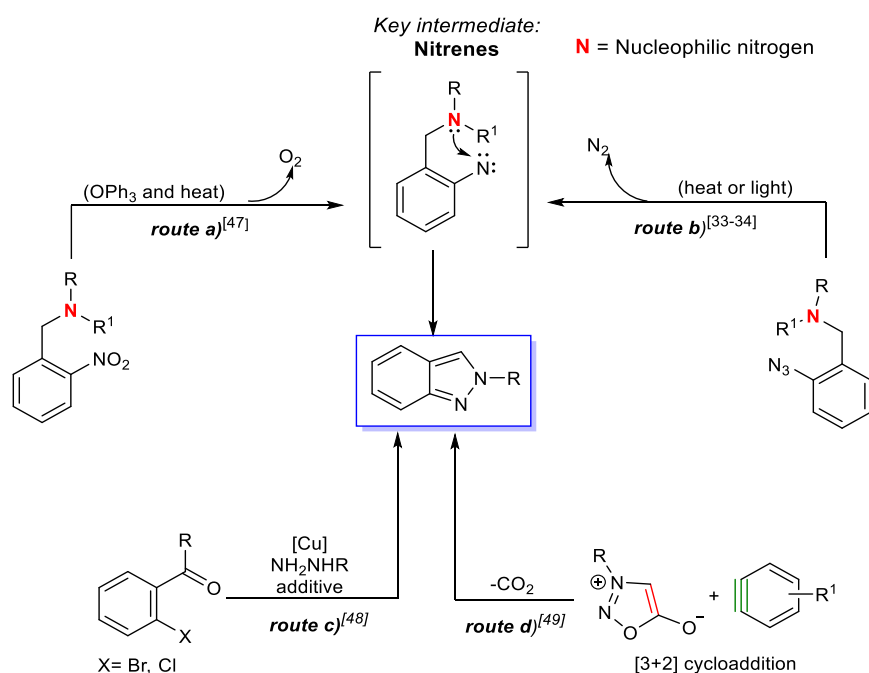
1) General synthesis

Indazole derivatives are heterocyclic molecules characterized by their N–N bond. Indazoles display a wide variety of pharmacological and biological actions, for instance, in anti-inflammatory and anti-tubercular uses.^[112] Some indazoles are fluorophores used to form fluorescent probes. They have demonstrated their diagnostic utility for cellular imaging in the field of medical biology (Scheme 38).^[113]



Scheme 38. Heteroarenes with N–N bond including indazole derivatives

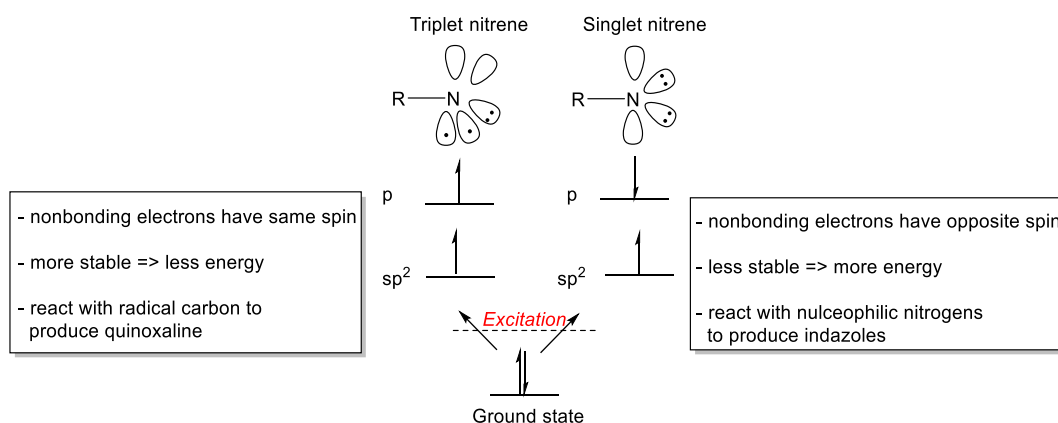
The synthesis of indazole derivatives is displayed *via* several organic and catalytic pathways (Scheme 39). The main organic pathways are known to be deoxygenation and denitrogenation processes of nitroso and azido heteroaryl amines *via* nitrene intermediates (routes **a** and **b**).^[114] On the other hand, palladium and copper metal precursors proved to be effective catalysts in the formation of the desired N–N bonds of indazoles (route **c**).^[115] Another route is based on [3+2] cycloaddition reactions from cycloalkynes and C=C bond containing heteroarenes (sydnones,^[116] for example, route **d**).^[117]



Scheme 39. The major organic and catalytic synthetic routes of indazole derivatives

A. The synthesis of indazoles from aryl azide and the nitrene intermediate

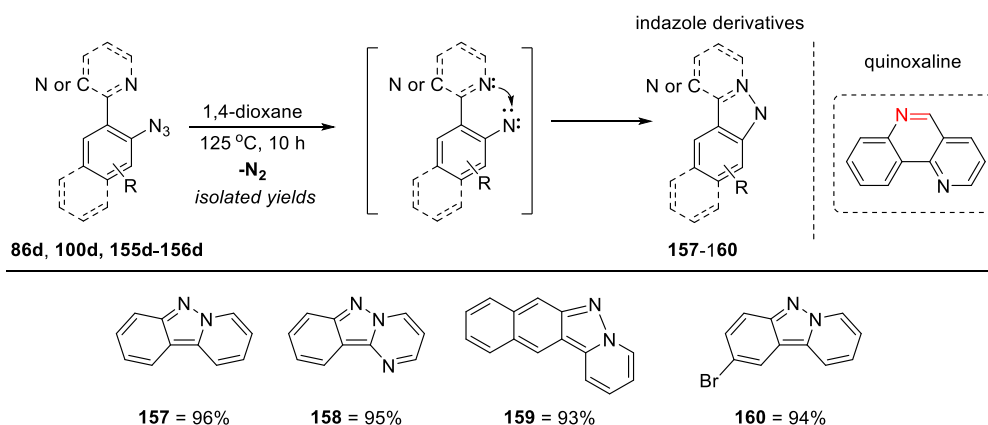
In the mid 1960's and 1970's, several groups exploited the N–N bond formations starting from nitrene intermediates.^[118] A nitrene is defined as the nitrogen-based analogue of a carbene, where the nitrogen atom is uncharged and univalent.^[119] Nitrenes have 6 electrons in its valence shell and two covalent bonds for four non-bonded electrons and are species with unsatisfied octet rule. This reactive intermediate can be attacked by a nucleophilic nitrogen to give different kind of N–N bond containing products.^[120] The main methods for obtaining nitrene intermediates are the deoxygenation and denitrogenation of nitro and azido groups, respectively. As carbene, nitrene exists in two different spin states, the singlet or triplet state. A triplet state nitrene has two nonbonding electrons with different spins in their excited states. The triplet state possesses less energy and therefore is the more stable form. One major pathway to form an indazole unit can be formed through N–N bond formation from the intramolecular attack of a nucleophilic nitrogen on the more reactive single state nitrene (Scheme 40).



Scheme 40. Spin states of excited nitrenes and their main characteristics

a. Pyridino and pyrimidino [1,2-*b*]indazole derivatives

The groups of Hao and Li have proposed azido phenylpyridines and pyrimidines as heteroaryl substrates that provide nitrenes in their singlet spin state. This intermediate is required for indazole synthesis through intramolecular N–N bond formation (Scheme 41).^[34] The reaction is performed by denitrogenative thermolysis of the azide functional group in *ortho*-position on the phenyl ring in 1,4-dioxane and leads to the formation of single state nitrene intermediates.



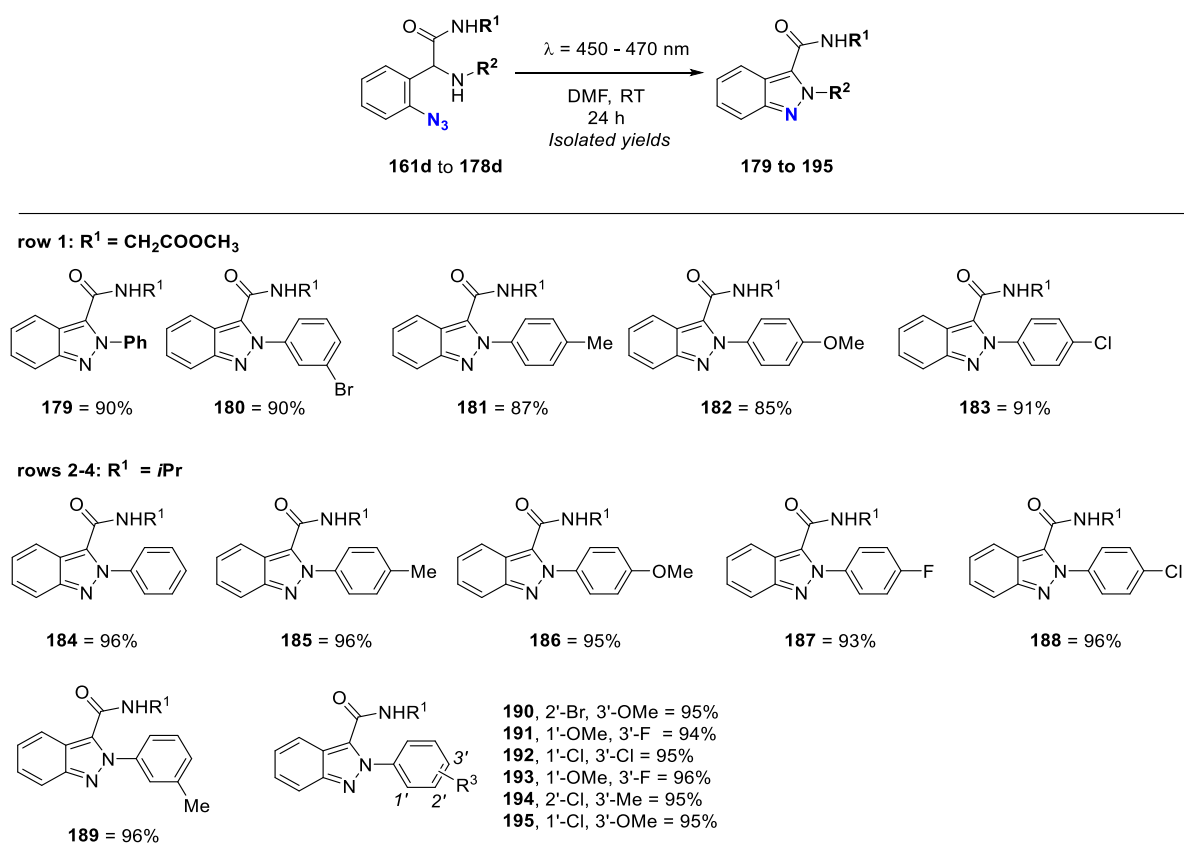
Scheme 41. The formation of pyridino and pyrimidino indazoles **157-160**

The nucleophilic heterocyclic nitrogen (pyridine or pyrimidine ring) attacks these electron-deficient nitrene, creating the N–N bond that results in the production of indazoles pyrido[1,2-*b*]indazole **157**, pyrimido[1,2-*b*]indazole **158**, benzo[*f*]pyrido[1,2-*b*]indazole **159**, 2-bromopyrido[1,2-*b*]indazole **160** and in 96%, 95%, 93% and 94% respectively. The high yields are attributed to the exclusive formation

of the single state nitrene ahead of its triplet counterpart, which is favored in non-polar solvents such as 1,4-dioxane. Interestingly, the presence of an electron-withdrawing substituent (Br) on **156d** which not direct the thermolysis towards the triplet state nitrenes intermediate, and thus subsequent production of quinoxalines as side products from single state nitrenes (shown in the structure) from N–C bond formations similar to the reported reactions with azido phenyl pyrazoles.^[121]

b. 2H-indazole derivatives by visible-light-driven photocyclization.

The group of Wang claimed that elevated temperatures –up to 130 °C– that are needed for thermolysis of azides for nitrene formation is not compatible with several functional groups, and cause their degradation. Therefore, they used photolysis to produce nitrene intermediates and their indazole products.^[122] Visible light (blue light, $\lambda = 455$ to 470 nm) was applied on compound **161** in DMF to produce 2-H indazole derivative **179** in 90% yield at RT. **179** was obtained in 85% to 88% in other solvents such as toluene, THF, HMPA and DMA. Polar solvents such as CCl₄, alcohols (CH₃COOH, MeOH), acetone and DMSO gave poorer yields (15% to 57%). The scope of the reaction was done on molecules modified at their nucleophilic amino group (NHR¹) (Scheme 42).



Scheme 42. The formation of 2H-indazole derivatives **179** to **195**

The photolysis and corresponding indazole formations went smoothly to give isolated 85% to 96% yields for **179** to **195**, regardless of the group connected to the amine. Similar reactivities were observed with molecules bearing either electron-donating or electron-withdrawing on the nitrogen of the amide moiety. The electronic nature of the substituent on the amide had no effect on the reactivity. The mechanism of the reaction is initiated by the attack of the nucleophilic amino group NHR^1 on the formed nitrene.

In summary, azide introduction onto organic molecules can occur *via* organic (diazotization, through inorganic reagents) and catalytic pathways. On organic molecules lacking directing groups such as nitrogen or oxygen, the organic pathways are mainly employed. This is reversed for heterocyclic organic molecules which *via* their directing group (nitrogen, oxygen...) can coordinate to the metal and facilitate the C–X (X = Halogen, H) transformation to C–N₃ bonds. Concerning the recent synthetic value of aryl and heteroaryl azides can be demonstrated *via* cycloaddition reactions on the azide group, which leads to the formation of highly tailored triazoles. The cycloaddition reactions involve an azide and some alkynes. Huisgen cycloaddition is performed upon employing normal or unstrained straight alkynes, in the presence of copper (terminal alkynes) or ruthenium catalysts (terminal or internal alkynes). The choice of the metal catalyst is a determining factor of the triazole regioisomer formation. Triazoles 1,4- and 1,5-disubstituted are obtained with copper and ruthenium catalysts, respectively, arguably following different mechanistic pathways. On the other hand, the cycloaddition reaction with cyclooctynes occurs spontaneously and does not require catalytic assistance from these strained alkynes that possess greater reactivity in comparison to straight alkynes. They form 1,4-disubstituted triazoles.

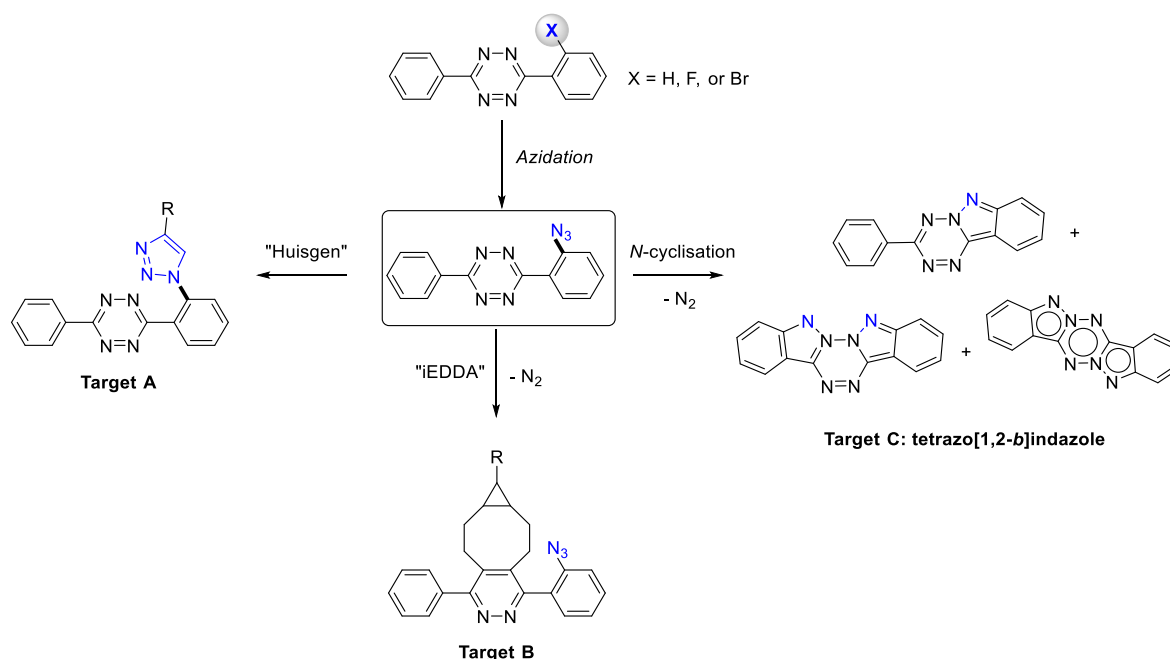
Another field of interest of azide bond formation is the cyclic formation of functional indazoles. Several synthetic routes have been explored for the synthesis of indazoles. Organic azides undergo thermo- or photolysis of their azide group, leading to the release of N₂ and a reactive intermediate, the nitrene. The N–N bond formation that is needed for indazoles formation occurs in the presence of a nucleophilic nitrogen, mostly of heterocycles such as pyridine or pyrimidine or an amine. The nucleophile attacks the electron-deficient nitrene and form the desired indazole. The indazoles of azido heteroaryl starting materials such as phenylpyridine, pyrimidine and (2-(2-azidophenyl)-2-(phenylamino) acetyl)glycinate are produced *via* nitrene intermediates.

We present now our work in the fields of cycloaddition chemistry and indazoles formation from different heteroaryl derivatives and notably, the *s*-tetrazine core that incorporates four nitrogen atoms, as potential directing groups for the introduction of azide reactive groups.

V. Results and discussion

1) Azidation of *s*-aryltetrazines: synthesis and applications

s-Tetrazines are the object of high interest in biochemistry and photophysics.^[3] Notably, the presence of a reactive azide group can facilitate the expansion and thus introduction of new properties into this family of molecules. Thus, our first target was to develop an efficient synthetic route to introduce the azide group on *s*-aryltetrazines. Then, since azido bearing *s*-tetrazines can perform the Huisgen coupling reaction and the inverse electron-demand Diels-Alder (IEDDA) reaction reactions on the azide or on the *s*-tetrazine core (Scheme 43, target **A** and **B** respectively), we intended to find conditions to achieve either cycloaddition reaction selectively. Finally, we focused our attention on the *N*-cyclisation on the *s*-tetrazine core based on the azide *s*-tetrazine intermediate, in order to form a new class of N-rich heterocycle namely tetrazo[1,2-*b*]indazole (Scheme 43, target **C**).

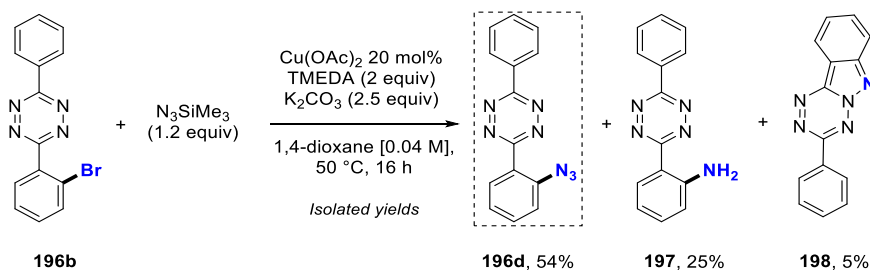


Scheme 43. Azidation of *s*-aryltetrazines (top) and its applications (Targets A-C)

A. Azide *s*-aryltetrazine in click chemistry

Based on the 3-(2-bromophenyl)-6-phenyl-1,2,4,5-tetrazine **196b** as starting material, we firstly developed the Cu-catalyzed azidation (Scheme 44). By employing 1 equivalent of **196** with 1.2 equiv of N₃SiMe₃ in the presence of 20 mol% of Cu(OAc)₂, 1.2 equiv of TMEDA as the ligand, and K₂CO₃ (2.5 equiv) as the base, we formed the target 3-(2-azidophenyl)-6-phenyl-1,2,4,5-tetrazine **196d** as the

major product in 54% yield in 1,4-dioxane at 50 °C.^[123] The side-products were 2-(6-phenyl-1,2,4,5-tetrazin-3-yl)aniline **197** and 3-(phenyl)-1,2,4,5-tetrazo[1,2-*b*]indazole **198** in 25% and 5% yields respectively (*vide infra*). The Staudinger reaction,^[124] led to the formation of primary amine by reduction of the azide function in the presence of water.



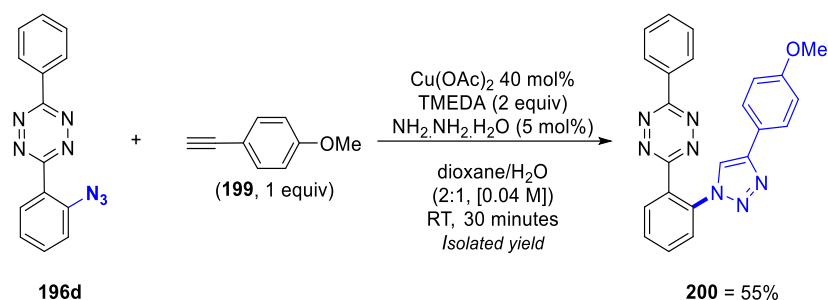
Scheme 44. Synthesis 3-(2-azidophenyl)-6-phenyl-1,2,4,5-tetrazine **196d**

With the 3-(2-azidophenyl)-6-phenyl-1,2,4,5-tetrazine **196d** in our hands, we studied the selective “click chemistry” reaction named Huisgen and iEDDA cycloadditions.

B. Cycloaddition chemistry: The Huisgen and iEDDA cycloaddition reactions

a. Selective Huisgen cycloaddition reaction

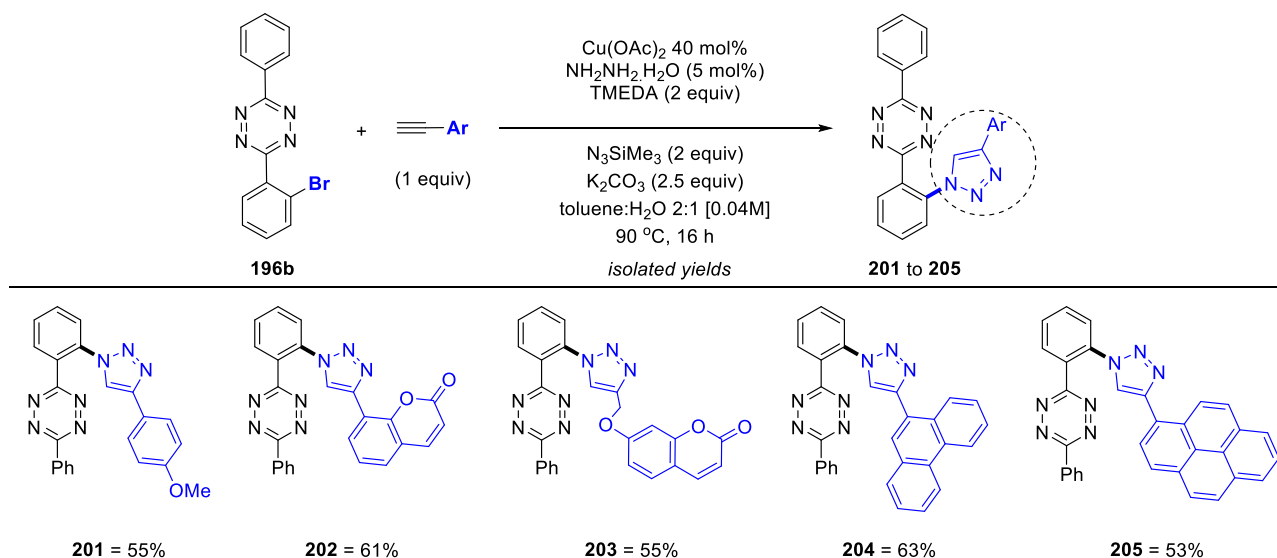
After successfully isolating the azido-aryl-*s*-tetrazine **196d**, we used the azide function for the introduction of various functional groups by “click chemistry” (Scheme 45). The reactive azido-aryl-*s*-tetrazine **196d** (1 equiv) easily achieved coupling with unstrained alkyne 1-ethynyl-4-methoxybenzene **199** (1 equiv) at 20 °C, yielding after 30 minutes the triazole-tetrazine 3-(2-(4-(4-methoxyphenyl)-1*H*-1,2,3-triazol-1-yl)phenyl)-6-phenyl-1,2,4,5-tetrazine **200** in 55% isolated yield. The reaction was catalyzed by 40 mol% Cu(OAc)₂ and 5 mol% hydrazine and performed in a mixture (dioxane:H₂O, 2:1). The Huisgen azide-alkyne cycloaddition occurred selectively and the tetrazine core remains untouched.



Scheme 45. Huisgen cycloaddition of the azide on the 1,2,4,5-tetrazine **196d**

b. One-pot azidation/Huisgen cycloaddition for incorporating fluorophores

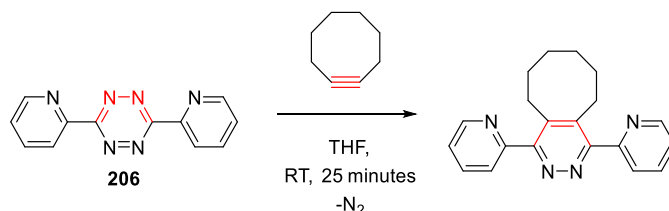
We then optimized a one-pot azidation/Huisgen cycloaddition leading to a series of tetrazines incorporating useful moieties such as coumarin or pyrene moieties (Scheme 46). Starting from the **196b** (1 equiv), we achieved the synthesis of the triazole products **201** to **205** in yields ranging from 53% to 63%, using 40% Cu(OAc)_2 , TMEDA (2 equiv), $\text{NH}_2\text{NH}_2\cdot\text{H}_2\text{O}$ (5 mol%), K_2CO_3 (2.5 equiv), TMSN_3 (2 equiv) and 1 equiv of various terminal alkynes. Under such protocol, the *s*-tetrazine core was preserved, and thus available for further iEDDA reactivity.



Scheme 46. One-pot azidation-cyclization for the synthesis of **201** to **205**

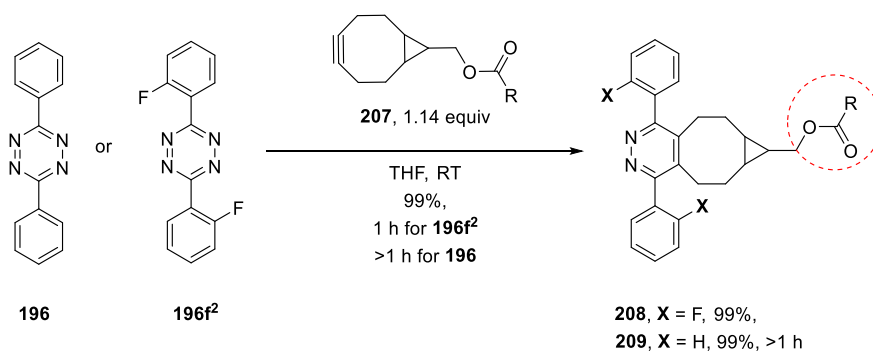
c. Selective iEDDA cycloaddition reactions

The iEDDA reaction with cyclic alkynes is a fast reaction and proceeds under metal free conditions, such as reported by Blackman *et al.* on the 3,6-bis(2-pyridinyl)-tetrazine **206**.^[125] The reaction proceeds at RT during 25 minutes in THF (Scheme 47).



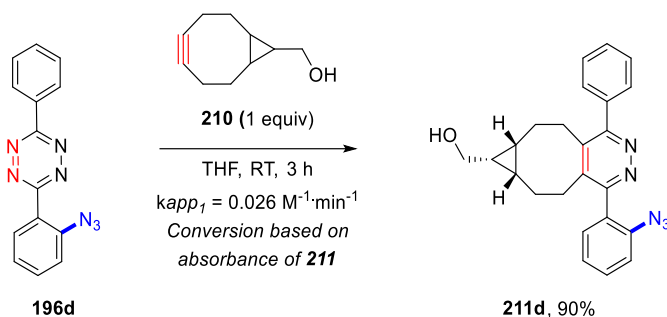
Scheme 47. The iEDDA reaction on the tetrazine core of **206**

The Hierso group reported the reactivity of the *s*-tetrazine core in iEDDA reaction with high yields (Scheme 48).^[5] The strain-promoted [2+2] cycloaddition of electron-deficient 1,2,4,5-tetrazines **196** and **196f²** reacted in THF with the electron-rich dienophile cyclooctyne **207** to form a Diels–Alder adduct. The complete reaction (99%) was achieved in 1 h when tetrazine **196f²** was used, and within a slightly longer reaction time in the presence of **196**. The difference of reactivity provided by the presence of electron-donating the *o*-fluorine atoms favorably influenced the electron-density of the dienophile and thus increased the rate of the reaction : the rate for **208** formation was $k_{app} = 0.0755 \text{ min}^{-1}$ vs. 0.0355 min^{-1} for **209**). The presence of the ester functional group at the terminus of the cyclooctyne opens to further functionalization with biochemicals from peptide coupling.^[126]



Scheme 48. The iEDDA reaction of the diene of the tetrazine core of **196f²** and **196**

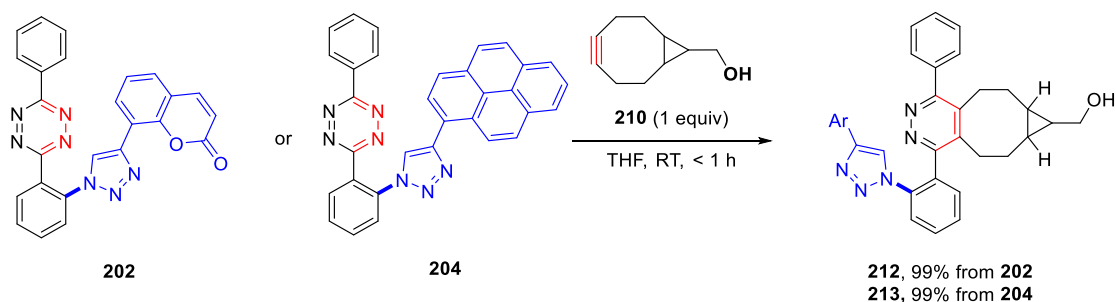
Despite the presence of the reactive azide group on the *s*-tetrazine **196d**, the also iEDDA proceeded fairly selectively on the nitrogen core by employing strained cyclooctyne **210** at RT (Scheme 49). A conversion up to 90% to give **211** in less than 3 h, which allows for further azide click chemistry, was achieved.



Scheme 49. The iEDDA cycloaddition of the diene of tetrazine of **194d**

d. Double cyclization by Huisgen and iEDDA reactions

The potential of the azide-tetrazines, having two different clickable positions, was further explored by an iEDDA cyclization reaction of the fluorophore-containing tetrazotriazoles **202** and **204**. A second cyclization located at the *s*-tetrazine-core using the cyclooctyne **210** was achieved with full conversion in THF at RT in less than 1 h to give the doubly cyclized **212** and **213** in 99% yields (Scheme 50).

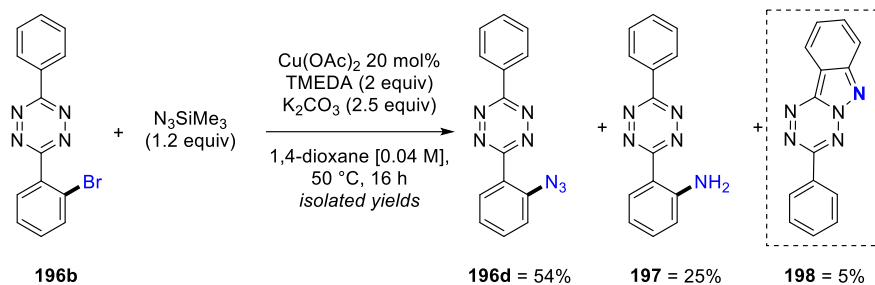


Scheme 50. The formation of doubly cyclized *s*-aryl tetrazines **212** and **213**

After the synthesis of azido *s*-tetrazine was disclosed, and the selective cycloaddition reactivity was demonstrated, the use of azide *s*-tetrazine derivative **196d** in the synthesis of tetrazo-indazole was investigated in this thesis, as described below.

2) Azide *s*-aryltetrazine in *N*-cyclisation: formation of tetrazo[1,2-*b*]indazole

During the copper-catalyzed functional group interconversion from **196b** to **196d** depicted in Scheme 44 and Scheme 51, we observed the formation of the 2-(6-phenyl-1,2,4,5-tetrazin-3-yl)aniline **197** and the 3-(phenyl)-[1,2,4,5]-tetrazo[1,2-*b*]indazole **198** in addition to 3-(2-azidophenyl)-6-phenyl-1,2,4,5-tetrazine **196d**. Under these conditions, **198** was formed in very low yields (5%).



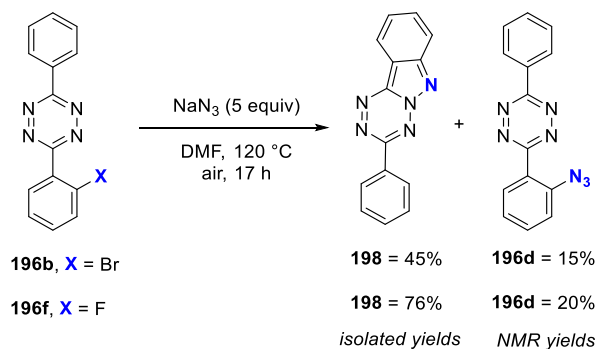
Scheme 51. Products of the copper-catalyzed synthesis of **196d**

Interested in the exploitation of the properties of these heterocycles, we tried to develop a more quantitative synthetic route towards 3-(aryl)-[1,2,4,5]-tetrazo[1,2-*b*]indazole **198** based on a free-metal nucleophilic azidation.

A. Formation of 3-aryltetrazo[1,2-*b*]indazole

a. Thermal *N*-cyclization

To avoid the reduction of the azido group in amine, the reaction was performed in the absence of copper catalysts starting from halogenated *s*-aryltetrazine. From **196b**, we achieved the protocol by directly substituting the *o*-halide by an azide on the phenyl group (Scheme 52).

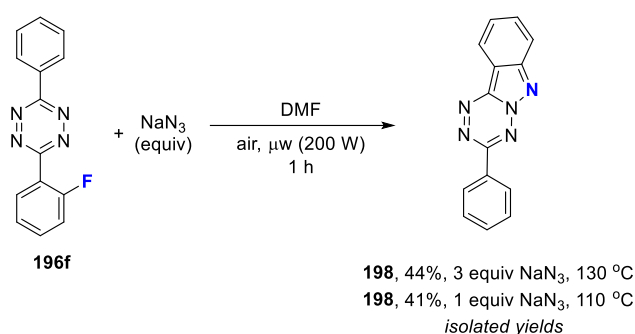


Scheme 52. Metal-free thermal azidation of bromo-*s*-aryl tetrazine towards **198**

The addition of 5 equiv of NaN₃ (instead of TMSN₃) at 120 °C in DMF produces **198** in 45% isolated yield, as the major product, in addition to the intermediate azide derivative in 15% (NMR yield). With this significant improvement, compared to the copper-catalyzed reaction, we then began to use fluorinated *s*-tetrazine as precursors to produce the azide form. We used **196f**² as starting material having fluorine as the leaving group. Under these conditions, 76% yield of **198** were isolated. In both syntheses, the aniline product was not observed, and only the azide derivative **196d** was observed as the side-product. Unsurprisingly, the fluorine is a better leaving group than bromine for the reactions on the phenyl.

b. *N*-cyclization by microwave irradiation

To improve the global efficiency of the cyclisation process we performed the cyclization reaction under microwave irradiations (Scheme 53). The *s*-tetrazine **196f** reacted with 3 equiv of NaN₃ in DMF for 1 h under 130 °C leading to 44% isolated yield of **198**. Decreasing the temperature to 110 °C and the NaN₃ loading to 1.1 equiv gave a similar in 41% isolated yield, in the range of standard error. The cyclization under microwave irradiations could be a useful tool due to the fairly good isolated yields *ca* 40% in short reaction times of 1 h instead of 17 h, and using a lesser amount NaN₃. However, in terms of overall yield, the reaction under thermal temperature more efficient to produce **198** in 76% yield despite using 5 equiv of NaN₃.



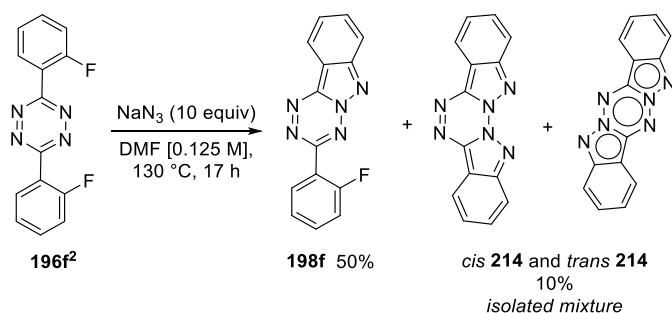
Scheme 53. The microwave-assisted metal-free synthesis of **198**

B. Formation of the *bis*-tetrazo[1,2-*b*]indazole

a. Thermal *N*-cyclization

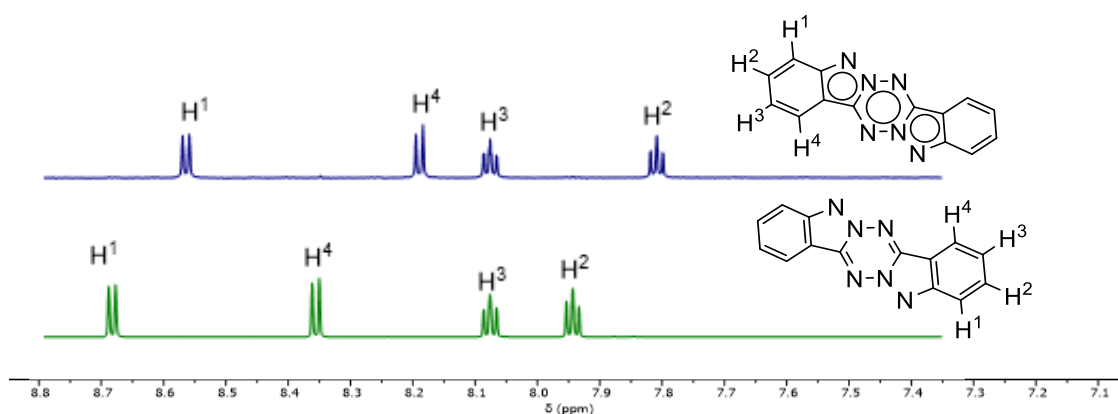
Taking advantage of the difunctionalized *s*-aryltetrazines, we carried out the formation of *bis*-tetrazo[1,2-*b*]indazole **214** (Scheme 54). From **196f**², which holds two fluorine atoms, we attempted

the double cyclization reaction with 10 equiv of NaN₃ in DMF at 130 °C for 17 h. In this reaction, the 3-(2-fluorophenyl)-[1,2,4,5]-tetrazo[1,2-*b*]indazole **198f**, obtained after the first cyclization was the major product with 50% isolated yield. On the other hand, two isomers of the desired double cyclization were synthesized: 1) the *cis*-isomer **214** and 2) the *trans*-isomer **214**, both detected by NMR, and their mixture was isolated in 10% yields due to their lower solubility in dichloromethane.



Scheme 54. The formation of the *cis* and *trans* isomers of **214**

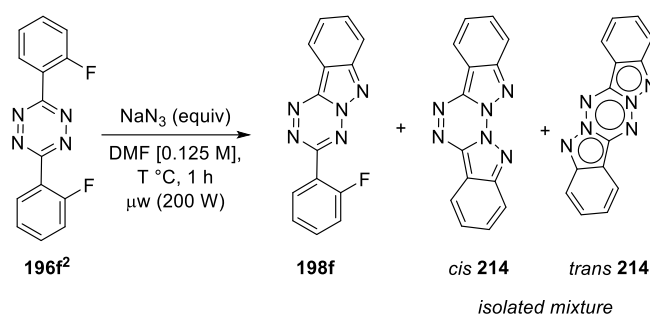
We separated the two isomers and identify it by NMR (¹H and ¹³C) techniques. We propose that the ¹H NMR chemical shift (in ppm) of the *trans*-isomer has a shift at low field for all the hydrogen atoms (H¹ to H⁴, Scheme 55) in comparison to the *cis*-isomer.



Scheme 55. ¹H NMR (600 MHz, DMSO-*d*₆, 298K) for *cis*-**214**, *trans*-**214**

b. Microwave-assisted azide-cyclization

By thermal heating, the double *N*-cyclization was not efficient. With the view to increase the conversion of the double *N*-cyclization, we performed the reaction under microwave conditions starting from **196f²** (Table 1). Under microwave irradiations at 130 °C for 1 h, the addition of 1.1 equiv of NaN₃ mainly leads to the monocyclization and produces **198f** as the major product (47%, Table 1, entry 1); whereas the mixture of bis-tetrazo[1,2-*b*]indazole isomers is isolated in 9% (45%, Table 1, entry 1). Increasing the loading of added NaN₃ to 3 equiv increases the amounts of obtained mixture of isomers to 34% (Table 2, entry 2). Further addition of the NaN₃ load to 6 equiv decreases the amounts of isolated isomer mixture to only 20% (entry 3 vs entry 2). The latter result can be explained by the disruption of the reaction by the presence of high amounts of waste products from the decomposition of NaN₃ under high temperatures.

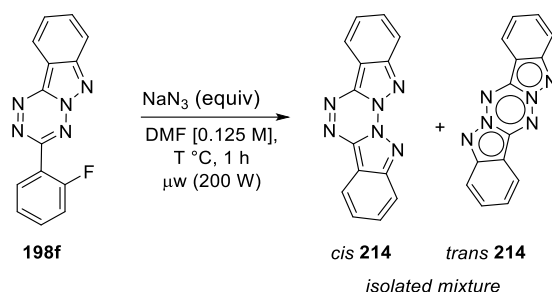


Entry	NaN ₃ (equiv)	T (°C)	Conv. (%) ^[b]	198f (%) ^[c]	214 (<i>cis</i> + <i>trans</i>) (%) ^[c]
1	1.1	130	99	47	9
2	3.0	130	99	45	34
3	6.0	130	99	39	20

Table 1. ^[a] Conditions: **196f²** (1 equiv, 0.25 mmol), NaN₃ (1.1-6.0 equiv), DMF (0.125 M, 2 ml), 130 °C, under microwave irradiation (200 Watts) under air, 1 h. ^[b] Conversion based on the **196f²** consumption (¹H and ¹⁹F NMR). ^[c] Isolated yield. *nd* (non-determined).

We assumed that performing the reaction starting from the mono-cyclized **198f** instead **196f²** under microwave conditions in DMF for 1 h might improve the results (Table 2). With **198f** as a starting material, 1.1 equiv of NaN₃ under 110 °C, an isolated of the isomers was formed in 14% yields (Table 2, entry 1). Increasing the temperature to 130 °C. Finally, produces a fairly good isolated yield of the

mixture in 36% (Table 2, entry 2). Finally, increasing the amounts of added NaN₃ to 3 equiv at 130 °C results in obtaining the bis-tetrazo[1,2-*b*]indazole isomer mixture 44% yields (Table 2, entry 3).



Entry	NaN ₃ (equiv)	T (°C)	214 (<i>cis</i> + <i>trans</i>) (%) ^[c]
1	1.1	110	14
2	1.1	130	36
3	3	130	44

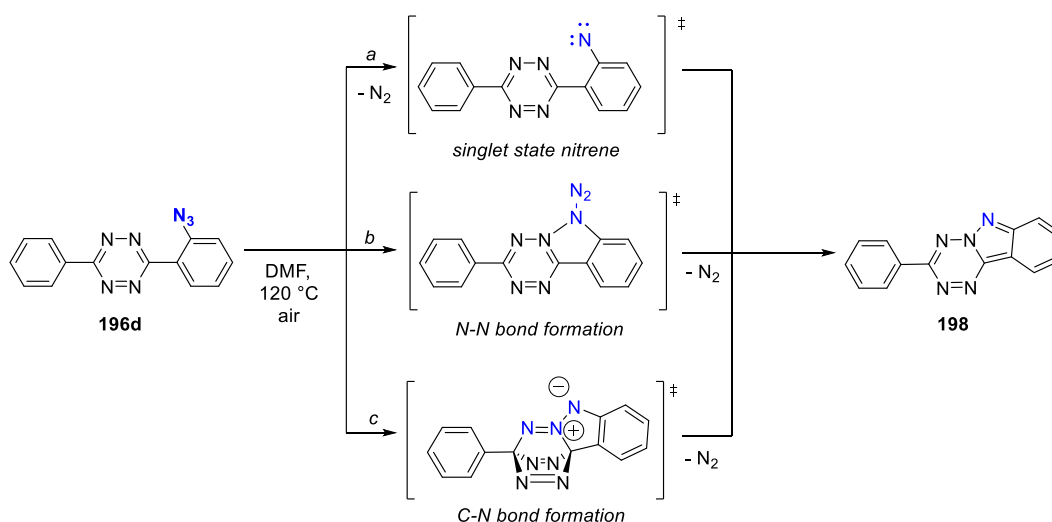
Table 2. Conditions: **198f** (1 equiv, 0.25 mmol), NaN₃ (1.1 equiv), DMF (0.125 M, 2 ml), 110-130 °C, under microwave irradiation (200 Watts) and air, 1 h. ^[b] Conversion based on the **198f** consumption (¹H NMR). ^[c] Isolated yield.

VI. Mechanism formation of the tetrazo[1,2-*b*]indazole

1) Formation of 3-(aryl)-tetrazo[1,2-*b*]indazole

The team of theoretical chemistry at the ICMUB led by Pr. Paul Fleurat-Lessard examined the mechanisms of the formation of the tetrazo[1,2-*b*]indazole **198** from **196d**, *via* density functionalized theory (DFT) calculations. Different possible routes were envisioned for the N–N bond formation to reach the *N*-rich heterocycle (Scheme 56).

Based on the literature reports previously discussed, a first route envisaged may occur *via* a nitrene intermediate. This is a two-step process where the electron-deficient nitrene is first formed and then the nitrogen of the tetrazine core attacks the nitrene forming the desired cyclic heterocycle *via* the N–N bond formation (route *a*). The second possible synthetic route occurs *via* the direct attack of the first nitrogen of the azide to the tetrazine core, which lead to the formation of the new N–N bond with the release of the second part of the azide (route *b*). Finally, the last possible synthetic route is the attack at the carbons of the tetrazine core by the azide, to form the tetrazo[1,2-*b*]indazole with the release of dinitrogen from the tetrazine core (route *c*).



Scheme 56. Possible mechanism pathways for the formation of **198** from **196d**

The DFT calculations were performed by Dr Iogann Tolbatov for these pathways. The nitrene formation is high in terms of energy, compared to the other synthetic routes, and the subsequent full mechanism was no longer considered. The second approach, route b, with the N–N formation is apparently energetically favored compared to the C–N bond formation with a transition structure (TS) at +34.1 Kcal mol⁻¹ compared to a TS at +46.2 Kcal mol⁻¹ in route c (Figure 1, blue line and a black line, respectively).

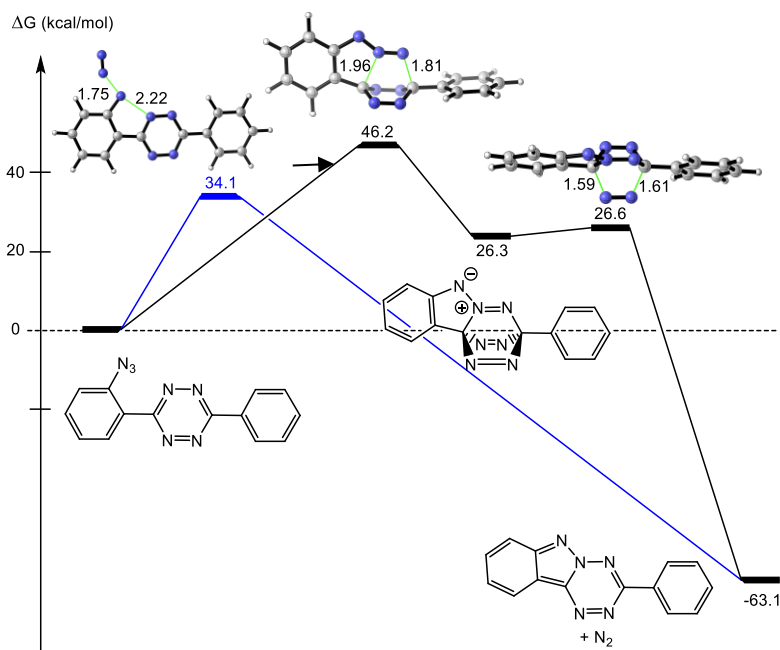


Figure 1. Formation of the **198**. Values represent Gibbs free energies in kcal mol⁻¹

As for the second cyclization leading to bis-tetrazo[1,2-*b*]indazole, the same mechanism is applied.

2) Formation of the *bis*-tetrazo[1,2-*b*]indazole

The second cyclization pathway was also examined by DFT calculations in order to evaluate the *cis/trans* formation and the ratio of the *bis*-tetrazo[1,2-*b*]indazole products (Figure 2). DFT calculations permitted to conclude that the most favourable reaction route for the formation of the *cis*-*bis*-tetrazoindazole follows the same mechanism as previously described for tetrazo-indazole. The cyclization of azide-functionalized complex upon approach of the azide nitrogen toward the tetrazine nitrogen. The calculations showed that the formation of the *trans*-isomer is favoured by 1.1 kcal/mol where $\Delta G^\ddagger\text{-cis} = 35.5\text{kcal/mol}$ vs $\Delta G^\ddagger\text{-trans} = 34.4\text{kcal/mol}$. At 130 °C, this energy gap would lead to a 80:20 *trans*:*cis* ratio.

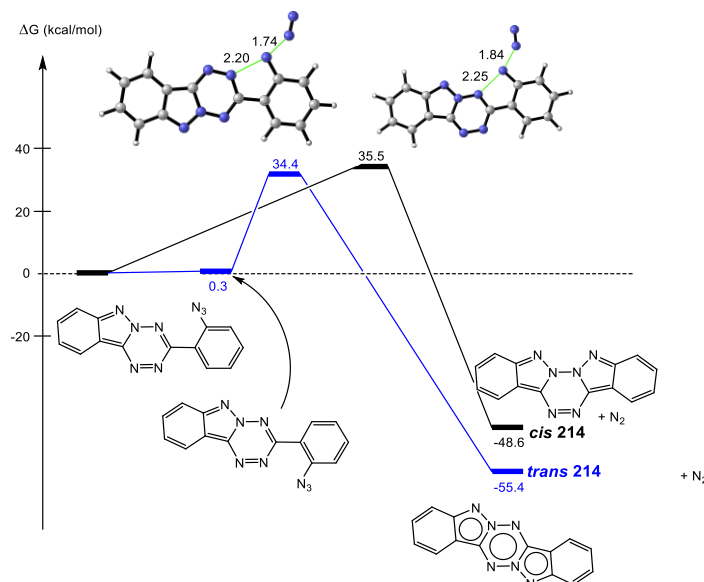
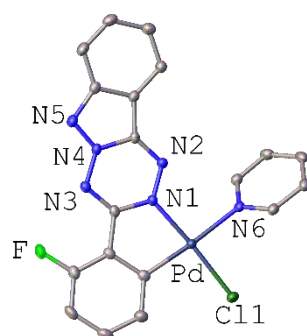
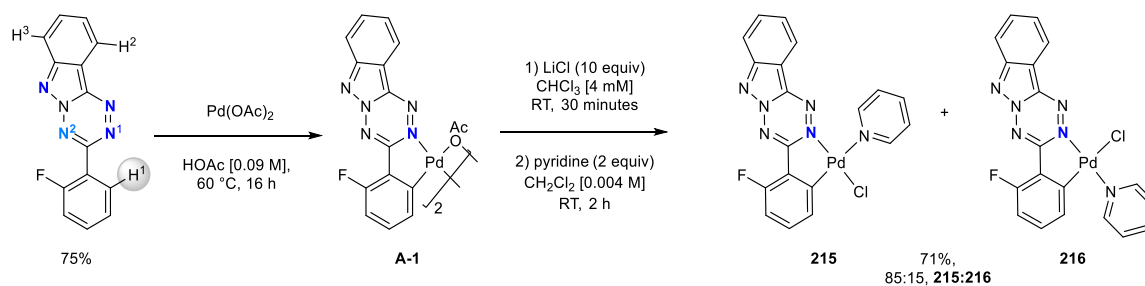


Figure 2. Formation of isomeric *cis*- and *trans*-214. Gibbs free energy profile (in kcal mol⁻¹)

VII. Post-functionalization of 3-(aryl)-tetrazo[1,2-*b*]indazole

1) Palladium metallacycle formation

198 contains different nitrogen atoms that may be eventually used as *N*-directing groups for the C–H bond activation on three potentially accessible functionalization positions (H¹ to H³, Scheme 57).

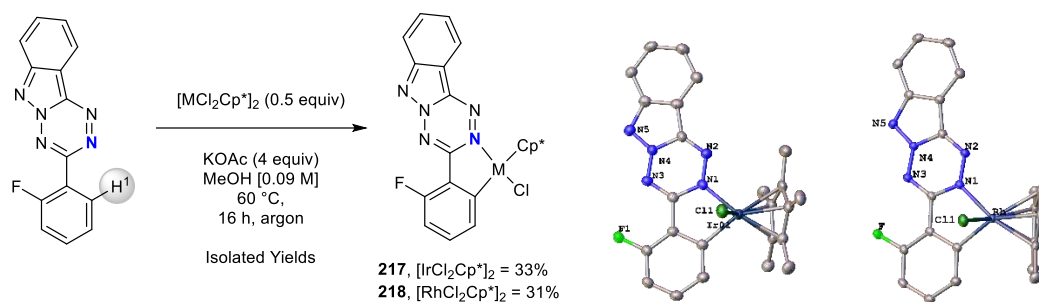


Scheme 57. Synthesis of different palladacycles and the molecular structure for **215** (ORTEP with hydrogen omitted)

Mechanistic studies on *N*-directed C–H activation/functionalization have identified the formation of *N*-containing metallacycles as pertinent intermediates for mastering the selectivity in the catalytic process.^[127] We selected the ligand 3-(2-fluorophenyl)tetrazo-[1,2-*b*]indazoles **198f** as the pertinent ligand to study the metallacycle formation by *N*-directed C–H activation, and subsequent applications in various cross-coupling reactions.

The palladacycle **A-1** was isolated in 75% yield by precipitation from the reaction of Pd(OAc)₂ and **198f** in HOAc (Scheme 57). Our attempts to get single crystals of **A-1** were unsuccessful, and we synthesized by an exchange of OAc ligands with chlorides and addition of pyridine the monomeric palladacycles **215** and **216** as a mixture of isomers. After column chromatography, we isolated 71% of complexes, based on the ¹⁹F and ¹H NMR spectroscopy in solution, and confirmed by X-ray diffraction analysis in the solid state. We identified a mixture with a ratio 85:15 of **215** and **216**, respectively, complexes which differ by the presence of the pyridine moiety in *cis* or *trans* of the tetrazo-indazole core (Scheme 57).

The analogous iridacycle and rhodacycle **217** and **218** (Scheme 58) were synthesized using the precatalyst [MCl₂Cp*]₂ (M = Ir and Rh), KOAc as the base in MeOH, giving 33% and 31% isolated yields, respectively. The metallacycles were the major products alongside traces of some other unidentified complexes. The XRD structure analysis of the metallacycles **217** and **218** confirmed the coordination mode at the N1 and C1.



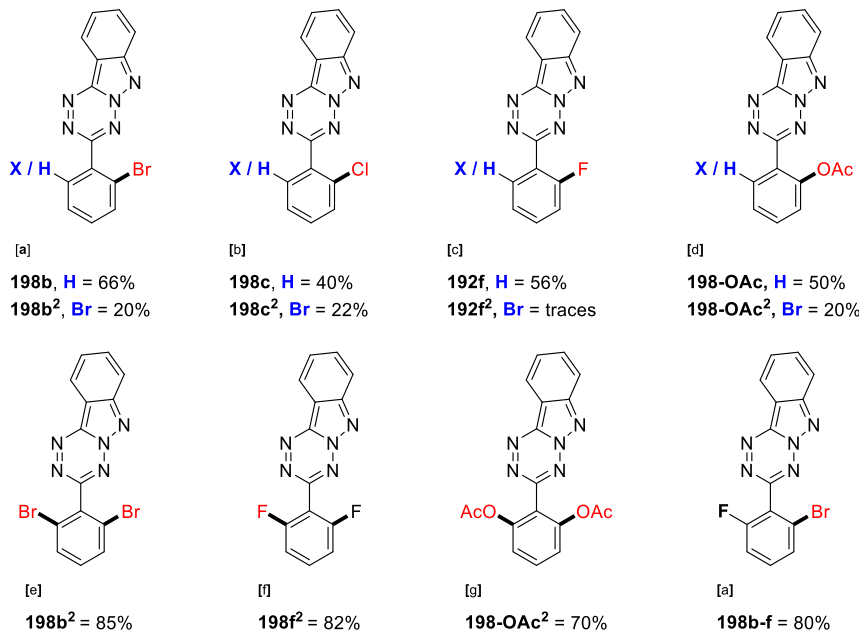
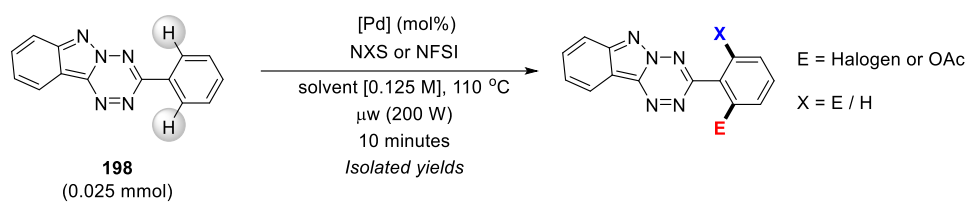
Scheme 58. Synthesis of the iridacycle and rhodacycle **217** and **218**

With these metallacycles in our hands, we studied the selective *o*-functionalization of the aryl-tetrazolo-indazole.

2) *Ortho*-functionalization of tetrazo-indazole

Compound **198** was employed as an *N*-directing ligand in the electrophilic Pd-catalyzed C–H bond activation and functionalization. Both mono- and dihalogenation (or acetoxylation) reactions were achieved on **198**, affording mono- and difunctionalized derivatives, in short reaction times under microwave conditions (Scheme 59).

Palladium-catalyzed C–H monofunctionalization was performed under microwave radiation for 10 minutes, using either 1 equiv of the *N*-halosuccinimide (NBS, NCS), or NFSI for halogenation, or PIDA for acetoxylation, in nitromethane or acidic acid at 100 °C. From these reactions, **198b**, **198c**, **198f** and **198-OAc** were isolated in 66%, 56%, 40% and 50% yields, respectively. The major side-product was the difunctionalization product obtained in *ca* 20% yields, except in the case of fluorination that showed traces of the dihalogenated product.

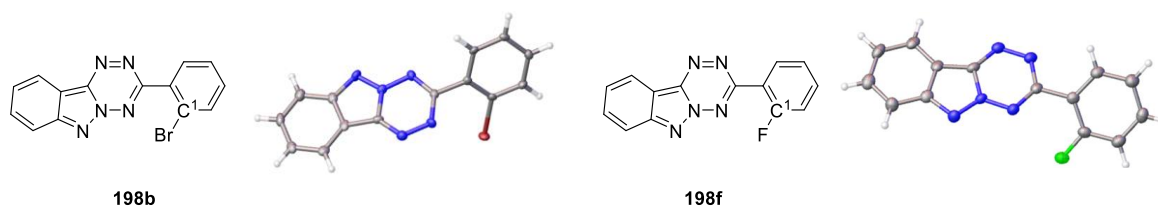


^[a] **198** (1.0 equiv), Pd(OAc)₂ 10 mol%, NBS (1.0 equiv), CH₃NO₂ [0.04 M], 110 °C, 200 W, under air. ^[b] Pd(dba)₂ 20 mol%, NCS (3.0 equiv), HOAc [0.04 M]. ^[c] Pd(dba)₂ 20 mol%, NFSI (1.0 equiv). ^[d] Pd(OAc)₂ 15 mol%, PIDA (1.0 equiv), HOAc [0.04 M]. ^[e] Pd(OAc)₂ 20 mol%, PIDA (2.2 equiv), HOAc [0.04 M]. ^[f] NFSI (5.0 equiv). ^[g] PIDA (2.2 equiv)

Scheme 59. *o*-C–H bond functionalization of **198**

Difunctionalization was also achieved for isolating **198b²**, **198f²**, **198-OAc²** in 85%, 82% and 70% yields, respectively. This was achieved upon increasing the amounts of electrophilic reagent to 2.2 equiv of NBS for dibromination or PIDA for diacetoxylation. Five equivalents of NFSI were required for operating difluorination. Difunctionalized tetrazo-indazoles with two different functions could be obtained using **198** as the starting material, and employing for instance one equivalent of NBS on **198f** to obtain **198b-f** in 80% reaction yield.

Single crystal X-ray diffraction structure of the brominated **198b** and the fluorinated **198f** are reported in Scheme 59. The halogen insertion clearly occurs on the *o*-position of the phenyl ring of tetrazo[1,2-*b*]indazole.



Scheme 60. Molecular structures of **198b** and **198f**

VIII. Photophysical analysis of the mono and bistetrazo[1,2-*b*]indazole

1) UV-visible analysis

A. UV-visible analysis of 3-(aryl)-tetrazo[1,2-*b*]indazoles

The spectroscopic properties of monohalogenated (**198a-198b-198c-198f** and **198-OAc**) and dihalogenated (**198a²-198f²** and **198-OAc²**) were investigated in diluted CH₂Cl₂ solutions ($c = 5.10^{-6}$ mol.L⁻¹, Figure 3). The 3-(aryl)-tetrazo[1,2-*b*]indazole display large absorption with moderate extinction coefficient in the visible range ($\lambda_{\text{abs}}(\text{PhTzIn}) = 435$ nm; $\lambda_{\text{max}} = 2300$ L. mol⁻¹.cm⁻¹). Such *transition* is assigned to π - π^* *transition* in the tetrazo[1,2-*b*]indazole core. The effect of post-*ortho*-functionalization has limited impact on the optical properties. This is explained as the modifications are performed in *o*-position of the lateral phenyl ring.

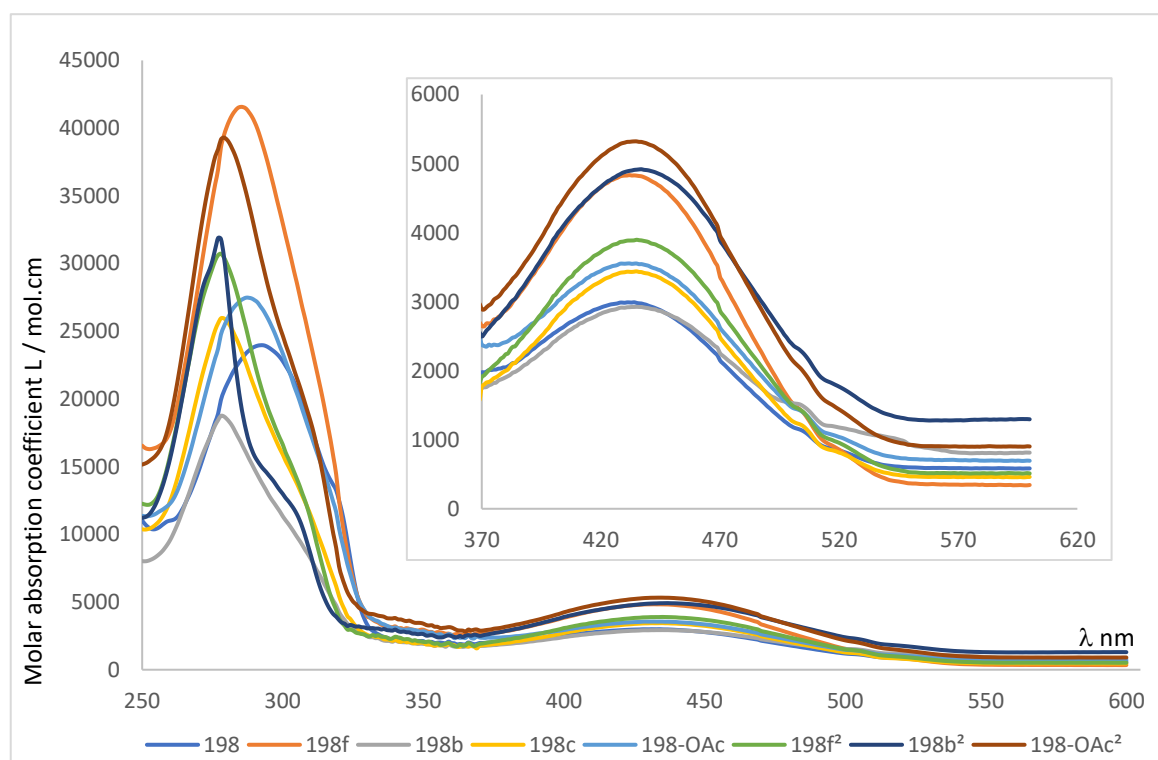


Figure 4. The UV-Vis of **198** and its functionalized derivatives

B. UV-visible analysis of bis-tetrazo[1,2-*b*]indazoles

As expected, the presence of the second fused cycle in *cis*-**214** red-shifts the UV-vis absorption with an increase of the molar absorption ($\lambda_{\text{abs}}(\textit{cis } \mathbf{214}) = 455 \text{ nm}$; $\lambda_{\text{max}} = 14000 \text{ L}\cdot\text{mol}^{-1}\cdot\text{cm}^{-1}$; Figure 5). Here also, the *transition* is assigned to π - π^* *transition* in the bis-tetrazo[1,2-*b*]indazole core. While the monofunctionalized derivatives of **198** showed no fluorophore properties, the bis-tetrazo[1,2-*b*]indazole *cis*-**214** display intense luminescence at 532 nm fluorescent ($\phi = 52\%$) with a lifetime of 7 ns (Figure 5). Indeed, the molecular structure of *cis*-**214** has a dramatic impact on its luminescent properties, and nicely fit with its planar and fully rigid structure.

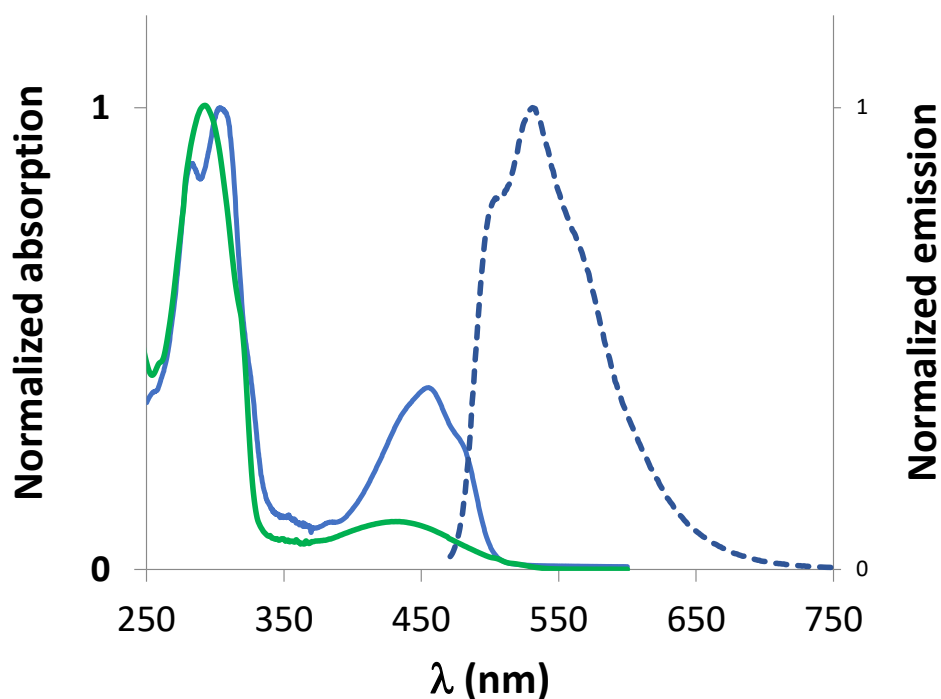
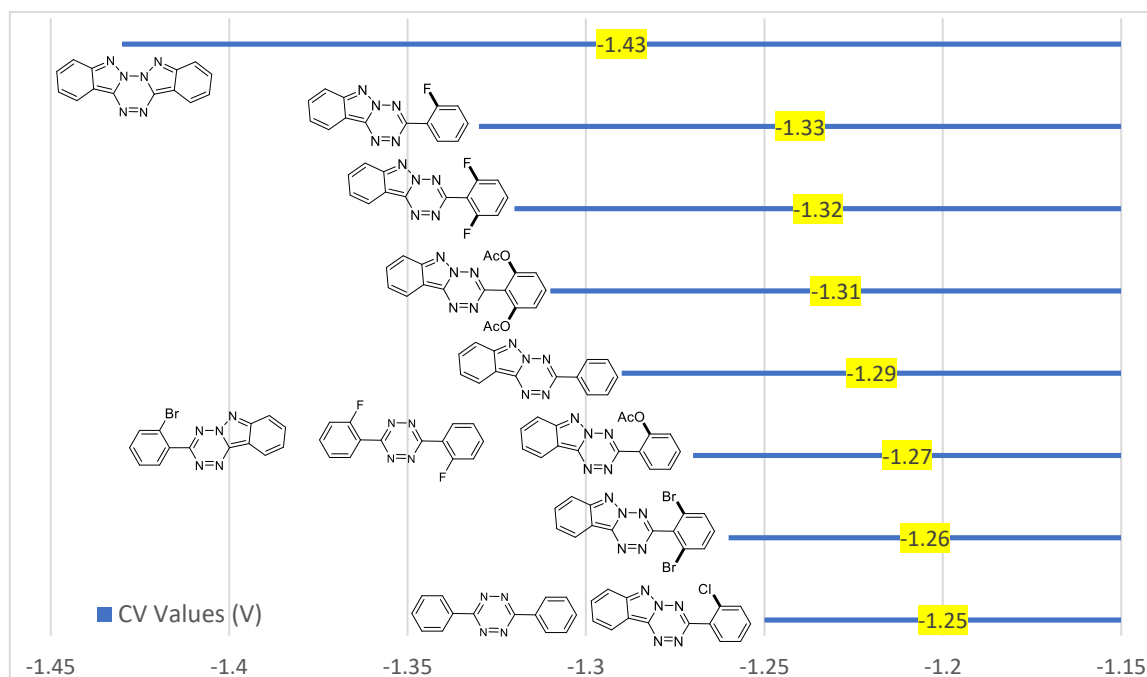


Figure 5. UV/Vis absorption of **198** (green) and *cis* **214** (blue) and emission of *cis* **214** (blue, dotted) in solution (CH_2Cl_2)

2) Cyclic voltammetry measurements

We have found out that 3-(aryl)-tetrazo[1,2-*b*]indazoles and bis-tetrazo[1,2-*b*]indazoles, have high electron-accepting capabilities. This is proved by their cyclic voltametric measurements where similar to *s*-aryltetrazine platforms,^[3] the newly synthesized tetrazo[1,2-*b*]indazoles can solely perform facile reduction. Typical *s*-aryltetrazine platforms **196** and **196c** are reduced at -1.25 V . Similarly, the 3-

(phenyl)-tetrazo[1,2-*b*]indazole **198** showed reduction close in value at -1.29 V. Tailoring **198** with electron-withdrawing halogen or acetyl groups had no significant effect on the electron-acceptance capabilities and thus reduction values (between -1.25 V and -1.33 V). However, the second cyclization slightly decreased this property as the *cis*-bis-tetrazo[1,2-*b*]indazole isomer demanded higher values at -1.43 V for *cis*-**214** to be reduced (Graph 15). One main significance of these values is the possibility of such novel heterocycles to be considered as electron-acceptor in organic solar cells.^[128]



Graph 15. CV of a 10^{-3} M solution of tetrazo[1,2-*b*]indazoles (mono and bis) (CH_2Cl_2 0.1 M, TEABF_4 , $\nu = 100 \text{ mV}\cdot\text{s}^{-1}$, vs SCE)

We also analyzed the cyclic voltammetry values of the *cis*- and *trans* bis-tetrazo[1,2-*b*]indazole isomers in DMF and vs the ferrocene. We found out that both isomers undergo irreversible reductions at -1.43 V and -1.17 V. Moreover, *trans*-**214** can perform oxidation at 0.75V unlike any tetrazine precursors or tetrazo[1,2-*b*]indazole **198** and its derivative (Table 3). This indicates that the *cis*-**214** has higher electron-density with respect to *trans*-**214**.

Molecule	Values (V vs Fe/Fe ⁺) for reduction	Values (V vs Fe/Fe ⁺) for oxidation
<i>Cis</i> 214	-1.43	-
<i>Trans</i> 214	-1.17	0.75

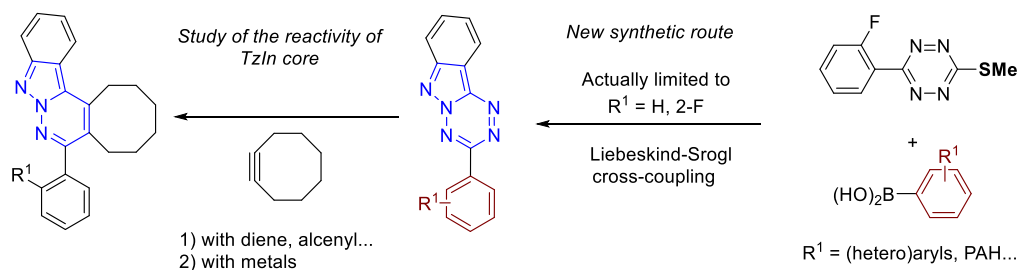
Table 3. CV of a 10^{-3} M solution of *cis* and *trans* bis-tetrazo[1,2-*b*]indazole **214** (DMF 0.1 M, TEABF₄, $v = 100$ mV.s⁻¹, WE: Pt, $\varnothing = 1.6$ mm).

IX. Conclusion and perspectives

In this chapter, we described the synthetic route to introduce azide in *ortho*-position of the tetrazine core by a copper-catalyzed pathway or a nucleophilic reaction. The azide heterocycle was used with success in the Huisgen coupling in order to introduce various chromophores such as coumarin or pyrenyl and the selective iEDDA reaction which occurred only on the *s*-tetrazine core.

More important, we described the synthesis of a new class of *N*-rich heterocycle: the tetrazo[1,2-*b*]indazole. We developed a new synthetic route starting from the corresponding fluorinated *s*-aryltetrazine under microwave irradiations. With the *N*-heterocycle, we applied the Pd-catalyzed *N*-directed C–H bond halogenation and acetoxylation in short reaction times (10 min). The bis-tetrazo[1,2-*b*]indazole **198** was found to have two *cis*- and *trans*-isomers. The 3-(aryl)-tetrazo[1,2-*b*]indazoles and the bis-tetrazo[1,2-*b*]indazoles showed interesting properties in terms of high electron affinity and intense luminescence, especially the more planar heterocycle.

As the perspectives (Scheme 61), in comparison with the *s*-tetrazine core, the reactivity of the tetrazo[1,2-*b*]indazole must be explored. As an example, the iEDDA with cyclooctyne must be tested to open the way to new applications as a click agent or to modify the fluorescence properties.^[129] The synthesis of the 3-(aryl)-tetrazo[1,2-*b*]indazole **198** is limited to the phenyl, or the fluorinated derivatives following by their post-functionalization. A new synthetic route is currently studied in the group based on the Liebeskind-Srogl cross-coupling strategy followed by a *N*-cyclization process on the *s*-tetrazine core in order to introduce new functions, which could valuably modify the properties, including from photophysical perspective.



Scheme 61. Perspectives on the tetrazo[1,2-*b*]indazoles chemistry

Supporting Information

General conditions

All commercial reagents were purchased from commercial suppliers and used without purifications. All reactions were performed in a Schlenk tube or in a microwave reaction vessel. Microwave heating was carried out using a CEM Discover microwave reactor. The microwave reactions were run in closed reaction vessels with magnetic stirring and with the temperature controlled *via* IR detection. ^1H (500 MHz or 600 MHz), ^{13}C (125 MHz or 150 MHz), ^{19}F (470 MHz) spectra were recorded. Chemical shifts are reported in ppm relative to CDCl_3 (^1H : 7.26 ppm and ^{13}C : 77.16 ppm) or CD_2Cl_2 (^1H : 5.32 ppm and ^{13}C : 54.00 ppm) or DMSO (^1H : 2.50 ppm and ^{13}C : 39.52 ppm) and coupling constants J are given in Hz.

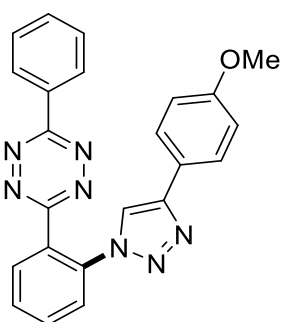
High resolution Mass Spectra (HRMS) were obtained on a Thermo LTQ-Orbitrap XL with ESI source.

Optical properties: UV-Visible spectra were recorded at room temperature on a Specord 205 UV/Vis/NIR spectrophotometer and with a Varian UV-vis spectrophotometer Cary 50 scan using quartz cells (Hellma). The UV-Vis emission spectra measurements were recorded on a FL 920 Edinburgh Instrument equipped with a Hamamatsu R5509-73 photomultiplier for the NIR domain (300-1700 nm) and corrected for the response of the photomultiplier. The absolute quantum yields were measured with a C9920-03 Hamamatsu. Life-times measurements were conducted with 375 nm diode laser excitation (EPL-series) plugged to a TCSPC pulsed source interface using an Edinburgh FS920 Steady State Fluorimeter combined with a FL920 Fluorescence Lifetime Spectrometer.

Typical experimental procedures

1) General procedure for the one-pot azidation and alkyne cycloaddition of bromo-Tz

3-(phenyl)-[1,2,4,5]-tetrazo[2-*b*]indazole (198)



55%, (heptane/ethylacetate: 6/4); R_f = 0.33

^1H NMR (500 MHz, CDCl_3): δ (ppm) = 8.59–8.54 (m, 2H), 8.36–8.31 (m, 1H), 8.11 (s, 1H), 7.83–7.77 (m, 4H), 7.69–7.65 (m, 1H), 7.62 (d, J = 5.8 Hz, 1H), 7.59–7.54 (m, 1H), 6.98 (d, J = 8.8 Hz, 2H), 3.85 (s, 3H)

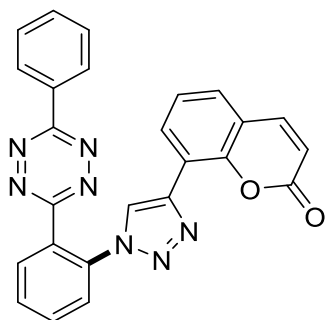
^{13}C NMR (125 MHz, CDCl_3): δ (ppm) = 165.3, 163.3, 159.8, 148.0, 136.1, 132.9, 132.4, 132.1, 131.5, 130.3, 129.3, 129.2, 128.4, 127.3, 126.1, 122.9, 120.0, 114.3, 55.4

HRMS + p ESI (m/z) [$\text{M}+\text{H}^+$] calcd for $\text{C}_{23}\text{H}_{18}\text{N}_7\text{O}^+$: 408.15673;

Found: 408.15633.

3-(phenyl)-[1,2,4,5]-tetrazo[2-*b*]indazole (198)

61%, (heptane/ethylacetate: 6/4); R_f = 0.1



¹H NMR (500 MHz, CDCl₃): δ (ppm) = 8.60-8.53 (m, 2H), 8.40 (dd, J = 5.8, 3.5 Hz, 1H), 8.31 (s, 1H), 7.86 (m, 3H), 7.80 (s, 1H), 7.75-7.67 (m, 2H), 7.63 (t, J = 7.3 Hz, 1H), 7.61-7.52 (m, 3H), 6.44 (d, J = 9.5 Hz, 1H)

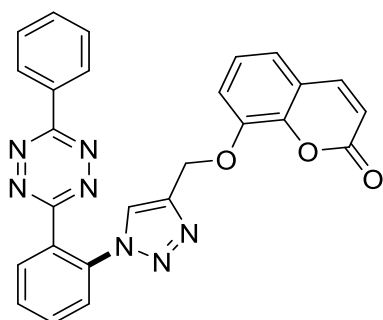
¹³C NMR (125 MHz, CDCl₃): δ (ppm) = 164.0, 159.6, 153.5, 145.5, 141.9, 134.7, 132.9, 132.0, 131.5, 131.2, 130.3, 129.7, 128.3, 128.2, 127.4, 127.4, 125.4, 121.2, 121.0, 117.7, 115.7, 112.8.

HRMS + p ESI (m/z) [M+H⁺] calcd for C₂₅H₁₆N₇O₂⁺: 446.13600;

Found: 446.13509.

3-(phenyl)-[1,2,4,5]-tetrazo[2-*b*]indazole (198)

57%, (heptane/ethylacetate: 6/4); R_f = 0.18



¹H NMR (500 MHz, CDCl₃): δ (ppm) = 8.61-8.51 (m, 2H), 8.42-8.34 (m, 1H), 8.06 (d, J = 0.8 Hz, 1H), 7.85-7.78 (m, 2H), 7.68-7.56 (m, 5H), 7.39 (d, J = 9.2 Hz, 1H), 6.97 (dq, J = 5.4, 2.5 Hz, 2H), 6.27 (d, J = 9.5 Hz, 1H), 5.36 (s, 2H)

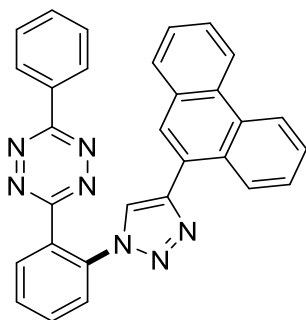
¹³C NMR (125 MHz, CDCl₃): δ (ppm) = 164.9, 163.3, 161.3, 161.0, 160.9, 155.8, 143.5, 143.2, 135.9, 133.1, 132.5, 132.1, 131.4, 130.7, 129.3, 129.3, 128.9, 128.4, 126.6, 126.5, 124.7, 113.6, 113.1, 112.68, 102.4, 62.4

HRMS + p ESI (m/z) [M+H⁺] calcd for C₂₅H₁₈N₇O₃⁺:

476.14656; Found: 476.14641.

3-(phenyl)-[1,2,4,5]-tetrazo[2-*b*]indazole (198)

63%, (heptane/ethylacetate: 6/4); R_f = 0.42



¹H NMR (500 MHz, CDCl₃): δ (ppm) = 8.79 (dd, J = 8.4, 1.2 Hz, 1H), 8.73 (d, J = 8.3 Hz, 1H), 8.65-8.57 (m, 2H), 8.48-8.39 (m, 2H), 8.27 (s, 1H), 8.07 (s, 1H), 7.96-7.90 (m, 1H), 7.88-7.84 (m, 2H), 7.83-7.79 (m, 1H), 7.70 (m, 2H), 7.66-7.58 (m, 4H), 7.58-7.52 (m, 1H)

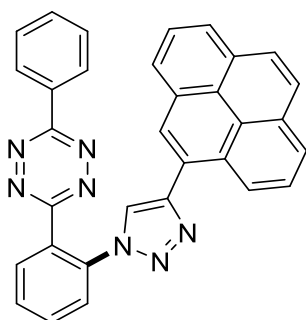
¹³C NMR (125 MHz, CDCl₃): δ (ppm) = 165.1, 163.3, 147.1, 136.2, 133.0, 132.0, 131.9, 131.5, 131.3, 130.8, 130.6, 130.3, 129.4, 129.3, 129.0, 128.9, 128.7, 128.4, 127.3, 127.2, 127.0, 126.9, 126.8, 126.6, 126.4, 124.8, 122.9, 122.6

HRMS + p ESI (m/z) [M+H⁺] calcd for C₃₀H₂₀N₇⁺: 478.17747;

Found: 478.17700.

3-(phenyl)-[1,2,4,5]-tetrazo[2-*b*]indazole (198)

53%, (heptane/ethylacetate: 99/1); R_f = 0.4



¹H NMR (500 MHz, CDCl₃): δ (ppm) = 8.70 (d, J = 9.3 Hz, 1H), 8.64-8.59 (m, 2H), 8.45-8.40 (m, 1H), 8.36 (s, 1H), 8.31 (d, J = 7.8 Hz, 1H), 8.25-8.16 (m, 3H), 8.13-8.06 (m, 3H), 8.02 (t, J = 7.6 Hz, 1H), 7.86-7.79 (m, 3H), 7.65-7.60 (m, 1H), 7.58 (ddd, J = 8.4, 6.5, 1.6 Hz, 2H)

¹³C NMR (125 MHz, CDCl₃): δ (ppm) = 165.2, 163.3, 147.7, 136.2, 133.0, 132.5, 132.0, 131.5, 131.5, 131.4, 130.9, 130.5, 129.3, 129.3, 128.9, 128.4, 128.3, 127.9, 127.4, 127.3, 126.6, 126.1, 125.5, 125.2, 125.1, 124.9, 124.8, 124.7.

HRMS + p ESI (m/z) [M+H⁺] calcd for C₃₂H₂₀N₇⁺: 502.17747;

Found: 502.17702.

2) General procedure for functionalization of 3,6-diaryl-1,2,4,5-tetrazine

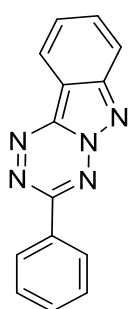
As a typical experiment, the 3,6-diphenyl-1,2,4,5-tetrazine (1.0 equiv, 0.25 mmol), the electrophilic source (NBS or NFSI), and palladium source (10 mol%) were introduced in a 10 mL microwave reaction vessel, equipped with a magnetic stirring bar. The solvent (2 mL, 0.125 M) was added, and the reaction mixture was heated in the microwave at 110 °C for corresponding reaction time (200 W, 2 minutes ramp). After cooling down to RT, the reaction mixture was diluted with DCM, and was washed three times with water + 3% of TEA. The combined organic layer was washed with water and dried over MgSO₄. The solvent was removed under *vacuum*. Then, the crude product was purified by silica gel column chromatography using an appropriate ratio of the eluent.

For alternative synthesis of monohalogenated tetrazine by normal heating, see: *Angew. Chem. Int. Ed.* **2016**, *55*, 5555–5559 (10.1002/anie.201601082).

3) General procedure of the synthesis of 3-(aryl)-[1,2,4,5]-tetrazo[1,2-*b*]indazole

As a typical experiment, the *s*-tetrazine (1.0 equiv, 0.25 mmol), sodium azide (3.0 equiv) were introduced in a 10 ml microwave reaction vessel equipped with a magnetic stirring bar. The DMF (2 ml, 0.125 M) was added, and the reaction mixture was heated at 130 °C under air. After cooling down to room temperature, the solvent was removed under *vacuum*. The crude product was purified by silica gel column chromatography (Pentane/CH₂Cl₂ or Heptane/Ethyl acetate) to afford the corresponding product.

3-(phenyl)-[1,2,4,5]-tetrazo[1,2-*b*]indazole (198)



(Pentane/CH₂Cl₂: 2/8). Yield: 70% as an orange solid.

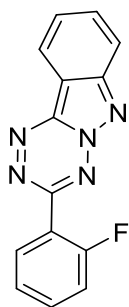
¹H NMR (500 MHz, CDCl₃): δ (ppm) = 8.66–8.63 (m, 3H), 8.15 (d, *J* = 8.5 Hz, 1H), 7.93 (t, *J* = 7.7 Hz, 1H), 7.76 (t, *J* = 7.6 Hz, 1H), 7.65–7.63 (m, 3H).

¹³C NMR (125 MHz, CDCl₃): δ (ppm) = 157.5, 148.3, 141.3, 132.4, 132.3, 132.1, 129.2, 128.5, 126.5, 121.2, 118.5, 114.0.

HRMS + p ESI (*m/z*) [*M*+*H*⁺] calcd for C₁₄H₁₀N₅⁺: 248.09307; Found: 248.09278.

3-(2-fluorophenyl)-[1,2,4,5]-tetrazo[1,2-*b*]indazole (198f)

(Pentane/CH₂Cl₂: 2/8). Yield: 45% as an orange solid.



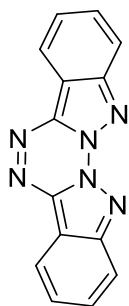
¹H NMR (500 MHz, CDCl₃): δ (ppm) = 8.66 (dt, *J* = 8.1 and 1.0 Hz, 1H), 8.32 (td, *J* = 7.7 and 1.8 Hz, 1H), 8.18 (dt, *J* = 8.5 and 0.7 Hz, 1H), 7.96 (ddd, *J* = 8.4, 7.0 and 1.2 Hz, 1H), 7.81–7.78 (m, 1H), 7.67–7.62 (m, 1H), 7.43 (td, *J* = 7.6 and 1.2 Hz, 1H), 7.35 (ddd, *J* = 11.0, 8.4 and 1.2 Hz, 1H).

¹⁹F NMR (470 MHz, CDCl₃): δ (ppm) = –112.0.

¹³C NMR (125 MHz, CDCl₃): δ (ppm) = 160.5 (d, *J* = 258.8 Hz), 156.7 (d, *J* = 5.1 Hz), 148.5, 140.9, 133.7 (d, *J* = 8.7 Hz), 132.4, 132.2, 126.8, 124.8 (d, *J* = 3.9 Hz), 121.4, 121.3 (d, *J* = 10.0 Hz), 118.7, 117.4 (d, *J* = 21.8 Hz), 113.9.

HRMS + p ESI (*m/z*) [*M*+*H*⁺] calcd for C₁₄H₉N₅⁺: 266.08365; Found: 266.08346.

bis-[1,2,4,5]-tetrazo[1,2-*b*]indazole (*cis* 214)



(Pentane/CH₂Cl₂: 2/8).

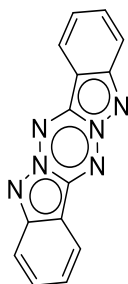
¹H NMR (600 MHz, DMSO-d⁶) δ (ppm) = 8.72 (d, *J* = 8.1 Hz, 2H), 8.31 (d, *J* = 8.5 Hz, 2H), 7.96 (dd, *J* = 8.3 and 7.3 Hz, 2H), 7.79 (sb, 2H).

¹³C NMR (150 MHz, CDCl₃): δ (ppm) = 145.2, 137.8, 130.5, 125.6, 120.3, 117.9, 114.7.

RMS + p ESI (m/z) [M+Na⁺] calcd for C₁₄H₈N₆Na⁺: 283.07027; Found: 283.07028.

bis-[1,2,4,5]-tetrazo[1,2-*b*]indazole (*trans* 214)

trans 214 exhibit a very low solubility compare to *cis* 214 in CH₂Cl₂. After DMF evaporation, the crude is dissolved in CH₂Cl₂ then filtered, and washed with CH₂Cl₂ and water.



¹H NMR (600 MHz, DMSO-d⁶) δ (ppm) = 8.58 (dt, *J* = 8.0 and 1.0 Hz, 2H), 8.11 (dt, *J* = 8.6 and 0.9 Hz, 2H), 7.96 (ddd, *J* = 8.3, 6.9, 1.2 Hz, 2H), 7.63 (ddd, *J* = 7.9, 6.9 and 0.8 Hz, 2H).

¹³C NMR (150 MHz, DMSO-d⁶): δ (ppm) = 149.9, 137.1, 132.5, 122.9, 121.5, 116.6, 110.3.

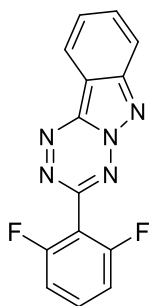
HRMS + p ESI (m/z) [M+H⁺] calcd for C₁₄H₉N₆⁺: 261.08832; Found: 261.08831

4) General procedure of the functionalization of 3-(aryl)-tetrazo[1,2-*b*]indazole

As a typical experiment, the 3-(aryl)-tetrazo[1,2-*b*]indazole (1.0 equiv, 0.25 mmol), [E⁺] (1-5 equiv), and palladium source (10 - 20 mol%) were introduced in a 10 ml microwave reaction vessel, equipped with a magnetic stirring bar. The solvent (ml) was added, and the reaction mixture was heated in the microwave at 110 °C for corresponding reaction time (10 to 30 minutes) (200 W, 2 minutes ramp). After cooling down to room temperature, the reaction mixture was diluted with DCM, and was washed three times with water + 3% of TEA. The combined organic layer was washed with water and dried over MgSO₄. The solvent was removed under *vacuum*. The crude product was purified by silica gel column chromatography (Heptane/Ethyl acetate) to afford the corresponding product.

3-(2,6-difluorophenyl)-[1,2,4,5]-tetrazo[1,2-*b*]indazole (198f²)

(Heptane/Ethyl acetate: 9/1). Yield: 82% as an orange solid.



^1H NMR (500 MHz, CDCl_3): δ (ppm) = 8.70 (d, J = 8.0 Hz, 1H), 8.22 (d, J = 8.5 Hz, 1H), 7.98 (ddd, J = 8.3, 7.0 and 1.2 Hz, 1H), 7.81 (t, J = 7.6 Hz, 1H), 7.61–7.55 (m, 1H), 7.15 (t, J = 8.1 Hz, 2H).

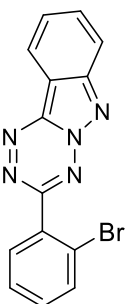
^{19}F NMR (470 MHz, CDCl_3): δ (ppm) = -112.5.

^{13}C NMR (125 MHz, CDCl_3): δ (ppm) = 160.2 (d, J = 255.5), 160.1 (d, J = 255.5), 153.2, 148.7, 141.3, 133.1 (t, J = 10.3 Hz), 132.8, 127.1, 121.7, 118.9, 113.9, 112.5 (d, J = 20.6 Hz), 112.4 (d, J = 20.5 Hz).

HRMS + p ESI (m/z) [$\text{M}+\text{H}^+$] calcd for $\text{C}_{14}\text{H}_7\text{F}_2\text{N}_5^+$: 284.07423; Found: 284.07408.

3-(2-bromophenyl)-[1,2,4,5]-tetrazo[1,2-*b*]indazole (198b)

(Heptane/Ethyl acetate: 9/1). Yield: 66% as an orange solid.



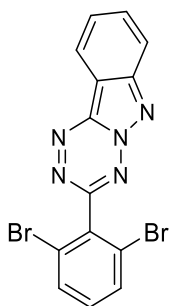
^1H NMR (500 MHz, CDCl_3): δ (ppm) = 8.68 (d, J = 8.1 Hz, 1H), 8.20 (d, J = 8.5 Hz, 1H), 7.97–7.95 (m, 1H), 7.94 (dd, J = 7.6 and 1.7 Hz, 1H), 7.83 (dd, J = 8.0 and 1.0 Hz, 1H), 7.79 (t, J = 7.6 Hz, 1H), 7.55 (td, J = 7.6 and 1.2 Hz, 1H), 7.46 (td, J = 7.7 and 1.7 Hz, 1H).

^{13}C NMR (125 MHz, CDCl_3): δ (ppm) = 159.5, 148.7, 141.0, 134.33, 134.32, 132.6, 132.5, 132.2, 127.9, 126.9, 122.9, 121.6, 118.8, 114.0.

HRMS + p ESI (m/z) [$\text{M}+\text{H}^+$] calcd for $\text{C}_{14}\text{H}_8\text{BrN}_5^+$: 326.00358; Found: 326.00327

3-(2,6-bromophenyl)-[1,2,4,5]-tetrazo[1,2-*b*]indazole (198b²)

(Heptane/Ethyl acetate: 9/1). Yield: 85% as an orange solid.



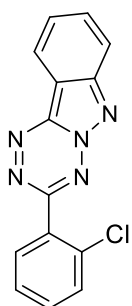
^1H NMR (500 MHz, CDCl_3): δ (ppm) = 8.72 (dt, J = 8.2 and 1.1 Hz, 1H), 8.24 (dt, J = 8.4 and 0.9 Hz, 1H), 7.99 (ddd, J = 8.4, 7.1 and 1.2 Hz, 1H), 7.82 (ddd, J = 8.0, 7.1 and 0.9 Hz, 1H), 7.75 (d, J = 8.2 Hz, 2H), 7.33 (t, J = 8.1 Hz, 1H).

^{13}C NMR (125 MHz, CDCl_3): δ (ppm) = 159.6, 148.9, 141.4, 135.9, 132.8, 132.7, 132.2, 127.2, 124.3, 121.8, 119.0, 114.0.

HRMS + p ESI (m/z) [$\text{M}+\text{H}^+$] calcd for $\text{C}_{14}\text{H}_7\text{Br}_2\text{N}_5^+$: 403.91410; Found: 403.91215.

3-(2-chlorophenyl)-[1,2,4,5]-tetrazo[1,2-*b*]indazole (198c)

(Heptane/Ethyl acetate: 9/1). Yield: 40% as an orange solid.



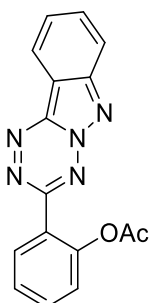
^1H NMR (500 MHz, CDCl_3): δ (ppm) = 8.68 (d, J = 8.1 Hz, 1H), 8.19 (d, J = 8.5 Hz, 1H), 7.98 (dd, J = 7.5 and 1.9 Hz, 1H), 7.95 (t, J = 7.8 Hz, 1H), 7.78 (t, J = 7.6 Hz, 1H), 7.63 (dd, J = 7.8 and 1.5 Hz, 1H), 7.54 (td, J = 7.7 and 1.9 Hz, 1H), 7.50 (td, J = 7.5 and 1.5 Hz, 1H).

^{13}C NMR (125 MHz, CDCl_3): δ (ppm) = 158.7, 148.6, 141.0, 134.0, 132.7, 132.5, 132.4, 132.2, 131.1, 127.3, 126.9, 121.5, 118.8, 113.9.

HRMS + p ESI (m/z) [$\text{M}+\text{H}^+$] calcd for $\text{C}_{14}\text{H}_9\text{ClN}_5^+$: 282.0541; Found: 282.05387.

3-(2-acetylphenyl)-[1,2,4,5]-tetrazo[1,2-*b*]indazole (198-OAc)

(Heptane/Ethyl acetate: 9/1). Yield: 82% as an orange solid.



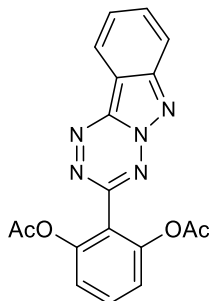
^1H NMR (500 MHz, CDCl_3): δ (ppm) = 8.65 (d, J = 8.1 Hz, 1H), 8.53 (dd, J = 7.9 and 1.6 Hz, 1H), 8.17 (d, J = 8.5 Hz, 1H), 7.93 (t, J = 7.8 Hz, 1H), 7.77 (t, J = 7.6 Hz, 1H), 7.65 (td, J = 7.8 and 1.7 Hz, 1H), 7.52 (t, J = 7.6 Hz, 1H), 7.31 (d, J = 8.0 Hz, 1H), 2.47 (s, 3H).

^{13}C NMR (125 MHz, CDCl_3): δ (ppm) = 170.3, 157.0, 149.9, 148.6, 140.9, 133.1, 132.4, 132.1, 126.9, 126.8, 125.7, 124.7, 121.4, 118.7, 113.9, 21.4.

HRMS + p ESI (m/z) [$\text{M}+\text{H}^+$] calcd for $\text{C}_{16}\text{H}_{11}\text{N}_5\text{O}_2^+$: 306.09855; Found: 306.09837.

3-(2,6-acetylphenyl)-[1,2,4,5]-tetrazo[1,2-*b*]indazole (198-OAc²)

(Heptane/Ethyl acetate: 7/3). Yield: 70% as an orange solid.



^1H NMR (500 MHz, CDCl_3): δ (ppm) = 8.67 (d, J = 8.2 Hz, 1H), 8.19 (d, J = 8.5 Hz, 1H), 7.96 (t, J = 7.8 Hz, 1H), 7.79 (t, J = 7.6 Hz, 1H), 7.64 (t, J = 8.3 Hz, 1H), 7.27 (d, J = 8.4 Hz, 2H), 2.25 (s, 6H).

^{13}C NMR (125 MHz, CDCl_3): δ (ppm) = 169.3, 154.9, 150.3, 148.6, 140.8, 132.6, 132.1, 126.9, 121.9, 121.5, 120.1, 118.8, 113.9, 21.0.

HRMS + p ESI (m/z) [$\text{M}+\text{H}^+$] calcd for $\text{C}_{18}\text{H}_{13}\text{N}_5\text{O}_4^+$: 364.10403; Found: 364.10372.

3-(2-fluoro-6-bromophenyl)-[1,2,4,5]-tetrazo[1,2-*b*]indazole (198b-f)

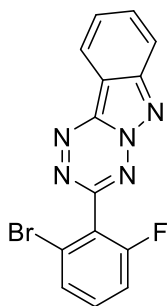
(Heptane/Ethyl acetate: 85/15). Yield: 80% as an orange solid.

^1H NMR (500 MHz, CDCl_3): δ (ppm) = 8.71 (dt, J = 8.2 and 1.1 Hz, 1H), 8.23 (dt, J = 8.5 and 0.9 Hz, 1H), 7.98 (ddd, J = 8.4, 7.1 and 1.2 Hz, 1H), 7.81 (ddd, J = 8.0, 7.0 and 0.7 Hz, 1H), 7.61 (dt, J = 8.1 and 1.0 Hz, 1H), 7.46 (td, J = 8.3 and 5.8 Hz, 1H), 7.28 (td, J = 8.6 and 1.0 Hz, 1H).

^{19}F NMR (470 MHz, CDCl_3): δ (ppm) = -110.0.

^{13}C NMR (125 MHz, CDCl_3): δ (ppm) = 162.2 (d, J = 255.1 Hz), 155.8, 148.6, 141.3, 132.9 (d, J = 9.1 Hz), 132.7, 128.9 (d, J = 3.6 Hz), 127.1, 124.0 (d, J = 8.7 Hz), 123.9 (d, J = 6.4 Hz), 121.6, 118.8, 115.4 (d, J = 21.6 Hz), 113.8.

HRMS + p ESI (m/z) [$\text{M}+\text{H}^+$] calcd for $\text{C}_{14}\text{H}_7\text{BrFN}_5$: 343.99416; Found: 343.99249.



X. Thermal properties

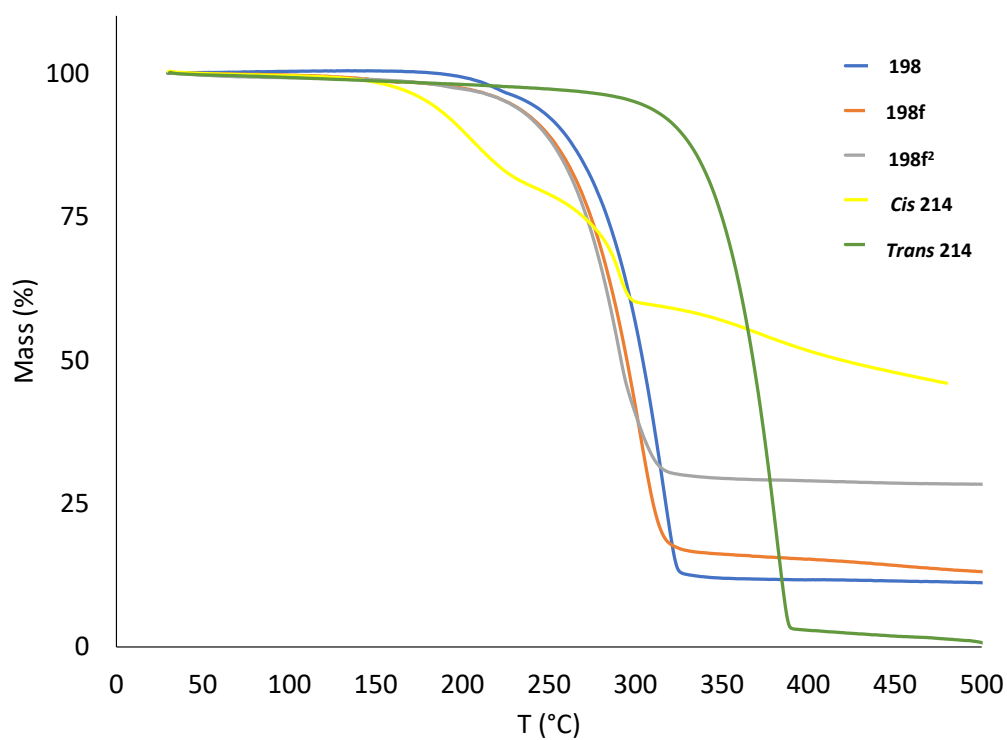


Figure S-1. Thermogravimetric analysis of **198-214**.

XI. Optical properties

1) UV-visible analyses

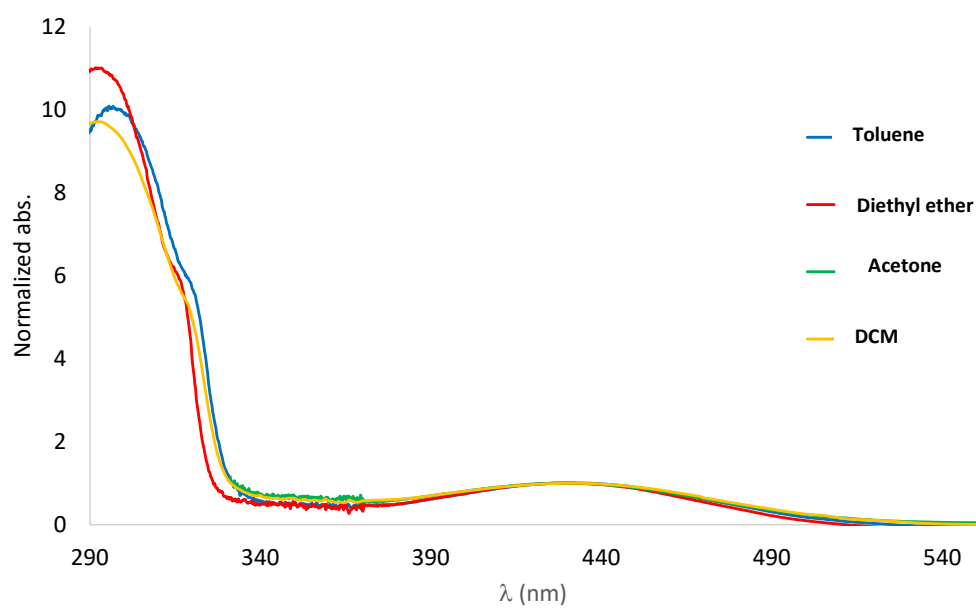


Figure S-2. UV-visible absorption of **198** in different solvents [$10^{-5}M$].

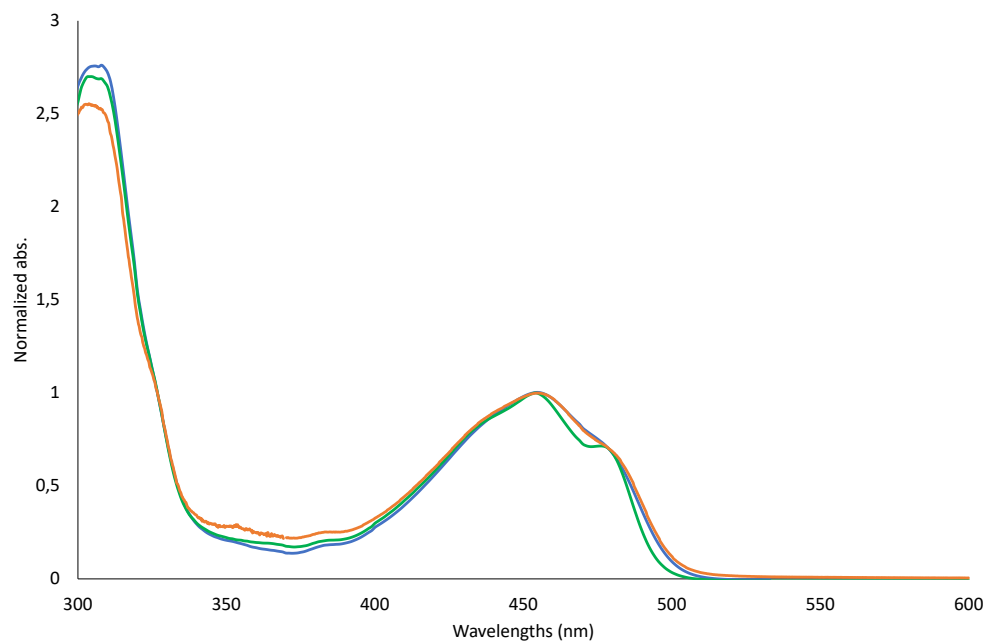


Figure S-3. Normalized UV-visible absorption of **cis 214** in toluene (green), CH_2Cl_2 (orange) and DMSO (blue) [10^{-5}M].

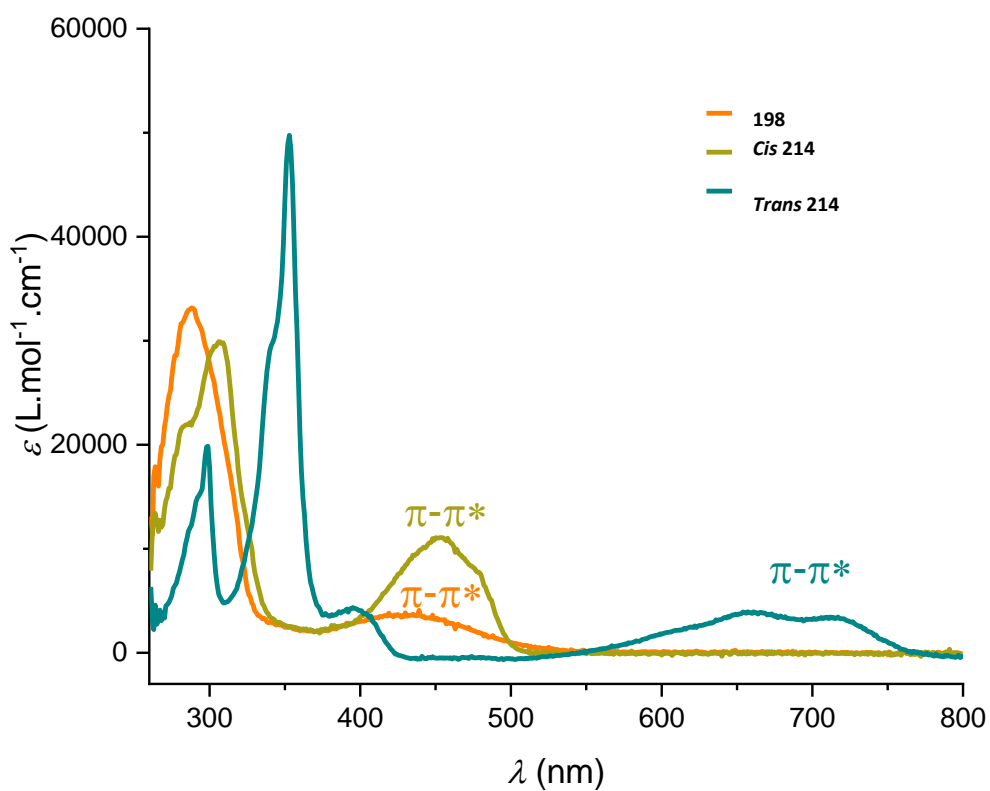


Figure S-4. UV-visible absorption of **198f**, **cis 214** and **trans 214** in diluted DMSO solution [10^{-5}M].

2) Emission spectra

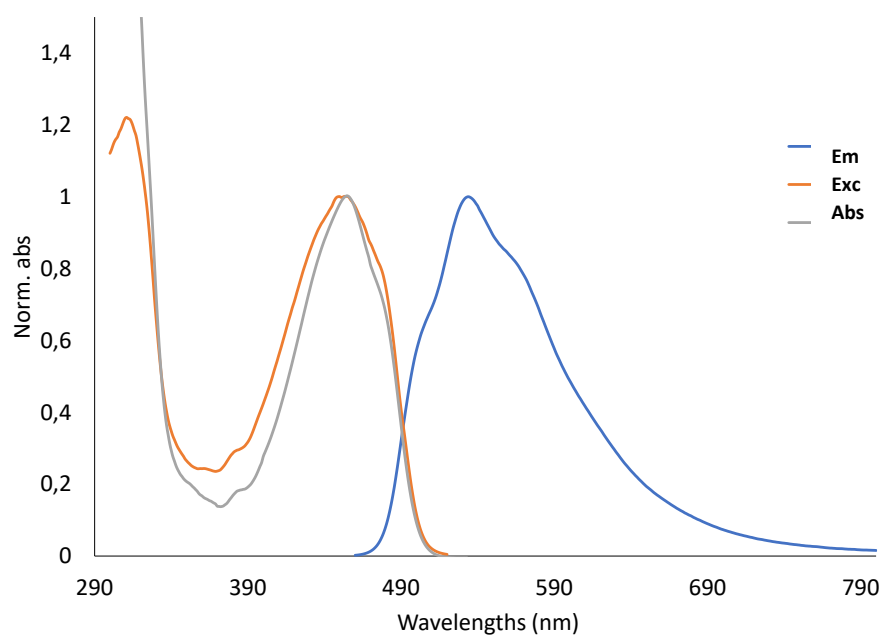


Figure S-5. Normalized UV-visible absorption, emission and excitation spectra of **cis 214** in DMSO.

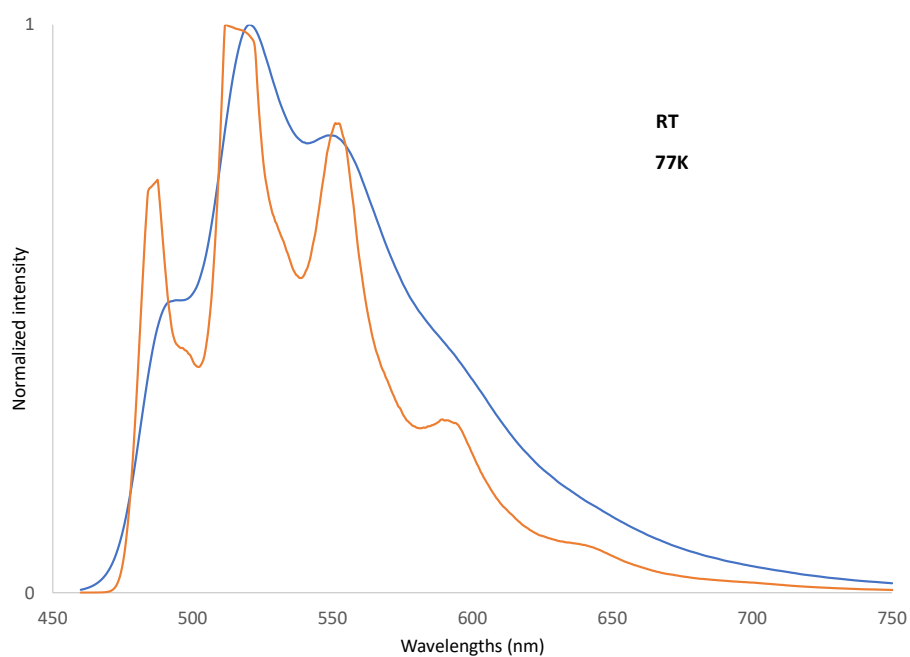


Figure S-6. Emission spectra of **cis 214** in diluted MeTHF at RT (blue) and 77K (orange).

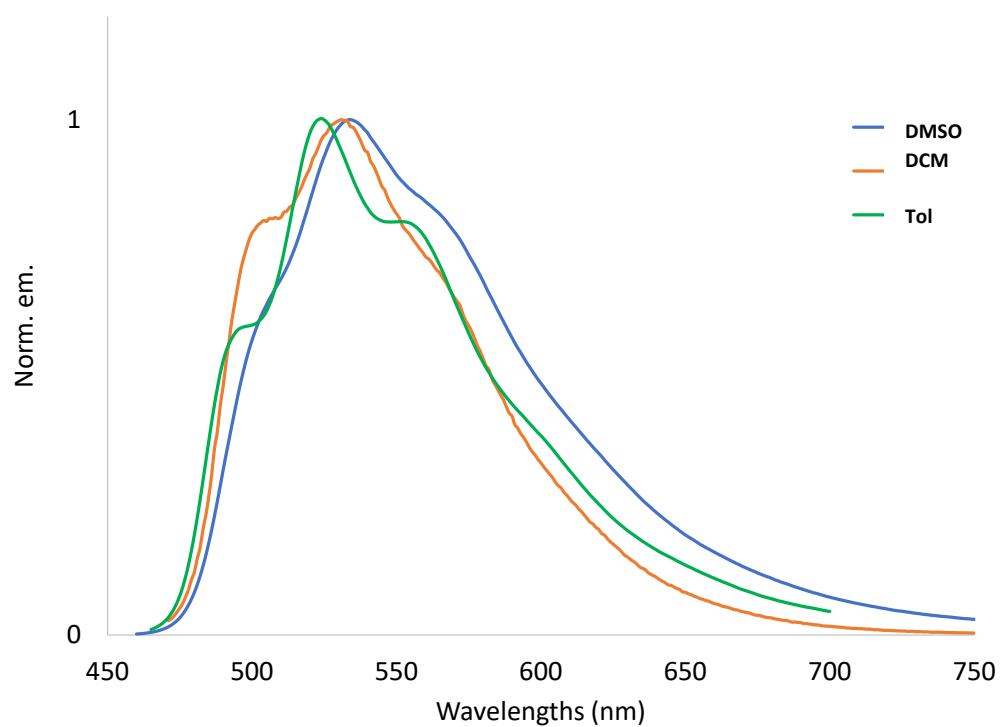


Figure S-7. Emission of **cis 214** in different solvents [$10^{-5}M$].

XII. Cyclic voltammetry

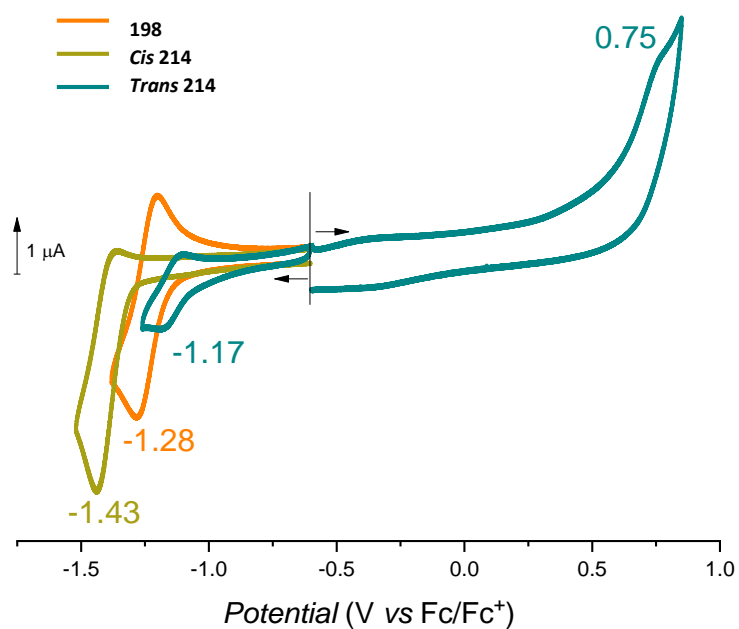


Figure S-8. Cyclic voltammograms of **198f**, **cis 214** and **trans 214** [$10^{-3} M$], recorded in DMF ($TEABF_4$ [$0.1 M$], $100 mVs^{-1}$, WE: Pt, $\phi = 1.6 mm$ potentials vs Fc^+/Fc).

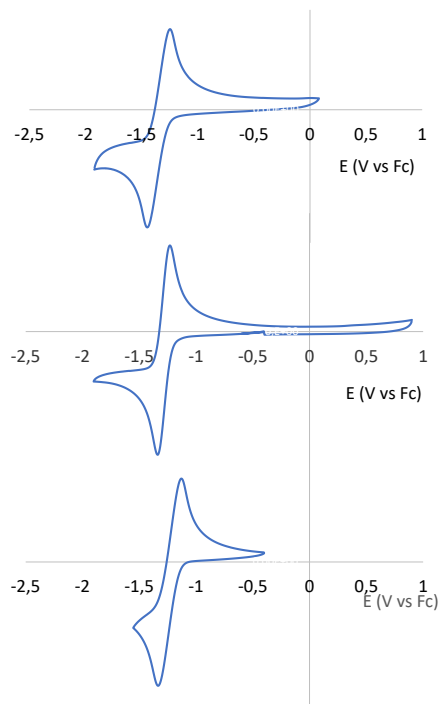


Figure S-9. Cyclic voltammograms of **198** (up), **198f** (middle), **198f²** (down) [10^{-3} M], recorded in CH_2Cl_2 (Bu_4NPF_6 [0.2 M], 200 mVs^{-1} , potentials vs Fc^+/Fc).

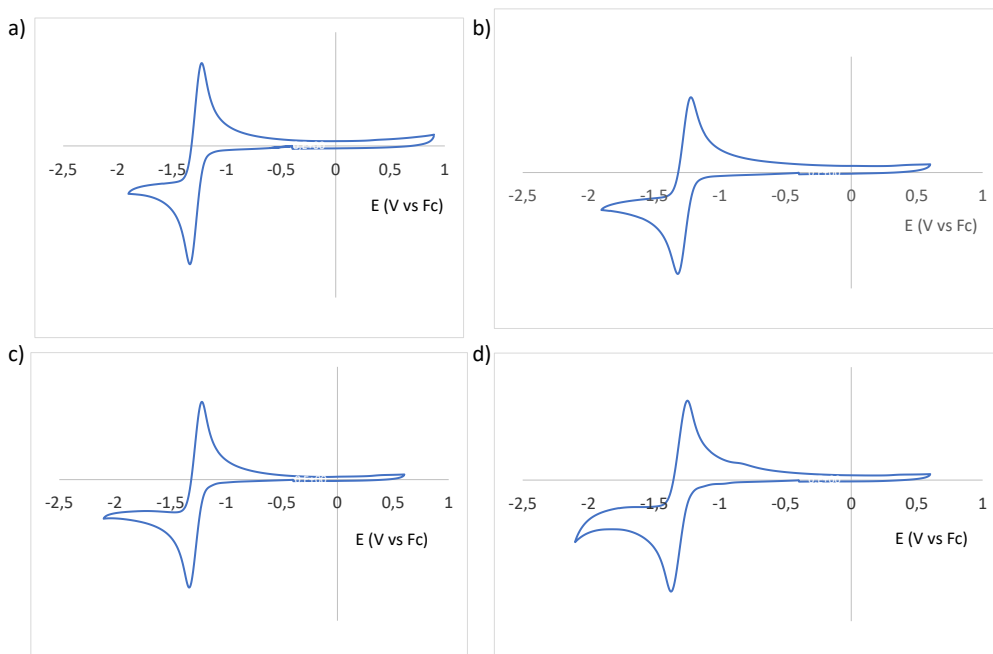


Figure S-10. Cyclic voltammograms of (a) **198f**, (b) **198b**, (c) **198c**, (d) **198-OAc** [10^{-3} M], recorded in CH_2Cl_2 (Bu_4NPF_6 [0.2 M], 200 mVs^{-1} , potentials vs Fc^+/Fc).

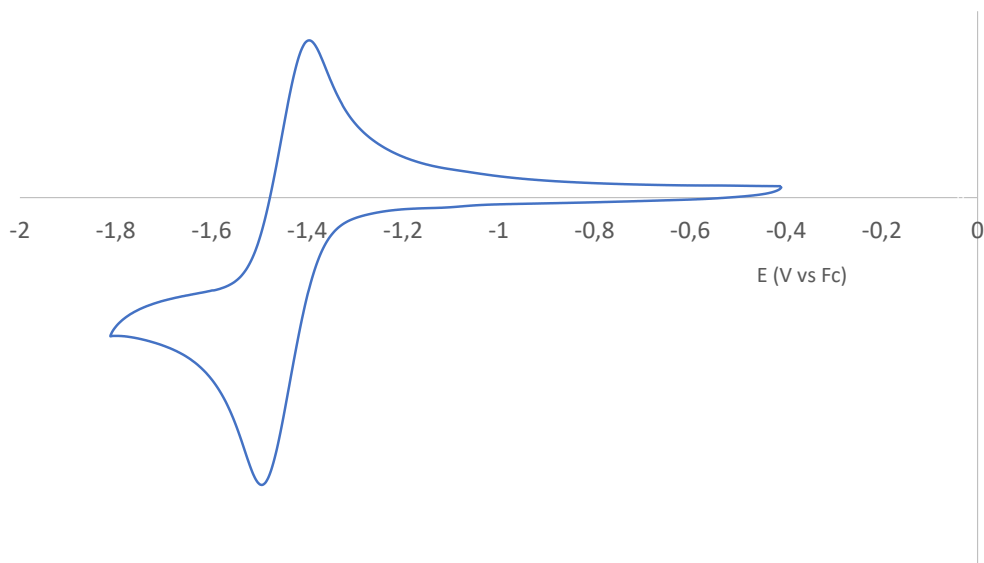


Figure S-11. Cyclic voltammogram of *cis* **214** [10^{-3} M], recorded in CH_2Cl_2 (Bu_4NPF_6 [0.2 M], 200 mVs^{-1} , potentials vs Fc^+/Fc).

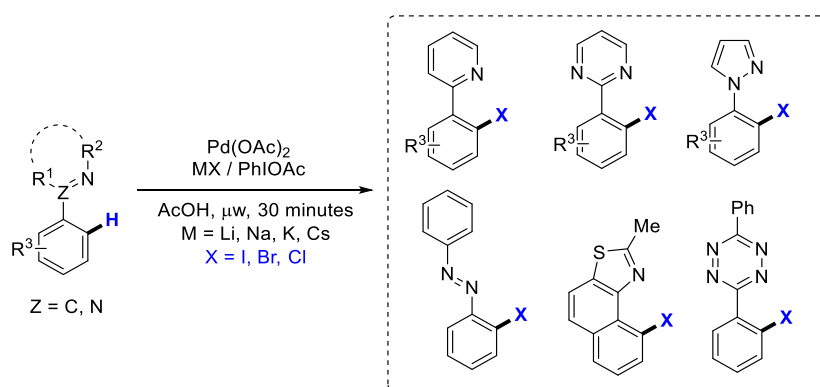
Table S-1. Photophysical and redox data.

Compound	$\lambda_{\text{abs}}^{[a]}$ [nm]	$\epsilon^{[a]}$ [$\text{M}^{-1}\text{cm}^{-1}$]	$\lambda_{\text{em}(\text{CH}_2\text{Cl}_2)}^{[a]}$ [nm]	$(\Phi)^{[a,b]}$	$E^{\text{red}} [c]$ [V]	Td_{10} [$^{\circ}\text{C}$] ^[d]
198	434	2400	-	-	-1.29	257
198f	432	3700	-	-	-1.33	247
198f²	435	3400	-	-	-1.32	246
198b	435	2100	-	-	-1.27	-
198b²	435	3600	-	-	-1.26	-
198c	435	3000	-	-	-1.25	-
198-OAc	435	2900	-	-	-1,27	-
198-OAc²	437	4400	-	-	-1,31	-
<i>cis</i> 214	455	14000	532	0.52	-1.43	200
<i>trans</i> 214 ^[e]	712	3400	-	-	-1.17	325

^[a] In CH_2Cl_2 [10^{-5} M]. ^[b] Measured in calibrated integrated sphere. ^[c] In CH_2Cl_2 with $\text{Bu}_4\text{N}^+\text{PF}_6^-$ [0.2 M] at a scan rate of $200 \text{ mV}\cdot\text{s}^{-1}$. Potentials vs Fc^+/Fc . ^[d] measured by TGA under N_2 ^[e] recorded in DMSO at a scan rate of $100 \text{ mV}\cdot\text{s}^{-1}$.

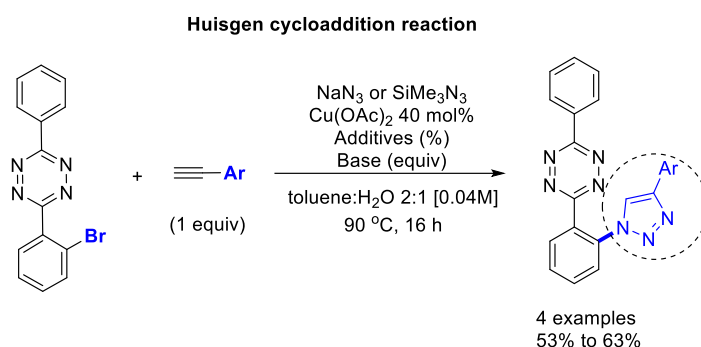
General conclusion and perspectives

In the first section of this thesis, the conditions for a broad range of N-directed o-halogenation of heteroaromatics employing PIDA as the oxidant and simple alkali metal halides as "nucleophilic" sources are presented (Scheme 1). The functionalized pyridines, pyrimidines, pyrazoles, oxazolines, naphtho[1,2-d]thiazoles, azobenzenes, and particularly the selectivity-challenging, clickable/bioconjugable, nitrogen-rich *s*-aryltetrazine are heteroaromatic substrates suited for direct C-H halogenation in this technique. These substrates, which also include N-directing groups, were effectively used with the entire range of alkali metals, including Li, Na, K, and Cs, for highly selective monohalogenation (X = I, Br, and Cl). The C-H-halogenated aryl was tested for a good tolerance to substituents, and microwave conditions effectively cut down a lengthy synthesis to less than an hour. The reaction was found to be appropriate for a wide variety of structurally various N-heteroaromatic mmsubstrates, where the bulk of monofunctionalization is achieved, generally along with the creation of around 15–25% of the dihalogenated product.



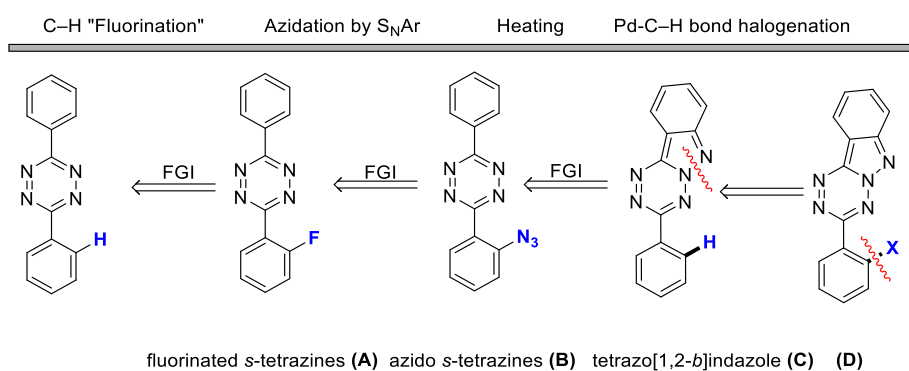
Scheme 1. N-directed palladium-catalyzed mono-halogenation using alkali halide nucleophilic sources (this work)

The second chapter begins in presenting the usefulness of the azide moiety on organic compounds and what kind of reactions and application can be done on such group. It precisely tackles the azide introduction on *s*-diphenyltetrazine derivatives in *ortho*-position with respect to the directing nitrogen of the tetrazine core. On these azido *s*-tetrazine derivatives, the most important application of this work was the introduction of fluorescent moieties utilizing the highly reactive N₃ group in Huisgen cycloaddition reactions (Scheme 2).



*Scheme 2. Introduction of fluorescent moieties by Huisgen cycloaddition reaction on the azide on *s*-tetrazines*

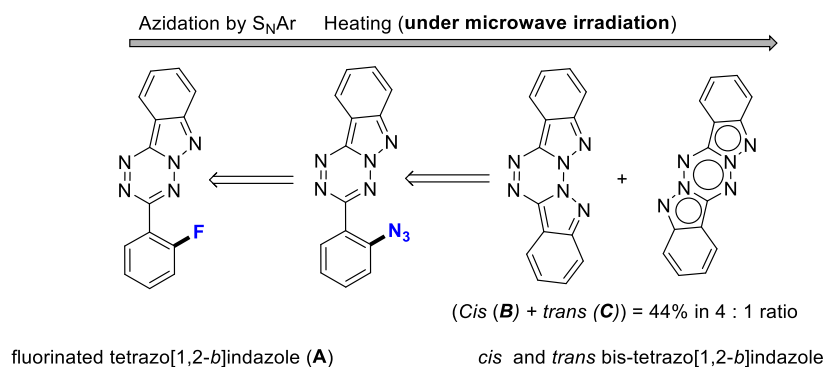
The second part first discusses the straightforward access to a new class of aza-polyaromatics, the tetrazo[1,2-*b*]indazole (**C**) from readily available fluorinated *s*-tetrazine (**A**). A cyclization process starts by inserting an azide group by S_NAr on fluorinated *s*-tetrazine (**A**) leading to the formation of an unprecedented tetrazo[1,2-*b*]indazole (**C**) *via* intramolecular cyclyziation. Based on the new nitrogen core on (**C**), further *N*-directed palladium-catalyzed ortho-C–H bond functionalization allows the introduction of halides or acetates to give halogenated and acetoxyated family of tetrazo[1,2-*b*]indazole in (**D**) (Scheme 3).



*Scheme 3. Synthesis and retrosynthesis strategy to novel tetrazo[1,2-*b*]indazoles (**D**)*

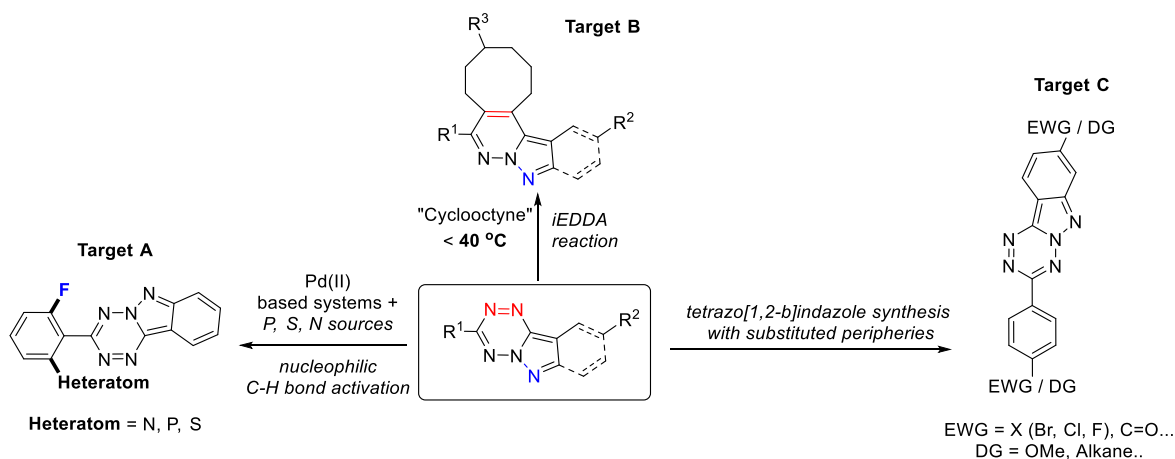
Similarly, the formation of bis-tetrazo[1,2-*b*]indazole (*cis* and *trans*) is presented. However, it was found more convenient to obtain these bis-tetrazo[1,2-*b*]indazole isomers from the prepared mono cyclized fluorinated tetrazo[1,2-*b*]indazole instead of difluorinated *s*-tetrazine. Mixtures of *cis*- and *trans* bis-tetrazo[1,2-*b*]indazole were isolated. The highest isolated mixture being in 44% yield. In these mixtures, the ratio of *trans* / *cis* isomers is 80% / 20% having the *trans* as the major product as

it has the lower energy between the two isomers. Interestingly, only the *cis* isomer was found fluorsenet in high quantum yield of $\phi = 52\%$ (in CH_2Cl_2) (Scheme 4).



Scheme 4. Retrosynthesis strategies to novel *cis* (**B**) and *trans* (**C**) bis-tetrazo[1,2-*b*]indazoles

Building on these results, we envisioned that several reactions could yet be done on both *s*-tetrazines and tetrazo[1,2-*b*]indazoles. Previously, we applied Cu-catalyzed C–Br bond activation to insert C–Heteroatom bonds on the *ortho* position.^[127] Our next target will be to find suitable conditions for direct C–Heteroatom bond formation on tetrazo[1,2-*b*]indazole (Target **A**, Scheme 5). Another interesting reaction would be the iEDDA reaction on the *trans* bis tetrazo[1,2-*b*]indazole due to the high delocalization which allows the [4 +2] cycloaddition reaction in the presence of suitable cyclooctynes (Target **B**, Scheme 5). Finally, after understanding the general properties of tetrazo[1,2-*b*]indazoles lacking substituents at the peripheries. It would be highly intriguing to initiate the synthesis of tetrazoindazoles with various moieties on its peripheries (Target **C**, Scheme 5).



Scheme 5. A general concept about some future work regarding the chemistry of tetrazo[1,2-*b*]indazoles

References

- 1 P. Arora, V. Arora, H. Lamba, D. Wadhwa, *Heterocyclic Chemistry* **2012**, *3*, 2947–2955
- 2 A. Pinner, *Mitteilungen Klosterneuburg* **1897**, *30*, 1871–1890
- 3 G. Clavier, P. Audebert, *Chem. Rev.* **2010**, *110*, 3299–3314
- 4 A. R. Katritzky, C. R. John A. Joule, V. Zhdankin, in *Handbook of Heterocyclic Chemistry*, Elsevier 24th August **2010**
- 5 (a) C. Testa, E. Gigot, S. Genc, R. Decreau, J. Roger, J.-C. Hierso, *Angew. Chem. Int. Ed.* **2016**, *55*, 5555–5559; (b) C. D. Mboyi, C. Testa, S. Reeb, S. Genc, H. Cattey, P. F. Lessard, J. Roger, J.-C. Hierso, *ACS Catal.* **2017**, *7*, 8493–8501
- 6 C. D. Mboyi, A. Daher, N. Khirzada, C. H. Devillers, H. Cattey, P. F. Lessard, J. Roger, J.-C. Hierso, *New J. Chem.* **2020**, *44*, 15235–15243
- 7 J. G. Erickson, P. F. Wiley V. P. Wystrach, In *The Chemistry of Heterocyclic Compounds; A Series of Monographs*; Interscience Publishers Inc.: New York, **1956**, 179
- 8 (a) P. O. Wennberg, R. C. Cohen, R. M. Stimpfle, J. P. Koplów, J. G. Anderson, J. G. R. J. Salawitch, D. W. Fahey, E. L. Woodbridge, E. R. Keim, R. S. Gao, C. R. Webster, R. D. May, D. W. Toohey, L. M. Avallone, M. H. Proffitt, M. Loewenstein, J. R. Podolske, K. R. Chan, S. C. Wofsy, *Science* **1994**, *266*, 398–404; (b) M. J. Molina, T. L. Tso, L. T. Molina, F. C. Y. Wang, *Science* **1987**, *238*, 1253–1257.
- 9 F. H. Vaillancourt, E. Yeh, D. A. Vosburg, S. Garneau-Tsodikova, C. T. Walsh, *Chem. Rev.* **2006**, *106*, 3364–3378
- 10 Natural combustion processes, such as volcanoes (and other geothermal events occurring in lakes, soils, salt mines, etc.) and forest or savannah fires, contribute measurable quantities of halogenated organic compounds to the environment, see for instance: E. J. Hoekstra, E. W. B.; de Leer, U. A. Th. Brinkman, *Environ. Sci. Technol.* **1998**, *32*, 3724–3729; A. Ruecker, P. Weigold, S. Behrens, M. Jochmann, J. Laaks, A. Kappler, *Environ. Sci. Technol.* **2014**, *48*, 9170–9178
- 11 H. China, R. Kumar, Kikushima, T. Dohi, *Molecules* **2020**, *25*, 6007–6039
- 12 H. H. Hodgson, *Chem. Rev.* **1947**, *40*, 251–277
- 13 (a) V. Snieckus, *Chem. Rev.* **1990**, *90*, 879–933; (b) D. W. Young, D. L. Comins, *Org. Lett.* **2005**, *7*, 5661–5664
- 14 M. Reddy, U. Kumar, E. B. Watkins, *Chem. Sci.* **2018**, *9*, 1782–1788
- 15 A. Vigalok, *Chem. Eur. J.* **2008**, *14*, 5102–5108
- 16 J. M. Brown, V. Gouverneur, *Angew. Chem. Int. Ed.* **2009**, *48*, 8610–8614
- 17 W. Liu, T. J. Groves, *Acc. Chem. Res.* **2015**, *48*, 1727–1735
- 18 M. G. Campbell, T. Ritter, *Chem. Rev.* **2015**, *115*, 612–633
- 19 D. A. Petrone, J. Ye, M. Lautens, *Chem. Rev.* **2016**, *116*, 8003–8104
- 20 T. W. Lyons, M. S. Sanford, *Chem. Rev.* **2010**, *110*, 1147–1169
- 21 (a) D. Kalyani, A. R. Dick, W. Q. Anani, M. S. Sanford, *Tetrahedron* **2006**, *62*, 11483–11498; (b) J. M. Racowski, M. S. Sanford, *Top. Organomet. Chem.* **2011**, *35*, 61–84; (c) S. R. Neufeldt, M. S. Sanford *Acc. Chem. Res.* **2012**, 936–946
- 22 (a) T. Furuya, A. S. Kamlet, T. Ritter, *Nature* **2011**, *473*, 470–477; (b) T. Liang, C. N. Neumann, T. Ritter, *Angew. Chem. Int. Ed.* **2013**, *52*, 8214–8264
- 23 (a) X. Jiang, H. Liu, Z. Gu, *As. J. Org. Chem.* **2012**, *1*, 16–24; (b) C. Chen, X. Tong, *Org. Chem. Front.* **2014**, *1*, 439–446; (c) A. Lin, C. B. Huehls, J. Yang, *Org. Chem. Front.* **2014**, *1*, 434–438
- 24 A. Vigalok, *Acc. Chem. Res.* **2015**, *48*, 238–247
- 25 K. M. Engle, T.-S. Mei, X. Wang, J.-Q. Yu, *Angew. Chem. Int. Ed.* **2011**, *50*, 1478–1491
- 26 (a) D. Kalyani, M. S. Sanford, *Org. Lett.* **2005**, *19*, 4149–4152; (b) K. L. Hull, W. Q. Anani, M. S. Sanford, *J. Am. Chem. Soc.* **2006**, *128*, 7134–7135
- 27 D. Kalyani, A. R. Dick, W. Q. Anani, M. S. Sanford, *Org. Lett.* **2006**, *8*, 2523–2526
- 28 D. R. Fahey, *J. Chem. Soc. Chem. Commun.* **1970**, 417a–417a
- 29 X. T. Maa, S. K. Tian, *Adv. Synth. Catal.* **2013**, *355*, 337–340

- 30 (a) R. B. Bedford, M. F. Haddow, C. J. Mitchell, R. L. Webster, *Angew. Chem.* **2011**, *123*, 5638–5641; *Angew. Chem. Int. Ed.* **2011**, *50*, 5524–5527; (b) J. W. Delord, T. Droge, F. Liu, F. Glorius, *Chem. Soc. Rev.* **2011**, *40*, 4740–4761
- 31 T. Mandal, M. Mondal, J. Choudhury, *Organometallics* **2021**, *40*, 2443–2449
- 32 H. Vardhan, A. M. Al-Enizi, A. Nafady, Y. Pan, Z. Yang, H. R. Gutiérrez, X. Han, S. Ma, *Small* **2020**, *17*, 2003970–2003977
- 33 B. Du, X. Jiang, P. Sun, *J. Org. Chem.* **2013**, *78*, 2786–2791
- 34 R. Das, M. Kapur, *J. Org. Chem.* **2017**, *82*, 1114–1126
- 35 Y. Jaiswal, A. Kumar, *Catal. Commun.* **2019**, *131*, 105784–105802
- 36 S. K. Santra, A. Banerjee, N. Khatun, A. Samanta, B. K. Patel, *RSC Adv.*, **2015**, *5*, 11960–11965
- 37 (a) C. Reddy, N. Bisht, R. Parella, S. A. Babu, *J. Org. Chem.* **2016**, *81*, 12143–12168; (b) J. Guo, H. He, Z. Ye, K. Zhu, Y. Wu, F. Zhang, *Org. Lett.* **2018**, *20*, 5692–5695
- 38 (a) H. D. Arman, R. L. Giesecking, T. W. Hanks, W. T. Pennington, *Chem. Commun.* **2010**, *46*, 1854–1856; (b) S. K. Sahoo, H. S. Jena, G. Majji, B. K. Patel, *Synthesis*, **2014**, *46*, 1886–1900
- 39 M. Saha, A. R. Das, *Org. Biomol. Chem* **2020**, *18*, 941–955
- 40 L. Chu, X. C. Wang, C. E. Moore, A. L. Rheingold, J. Q. Yu, *J. Am. Chem. Soc.* **2013**, *135*, 16344–16347
- 41 N. Schroeder, J. W. Delord, F. Glorius, *J. Am. Chem. Soc.* **2012**, *134*, 20, 8298–8301
- 42 Q. Ding, X. Zhou, S. Pu, B. Cao, *Tetrahedron* **2015**, *71*, 2376–2381
- 43 (a) Z. Li, C. J. Li, *J. Am. Chem. Soc.* **2006**, *128*, 56–57; (b) W. Wang, C. Pan, F. Chen, J. Cheng, *Chem. Commun.*, **2011**, *47*, 3978–3980
- 44 D. Zhijun, G. Lianxun, L. Yingjie, *Chem. Res. Chin. Univ.* **2015**, *31*, 167–170
- 45 D. Z. J., L. X. Gao, Y. J. Lin, F. S. Han, *Chem. Cat. Chem.* **2014**, *6*, 123–126
- 46 Z. L. Lia, P. Y. Wua, C. Cai, *New J. Chem.*, **2019**, *43*, 3462–3468
- 47 (a) T. Yoshino, H. Ikemoto, S. Matsunaga, M. Kanai, *Angew. Chem., Int. Ed.* **2013**, *52*, 2207–2211; (b) T. Yoshino, H. Ikemoto, S. Matsunaga, M. Kanai, *Chem. Eur. J.* **2013**, *19*, 9142–9146; (c) H. Ikemoto, T. Yoshino, K. Sakata, S. Matsunaga, M. Kanai, *J. Am. Chem. Soc.* **2014**, *136*, 5424–5431
- 48 D.-G. Yu, T. Gensch, F. Azambuja, S. Vasquez-Céspedes, F. Glorius *J. Am. Chem. Soc.* **2014**, *136*, 17722–17725
- 49 (a) J. D. Dooley, C. S. Reddy, H. W. Lam, *J. Am. Chem. Soc.* **2013**, *135*, 10829–10836; (b) L. Wang and L. Ackermann, *Org. Lett.* **2013**, *15*, 176–179
- 50 (a) W. Liu, L. Ackermann, *Org. Lett.* **2013**, *15*, 3484; (b) F. Yang, L. Ackermann, *Org. Lett.* **2013**, *15*, 718–720
- 51 (a) V. S. Thirunavukkarasu, K. Raghuvanshi, L. Ackermann, *Org. Lett.* **2013**, *15*, 3286–3289; (b) M. Bhanuchandra, M. R. Yadav, R. K. Rit, M. R. Kuram and A. K. Sahoo, *Chem. Commun.* **2013**, *49*, 5225–5527
- 52 L. Wang, L. Ackermann, *Chem. Commun.* **2014**, *50*, 1083–1085
- 53 C. Testa, J. Roger, P. F. Lessard, J.-C. Hierso, *Eur. J. Org. Chem.* **2019**, *2019*, 233–253
- 54 Y. Yuan, Y. Liang, S. Shi, Y. F. Liang, N. Jiao, *Chin. J. Chem.* **2019**, *38*, 1245–1251
- 55 H. He J. Guo, W. Sun, B. Yang, F. Zhang, G. Liang, *J. Org. Chem.* **2020**, *85*, 3788–3798
- 56 X. Chen, X. S. Hao, C. E. Goodhue, J. Q. Yu, *J. Am. Chem. Soc.* **2006**, *128*, 6790–6791
- 57 W. Wang, C. Pan, F. Chen, J. Cheng, *Chem. Commun.* **2011**, *47*, 3978–3980
- 58 Y. Lu, R. Wang, X. Qiao, Z. Shen, *Synlett* **2011**, *52*, 1038–1042
- 59 S. Mo, Y. Zhu, Z. Shen, *Org. Biomol. Chem.* **2013**, *11*, 2756–2760
- 60 (a) N. Schröder, J. W.-Delord, F. Glorius, *J. Am. Chem. Soc.* **2012**, *134*, 8298–8301; (b) N. Kuhl, N. Schröder, F. Glorius, *Org. Lett.* **2013**, *15*, 3860–3863
- 61 P. Zhang, L. Hong, G. Li, R. Wang, *Adv. Synth. Catal.* **2014**, *356*, 1–6
- 62 L. H. Choudhury, T. Parvin, A. T. Khan, *Tetrahedron* **2009**, *65*, 9513–9526
- 63 (a) Z. Li, H. Cai, M. Hassink, M. L. Blackman, R. C. D. Brown, P. S. Conti, J. M. Fox, *Chem. Commun.* **2010**, *46*, 8043–8045; (b) S. K. Hanson, J. M. Veauthier, D. A. Parrish, *Angew. Chem.* **2013**, *125*, 7014–7017
- 64 C. Testa, J. Roger, S. Schieb, P. F. Lessard, J.-C. Hierso, *Adv. Synth. Catal.* **2015**, *357*, 2913–2923

- 65 M. Gupta, S. Kumar, P. Kumar, A. K. Singh, V. Bahadur, B. K. Singh, *Chemistry Select* **2019**, *4*, 13992–13997
- 66 A. R. Dick, K. L. Hull, M. S. Sanford, *J. Am. Chem. Soc.* **2004**, *126*, 2300–2301
- 67 (a) E. Dubost, V. Babin, F. Benoist, A. Hebert, P. Barbey, C. Chollet, J. P. Bouillon, A. Manrique, G. Pieters, F. Fabis, T. Cailly, *Org. Lett.* **2018**, *20*, 6302–6305; (b) J. S. Hewage, S. Wanniarachchi, T. J. Morin, B. J. Liddle, M. Banaszynski, S. V. Lindeman, B. Bennett, J. R. Gardinier, *Inorg. Chem.* **2014**, *53*, 10070–10084
- 68 F. Kakiuchi, PCT Int. Appl. (**2010**), WO 2010104028 A1 20100916
- 69 B. Song, X. Zheng, J. Mo, B. Xu, Bin, *Adv. Synth. Catal.* **2013**, *352*, 329–335
- 70 Griess, P. Philos, *Trans. R. Soc. London* **1864**, *13*, 377–384
- 71 (a) E. F. V. Scriven, K. Turnbull, *Chem. Rev.* **1988**, *88*, 297–368; (b) G. L'Abbé, *Chem. Rev.* **1969**, *69*, 345–363
- 72 (a) F. D. Tropper, F. O. Andersson, S. Braun, R. Roy, *Synthesis* **1992**, *7*, 618–620; (b) R. Kumar, P. Tiwari, P. R. Maulik, A. K. Misra, *Eur. J. Org. Chem* **2006**, *2006*, 74–79
- 73 (a) C. I. Schilling, S. Brase, *Org. Biomol. Chem.* **2007**, *5*, 3586–3588
- 74 (a) J. H. Boyer, *J. Am. Chem. Soc.* **1951**, *73*, 5865–5866; (b) H. C. brown, A. Suzui, S. Sonao, M. Itoh, M. M. Midland, *J. Am. Chem. Soc.* **1971**, *93*, 4329–4330
- 75 (a) D. Kim, L. Wang, C. G. Caldwell, P. Chen, P. E. Finke, B. Oates, M. MacCoss, S. G. Mills, L. Malkowitz, S. L. Gould, J. A. DeMartino, M. S. Springer, D. Hazuda, M. Miller, J. Kessler, R. Danzeisen, G. Carver, A. Carella, K. Holmes, J. Lineberger, W. A. Schleif, E. A. Emini, *Bioorg. Med. Chem. Lett.* **2001**, *11*, 3103–3106; (b) H. Wang, H. Han, D. D. Von Hoff, *Cancer Res.* **2006**, *66*, 9722–9730
- 76 S. Bräse, *Organic Azides Syntheses and Applications*, K. Banert Institute of Chemistry, Chemnitz University of Technology, **2010**, Germany
- 77 R. J. Simmonds, M. F. G. Stevens, *J. Chem. Soc. Perkin Trans.* **1982**, *1*, 1821–1825
- 78 (a) C. K. L. Ma, R. A. Nissan, W. S. Wilson, *J. Org. Chem.* **1990**, *5*, 3755–3761; (b) W. Stadlbauer, W. Fiala, M. Fischer, G. Hojas, *J. Heterocycl. Chem.* **2000**, *37*, 1253–1256
- 79 P. Roschger, W. Fiala, W. Stadlbauer, *J. Heterocycl. Chem.* **1992**, *29*, 225–231
- 80 D. R. Miller, D. C. Svenson, E. G. Gillan, *J. Am. Chem. Soc.* **2004**, *126*, 5372–5373
- 81 P. Choi, C. W. Rees, E. H. Smith, *Tetrahedron Lett.* **1982**, *23*, 121–124
- 82 K. A. H. Chehade, H. P. Spielmann, *J. Org. Chem.* **2000**, *65*, 4949–4953
- 83 C. K. Lowe-Ma, R. A. Nissan, W. S. Wilson, *J. Org. Chem.* **1990**, *55*, 3755–3761
- 84 G. B. Barlin, *Aust. J. Chem.* **1983**, *36*, 983–892
- 85 J. Gavenonis, T. D. Tilley, *Organometallics* **2002**, *21*, 5549–5563
- 86 P. Zanirato, S. Cerini, *Org. Biomol. Chem.*, **2005**, *3*, 1508–1513
- 87 Y. H. Kim, K. Kim, S. B. Shim, *Tetrahedron Lett.* **1986**, *27*, 4749–4752
- 88 T. Itoh, Y. Matsuya, K. Nagata, A. Ohsawa, *Tetrahedron Lett.* **1997**, *38*, 4117–4120
- 89 (a) A. Zarei, A. R. Hajipour, L. Khazdooz, H. Aghaei, *Tetrahedron Lett.* **2009**, *50*, 4443–4445; (b) M. A. K. Zarchi, R. J. Nabei, *Appl. Polym. Sci.* **2012**, *124*, 2362–2369
- 90 Bretherick's Handbook of Reactive Chemical Hazards, 6th ed., 2; Urben, P., Ed.; Butterworth-Heinemann: Oxford, **1999**
- 91 B. Patro, M. Merrett, S. Makin, S. D. Murphy, J. A. Parkes, *K. E. B. Tetrahedron Lett.* **2000**, *41*, 421–424
- 92 K. V. Kutonova, M. E. Trusova, P. S. Postnikov, V. D. Filimonov, J. Parello, *Synthesis* **2013**, *45*, 2706–2710
- 93 H. Suzuki, K. Miyoshi, M. Shinoda, *Bull. Chem. Soc. Jpn* **1980**, *53*, 1765–1766
- 94 W. Zhu, D. Ma, *Chem. Commun.* **2004**, 888–889
- 95 J. Andersen, U. Madsen, F. Björkling, X. Liang, *Synlett* **2005**, *14*, 2209–2214
- 96 D. M. T. Chan, K. L. Monaco, R. P. Wang, M. P. Winters, *Tetrahedron Lett.* **1998**, *39*, 2933–2936
- 97 (a) J. Morgan, J. T. Pinhey, *J. Chem. Soc. Perkin Trans 1* **1990**, 715–720; (b) M. L. Huber, J. T. Pinhey, *J. Chem. Soc. Perkin Trans 1* **1990**, 721–722
- 98 K. Grimes, A. Gupte, C. Aldrich, *Synthesis* **2010**, *9*, 1441–1448

- 99 C. S. Azad, A. K. Narula, *RSC Adv.* **2015**, *5*, 100223–100227
- 100 J. Tat, K. Heskett, S. Satomi, R. B. Pilz, B. A. Golomb, G. R. Boss, *J. Toxicol. Clin. Toxicol.* **2021**, *59*, 683–697
- 101 (a) R. M. Moriarty, R. K. Vaid, V. T. Ravikumar, B. K. Vaid, T. E. Hopkins, *Tetrahedron* **1988**, *44*, 1603–1605; (b) Y. Kita, H. Tohma, M. Inagaki, K. Hatanaka, T. Yakura, *Tetrahedron Lett.* **1991**, *34*, 4321–4324; (c) P. Magnus, C. Hulme, W. Weber, *J. Am. Chem. Soc.* **1994**, *116*, 4501–4502; (d) D. Lubriks, L. Sokolovs, E. Suna, *J. Am. Chem. Soc.* **2012**, *134*, 15436–15422
- 102 V. V. Zhdankin, A. P. Krasutsky, C. J. Kuehl, A. J. Simonsen, J. K. Woodward, B. Mismash, J. T. Bolz, *J. Am. Chem. Soc.* **1996**, *118*, 5192–5197
- 103 (a) Y. V. Mironov, A. A. Sherman, N. E. Nifantiev, *Mendeleev Commun.* **2008**, *18*, 241–243; (b) B. Zhang, A. Studer, *Org. Lett.* **2013**, *15*, 4548–4551; (c) M. V. Vita, J. Waser, *Org. Lett.* **2013**, *15*, 3246–3249; (d) Q. H. Deng, T. Bleith, H. Wadepohl, L. H. Gade, *J. Am. Chem. Soc.* **2013**, *135*, 5356–5359
- 104 Y. Fan, W. Wan, G. Ma, W. Gao, H. Jiang, S. Zhu, J. Hiao, *Chem. Commun.* **2014**, *50*, 5733–5736
- 105 K. D. Hesp, R. G. Bergman, J. A. Ellman, *J. Am. Chem. Soc.* **2011**, *133*, 11430–11433; (b) J. Kim, S. Park, J. Ryu, S. Cho, S. Kim, S. Chang, *J. Am. Chem. Soc.* **2012**, *134*, 9110–9113; (c) D. G. Yu, M. Suri, F. Glorius, *J. Am. Chem. Soc.* **2013**, *135*, 8802–8805
- 106 (a) Y. Fan, W. Wan, G. Ma, W. Gao, H. Jiang, S. Zhu, J. Hao, *Chem. Commun.* **2014**, *50*, 5733–5736; (b) X. Chen, X.-S. Hao, C. E. Goodhue, J. Q. Yu, *J. Am. Chem. Soc.* **2006**, *128*, 6790–6791; (c) T. S. Mei, X. Wang, J. Q. Yu, *J. Am. Chem. Soc.* **2009**, *131*, 10806–10807; (d) A. E. King, L. M. Huffman, A. Casitas, M. Costas, X. Ribas, S. S. Stahl, *J. Am. Chem. Soc.* **2010**, *132*, 12068–12073; (e) X. Ribas, C. Calle, A. Poater, A. Casitas, L. Gómez, R. I. Xifra, T. Parella, J. Benet-Buchholz, A. Schweiger, G. Mitrikas, *J. Am. Chem. Soc.* **2010**, *132*, 12299–12306
- 107 R. Huisgen, *Angew. Chem. Int. Ed.* **1963**, *2*, 565–598; *Angew. Chem.* **1963**, *75*, 604–637
- 108 (a) M. Meldal, C. W. Tornøe, *Chem. Rev.* **2008**, *108*, 2952–3015; (b) H. C. Kolb, K. B. Sharpless, *Drug Discov. Today* **2003**, *8*, 1128–1137; (c) Z. P. Demko, K. B. Sharpless, *Org. Lett.* **2001**, *3*, 4091–4094
- 109 T. Harris, I. V. Alabugin, *Mendeleev Commun.* **2019**, *29*, 237–248
- 110 J. Dommerholt, F. P. J. T. Rujtes, F. L. Van Delft, *Top. Curr. Chem.* **2016**, *16*, 56–76
- 111 (a) B.R. Buckley, S. E. Dann, H. Heany, *Chem. Eur. J.* **2010**, *16*, 6278–6284; (b) V. V. Rostovtsev, L. G. Green, V. V. Fokin, K. B. Sharpless, *Angew. Chem. Int. Ed.* **2002**, *41*, 2596–2599; *Angew. Chem.* **2002**, *114*, 2708–2711; (c) V. O. Rodionov, V. V. Fokin, M. G. Finn, *Angew. Chem.* **2005**, *117*, 2250–2255; *Angew. Chem. Int. Ed.* **2005**, *44*, 2210–2215; (d) M. Ahlquist, V. V. Fokin, *Organometallics* **2007**, *26*, 4389–4391
- 112 (a) H. Cerecetto, A. Gerpe, M. Gonzalez, V. J. Aran, C. O. Ocariz, *Mini-Rev. Med. Chem.* **2005**, *5*, 869–878; (b) G. Picciòla, F. Ravenna, G. Carenini, P. Gentili, M. Riva, *Farmaco Ed. Sci.* **1981**, *36*, 1037–1056; (c) S. Vidyacharan, C. Adhikari, V. S. Krishna, R. S. Reshma, D. Sriram, D. S. Sharada, *Bioorg. Med. Chem. Lett.* **2017**, *27*, 1593–1597
- 113 O. S. Kim, J. H. Jang, H. T. Kim, S. J. Han, G. C. Tsui, J. M. Joo, *Org. Lett.* **2017**, *19*, 1450–1453
- 114 J. Schoene, H. B. Abed, P. Schmieder, M. Christmann, M. Nazaré, *Chem. Eur. J.* **2018**, *24*, 9090–9100
- 115 (a) D. Vina, E. del Olmo, J. L. L. Perez, A. S. Feliciano, *Org. Lett.* **2007**, *9*, 525–528; (b) J. J. Song, N. K. Lee, *Org. Lett.* **2000**, *2*, 519–521
- 116 F. H. C. Stewart, *Chem. Rev.* **1964**, *64*, 129–147
- 117 C. Wu, Y. Fang, R. C. Larock, F. Shi, *Org. Lett.* **2010**, *10*, 2234–2237
- 118 (a) L. Horner, A. Christmann, *Angew. Chem. Int. Ed.* **1963**, *2*, 599–608; (b) W. Lwowski, *Angew. Chem. Int. Ed.* **1967**, *6*, 897–906; (c) B. V. Ioffe, M. A. Kuznetsov, *Russ. Chem. Rev.* **1972**, *41*, 131–145
- 119 Compendium of Chemical Terminology, 2nd ed. (the "Gold Book")
- 120 I. M. McRobbie, O. M. Cohn, H. Suschitzky, *Tetrahedron Lett.* **1976**, *17*, 925–928
- 121 J. M. Lindley, I. M. McRobbie, O. M. Cohn, H. Suschitzky, *J. Chem. Soc. Perkin Trans. 1* **1980**, 982–994
- 122 J. Liu, N. Liu, Q. Yang, L. Wang, *Org. Chem. Front.* **2021**, *8*, 5296–5302

- 123 C. M. Mboyi, D. Vivier, A. Daher, P. F. Lessard, H. Cattey, C. H. Devillers, C. Bernhard, F. Denat, J. Roger, J.-C. Hierso, *Angew. Chem. Int. Ed.* **2020**, *59*, 1149–1154; *Angew. Chem.* **2020**, *132*, 1165–1170
- 124 J. E. Leffler, R. D. Temple, *J. Am. Chem. Soc.* **1967**, *89*, 5235–5246
- 125 M. L. Blackman, M. Royzen, J. M. Fox, *J. Am. Chem. Soc.* **2008**, *130*, 13518–13519
- 126 (a) H. E. Murrey, J. C. Judkin, C. W. A. End, T. E. Ballard, Y. Fan, K. Riccardi, L. Di, E. R. Guilmette, J. W. Schwartz, J. M. Fox, D. S. Johnson, *J. Am. Chem. Soc.* **2015**, *137*, 11461–11475; (b) Y. Sun, X. Ma, K. Cheng, B. Wu, J. Duan, H. Chen, L. Bu, R. Zhang, X. Hu, Z. Deng, L. Xing, X. Hong, Z. Cheng, *Angew. Chem. Int. Ed.* **2015**, *127*, 5981–5984
- 127 (a) R. Das, M. Kapur, *Asian J. Org. Chem.* **2018**, *7*, 1524–1541; (b) W. Hao, Y. Liu, *Beilstein J. Org. Chem.* **2015**, *11*, 2142–2144; (c) J. Slater, J. Rourke, *Org. Chem* **2003**, *688*, 112–120
- 128 N. Marinova, S. Valero, J. L. Delgado, *J. Colloid Interf. Sci.* **2017**, *488*, 373–389
- 129 Y. Qu, P. Pander, O. Vybornyi, M. Vasylieva, R. Guillot, F. Miomandre, F. B. Dias, P. Skabara, P. Data, G. Clavier, P. Audebert, *J. Org. Chem.* **2020**, *85*, 3407–3416

Titre : Fonctionnalisation directe par activation C–H de *s*-tétrazines pour le développement de nouvelles applications

Mots clés : *s*-tétrazines, activation de la liaison C–H, halogénéation, azidation, tétrazo[1,2-*b*]indazole

Résumé : Cette thèse vise à décrire la diversité des dérivés de la *s*-tétrazine en termes de synthèses et d'applications. Elle se concentre principalement sur le développement des stratégies d'activation des liaisons C–H de la *s*-tétrazine afin d'introduire des halogénures et des azotures en positions *ortho*, afin d'atteindre des molécules et des applications innovantes.

Le premier chapitre met en évidence l'importance des halogénures d'hétéroaryle en tant que plateformes. Il se focalise sur l'introduction d'halogénures sur les *N*-hétéroaryles par une activation de la liaison C–H *N*-dirigée par des complexes du palladium. En utilisant des sources d'halogène nucléophiles, l'insertion d'halogène a été réalisé sur plusieurs molécules contenant de l'azote (telles que la *s*-tétrazine) dans des conditions douces et des

temps de réaction courts par catalyse au palladium.

Le deuxième chapitre présente les principales voies de synthèses et applications des dérivés azido *s*-tétrazine. A partir de l'azoture présent sur la *s*-tétrazine, des réactions de cycloaddition de Huisgen ont été réalisées pour synthétiser des triazoles cycliques fluorescents. La deuxième application est la synthèse d'une nouvelle famille de dérivés hétéroaryle 2*H*-indazole : les tétrazo[1,2-*b*]indazoles. Leurs propriétés ont été analysées et comparées à leur parent d'origine, les *s*-tétrazines.

Les informations complémentaires contenant les données RMN et UV-Vis sont fournies après chaque chapitre.

Title: Direct functionalization by C–H activation of *s*-tetrazines for the development of new applications

Keywords : *s*-tetrazines, C-H bond activation, halogenation, azidation, tetrazo[1,2-*b*]indazole

Abstract : This PhD thesis is planned to describe the diversity of *s*-tetrazine derivatives in terms of synthesis and applications. It is mainly focused on the development of the C–H bond activation strategies on *s*-tetrazines in order to insert halides and azide groups in *ortho*-positions to reach innovative molecules and applications.

The chapter one highlights the importance of heteroaryl organic halides as primary platforms. It focuses on the introduction of halides on *N*-heteroaryls by a palladium *N*-directed C–H bond activation. Using nucleophilic halogen sources, halogen insertion was achieved on several *N*-containing molecules (such as the topical *s*-tetrazine) under mild conditions and short reaction times by Pd-catalysis.

The second chapter presents the major synthetic routes and major applications of azido *s*-tetrazine derivatives. From azido *s*-tetrazines, huisgen cycloaddition reactions were performed to synthesis fluorescent triazole cycles . The second application is the synthesis of a novel family of 2*H*-indazole heteroaryl derivative, the tetrazo[1,2-*b*]indazole. Their properties were analyzed and compared to their parent-of-origin, the *s*-tetrazines.

The supporting information containing NMR and UV-Vis data is provided after each chapter.